

# EV clustering methods for flexibility services

**Striani, Simone**

*Publication date:*
2024

*Document Version*
Publisher's PDF, also known as Version of record

**DTU Wind and Energy Systems**
Department of Wind and Energy Systems

# EV clustering methods for flexibility services

Ph.D. Thesis

Simone Striani

Risø, Denmark, September 2024

**EV clustering methods for flexibility services**

**Author**
Simone Striani

**Supervisors**
Mattia Marinelli, Associate Professor
Department of Wind and Energy Systems, Technical University of Denmark, Denmark

Peter Bach Andersen, Senior Researcher
Department of Wind and Energy Systems, Technical University of Denmark, Denmark

Jan Engelhardt, Assistant Professor
Department of Wind and Energy Systems, Technical University of Denmark, Denmark

**Dissertation Examination Committee:**
Yi Zong, Senior Researcher (Internal examiner)
Department of Wind and Energy Systems, Technical University of Denmark, Denmark

Merkebu Zenebe Degafa, Associate Professor
Department of Electrical Engineering and Computer Science, University of Stavanger, Norway

Matej Zajc, Full Professor
Department of Information and Communication Technology, University of Ljubljana, Slovenia

**Division of Power and Energy Systems (PES)**
DTU Wind and Energy Systems
Frederiksborgvej 399, DTU Risø Campus
4000 Roskilde, Denmark
https://windenergy.dtu.dk/english
Tel: (+45) 46 77 50 85
E-mail: communication@windenergy.dtu.dk

Release date: September 2024
Class: Public
Field: Wind and Energy Systems
Remarks: The dissertation is presented to the Department of Wind and Energy Systems of the Technical University of Denmark in partial fulfillment of the requirements for the degree of Doctor of Philosophy.

# Preface

This thesis was prepared at the Department of Wind and Energy Systems of the Technical University of Denmark (DTU), in partial fulfillment of the requirements for acquiring the degree of Doctor of Philosophy in Engineering. The Ph.D. project was financially supported by the Danish research projects Autonomously Controlled Distributed Chargers-ACDC (EUDP grant number: 64019-0541) and Frederiksberg Urban Smart Electromobility-FUSE (EUDP grant number: 64020-1092).

The thesis summarizes the work carried out by the author during his Ph.D. project, between 30$^{\text{th}}$ July 2021 and 30$^{\text{th}}$ September 2024. During this period, he was employed as a Ph.D. student in the Division of Power and Energy Systems at DTU Wind and Energy Systems. The thesis is composed of a report, organized in six chapters, with seven attached scientific papers and one extended abstract. Five of these articles have been peer reviewed and published, whereas the remaining two are currently under review.

Copenhagen, 29$^{\text{th}}$ September, 2024

Simone Striani

# Acknowledgements

Over the past few years, many people have shaped my journey, and I owe a deep debt of gratitude to each one of them. This period has been one of immense personal growth, and I'd like to take this opportunity to express my sincere thanks to all who have contributed to it.

First and foremost, my heartfelt thanks go to my thesis supervisors, Mattia Marinelli, Peter Bach Andersen, and Jan Engelhardt. They gave me the invaluable opportunity to pursue this PhD and guided me throughout my studies with constructive feedback and support. I have learned a tremendous amount from them—not only scientifically but also about the academic community as a whole. Also, they have had the patience to put up with me, which I'm sure has sometimes been quite a challenge! :)

I also extend my gratitude to Kenta Suzuki and Kiuchi Hironobu for their warm hospitality and assistance during my time at the Nissan Research Center and for their many stimulating and insightful discussions that helped shape my work. I also want to thank Yuki Kobayashi for a great collaboration that grew into a friendship beyond work.

During the three years I spent at the DTU Risø campus, I was fortunate to be part of an inspiring and joyful working environment. I am grateful to all my colleagues, particularly Anya, Kristoffer, Xihai, Kristian, Eva, Helle, Daniel, Tom, and Oliver, with whom I had the pleasure of working. Thank you for all the conversations, laughter, and camaraderie, both in and out of work.

I also wish to extend my deepest thanks to my family—my brother Stefano, my sister Silvia, and especially my parents, Antonella and Adolfo, to whom this thesis is dedicated. Your love and support have been the bedrock of my journey.

My friends, both in Italy and Denmark, have been a constant source of encouragement and joy. A special thanks to Don Pietro, who holds a central place in my life, and to Lord Holsen, Sigurd, who graciously hosts me in his dwellings and brings joy to my days. I am also grateful to Lorenzo and Anna for their friendship, fun, and countless moments of happiness, and to Chris for reminding me how beautiful Australia is. Lastly, I thank Annesofie, the greatest partner in crime I could have ever hoped for.

# Abstract

As the world embraces cleaner energy, electric vehicles (EVs) are becoming increasingly prevalent, gradually replacing conventional combustion engine vehicles on our roads. While some EV smart charging technologies are commercially available, they are not widely used in public EVs chargers. Deploying smart charging functionalities on a large scale could reduce grid impact, accelerate the roll-out of charging infrastructure, and proactively integrate EVs clusters in grids and flexibility markets, making them a key asset in the green transition. However, the novel nature of the technology and the underdeveloped framework for EV-based flexibility services present significant unknowns, leading charging point operators (CPOs) to question the viability of its value chain. Research in smart charging technologies aims to develop EV chargers that can control power dispatch based on grid conditions and introduce a framework to marketise such controllability in flexibility markets.

This thesis investigates the potential of smart EV clusters to operate autonomously as controllable loads, providing flexibility services to grid operators (GOs) while ensuring an optimal charging experience for EV users. The analysis is conducted in two parts: first, the design of an analytical framework to streamline the planning and sizing of smart EV clusters in preparation for future flexibility market opportunities; second, the development of an autonomous distributed control architecture capable of coordinating multiple clusters to deliver flexibility services under the control of aggregators and GOs, while still maintaining a user-centred charging experience.

The first part of the thesis investigates the flexibility potential of smart EV clusters and the factors that influence it. It opens with an overview of the deployment status of smart EV infrastructures, identifying key technological, economic, and policy barriers to their integration as providers of flexibility services. The combination of these barriers creates uncertainties about the flexibility potential and profitability of smart EV clusters, slowing their deployment. To address this uncertainty, the thesis presents an analytical framework designed to quantify the suitability of clusters for behind-the-meter (BTM) and in-front-of-the-meter (FTM) flexibility services. This tool is valuable for CPOs and aggregators in estimating potential revenues from offering flexibility services to users and grid operators. The

study also examines how different cluster characteristics and user behaviour impact the suitability of the cluster for providing flexibility. By identifying barriers and proposing solutions, the first part of the thesis advances the discussion on smart EV infrastructure deployment, while offering insights on cluster dimensioning and suitability for different flexibility services based on forecasted operating conditions.

The second part of the thesis centers around the development of the autonomous distributed control architecture for EV clusters. It covers the design concept and implementation, development stages, computational analysis, and experimental validation of the system. A computational analysis evaluates the performance of the architecture in delivering flexibility services through smart charging functionalities, addressing the coordination of charging sessions within a single cluster for BTM services and the coordination of multiple EV clusters for FTM services. The findings provide computational evidence that distributed control is a promising alternative to centralized control for delivering flexibility services. Following the development of the chargers prototypes, an experimental campaign was conducted to validate the technical feasibility of this architecture. The experiments, which reproduced the simulated smart charging functionalities on a smaller scale, assessed the performance of the system in terms of accuracy and communication delay. The results confirmed the feasibility of the distributed control architecture, while also highlighting potential limitations of current EV models in supporting certain smart charging functionalities.

In conclusion, this thesis offers new perspectives on the key factors involved in designing smart EV clusters. It addresses both the physical attributes of the clusters——such as connection capacity, charger capacities, location, and type of cluster——and the impact of different charging strategies on their effectiveness. The study breaks new ground in the field of EV controllability by presenting and demonstrating the efficacy of a novel control architecture for smart EV chargers and by highlighting the potential and limitations of EVs as controllable loads.

# Resumé

Efterhånden som verden tager renere energikilder i brug, bliver elbiler stadig mere udbredte og erstatter gradvist konventionelle forbrændingsmotorer på vejene. Selvom nogle intelligente opladningsteknologier til elbiler allerede er kommercielt tilgængeligt, bliver de ikke anvendt i stor udstrækning i offentlige ladestandere til elbiler. Implementering af smarte ladefunktioner i stor skala kan reducere belastningen på elnettet, fremskynde udbygningen af opladningsinfrastrukturen og proaktivt integrere klynger af elbilsladere i el- og fleksibilitetsmarkederne, og derved gøre dem til et nøglekomponent i den grønne omstilling. Dog indebærer teknologiernes nye karakter og den underudviklede ramme for fleksibilitetsydelser baseret på elbiler betydelige usikkerheder, hvilket får ladeoperatører til at stille spørgsmål ved værdikædens levedygtighed. Forskning inden for smartladningsteknologier har til formål at udvikle elbilsladere, der kan styre effekten baseret på netforhold, samt at introducere en ramme til at markedsføre denne styring i fleksibilitetsmarkeder.

Denne afhandling undersøger potentialet for intelligente elbilsklynger til at fungere autonomt som styrbare belastninger, og derved leverer fleksibilitetsydelser til gavn for ladeoperatører og samtidig undgå kompromier med brugernes opladningsoplevelse. Analysen er i to dele: Først designes en analytisk ramme, der skal forenkle planlægning og dimensionering af intelligente elbilsklynger i forhold til fremtidige muligheder på fleksibilitetsmarkedet. Dernæst udvikles en autonom, distribueret kontrolarkitektur, der er i stand til at koordinere flere klynger for at levere fleksibilitetsydelser under kontrol af aggregatorer og netoperatører, samtidig med at der opretholdes en brugervenlig opladningsoplevelse.

Første del af afhandlingen undersøger fleksibilitetspotentialet i intelligente elbilsklynger og de faktorer, der påvirker det. Denne del begynder med et overblik over implementeringsstatus for intelligente elbilsinfrastrukturer, hvor de vigtigste teknologiske, økonomiske og politiske barrierer for deres integration som leverandører af fleksibilitetsydelser identificeres. Kombinationen af disse faktorer skaber usikkerhed omkring fleksibilitetspotentialet og rentabiliteten for intelligente elbilsklynger, hvilket hæmmer deres udbredelse. For at imødegå denne usikkerhed præsenterer afhandlingen en analytisk ramme designet til at kvantificere klyngernes egnethed til fleksibilitetsydelser inden for både tjenester bag el-måleren og tjenester foran måleren. Dette værktøj er værdifuldt for ladeoperatører og aggregatorer

til at estimere potentielle indtægter fra udbud af fleksibilitetsydelser til brugere og netoperatører. Undersøgelsen analyserer også, hvordan forskellige klyngekarakteristiker og brugeradfærd påvirker klyngernes egnethed til fleksibilitetsydelser. Ved at identificere barrierer og foreslå løsninger bidrager første del af afhandlingen til diskussionen om implementeringen af intelligente elbilsinfrastrukturer og tilbyder indsigt i dimensioneringen af klynger og deres egnethed til forskellige fleksibilitetsydelser baseret på forventede driftsforhold.

Anden del af afhandlingen fokuserer på udviklingen af en distribueret autonom kontrolarkitektur for elbilsklynger. Denne del omhandler designkonceptet, implementeringen, udviklingsstadierne, beregningsanalysen og den eksperimentelle validering af systemet. En beregningsanalyse evaluerer arkitekturens præstation i leveringen af fleksibilitetsydelser med smarte opladningsfunktioner. Analysen adresserer både koordineringen af opladningssessioner inden for en enkelt klynge til tjenester bag måleren og koordineringen af flere elbilsklynger til tjenester foran måleren. Resultaterne giver analytisk bevis for, at distribueret kontrol er et lovende alternativ til centraliseret kontrol for levering af fleksibilitetsydelser. Efter udviklingen af prototype-ladere blev der gennemført en eksperimentel test kampagne for at validere de tekniske styrker af arkitekturen. Eksperimenterne, som reproducerede de simulerede smarte opladningsfunktioner i mindre skala, vurderede systemets præstation i forhold til nøjagtighed og kommunikationsforsinkelse. Resultaterne bekræftede den distribuerede kontrolarkitekturs styrker, men fremhævede også potentielle begrænsninger i de nuværende elbilsmodeller i understøttelsen af visse smarte opladningsfunktioner.

Afslutningsvis giver denne afhandling nye perspektiver på de vigtigste omdrejningspunkter, der er involveret i designet af intelligente elbilsklynger. Den adresserer både de fysiske parametre ved klyngerne, såsom forbindelseskapacitet, ladekapaciteter, placering og klyngetype, samt virkningen af forskellige opladningsstrategier på lade effektivitet. Studiet baner ny vej inden for elbilernes styrbarhed ved at præsentere og demonstrere effektiviteten af en ny kontrolarkitektur til smarte elbilopladere og ved at fremhæve potentialet og begrænsningerne af elbiler som styrbare belastninger.

# Contents

# List of Acronyms

| | |
|---|---|
| BRP | balancing responsible party |
| BTM | behind-the-meter |
| CA | cloud aggregator |
| CAPEX | capital expenditures |
| CPO | charging point operator |
| DER | distributed energy resource |
| DSO | distribution system operator |
| EV | electric vehicle |
| EVSE | electric vehicle supply equipment |
| FTM | in-front-of-the-meter |
| GO | grid operator |
| ICT | information and communication techology |
| IoT | internet of things |
| OPEX | operational expenditures |
| PCC | point of chargers connection |
| RES | renewable energy sources |
| SOC | state-of-charge |
| TSO | transmission system operator |
| V2G | vehicle-to-grid |
| VA | virtual aggregator |
| VPP | virtual power plant |

# List of Figures

# List of Tables

# List of Publications

Papers included in the thesis

[**P1**] **S. Striani**, K. Sevdari, L. Calearo, P. B. Andersen, and M. Marinelli (2021). Barriers and solutions for EVs integration in the distribution grid. 2021 56th International Universities Power Engineering Conference (UPEC). IEEE, 2021. p. 1-6.

[**P2**] **S. Striani**, T. Unterluggauer, M. Marinelli, and P. B. Andersen, (2022). Flexibility Potential Quantification of Electric Vehicle Charging Clusters. Sustainable Energy, Grids and Networks (SEGAN). Under review.

[**P3**] **S. Striani**, K. Sevdari, P. B. Andersen, and M. Marinelli, (2022). Autonomously Distributed Control of EV Parking Lot Management for Optimal Grid Integration. 2022 International Conference on Renewable Energies and Smart Technologies (REST). IEEE, 2022. p. 1-5.

[**P4**] **S. Striani**, K. Sevdari, M. Marinelli, V. Lampropoulos, Y. Kobayashi, and K. Suzuki, (2022). Wind Based Charging via Autonomously Controlled EV Chargers under Grid Constraints. 2022 57th International Universities Power Engineering Conference (UPEC). IEEE, 2022. p. 1-6.

[**P5**] A. Malkova, **S. Striani**, J. M. Zepter, M. Marinelli, and L. Calearo, (2023). Laboratory Validation of Electric Vehicle Smart Charging Strategies. 2023 58th International Universities Power Engineering Conference (UPEC). IEEE, 2023. p. 1-6.

[**P6**] K. L. Pedersen, **S. Striani**, J. Engelhardt, and M. Marinelli, (2024). Implementation of Priority-based Scheduling for Electric Vehicles through Local Distributed Control. Proceedings of 2024 IEEE PES Innovative Smart Grid Technologies Europe (ISGT Europe 2024). Accepted manuscript.

[**P7**] **S. Striani**, K. L. Pedersen, J. Engelhardt, and M. Marinelli, (2024). Experimental Investigation of a Distributed Architecture for EV Chargers Performing Frequency Control. World Electric Vehicle Journal, 2024, 15.8: 361.

## Other publications

The following publications have been prepared during the course of the Ph.D. study, but are omitted from the thesis because they are not directly related to the primary research objectives, or partially covered by the selected papers.

### Papers

[P9] K. Sevdari, L. Calearo, **S. Striani**, P.B. Andersen, M. Marinelli, and L. Ronnow. (2021). Autonomously Distributed Control of Electric Vehicle Chargers for Grid Services. Proceedings of 2021 IEEE PES Innovative Smart Grid Technologies Europe: Smart Grids: Toward a Carbon-Free Future, ISGT Europe 2021, 1–5.

[P10] K. Sevdari, **S. Striani**, P. B. Andersen, and M. Marinelli, (2022). Power Modulation and Phase Switching Testing of Smart Charger and Electric Vehicle Pairs. 2022 57th International Universities Power Engineering Conference: Big Data and Smart Grids, UPEC 2022 - Proceedings, 1–6.

[P11] X. Cao, **S. Striani**, J. Engelhardt, C. Ziras, and M. Marinelli, (2023). A semi-distributed charging strategy for electric vehicle clusters. Energy Reports, 2023, 9: 362-367.

[P12] P. Zunino, J. Engelhardt, **S. Striani**, K. L. Pedersen, and M. Marinelli, (2024). Frequency Control in EV Clusters: Experimental Validation and Time Response Analysis of Centralized and Distributed Architectures. Innovative Smart Grid Technologies (PES ISGT), IEEE, under review.

### Technical reports

[R1] M. Marinelli, **S. Striani**, K. L. Pedersen, K. Sevdari, M. Hach, O. L. Mikkelsen, M. Rakowski (2023). ACDC project – Autonomously Controlled Distributed Chargers: Final report. Det Energiteknologiske Udviklings- og Demonstrationsprogram. (EUDP) 42 p.

### Co-supervision of Bachelor or Master's theses

[T1] T. K. Skogland, (2021). Charging flexibility from electric vehicles via autonomous chargers in a workplace (Master's thesis, NTNU, Norway).

[T2] V. Lampropoulos, (2022). Wind farm balancing via autonomously controlled electric vehicle chargers, M.Sc. in Electrical Engineering, DTU, Denmark.

[T3] B. Shan, (2022).Design of charging strategies with autonomous phase switching for an aggregation of EVs, M.Sc. in Electrical Engineering, DTU, Denmark.

[T4] K. L. Pedersen, (2023). Development and testing of smart charging strategies for a workplace parking lot, M.Sc. in Electrical Engineering, DTU, Denmark.

[T5] P. Zunino, (2024). Analysis and testing of frequency services provided by electric vehicle clusters, M.Sc. in Electrical Engineering, DTU, Denmark.

PART I

# Summary Report

CHAPTER 1

# Introduction

## 1.1 Context and motivation

To reduce $CO_2$ emissions, governments are promoting a shift away from fossil fuels in favour of sustainable technologies in both electricity production and transportation [1]. For electricity production, this involves promoting renewable energy sources (RES), while in the transportation sector, it means accelerating the adoption of electric vehicles (EVs) for both private and public transport [2]. The penetration of RES into the power system is crucial for reducing carbon emissions but introduces challenges related to their intermittent and unpredictable energy production [3]. Traditionally, stability and security of supply have been maintained through energy markets, including flexibility markets, where controllable energy suppliers and consumers offer flexibility to grid operators [4]. In these markets, flexibility is provided through standardised products known as flexibility services. However, as the traditional controllable power plants are replaced by less predictable RES, the grid faces increasingly volatile power production, creating a greater need for energy buffers that can absorb excess energy production and reduce consumption during shortages [5].

Smart charging offers a solution to these challenges by turning EV chargers into flexible grid assets [6]. Without smart management, large-scale EV charging could destabilise the grid [7], [8], but smart charging can provide substantial storage capacity, becoming an integral part of future smart grids [6]. Charging infrastructures are implemented as EV charging clusters owned and managed by charging point operators (CPOs) and aggregators [9], where multiple outlets share a common grid connection, referred in this thesis as point of chargers connection (PCC). These clusters typically modulate the power consumption of the connected EVs to avoid overloading their grid connection [10], but they lack advanced functionali-

ties. State-of-the-art smart EV clusters employ control strategies to offer flexibility services by adjusting charging power according to strategic power set-points and scheduling charging sessions based on user demand [11], [12]. The provision of these services to the grid operators will be remunerated in flexibility markets and be financially convenient for the EV users, as well as the CPOs and aggregators. Flexibility services from aggregated EV clusters can be monetised in flexibility markets, benefiting CPOs and aggregators and potentially lowering charging prices for users participating in these services.

Despite its potential, smart charging faces several obstacles, including technical, economic, and regulatory challenges [13]. These barriers create a feedback loop that discourages EV adoption among drivers and limits investment in smart EV charging infrastructure [14]. Overcoming these challenges requires coordination among multiple stakeholders, such as charger manufacturers, carmakers, CPOs, grid operators (GOs), and flexibility market operators, to standardise technologies and create compatible infrastructures. Government and policymakers must oversee and incentivise these efforts.

One major challenge in deploying smart EV charging clusters is the uncertainty about their flexibility potential and profitability. CPOs need to upgrade existing infrastructures, including hardware and software, to provide flexibility services and plan new clusters that align with future developments. They face the dual challenge of minimising costs while maximising potential revenues, a task made more difficult by the current uncertainty in flexibility markets. Decisions regarding the placement and sizing of EV clusters are crucial for optimising revenue and attracting EV users [15]. Developing robust and reliable control strategies and communication architectures is essential alongside cluster design [16], [17]. These strategies must leverage internet of things (IoT) and cloud computing for data management and offer a user-friendly experience to encourage EV owners to participate in flexibility services by offering lower charging prices.

Given this context, ongoing research should focus on developing and testing smart charging strategies, including control. Computational analysis should be conducted on various scales, from large-scale studies of user behaviour to guide the strategic placement of EV clusters in cities and ensure grid compatibility [18], to smaller-scale analyses aimed at optimising charging strategies and enhancing cluster flexibility based on specific connection patterns.

## 1.2 Research Objectives

The present thesis explores the quantification flexibility potential of EV clusters and proposes a novel distributed control architecture for EV chargers to harness

this potential. The control architecture was developed and installed in an office parking lot at the Risø campus of the Technical University of Denmark as part of the research project "Autonomously Controlled Distributed Chargers" (ACDC). The goal of the research project was to demonstrate the feasibility of the design and evaluate its prospective capabilities.

The developed control architecture consists of a two-layer system: the first layer consists of a cloud computing platform, referred to as cloud aggregator (CA), which coordinates the power set-points of each managed EV cluster controlled and treated as a whole unit. This coordination is based on user presence, grid conditions, and flexibility services scheduled from CPOs/aggregators. The second layer is an autonomous control unit, called virtual aggregator (VA), installed in each charger, which independently manages the charging sessions of connected EVs according to the set-points from the CA and conditions at the PCC. Additionally, the control architecture implements a priority system based on user inputs from a mobile app to prioritise the most urgent charging sessions. The thesis objectives are grouped into two distinct research perspectives.

The first perspective focuses on analysing EV clusters as distributed energy storage systems and mapping their flexibility potential in relation to their different characteristics. This requires designing a straightforward and comprehensive analytical framework and well-defined key performance indicators. The developed method aims to support policymakers, CPOs, and aggregators by enabling them to leverage charger metering data to optimise the sizing of new EV clusters and determine when to consider upgrading existing ones to provide flexibility services. The method is designed to aid the development of EV clusters tailored to future flexibility market opportunities and balancing trade-offs between BTM and FTM flexibility services. The key questions explored involve determining the characteristics shaping flexibility potential and assessing how significantly they impact it. The factors analysed relate to the electrical layout of the cluster (such as number of chargers, connection capacity, power capacity of the chargers), the control architecture, the type and location of the parking lot and consequently, user behaviour.

The second perspective focuses on developing and validating the distributed control architecture, assessing its performance in coordinating various EV clusters and their charging sessions to provide flexibility services. The local control layer of the control architecture must ensure autonomous smart charging functionalities, such as power-scheduling, power-sharing and prioritisation of charging sessions among the EVs within the clusters. Meanwhile, the global control layer must aggregate the power demand of the controlled EV clusters to provide various flexibility services, such as peak shaving, RES power matching and frequency regulation. The thesis aims to measure the effectiveness of this architecture and evaluate its performance through computational simulations and experimental val-

idation.

In conclusion, based on the findings from these two research perspectives, the thesis provides insights on design choices for improving the cost-effectiveness of smart EV clusters, including considerations for electrical layout, control architecture, and strategy design. Lastly, the thesis addresses current limitations in the controllability of existing EV models and outlines directions for future research.

## 1.3 Thesis outline

The thesis is divided into two parts. Part I is a comprehensive summary report outlining the thematic framework for the scientific publications and highlighting their main contributions and findings. This section consists of six chapters: an introduction, four technical chapters, and a conclusion. Part II includes the six scientific publications integrated into the thesis. This section provides an overview of the content covered in Part I.

Chapter 2 focuses on the integration of EV clusters as controllable loads for providing grid services. The first section contains an overview of the techno-economic and policy frameworks for integrating smart EV chargers into the grid as flexibility services providers. It then presents the content of **Paper** [**P1**], identifying the main barriers to the deployment of smart charging technologies and proposing action points to address these challenges. One key barrier discussed is the uncertainty surrounding the flexibility potential of EV clusters. The third section introduces an analytical framework developed to quantify this flexibility potential, as detailed in **Paper** [**P2**]. Starting with a thorough review of the current state-of-the-art methodologies on the topic, it introduces new criteria for assessing cluster flexibility. The criteria are demonstrated through computational analysis using metering data from chargers. A sensitivity analysis is employed to evaluate how various cluster characteristics——such as connection capacity, aggregated battery capacity of EVs, power capabilities of EVs and chargers, and the number of daily charging sessions——affect flexibility. The final section concludes with insights into the design of EV clusters and suggestions for further methodological improvements.

Chapter 3 introduces the autonomous distributed control architecture that has been developed, which is the focus of the remainder of the thesis. It starts by reviewing the state-of-the-art in control algorithms for EV chargers and the commercially available control architectures for both public and private applications. The second section describes in general terms the concept of the architecture, providing an overall overview of the functionalities it offers. The chapter then describes the design of Version 1 of the architecture and the characteristics of the simulation model for the computational analysis. The next section describes the

design of Version 2 of the architecture and its physical implementation employed in the experimental campaign. The final section summarises the advantages and disadvantages of the two versions of the architecture.

Chapter 4 examines the performance of the control architecture in a computational environment. The first section, based on **Paper** [**P3**], focuses on the simulation of a single cluster, evaluating the effectiveness of the VAs in coordinating the charging sessions under limited connection capacity while also assessing user charging fulfilment. The next section, based on **Paper** [**P4**], investigates the ability of the architecture to coordinate multiple EV clusters. In the simulation, four clusters are part of a virtual power plant (VPP) powered by a wind turbine and are connected to different transformers. The goal of the control is to simultaneously achieve wind power matching and peak shaving to avoid transformer overloading. The chapter concludes by summarising the findings and offering suggestions for improvements, leading to the updated version of the architecture.

Chapter 5 details the experimental campaign conducted to validate the technical feasibility of the design and methodology. The first section describes the experimental setup employed for the different test cases. The next sections discuss the results of different functionalities tested, which are power-sharing, power-scheduling, RES power matching, and peak shaving, as covered in **Paper** [**P5**] and **Paper** [**P6**]. The following section, summarising the study in **Paper** [**P7**], analyses the effectiveness of the system performing priority-based frequency regulation, which combines frequency regulation with the prioritisation of charging sessions based on user-provided urgency data via app. The chapter concludes with a summary of the results and key findings, and discusses potential improvements in the control design.

Chapter 6 provides a summary of the key contributions and findings of the thesis and suggests potential directions for future research.

CHAPTER 2

# The potential of smart charging

This chapter focuses on the integration of EV clusters as controllable loads for providing grid services. Section 2.1 provides an overview of the status of smart EVSE integration in the power system and discusses different barriers towards their full implementation for flexibility services. Section 2.2 then introduces the developed method for quantifying the flexibility potential of EV clusters, starting from the motivation and state-of-the-art methodologies and introducing the flexibility criteria. Subsequently, Section 2.3 introduces the model and assumption used for demonstrating the use of the analytical framework. Next, Section 2.4 discusses the results of the simulation and sensitivity analysis. At last, 2.5 concludes the chapter with a summary of the main findings and provides ideas for future work.

## 2.1 The status of EVSE integration

The management of EV charging has the potential to transform the power grid and serve as a foundational element for future smart cities. Depending on the technology employed, EVs can function both as flexible loads, by shifting charging times and modulating charging power, and as flexible sources, by feeding power back into the grid. Through the internet of things (IoT), aggregators and charging point operators (CPOs) can control the charging demands of large fleets of EVs across various clusters, providing flexibility services to grid operators (GOs). Flexibility services are power adjustments made by either the supply or demand side to maximise the security and stability of the energy supply. EV flexibility services

can be classified as behind-the-meter (BTM) or in-front-of-the-meter (FTM), with FTM further divided into local or system-wide services, depending on the specific application [19].

BTM flexibility mainly benefits EV users or charging site owners by reducing grid connection costs, minimising charging expenses, or maximising self-consumption of distributed energy resources (DERs), as discussed in [20]–[23]. Local EV flexibility, which benefits the power distribution network, encompasses various aspects, such as using smart charging to minimise grid losses [24], perform peak shaving and congestion management [25], [26], mitigate voltage imbalances [27], and reduce transformer loss-of-life [28]. System-wide flexibility services, aimed at benefiting the wholesale market or transmission system, include frequency control [29], [30] and using EV flexibility to facilitate the integration of variable renewable energy sources [31]. Table 2.1 summarises EV flexibility services and their standards.

Flexibility services are typically traded through flexibility markets, where smart charging could enable electric vehicle supply equipment (EVSE) to participate and generate revenue by providing such services. The EV market actors and stakeholders are briefly described in this section. However, this thesis refers to [32] for a more comprehensive outline. As the end-users of charging technologies, EV owners require reliable and efficient functionalities to ensure a seamless charging experience. Additionally, they need to be appropriately compensated for participating in flexibility services [33]. CPOs own EV clusters and are responsible for their monitoring, operation, and maintenance. Aggregators collect flexibility from multiple sources, such as several CPOs, to participate in electricity markets as a balancing responsible party (BRP) [9]. Aggregation is essential to meet market standards, such as minimum bid requirements for participation. GOs, including distribution system operators (DSOs) and transmission system operators (TSOs), are the primary buyers of these services in the markets. They compensate electricity suppliers and consumers for their capacity to adjust production and consumption to maintain grid stability and security. This market structure creates value for all participants, supporting the transition towards sustainable energy production and transportation.

### 2.1.1 Overcoming barriers for adopting EVs as flexibility providers

Several technological, economic, and regulatory barriers hinder the adoption of electric vehicles (EVs) as providers of flexibility services in the power grid. Overcoming these challenges requires coordinated efforts among stakeholders to harness the potential of EVs in flexibility markets fully [19].

From a technological standpoint, the current EV infrastructure, including charg-

**Table 2.1:** Classification of potential EV flexibility services for FTM applications (Own illustration based on the work in [32]).

## Frequency services

| *Services* | *Description* |
|---|---|
| 1. Fast frequency reserve | 1. Power injection starts within 2 seconds and lasts for several minutes; assists in reducing the *Rate of change of frequency*. |
| 2. Frequency containment reserve | 2. Power injection begins within 30 seconds and is fully activated within 2-5 minutes; it aids in containing deviations from the nominal frequency. |
| 3. Frequency restoration reserve | 3. Activated within 5-15 minutes and sustained until frequency is restored; assists in bringing the system frequency back to its nominal value. |
| 4. Replacement reserve | 4. Power delivered within 15 minutes to 1 hour; ensures sufficient active power reserves following a disruption and replaces the Frequency restoration reserve. |
| 5. Synthetic inertia | 5. Immediate response (<1 second) to frequency changes; emulates the behaviour of traditional rotating generators. |

## Grid stability

| *Services* | *Description* |
|---|---|
| 1. Emergency power | 1. Activated during emergencies to provide critical infrastructure with power; typically involves non-scheduled power plants that can start up quickly. |
| 2. Energy arbitrage | 2. Involves charging when prices are low (off-peak) and discharging when prices are high (peak). |
| 3. RES power smoothing | 3. Aims to reduce the variability of power output from renewable energy sources, which helps to mitigate issues like power flickering. |
| 4. Black start capability | 4. Helps the power grid to restart after a total or partial blackout by supplying power until the interconnected system is established again. |
| 5. Anti-islanding | 5. Prevents local generators from continuing to supply power during a wider network outage, ensuring the safety of repair crews and preventing the spread of faults. |
| 6. Low voltage ride through | 6. Requires power generation systems to maintain operation despite dips in grid voltage; contributing to overall grid stability. |
| 7. Fault ride through | 7. Requires power generation systems to maintain operation during grid faults or abnormal operating conditions, such as short circuits. |
| 8. Valley filling | 8. Involves charging energy storage systems during off-peak periods (when demand is low) and discharging them during peak times; helps to alleviate load peaks. |
| 9. Peak shaving | 9. Entails reducing or curtailing demand during peak times to relieve stress on the grid. |

## Congestion management

| *Services* | *Description* |
|---|---|
| 1. Time of use | 1. Involves varying electricity prices based on the time of the day to encourage consumers to shift their electricity use to periods of lower demand. |
| 2. Type of use | 2. Featured different rates depending on the type of electricity usage, with additional fees based on grid carbon intensity. |
| 3. Dynamic pricing | 3. Encompasses adjusting electricity prices in real-time according to supply and demand; requires advanced metering infrastructure and sophisticated rate design. |
| 4. Extreme day pricing | 4. Refers to significantly increased electricity prices on days with expected extremes, often in response to weather events; it aims to incentivise consumers to shift their usage away from these peak periods. |
| 5. Peak time rebate | 5. Offers discounts or rebates to customers who reduce their electricity usage during peak demand periods. |
| 6. RES power matching | 6. Involves scheduling the operation of Renewable Energy Sources (RES) to align with demand profiles, helping to mitigate the issues caused by the intermittency of RES. |
| 7. Phase balancing | 7. Aims to distribute electrical loads evenly across all phases in a three-phase power system to improve efficiency and reduce losses. |
| 8. DER power matching | 8. Matches supply with demand in systems with DERs, often through demand response programs or adjustments to DER output. |

ers and communication networks, presents significant obstacles. Most EV chargers deployed today are not equipped with smart functionalities and cannot perform advanced tasks like dynamic load management and scheduling [34]. For existing smart chargers, a major technological challenge across the entire range of involved devices (from chargers to EVs) is the lack of standardisation in communication protocols [35] and inconsistencies in EV response accuracy and behaviour. Additionally, the limited deployment of smart meters and the absence of standardised protocols impede effective data sharing and grid management. Smart meters, which must be certified and installed by DSOs, provide essential real-time data to manage grid conditions but require precise specifications for parameters like sampling rates to balance speed and cost. The European Clean Energy Act mandates that smart meters include remote reading with two-way communication and a maximum 15-minute sampling rate [36], but the lack of standardised implementation across Europe remains a barrier. Developing robust information and communication techology (ICT) systems is crucial for effective metering, control, and communication among stakeholders, which are necessary for a functional flexibility market framework.

From an economic standpoint, the lack of a robust economic framework for flexibility services is a significant barrier to adopting EVs as flexibility providers. System-wide ancillary services markets, such as frequency and balancing markets, are already active but offer limited services and require high minimum bids of power or energy. At the distribution level, however, flexibility markets are still in their infancy [37]. In Europe, several research initiatives, including Piclo, Enera, Flex, GOPACS, NODES [38], and Ecogrid 2.0 [39], are leading efforts to establish local flexibility markets. These markets will facilitate trading between GOs, aggregators, and CPOs [40]. To facilitate this development, regulators should promote the creation of additional local flexibility markets based on nodal pricing systems [41]. Furthermore, DSOs should take on the role of defining the flexibility requirements for aggregators, CPOs or prosumers.

Regulatory challenges also play a crucial role in limiting the deployment of EVs as flexibility providers. The transition towards smart grids requires DSOs to move beyond the traditional "fit-and-forget" approach, focusing primarily on minimising capital expenditures (CAPEX) by reinforcing the grid when needed. Instead, they should shift to a total expenditure (TOTEX) framework that balances both operational expenditures (OPEX) and CAPEX to optimise overall costs [42]. Regulatory reforms are necessary to encourage proactive management of expenditures by DSOs and to capitalise on load flexibility opportunities [43]. Additionally, the adoption of vehicle-to-grid (V2G) technologies encounters regulatory obstacles due to its novelty, including cumbersome administrative procedures that discourage user adoption [35]. These hurdles stem from the lack of comprehensive standards

for connection requirements, classification, and interconnection of V2G systems. To address these issues, regulators, system operators, and manufacturers need to collaborate on standardising these requirements to streamline administrative processes and ensure safety. Effective grid management also necessitates enhanced coordination between DSOs, TSOs, and EV users. Whether grid code-based, contract-based, or market-based, flexible provision strategies rely on a coordinated approach among these stakeholders. The interaction between DSOs and TSOs becomes particularly critical as the penetration of renewable energy sourcess (RESs) and DERs increases, often resulting in conflicting demands between distribution and transmission networks. In such cases, prioritising the needs of the transmission network over the distribution network is frequently required to preserve grid stability.

## 2.2 Quantifying the flexibility potential of EV clusters

The underdeveloped flexibility framework for smart charging technologies, described in 2.1.1, generates uncertainty about the ability of EV clusters to provide flexibility services profitably [44]. This uncertainty discourages CPOs from adopting smart charging technologies, leading them to rely on traditional charging methods instead. However, the growing adoption of meter-integrated smart chargers enables new data-driven approaches for planning the electrical layout and designing smart charging strategies for future EV clusters. By utilising historical data from clusters, CPOs can predict the flexibility potential and profitability of these clusters based on their characteristics.

The flexibility potential of EV clusters is influenced by several key factors, including location (workplace, curbside, residential, etc.) and type (fast charging, slow charging) [15]. For example, residential and workplace clusters generally provide the highest flexibility due to longer connection times [45], whereas highway fast-charging clusters tend to offer minimal flexibility because of their shorter connection durations [46]. By leveraging metering data, CPOs can tailor the hardware configurations of clusters——such as connection capacity, charger power capacity, and the number of chargers——to optimise return on investment. This optimisation helps reduce CAPEX by avoiding oversized grid connections and reduces OPEX by providing flexibility services.

The rest of this chapter outlines the analytical framework developed in **Paper [P2]** to evaluate the flexibility potential of EV clusters and examine the factors influencing it. The method is designed to aid CPOs and aggregators in making informed design decisions for new EV clusters, enhancing their ability to provide flexibility services while improving profitability.

### 2.2.1 Available methods in literature

Quantifying the flexibility potential of electric vehicles (EVs) is a complex and underexplored area, with most studies focusing on specific dimensions such as time, power, or energy. Time-based flexibility is investigated by works like [47]–[49], which focus on public and office charging, while [50] looks at non-residential charging, defining flexibility as the ratio of idle to total connection time. Other studies, such as [51]–[53], explore power or energy-based flexibility, examining public and workplace charging in locations like Helsinki and Germany. Additionally, [45] focuses on flexibility in residential apartment complexes, using idle capacity as the primary metric.

Recent work has adopted a more multidimensional approach to flexibility quantification. For example, [54] introduces a distributed coordination strategy using indexes that measure SoC deviation, target violation, and battery degradation. Similarly, [55] proposes metrics like load shift, peak reduction, and load curve flatness to assess the impact of charging strategies. In a systematic review, [56] evaluates flexibility across four dimensions—temporal, durational, quantitative, and locational—highlighting that flexibility remains underutilised and unevenly applied.

The research in [57] emphasises that flexibility quantification depends on the stakeholder involved, with a Norwegian case study examining power and energy KPIs like peak power reduction and self-consumption. Finally, [58], [59] use extensive mathematical models to quantify aggregated flexibility across EV fleets, though the complexity and data requirements of these models limit their practical application.

Overall, most studies focus on single dimensions, which provide limited perspectives. While recent work attempts more comprehensive evaluations, these approaches are often theoretical and challenging to implement in real-world scenarios. Additionally, existing methods generally overlook the trade-offs between BTM and FTM flexibility goals.

### 2.2.2 Flexibility evaluation criteria

This subsection outlines the criteria developed in **Paper [P2]** to evaluate the flexibility potential of EV charging clusters. The criteria aim to assess both the qualitative and quantitative aspects of flexibility, focusing on the ability of the cluster to provide flexibility services without compromising user needs. We refer to **Paper [P2]** for a more comprehensive description of the mathematical derivation of the criteria and examples of how they relate to different flexibility services.

To quantify the flexibility potential of an EV charging cluster, it is important to define its boundaries in terms of power, time and energy capabilities. The connection capacity of the cluster sets the upper power limit of the aggregated power consumption, while the minimum charging power of the EVs/chargers sets the lower limit. The minimum charging power depends on the charging technology deployed: for example, bidirectional chargers would allow negative power values, while unidirectional chargers (which are the focus of this study) allow a minimum of 0 kW. The maximum power capacity of the EVs/charger is another important boundary to consider, again dependent on the charging technology. Building up from the boundaries mentioned above, we define the maximum energy potential $E_{pot}$, as the energy that the charging cluster could potentially charge to EVs with infinite energy storage within the boundaries of the power capacity of the chargers, connection pattern and connection capacity of the cluster (i.e., all EVs charge at full power for the entire duration of their connection time).

In the study, we define four qualitative criteria and one quantitative criterion for the comprehensive assessment of the flexibility potential of clusters. The qualitative criteria, called flexibility indexes, are the Energy Flexibility Index (EFI), Minimum Power Flexibility Index (MPFI), Average Power Flexibility Index (APFI) and Time Flexibility Index (TFI). In contrast, the quantitative criterion is the Hourly Energy Flexibility (HEF). The qualitative criteria are tailored to take into account short-term power adjustments (addressed by the MPFI and APFI), long-term power adjustments/scheduling (addressed by the EFI) and available idle time useful for scheduling purposes (addressed by TFI). Each index assigns a score between 0, representing no flexibility potential, and 1, representing infinite flexibility potential within their respective domains. Within this framework, flexibility potential is defined as the capability of delaying power consumption over time without influencing the charging fulfilment of the cluster.

From the energy perspective, the EFI is defined as:

$$EFI = 1 - \frac{E_{ch}}{E_{pot}}. \tag{2.1}$$

In the formula, $E_{ch}$ is the aggregated energy demand, defined as the total energy delivered to all the EVs connected during the time period under analysis. The EFI is relevant to understand the suitability of the charging cluster to delay energy in time.

The MPFI is defined as:

$$MPFI = 1 - \frac{P_{max,avg}}{CC}, \tag{2.2}$$

where $P_{max,avg}$ is the average daily maximum that the aggregated power of the charging cluster reaches over a given period, and $CC$ is the connection capacity. The MPFI estimates the remaining power flexibility during peak utilisation of the charging cluster.

On the other hand, the APFI is:

$$APFI = 1 - \frac{P_{mean,ch}}{CC}, \tag{2.3}$$

where $P_{mean,ch}$ is the average charging power dispatched by the charging cluster, considering only the time periods during which at least one EV is charging. The MPFI and APFI are important for understanding the ability of the charging cluster to make short-term power adjustments under peak demand conditions and average operating conditions, respectively. A significant difference between the MPFI and APFI indicates a highly variable utilisation rate throughout the day.

Lastly, in the time domain, the TFI is defined as:

$$TFI = \frac{t_{idle,avg}}{t_{tot,avg}}. \tag{2.4}$$

While $t_{idle,avg}$ represents the average idle time of the EVs connected to the charging cluster when fully charged, $t_{tot,avg}$ depicts the average total connection time of the EVs. The TFI estimates how much the charging sessions can be shifted in time without influencing the charging fulfilment.

For defining the HEF, we use two other boundaries, which correspond to the aggregated demand resulting from two charging strategies with opposite objectives: one, $P_{max}$ *Strategy*, which charges EVs as quickly as possible, and the second, $P_{min}$ *Strategy*, which delays the charging time as much as the connection time allows. It is important to emphasize that the two strategies depend on the specific charging technology and the EVs utilised; therefore, the strategies designed in this study should be replaced with those tailored to the characteristics of the analysed cluster. In our study, $P_{max}$ *Strategy* maximises the aggregated power consumption within the limit of the connection capacity; such strategy corresponds to the most common commercialized strategy [16], [17], [60]. On the other hand, we designed the $P_{min}$ *Strategy* to dispatch a constant power value for each EV, corresponding to the power needed to reach the energy requested within the EV connection time. By comparing the energy accumulated over time between these two strategies, we can quantify the hourly flexibility, which represents the amount of energy that can be deferred each hour without compromising charging fulfilment. The HEF is defined as:

$$HEF = \Delta E = \int_{t}^{t+1} \Delta P(t) dt, \tag{2.5}$$

where $t$ and $t+1$ denote the interval between the beginning and the end of each hour of the day, and $\Delta P(t)$ is the difference in power consumption between the charging strategies at time $t$. Understanding the profile of HEF is crucial for identifying when and how much energy flexibility is available.

## 2.3 Computational framework for method demonstration

### 2.3.1 Description of the model

The method for quantifying the fexibility of EV clusters is demonstrated through a simplified model of a hospital charging cluster located in Copenhagen, Denmark, using real charging session data provided by the CPO Spirii for the year 2022. The inputs given to the model are user behaviour data from the charging sessions, consisting of connection and disconnection times and energy demand. The model is tailored to the electrical layout of the existing cluster, having in the base case scenario ten chargers with a power capacity of 22 kW and a connection capacity of 82 kW. Using these inputs, the model calculates the aggregated demand of the $P_{max}$ *Strategy* and the $P_{min}$ *Strategy*. In both cases, the outputs are the end-time of each charging session, the idle time for each EV, total power consumption and the total energy charged for the entire charging cluster. These outputs are then processed to calculate the flexibility index scores and the HEF. A simplified flowchart of the model is illustrated in Fig. 2.1. More details on the model used for the simulation can be found in **Paper** [**P2**].

### 2.3.2 Assumptions of the model

During the design of the simulation model to demonstrate the flexibility quantification method, several assumptions were made to simplify the analysis and address the lack of more detailed EV charging data. It is important to note that this study aims to demonstrate the flexibility quantification method and its practical application rather than provide an exhaustive analysis of the charging cluster in question. Larger datasets and more realistic models are recommended for a more comprehensive performance evaluation. Specifically, larger datasets may improve result accuracy, reveal additional patterns, and reduce the risk of biased outcomes due to the limited statistical sample size.

The first concerns the creation of user inputs: Since the original cluster lacked smart charging capabilities, it did not request any user inputs. Instead, the study

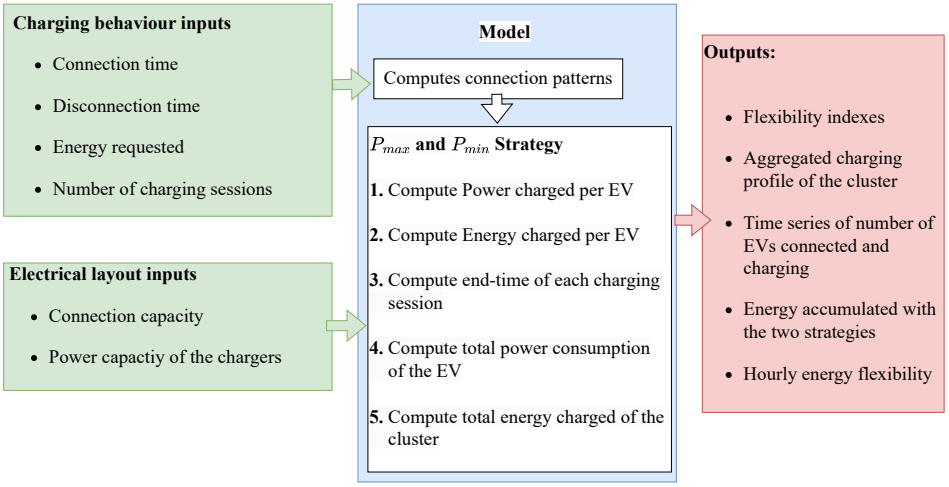


**Figure 2.1:** Flowchart of the model, illustrating the inputs (in green), the intermediate calculations of the model (in blue), and the outputs (in red).

used data from charger meters, which recorded the arrival time, departure time, and total energy charged during each session. This data is repurposed as user inputs. This assumption is considered a necessary part of the methodology since the analysis needs to be done on past data from clusters, and the metering data gives the most accurate description of user behaviour.

Another assumption is that the onboard chargers of the EVs have maximum efficiency regardless of the extent of power modulation. However, existing literature shows that power modulation reduces the charging efficiency of the EVs, increasing energy losses and slowing down the charging process [61]. This assumption would likely impact the $P_{min}$ Strategy, possibly increasing the energy needed for charging fulfilment. Nonetheless, for the scope of the analysis, the influence on the results is considered acceptable and does not influence the overall reliability of the evaluation method.

Additionally, the study assumed that all EVs had constant and equal charging power, regardless of their state-of-charge (SOC) or model, despite real-world variations. This simplification was necessary due to the lack of specific data, although accounting for these variations could improve the accuracy of the model. While this level of approximation is considered acceptable for the current analysis, incorporating second-based metering data of power consumption from the charger

meters would be an ideal solution.

## 2.4 Results of the demonstration

This section presents the results of applying the proposed flexibility criteria to the modelled EV cluster. Subsection 2.4.1 evaluates the flexibility potential of the EV cluster under original conditions. This analysis draws conclusions regarding the optimal dimensioning of its electrical layout and proposes a suitable charging strategy. Finally, the method is deployed with a sensitivity analysis to offer insight into the flexibility potential of the cluster under varying conditions. Specifically, the study examines the effects of connection capacity in Subsection 2.4.2, EV battery capacity in Subsection 2.4.3, charger capacity in Subsection 2.4.4, and the number of charging events in Subsection 2.4.5.

### 2.4.1 The flexibility potential of the cluster

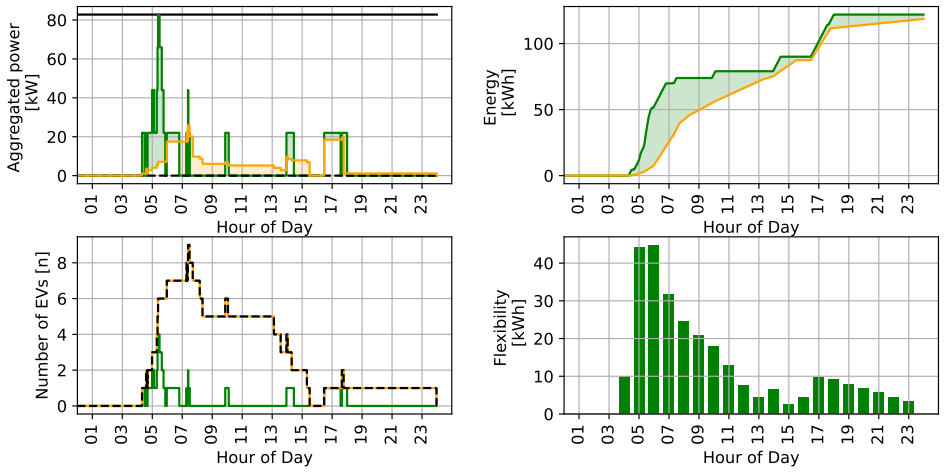


**Figure 2.2:** Analysis of the flexibility potential of the EV charging cluster on August 31, 2022, using two different charging strategies: $P_{max}$ *Strategy* (in green) and $P_{min}$ *Strategy* (in yellow). The figure includes the aggregated power time series in the top-left, the number of EVs connected (black dotted line) and charging (green and yellow line) in the bottom-left, the accumulated energy demand in the top-right, and the HEF in the bottom-right.

The evaluation of the cluster using original input data from August 31, 2022, reveals that the cluster has significant flexibility potential. The flexibility indexes show that the cluster experiences high demand during peak hours, indicated by a low MPFI of 0 (no flexibility during peak times). However, the APFI of 0.67 highlights considerable power flexibility during the rest of the day. Additionally, the high EFI of 0.88 and TFI of 0.91 suggest substantial potential for delaying energy consumption. Overall, the cluster appears to be largely over-dimensioned for current usage, suggesting excessive CAPEX. However, as EV adoption increases, this capacity may become more appropriate. In the short term, operational savings could be achieved by implementing smart charging strategies for BTM or FTM services according to local resources.

Fig. 2.2 displays the results of the quantitative analysis using the $P_{max}$ *Strategy* (in green) and the $P_{min}$ *Strategy* (in yellow). The figure showcases the time-histories of the aggregated power, the number of EVs charging (green and yellow lines) and connected (black dotted line), the total accumulated energy, and the HEF. The analysis shows two peak utilisation periods for the cluster, with the main peak occurring at 5:30 and a minor one at 17:00, corresponding to working shifts of the hospital personnel. While both strategies charge the same total energy (124 kWh), the $P_{min}$ *Strategy* significantly flattens the aggregated power curve, reducing the peak consumption from 82 kW to 25 kW and shifting the morning peak demand to 7:30 instead of 5:30. Additionally, the HEF is directly proportional to the amount of EVs charging, with flexibility peaks of 45 kWh at 6:00 and 10 kWh at 17:00. These findings highlight the significant impact of user behaviour, influenced by the type and location of the cluster, on both the timing and the amount of flexibility that can be harnessed.

### 2.4.2 Impact of connection capacity

The first sensitivity analysis explores how different grid connection capacities affect the flexibility of the EV cluster. The connection capacities tested are 30%, 50%, and 80% of the original 82 kW capacity. The results reveal that reducing the connection capacity decreases scores in all flexibility indexes. However, the most affected indexes are the power indexes, while the EFI shows less variation and the TFI shows only marginal variation. Fig. 2.3 displays the flexibility index scores and HEF for each scenario, while Table 2.2 summarises the results.

The HEF also decreases with decreasing connection capacity, with its major peak ranging from 37 kWh to 31 kWh and its average from roughly 11.5 kWh to 11 kWh. In the $P_{max}$ *Strategy* scenario with the lowest connection capacity, the HEF further indicates a degradation of the energy fulfilment. Specifically, at least

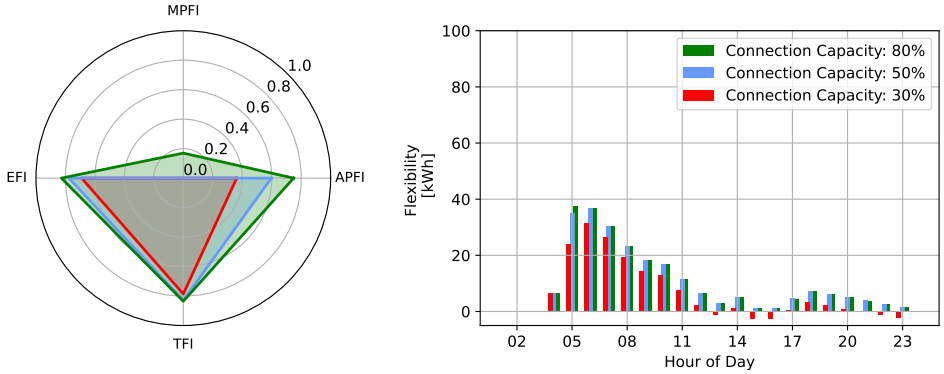


**Figure 2.3:** Impact of the grid connection capacity on the charging cluster performance. The colours green, blue, and red represent scenarios in which the connection capacity is 80%, 50%, and 30% of the original grid connection (82 kW), respectively. On the left, flexibility indexes are evaluated, while the HEF is depicted on the right.

**Table 2.2:** Flexibility criteria results for various connection capacities. The connection capacity, expressed as a percentage, is based on the original grid connection of 82 kW.

| **Grid connection capacity** [%] | **30** | **50** | **80** |
|---|---|---|---|
| MPFI | 0.00 | 0.00 | 0.17 |
| APFI | 0.36 | 0.60 | 0.75 |
| EFI | 0.69 | 0.78 | 0.83 |
| TFI | 0.79 | 0.83 | 0.84 |
| Maximum HEF [kWh] | 31.37 | 36.83 | 37.45 |
| Average HEF [kWh] | 10.95 | 11.40 | 11.51 |

one EVs disconnects without being fully charged, highlighting the need for scheduling strategies in connection with limited connection capacities. This result is not evident from analysing the TFI alone, which instead shows an average idle time of all EVs being 79%. However, since the idle time can vary significantly between individual EVs, a single value does not accurately represent all cases. In future work, we plan to modify the TFI to better reflect the time flexibility of EVs with the lowest idle time.

Overall, this sensitivity analysis shows that reducing the connection capacity diminishes the ability of the cluster to provide power-based flexibility, while having

only a marginal impact on energy-based and time-based flexibility. This reduction limits the potential for effective energy management throughout the day. A significant challenge arises when the connection capacity is constrained too much, as it hinders the ability to meet demand during peak utilization periods. This issue can be mitigated by implementing priority-based charging schedules, ensuring that charging sessions are efficiently managed even during times of high demand.

### 2.4.3 Impact of battery capacity

The second sensitivity analysis evaluates how varying battery capacities affect the flexibility potential of the cluster. Three scenarios were analyzed: the original battery capacity, and increases of 15 kWh and 30 kWh for all EVs in the cluster. Fig. 2.3 displays the flexibility index scores and HEF for each scenario, while Table 2.2 summarises the results.

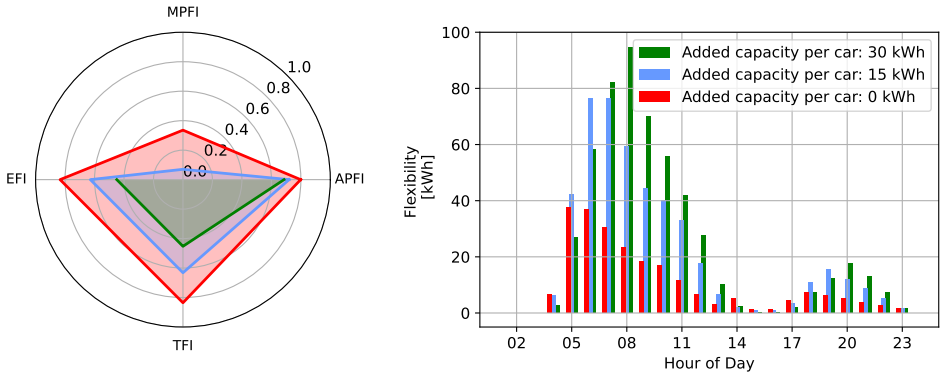


**Figure 2.4:** Impact of the battery size on the charging cluster performance. The colours green, blue, and red represent scenarios with an additional battery capacity of 30, 15, and the base case. The flexibility indexes are assessed on the left, whereas the HEF is assessed on the right.

The results reveal that increasing the battery capacity decreases scores in all flexibility indexes. The analysis shows that as battery capacities increase, the EFI and TFI decrease significantly, with the EFI dropping from 0.83 to 0.45 and the TFI from 0.84 to 0.45 as battery size increases. This decline is attributed to the higher energy demand from larger batteries, which limits the idle time of EVs and the overall capability to delay charging. On the other hand, the MPFI shows lower variation, and the APFI only has marginal variation, indicating that although the

**Table 2.3:** Flexibility criteria results for various battery capacities. The table shows the additional capacity beyond the initial energy capacity, which is assumed to be equal to the energy requests of the EVs.

| **Additional battery capacity [kWh]** | **0** | **15** | **30** |
|---|---|---|---|
| MPFI | 0.34 | 0.07 | 0.00 |
| APFI | 0.80 | 0.72 | 0.69 |
| EFI | 0.83 | 0.63 | 0.45 |
| TFI | 0.84 | 0.63 | 0.45 |
| Maximum HEF [kWh] | 37.4 | 76.5 | 94.5 |
| Average HEF [kWh] | 11.5 | 23.1 | 26.7 |

aggregated power consumption has a higher peak, it is not significantly affected overall. Fig. 2.3 displays the flexibility indexes scores and HEF for each scenario, while Table 2.2 summarises the results.

One key finding is that, although the EFI and TFI decrease for higher battery capacities, the HEF shows a substantial increase, with its peak in HEF ranging from 37.4 kWh to 94.5 kWh, and it average from 11.5 kWh to 26.7 kWh. The reason lies in the definition of the qualitative and quantitative criteria: indeed, although the amount of energy that can be delayed in time increases due to increased storage capacity (measured by the HEF), the cluster has less capacity to delay it due to longer due to reduction in idle time. These results highlight the complementarity between the qualitative and quantitative flexibility criteria developed in this study. Another important finding from the HEF is that as battery capacities increase, the peaks of HEF shift to later times. For example, the major HEF peak shifts from 5:00 in the base scenario to 8:00 in the scenario with the largest battery capacity.

Overall, this sensitivity analysis shows that, in the absence of a charging strategy, increasing battery capacities reduces the idle times of individual EVs and increases overall the urgency of meeting energy demands, limiting the ability of the cluster to delay energy demand for long periods. However, implementing a smart charging strategy that incorporates charging prioritization enhances the potential to defer energy consumption on an hourly basis. The cluster can still provide energy flexibility over longer durations by alternating charging sessions.

### 2.4.4 Impact of charging power

The third analysis examines how different charging power capacities——6 kW, 11 kW, and 22 kW——affect the flexibility potential of the cluster. Fig. 2.5 and Table 2.4 summarise the analysis results. The results show that increasing charging

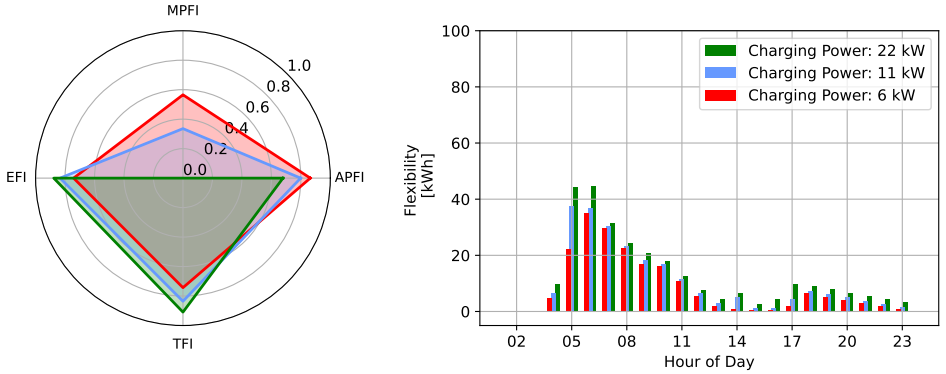


**Figure 2.5:** Impact of the charging power on the charging cluster performance. The colours green, blue, and red represent scenarios where the charging power is set to 22 kW, 11 kW, and 6 kW, respectively. Flexibility indexes are evaluated on the left, while HEF is depicted on the right.

**Table 2.4:** Flexibility criteria results for different charging power capabilities.

| **Charging power [kW]** | **6** | **11** | **22** |
|---|---|---|---|
| MPFI | 0.57 | 0.34 | 0.00 |
| APFI | 0.86 | 0.80 | 0.68 |
| EFI | 0.74 | 0.83 | 0.88 |
| TFI | 0.74 | 0.84 | 0.91 |
| Maximum HEF [kWh] | 35.2 | 37.5 | 44.7 |
| Average HEF [kWh] | 9.6 | 11.5 | 14.0 |

power reduces power-based indexes, particularly the MPFI, which falls to zero in the highest power scenario. However, the EFI and TFI improve with greater charging power, showing inverse proportionality with the power-based indexes. This result indicates that, although faster charging decreases the capability for power-based flexibility services due to more volatile power consumption, it facilitates the energy-based flexibility services due to more room for scheduling energy consumption in time. The HEF also indicates an overall increase in energy flexibility, with its maximum peak ranging from 35 kWh to 45 kWh. Faster chargers shift these HEF peaks to earlier times, with both peaks moving one hour earlier. Overall, this sensitivity analysis demonstrates that increasing the charging power capacities is an effective solution to reducing the charging time of EVs. This approach enhances

the capability to delay shorter charging sessions, thereby improving the capacity of the cluster to provide energy-based and time-based flexibility services when paired with a tailored smart charging strategy.

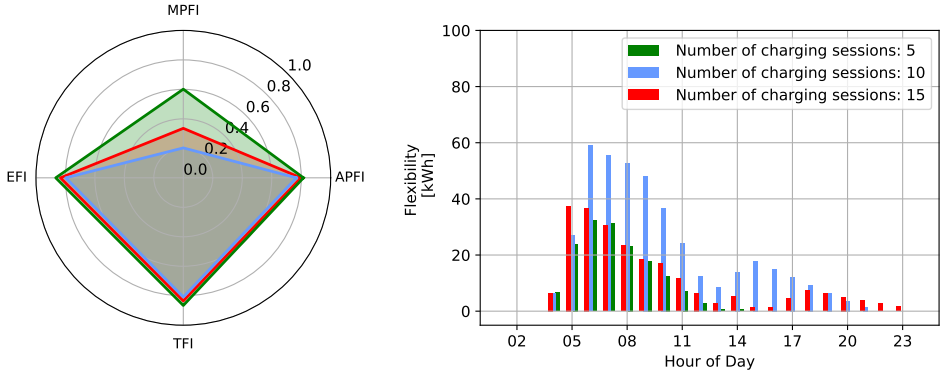


**Figure 2.6:** Impact of the number of charging sessions on the charging cluster performance. The colours green, blue, and red represent scenarios where 5, 10, and 15 charging sessions are considered, respectively. On the left, flexibility indexes are evaluated, while the HEF is shown on the right.

**Table 2.5:** Flexibility criteria results for different numbers of charging sessions. The analysis is based on simulations from different days, each varying in the total number of recorded charging events.

| **Number of charging events** | **5** | **10** | **15** |
|---|---|---|---|
| MPFI | 0.34 | 0.20 | 0.60 |
| APFI | 0.80 | 0.77 | 0.82 |
| EFI | 0.83 | 0.80 | 0.87 |
| TFI | 0.84 | 0.81 | 0.87 |
| Maximum HEF [kWh] | 37.5 | 58.9 | 32.2 |
| Average HEF [kWh] | 11.5 | 22.8 | 14.4 |

## 2.4.5 Impact of number of charging events

The final sensitivity analysis focuses on the impact of the number of daily charging sessions on flexibility potential. As described in Fig. 2.6 and Table 2.5, three

scenarios were tested: five charging sessions, ten sessions, and fifteen sessions. Interestingly, the number of charging events does not appear to be the primary factor influencing flexibility. Instead, the total energy requested by the EVs and their connection patterns have a more significant impact. For example, the intermediate scenario records the lowest flexibility index values, despite having fewer sessions than the third scenario. This discrepancy is explained by the higher total energy demand in the intermediate scenario, which resulted in lower flexibility scores. The HEF further confirms the major influence of the energy demand. This suggests that flexibility potential is more closely related to the total energy requested by EVs and the timing of their connection rather than the sheer number of charging events. Overall, this sensitivity analysis suggests that the number of charging sessions alone does not significantly influence the flexibility potential of the cluster. Instead, the energy requests and the connection patterns play a crucial role in the amount, timing and duration of flexibility.

## 2.5 Summary

This section provides a summary of the findings provided from the studies in **Paper** [**P1**] and **Paper** [**P2**].

Regarding the study in **Paper** [**P1**], the key findings consist of recommendations for an action plan for overcoming the technological, economic and regulatory barriers found in the literature. The action plan on these three domains is summarised in table 2.6: From a technical point of view, a recurrent theme is the effort to standardise smart charging technologies and ensure interoperability among their related devices (EVs, EVSEs and smart meters). On the economic front, we highlight the need to take action towards a clear definition of the economic framework for providing flexibility services. This action would empower investors in smart EV infrastructures. The regulatory framework should redefine the roles of the GOs and their responsibilities and interactions and incentivise standardisation of flexibility markets framework and smart charging technologies.

Regarding the design of the flexibility quantification tool, the findings from **Paper** [**P2**] suggest that the presented analytical framework is a promising, comprehensive and user-friendly tool to analyse the flexibility potential of an EV cluster for BTM and FTM flexibility services. Given a model of a cluster and large historical data from the chargers, it is possible to deploy the flexibility indexes to gain insight into the average idle time of the EVs, the peak and average power consumption of the cluster in relation to its connection capacity, and the rate of energy charged against the potential that the cluster could provide. Furthermore, the quantitative analysis, consisting of the HEF, proved to be complementary to

**Table 2.6:** Future steps needed to push the development of robust EV infrastructures for distribution grid services in each of the fields analysed

| **Technical** | **Economic framework** | **Regulatory framework** |
|---|---|---|
| Further R&D on smart charging capabilities. | Keep or introduce temporary incentives for cars, shared mobility and Mobility-as-a-service | Enhance active management requirement to DSOs |
| Standardise and ensure interoperability between different EVs and EVSE. | Research on business models for aggregators and charge point operators | Standardize cost-benefit analysis for smart meters |
| Develop and test ICT and standards (especially V2G) | Develop and test new Network tariff structures | Ensure a clear classification and standardisation of V2G connection requirements for V2G prosumers |
| User interactivity and interconnectivity | Strategical location for different types of chargers to ensure trust in EV infrastructure investors | Create incentives for smart chargers purchase |
| Continue the demonstration project campaigns to gather data. | Establish local flexibility platforms with increasingly competitive approaches. | Define DSO-TSO priorities and the interaction between every stakeholder |
| Increase grid observability | Continuous revision and improvement of economic framework of flexibility based on the lessons learned | Set ambitious targets ($CO_2$ reduction, targets for different transport types) |

the qualitative analysis of the cluster to provide the timing and quantity of energy that can be delayed to later hours, as well as unfulfilled charging demand. While performing the sensitivity analysis, one improvement proved necessary regarding the TFI: in detail, showing a single value for indicating the average idle time is not comprehensive of the large variability that can occur in the idle time of different EVs. Future studies will consider modifying the TFI to include the idle time of all the EVs.

The application of the method to the simulated hospital cluster revealed several important insights. The base case simulation showed that the EV cluster is significantly over-dimensioned in relation to the user behaviour recorded in 2022. As a result, the cluster is well-suited for a wide range of flexibility services, BTM and FTM, as indicated by the high score across all the flexibility indexes. The sensitivity analysis further revealed that user energy requests and connection patterns are the most critical factors to consider when dimensioning an EV cluster and selecting the appropriate strategy. These factors were identified as the strongest predictors of flexibility amount and timing, respectively. For example, the cluster could provide flexibility primarily at the beginning of personnel work shifts, with reduced potential during the rest of the day due to the absence of new connections. Regarding connection capacity, the findings suggest that clusters with undersized connection capacities and no priority-based scheduling strategies risk

decreasing user satisfaction, particularly as EV adoption increases. Additionally, increasing the power capacity of chargers can enhance the ability of the cluster to distribute energy consumption more effectively over time through smart charging strategies. Lastly, the sensitivity analysis on daily connection capacity suggested that the number of EVs alone does not significantly impact flexibility potential. The sensitivity analysis confirmed the higher influence of connection patterns and energy requests.

CHAPTER 3

# The concept of autonomous chargers

This chapter focuses on the description of the novel distributed architecture and the concept of autonomous smart chargers developed during the Autonomously Controlled Distributed Chargers (ACDC) project. Section 3.1 provides an overview of the existing control architectures for electric vehicle supply equipment (EVSE) and introduces the motivation for research in new architecture strategy. Section 3.2 introduces, in general terms, the control and communication structure of the architecture. Section 3.3 describes the design of the first version of the control architecture and the model deployed for the computational analysis. Section 3.4 introduces the improved version of the architecture currently deployed at the workplace EV cluster in Risø campus.

## 3.1 Background

Current research in smart EV charging primarily focuses on developing strategies to optimise charging schedules, integrate renewable energy sources (RES), and adapt to grid conditions, balancing user convenience and grid stability. The literature offers various approaches for implementing smart charging, such as data-driven and predictive models, decentralised frameworks, optimisation techniques, and fuzzy logic-based scheduling algorithms.

However, much of the research remains theoretical and simulation-based, with limited emphasis on practical implementation within EV clusters. For example, the study in [62] uses predictive models for heterogeneous EV fleets, while Nour

et al. [63] propose an algorithm aligning EV charging with fluctuating electricity prices. Decentralised approaches are explored by [64] and [65], focusing on load distribution and real-time grid management, respectively. Reinforcement learning for fleet optimisation is investigated in [66], and utility-maximising algorithms based on urban mobility are proposed in [67]. Additionally, Hussain et al. [68] analyse flexibility in smart grids, and Khalkhali and Hosseinian [69] propose a multi-class charging strategy to improve grid flexibility in residential parking lots.

While these studies enrich the theoretical framework of smart charging, they do not focus on real-world implementation. Some studies offer solutions suitable for practical application, such as the integration of renewable energy in EV clusters [70], fuzzy logic scheduling for dynamic charging [71], and cloud-based smart charging systems [72]. Others investigate grid balancing and peer-to-peer coordination mechanisms for charging stations [73], [74].

Despite these contributions, the majority of smart charging strategies lack experimental validation, as most research relies on simulations. Experimental work in this field is still limited, with only a few studies bridging the gap between simulation and practice. Examples include experimental validations of fleet management algorithms [75] and frequency regulation [76], [77].

Ultimately, developing effective smart charging strategies requires coupling theoretical models with experimental validation to gather empirical evidence and address the real-world challenges posed by EV behaviour. Such a combination is crucial for assessing the performance and reliability of these strategies, as simulations alone cannot fully capture the complexities of EV controllability and operation.

### 3.1.1 Existing control architectures for EV clusters

Control architectures for EV charging infrastructure can generally be categorised into three types: centralised, decentralised, and distributed [78]. Centralised control has been the most common in smart charging applications due to its simplicity and technological maturity. This system relies on a single central control unit that collects data from the grid and remotely manages power demands for each device. While centralised control offers operational transparency, it faces significant challenges with scalability, vulnerability to cyber-attacks, and privacy concerns [79]. A crucial scalability limitation lies in the need for increasingly powerful server infrastructures to manage both the computational requirements and the large volumes of data generated by individual EV chargers. Furthermore, the costs of leading cloud computing platforms increase exponentially with the volume of data processed and the computational power required by the deployed machines [80], [81].

Decentralised control architectures, on the other hand, are frequently used in

stand-alone charging infrastructures. In these systems, local control units operate independently, relying solely on local measurements and actuators to achieve their control objectives. While decentralised control brings benefits like enhanced scalability, robustness, and simplified communication with users, it lacks the global coordination needed for optimal overall performance [82]–[84]. As a consequence, the controlling capabilities of the architecture remain limited.

Distributed control architectures combine elements of both centralised and decentralised systems. This approach involves a central controller, typically hosted on a cloud server and local controllers on each controlled device. The central controller manages the charging clusters globally by processing grid information and sending set-points to the local controllers. The local controllers provide another control layer, distributing new set-points among devices using local communication. This hybrid approach leverages the advantages of centralized systems (e.g., precision) and decentralised systems (e.g., scalability and robustness) to provide a more comprehensive control solution [85], [86]. In terms of scalability, distributed control reduces communication nodes and lowers the required frequency of communication. Even if communication with the central controller is disrupted or a charger malfunctions, the system remains operational, and the local controllers maintain local smart charging functionalities, further enhancing its resilience. At last, the local communication between controllers is potentially faster and more reliable, further improving the reliability of the system [87].

The advantages and limitations of centralised, decentralised, and distributed control approaches are further analysed in [86]. Table 3.1 consolidates the findings on the pros and cons of each control method, based on several studies [84], [88], [89].

## 3.2 The general concept of the architecture

Fig. 3.1 presents the global communication architecture for a generic node in the distribution grid supplied by a transformer. The global controller, called cloud aggregator (CA), operates from a cloud server equipped with computational power for data processing and communication and memory for storage. For simplicity, the figure focuses on a single node containing two EV clusters, though in reality, the CA can manage multiple clusters across various nodes. The flowchart details the communication pathways and the devices involved. Each transformer feeds different EV clusters, which can also incorporate power consumption from the buildings and power generation from distributed energy resources (DERs), connected to the same point of chargers connection (PCC).

**Table 3.1:** Advantages and drawbacks of chargers control approaches.

| Control approach | Advantages | Drawbacks |
|---|---|---|
| **Centralized** | Mature architecture.<br>System wide observation.<br>Easier implementations of optimization algorithms. | Vulnerable to cloud aggregator malfunction being spread on all chargers.<br>Need of a backup server system.<br>Heavy communication and computation when scaled-up.<br>Subject to cyber-attacks and possible data privacy violation. |
| **Decentralized** | Diverts data privacy challenges.<br>Low communications and computation capabilities when scaled-up.<br>Low sensitivity to errors and cyber-attacks, thus high system robustness.<br>High deployment scalability.<br>Low communication delays. | Lack of grid observability.<br>Immature control architecture.<br>Risk of avalanche effects.<br>Difficult to reach optimal solutions from optimization algorithms. |
| **Distributed** | High scalability and autonomy.<br>System wide observation.<br>Low sensitivity to errors, thus high system robustness.<br>Diverts data privacy challenges.<br>Possibility of plug and play protocols.<br>Low communication delays. | Novel control architecture, thus not mature.<br>Prone to cyber-attacks.<br>High complexity on charger design. |

The CA is monitored and controlled by the aggregator to provide services in flexibility markets or to comply with agreements with transmission system operators (TSOs) and distribution system operators (DSOs). Based on the flexibility service bid by the aggregator, the CA processes inputs from various smart meters that monitor factors like RES power production and transformers loading to regulate the power consumption of each EV cluster. Additionally, the CA provides real-time information to users via a mobile app, including charger availability and energy prices. Upon arriving at the EV cluster, users can input their charging preferences, enabling the system to coordinate the charging sessions effectively.

The final output of the CA for each EV cluster consists of power set-points, which are sent to the local controllers of each cluster, called virtual aggregator (VA), alongside user requests. The VA is the autonomous intelligence embedded within each charger, managing power consumption in alignment with the set-points from the CA, measurements from the PCC and user inputs. User input is essential for the VA to prioritise charging sessions and allocate power accordingly. In the final step of the control loop, the VAs coordinate the power consumption of chargers based on user priorities to align with the set-points provided by the CA. This coordination is achieved through several smart charging functionalities: power-sharing, power-scheduling, prioritisation, and an anti-overshooting function.

The power-sharing functionality is a commercially available feature that mod-

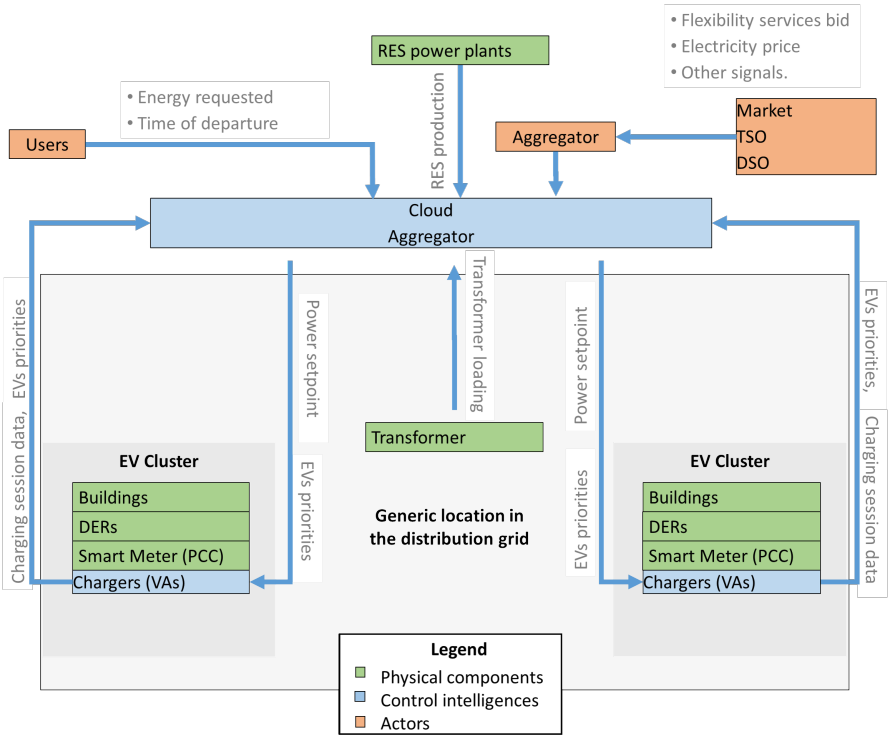


**Figure 3.1:** Global system architecture and communication paths between different actors.

ulates power consumption across charging sessions to prevent exceeding the power reference or connection capacity assigned to the cluster. The power-scheduling functionality, which is not yet commercially available, involves pausing and resuming EV charging sessions according to strategic patterns to avoid overshooting power limits. Prioritisation tailors both power-sharing and power-scheduling to the charging urgency set by users, ensuring that sessions are managed according to their priority. The anti-overshooting functionality temporarily reduces the power consumption of the charging EVs when a new session starts to create a power window, allowing the EV to reach its target power set-point without exceeding the connection capacity or power reference of the cluster. These functionalities work together to ensure optimal and safe coordination of charging sessions within the cluster. Additionally, the VAs and the PCC send feedback data back to the CA to

complete the loop, ensuring continuous monitoring and adjustment of the system.

Thanks to the collaboration of DTU with the companies Nissan and Circle Consult, the architecture has been refined and enhanced throughout the ACDC project. Although the core concept of the project remained unchanged, minor adjustments were made to the control and communication structure between the CA and the VAs and to the electrical layout of the chargers. This section details the two primary versions of the architecture developed throughout the project.

## 3.3 Version 1 of the architecture

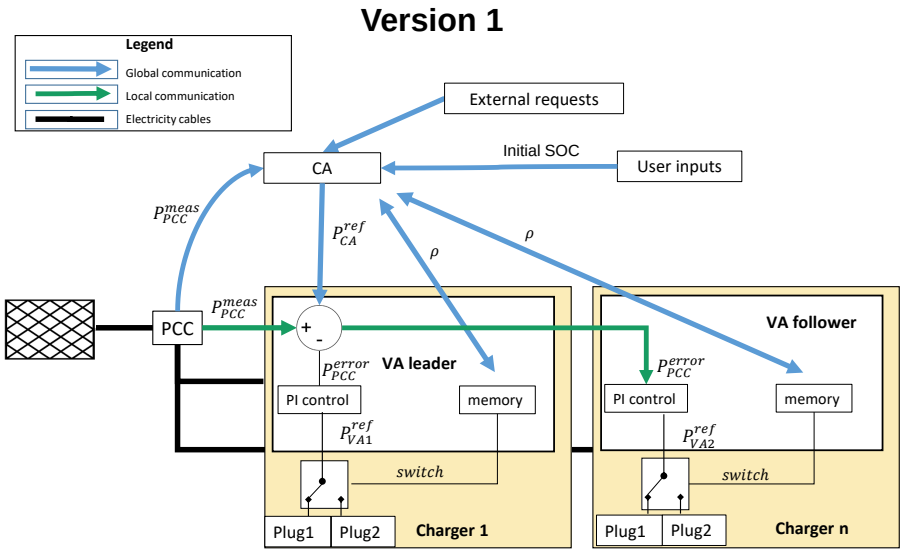


**Figure 3.2:** Flowchart illustrating the design of Version 1, focusing on the local communication and the layout of the chargers

Fig. 3.2 illustrates the detailed layout of the control architecture, focusing on the communication and electrical design of the chargers. Version 1 builds up from the study in Paper [P9], which lays the ground for the control architecture. The architecture is developed in a computational environment and tested with the test cases described in Chapter 4.

In Version 1, the CA receives the aggregated power measurement from the PCC of the cluster ($P_{PCC}^{meas}$). This allows the CA to monitor the power consumption of

each cluster and coordinate their operation by assigning different power set-points ($P_{CA}^{ref}$). Specifically, if a cluster is unable to meet its assigned power set-point due to insufficient connected EVs or an overloaded transformer, other clusters with sufficient EVs can increase their consumption to compensate. Additionally, the CA is responsible for receiving user inputs and relaying them to the VAs, enabling each VA to calculate its priority relative to others.

For the local control, the architecture employs two types of VAs in each cluster: a $VA_{leader}$ for one charger and a $VA_{follower}$ for each additional charger. The $VA_{leader}$ receives $P_{CA}^{ref}$ and $P_{PCC}^{meas}$, calculates the error $P_{PCC}^{error}$, and then transmits the $P_{PCC}^{error}$ to all the $VA_{follower}$ via cable or Bluetooth. Based on the received $P_{PCC}^{error}$, all VAs determine their power set-point ($P_{VA}^{ref}$) for each EV and schedule the charging sessions according to the priority ($\rho$) of the connected vehicles. The local communication setup ensures that smart charging functions like power-sharing and power-scheduling remain operational even if there are connectivity issues with the CA.

The chargers are limited to activating one plug at a time. Each plug can deliver a maximum current of 16 A, supplying 11 kW for three-phase EVs and 3.7 kW for single-phase EVs. Each VA is responsible for scheduling the charging of the two connected EVs based on their $\rho$.

The priority system relies on two criteria for scheduling the charging sessions. The first is the SOC reported by the user at the start of the session, and the second is the amount of energy charged during the session. The priority $\rho$ is a value in the range from 0 to 1 and decreases proportionally as the SOC and charged energy increase. When two EVs on the same charger have equal $\rho$, the system activates the switch to supply power to the idle EV, with each charging window allowing for roughly 5 kWh. The VAs continuously monitor the $\rho$ of each EV, and in case of limited $P_{CA}^{ref}$, if all sessions have reached their minimum power capacity of 6 A, the charger with the lowest $\rho$ will halt its session to prioritise others.

### 3.3.1 The model - Version 1

Version 1 is simulated using Matlab Simulink, with each simulation spanning 24 hours and a time resolution of 0.1 s. The communication structure follows the layout shown in Fig. 3.2, where data transmission in the global communication layer (shown with blue arrows) has a delay of 0.5 s. In contrast, the local communication (shown with green arrows) experiences a 0.1 s delay. For a more technical description of the model the reader is referred to **Paper [P3]**.

The EV model in the simulation incorporates two key simplifications. First, the AC-DC converter efficiency decreases linearly, starting from 90% at 16 A (11

kW for three-phase EVs and 3.68 kW for single-phase EVs) to 80% at 6 A (4.15 kW for three-phase and 1.38 kW for single-phase EVs). Second, the maximum charging power of the EV remains constant throughout the entire charging session, regardless of the SOC. These simplifications are deemed necessary due to the lack of detailed behavioural data from the EVs; however, they may introduce some marginal inaccuracies in the results.

## 3.4 Version 2 of the architecture

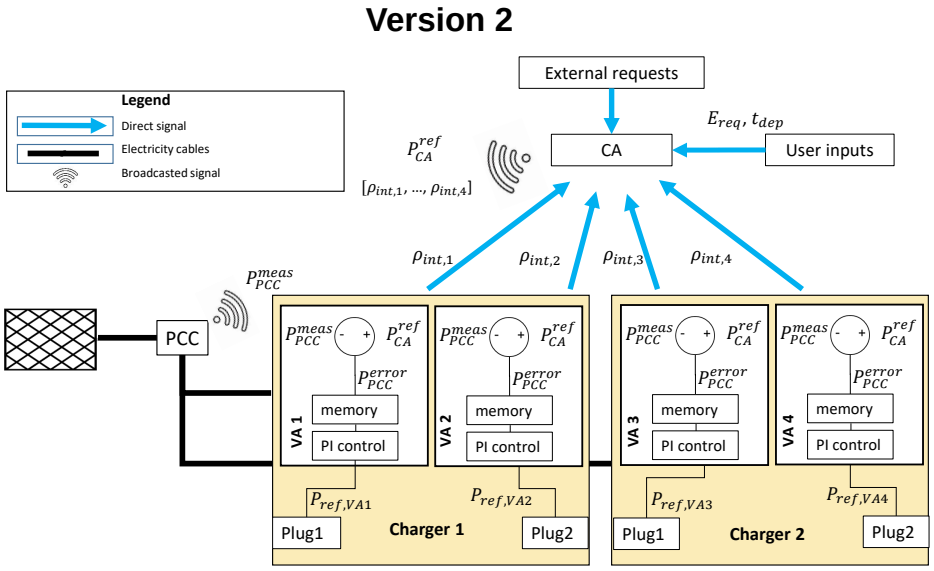


**Figure 3.3:** Flowchart illustrating the design of Version 2, focusing on the local communication and the layout of the chargers

Version 2 represents the final iteration of the architecture, improved based on the insights gained from computational analysis. This version was utilised during the experimental campaign and is now implemented at the Risø campus EV cluster. Fig. 3.3 outlines the control and communication of the architecture and the electrical layout of the chargers.

Unlike the previous version, Version 2 eliminates direct feedback of cluster consumption from the PCC $P_{PCC}^{meas}$ to the CA. Instead, the CA receives only the priority

values from each VA, which provide insights into the availability of EVs and their charging urgency. Based on external requests, the charging mode of the cluster, and the priorities of all VAs within a cluster, the CA sends each cluster $P_{CA}^{ref}$.

A key change in this version is the removal of the hierarchical VA structure (leader-follower). Instead, each VA operates independently, receiving both $P_{CA}^{ref}$ and $P_{PCC}^{meas}$. This allows each VA to calculate its power set-point $P_{VA}^{ref}$ based on the power error $P_{PCC}^{error}$ and priority.

The chargers in this version are capable of charging two EVs simultaneously, with each plug providing a maximum current of 32 A, equivalent to 22 kW for three-phase EVs and 7.4 kW for single-phase EVs. However, the total current capacity of the charger remains 32 A, which limits the power per plug when both plugs are active.

To determine the priority, users input their energy request $E_{req}$ and departure time $t_{dep}$. Two values are used to calculate priority: the internal priority $\rho_{int}$ and the relative priority $\rho_r$. $\rho_{int}$ is shared among the chargers through the CA, providing the VAs with a scheduling order for the EVs. It ranges from 0 to 0.99 and is used to signal the charging state of the plug (e.g., starting the charge, idle, charging, no EV connected, or errors). $\rho_r$ is calculated by each VA using the $\rho_{int}$ from all the VAs. It is not shared among the VAs and serves as a control parameter for the PI controller within each individual VA. The reader is referred to **Paper [P6]** for a more comprehensive description of the priority system, including its mathematical formulation.

### 3.4.1 Implementation of the architecture - Version 2

This subsection details the architecture implementation as explained in Fig. 3.4, including the hardware and software utilised.

The VAs and the CA are hosted on "Beaglebone® black industrial" microcontrollers, which are equipped with an ARM Cortex-A8 1 GHz processor, 521 MB of RAM and 4GB of embedded flash memory. The microcontrollers are connected via Ethernet and deploy a Debian OS operating system. The control strategy is actuated on stand microcontrollers located outside the chargers, while the chargers are only responsible for the actuation of the final set-points. The chargers are linked to the Internet through a 4G connection, while all the other devices are connected to the university WiFi network, which is secured by a firewall. A public server database (Database 1 in the figure) mediates the communication through the firewall between the chargers and the microcontrollers. This server acts as a central hub and is the intermediate node of most control-related data communication.

The charging system incorporates an Android mobile app for providing user requests and monitoring the charging sessions. A web interface on the university server (Visualization Webpage) allows to monitor in real time the status of the cluster.

The data management of the chargers is hosted on Amazon Web Services, which is responsible for the communication between the app, the chargers and the final power set-points from the VAs.

The chargers convert the received power set-points to a current set-point, which is transmitted to the actuators. The charger follows the IEC 61851-1:2019 [90] type 2 charging protocol, using a 32 A 5-wire connection. Each charger has a total three-phase power capacity of 22 kW, distributed across two plugs, which are both capable of providing up to 22 kW of three-phase power. A smart meter (DEIF Multi-instrument MIC-2 MKII) at the PCC measures and publishes on the data broker energidata.dk (Database 2), different parameters on a second basis, useful for data storage and post-processing. All the data from smart meters of external devices, such as transformers, RES and DEIF is handled with the framework of the Energy System Integration Lab – SYSLAB (Syslab node).

## 3.5 Summary of the development

This section summarises the differences between the two versions of the control architecture and explains their advantages and disadvantages.

In the second version of the architecture, a significant change involves removing the direct feedback of $P_{PCC}^{meas}$ of each cluster to the CA. While this feedback allows the CA to receive real-time consumption data and optimise power distribution across the clusters, it is computationally intensive due to the high-frequency data transmission required from each cluster. In the updated version, this real-time feedback has been replaced by priority updates sent from the VAs to the CA, which are necessary for the system regardless. In Version 2, the $\rho_{int}$ from each VA contains sufficient information for the CA to determine the number of connected EVs and their charging urgency. This approach reduces the need for high-frequency data transmission (previously every second) by utilising an existing data stream, which operates at a much lower frequency, such as once every five minutes. Although less optimal in terms of real-time power distribution, this solution alleviates the computational load while still providing the necessary information to manage the clusters effectively.

In Version 2, the hierarchical structure among the VAs is also eliminated. This hierarchical structure of Version 1 ensures that only one communication line for the $P_{CA}^{ref}$ is needed per cluster. However, during the prototyping of the first chargers

with this setup, local communication via cable or Bluetooth proved to be technically challenging, particularly for large EV clusters. As WiFi became the only viable communication method, Version 2 is designed so that each charger receives the $P_{CA}^{ref}$ directly, eliminating the need for VA-to-VA communication. While this change improves the technical feasibility of the system, it increases the computational burden on the cloud infrastructure.

The chargers are equipped with two type 2 plugs in both versions, but the electrical layout differs significantly. In Version 1, each charger could only activate one plug at a time and provide a maximum current of 16 A, which limits the scheduling options for EV charging. In Version 2, however, the chargers can charge two EVs simultaneously. Moreover, each plug can provide up to 32 A, although the total current for the charger remains capped at 32 A. This design change also came about during the charger prototyping process, where it was found that the 32 A solution was a standard solution in commercially available chargers. This upgrade improves overall charging efficiency and minimises reactive power consumption caused by the power modulation of the EVs.

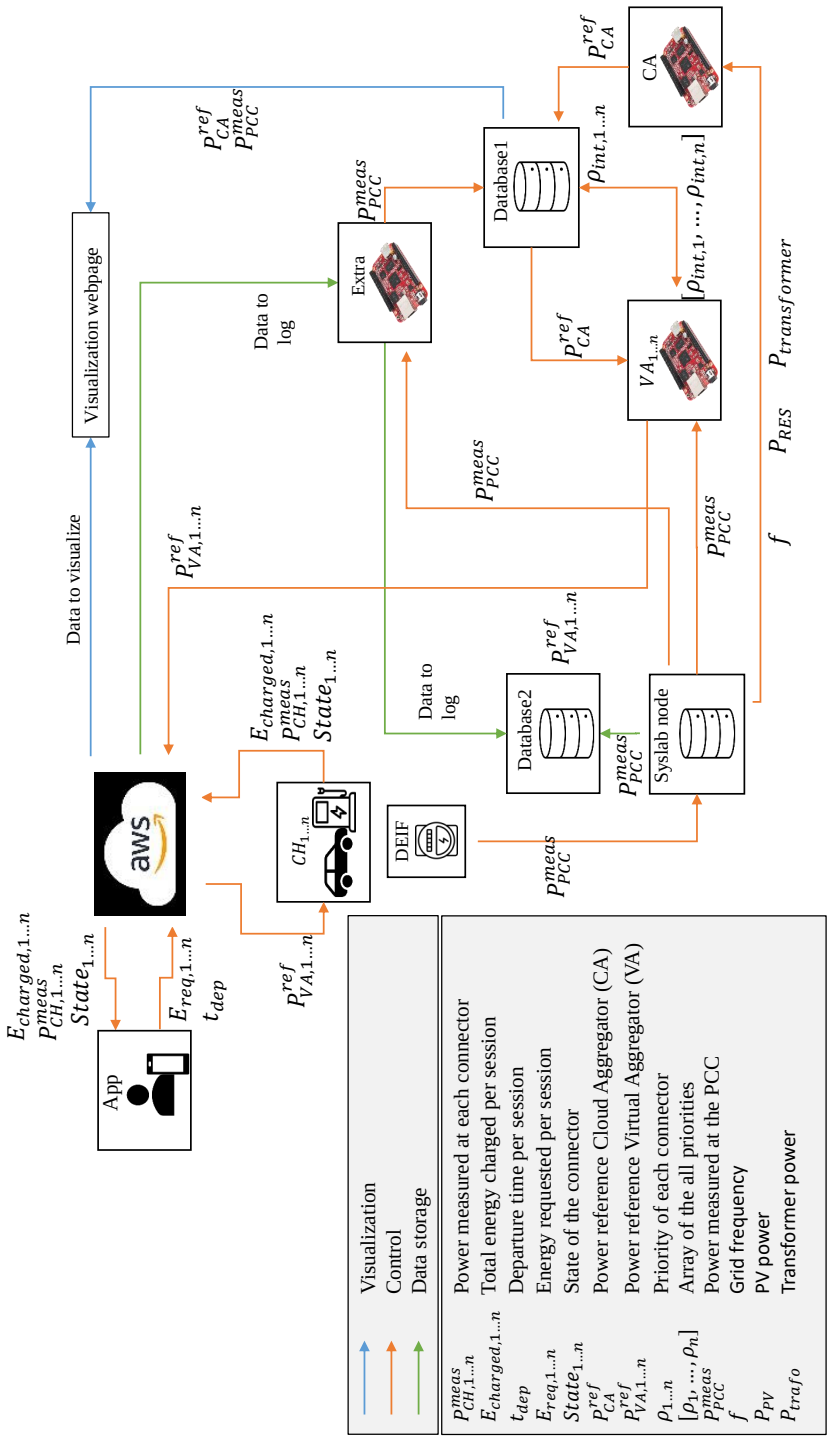


**Figure 3.4:** Overview of the implementation of the architecture, including data communication among the different nodes of the architecture

CHAPTER 4

# Computational analysis

This chapter describes the computational investigation of the distributed system capabilities, focusing initially on the functionalities of the VA within a single EV cluster in Section 4.1. It then examines the coordination of the power consumption of multiple clusters through the CA as a part of a virtual power plant (VPP) in Section 4.2. Finally, Section 4.3 provides a summary of the results and discusses the key findings that led to the version upgrade of the architecture.

## 4.1 Single EV cluster

In this test case, the technical feasibility of the system has been investigated via simulation, focusing mainly on the performance of the VA control. The model has eight chargers and represents the workplace EV cluster at the Risø research campus of the Technical University of Denmark. In the simulation, the CA does not provide any control apart from providing a PCC protection functionality, which lowers the power reference of 6 kW any time an EV starts charging to avoid overshooting the PCC limit. On the other hand, the VAs provide power-scheduling and power-sharing in the cluster according to the charging urgency set by the user inputs. The study compares an unconstrained scenario (Scenario 1), where the aggregated power of the cluster has no upper boundary and a constrained scenario (Scenario 2), where the system has a connection capacity at the point of chargers connection (PCC) of 43 kW. Although power-sharing functionalities are deployed only in the constrained scenario to prevent overloading of the PCC, both scenarios deploy power-scheduling within the chargers, as only one plug per charger can be activated at a given time.

Nissan EV telematics supplies key inputs for the simulation, such as the ar-

rival time, departure time, and initial SOC of the EVs virtually connecting to the chargers. Additionally, the simulation incorporates battery capacity based on the types of EVs commonly used at the workplace. More details on the inputs of the simulation can be found in **Paper [P1]**.

### 4.1.1 Performance overview of the cluster

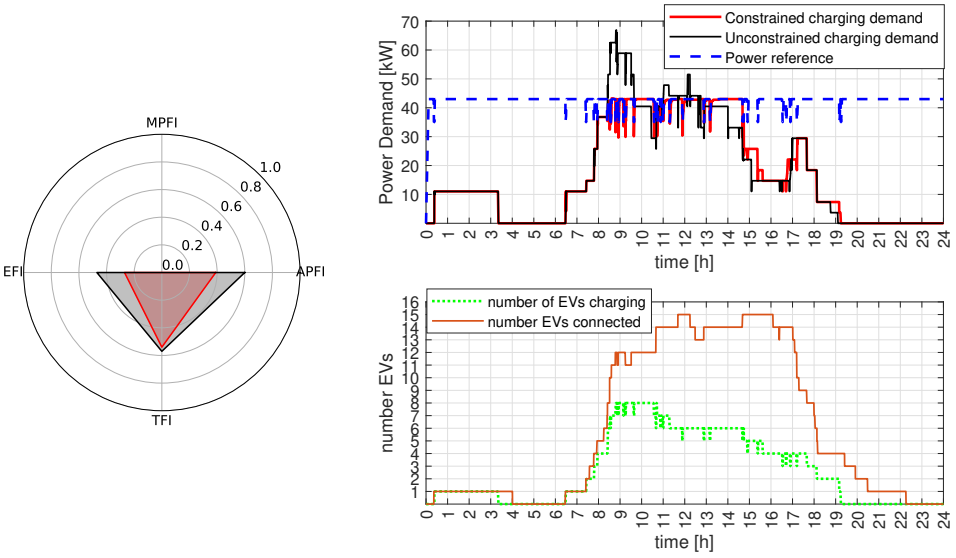


**Figure 4.1:** General performance of the simulated cluster: Score of the cluster on the flexibility indexes (left); time-history of the aggregated power consumption (top-right); and time-history number of EVs connected and charging (bottom-right).

This section provides an overview of the results of the simulation; Fig 4.1 provides an overview of the score of the system on the flexibility indexes in the two scenarios, together with the time histories of aggregated power consumption and the number of charging and connected EVs. The flexibility indexes for Scenario 1 and Scenario 2 are calculated considering a connection capacity of 66 kW and 43 kW respectively. Since the connection capacity is reached by the aggregated power consumption in both cases, the MPFI is 0. Compared with Scenario 1, in

Scenario 2, the radar graph shows a steep reduction in the APFI and the EFI occurring when reducing the connection capacity. At the same time, the TFI does not change significantly. These results align with the results from 2.4.2 and suggest that there are only marginal effects on idle time and charging fulfilment. The time-history of the aggregated power shows that the power reference from the CA, in blue in the graph, is constant overall, showing only the effects of the PCC protection functionality. While in Scenario 1 the aggregated power consumption (in black) has a peak demand of 66 kW, in Scenario 2 the aggregated power (in red) is correctly following the $P_{CA}^{ref}$ without showing overshoots. The bottom graph shows that, while the number of EVs connected peaks at 12:00 and stays almost constant until 17:00, the amount of active plugs reaches its maximum only from 9:00 to 10:45 and lowers gradually after. Overall, these results outline the efficacy of the distributed control architecture in operating the clusters with reduced connection capacity.

Fig. 4.2 illustrates the scheduling action of the chargers; the y-axis indicates the plug number, and the x-axis shows the time in hours. For each charging session, the dotted and solid lines indicate, respectively, connection and charging time. Charging sessions from the same charger have the same dedicated colour for a clear distinction of the alternation of charging sessions performed by the switch within the chargers. Additionally, the table provides an overview of the idle time and final state-of-charge (SOC) for all the EVs in both scenarios. Together, Fig. 4.2 showcases the effective action of the control system, as there are no significant differences in the two scenarios either in terms of final SOC or in terms of idle time. In detail, the maximum difference in final SOC between the two scenarios is six percentage points (EV2). Also the idle time shows only marginal variation. While all the EVs have a final SOC equal or higher than 92%, EV11 has a final SOC of 78%. EV11 is, however, a one-phase EV with a large battery capacity (62 kWh) and charges 25 kW in both scenarios, showing that the reduction of the connection capacity did not affect its final SOC.

The major drawback of the power-sharing is seen in the charging efficiency of the EVs: Indeed, Scenario 2 shows a power consumption of 414 kWh of which 368 kWh were stored in the batteries (88% efficiency), the Scenario 1 shows a consumption of 413 kWh of which 373 kWh were stored in the batteries (90% efficiency). With the latest knowledge in efficiency losses in the onboard chargers, we know that the losses due to power-sharing could be even more significant, and therefore, the effects of power-sharing need to be reconsidered [91]. These losses can be minimised by prioritising power-scheduling over power-sharing functionalities.

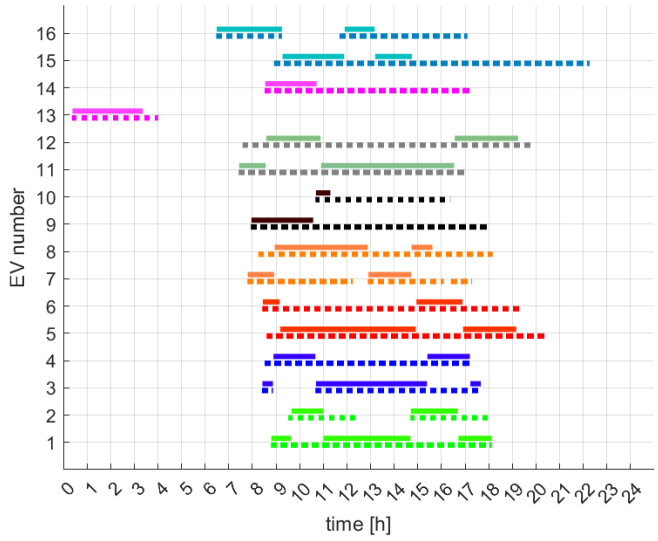


| | EV1 | EV2 | EV3 | EV4 | EV5 | EV6 | EV7 | EV8 | EV9 | EV10 | EV11 | EV12 | EV13 | EV14 | EV15 | EV16 |
|---|---|---|---|---|---|---|---|---|---|---|---|---|---|---|---|---|
| idle time unconstrained [hh:mm] | 03:40 | 02:22 | 01:56 | 05:03 | 04:00 | 08:36 | 04:32 | 05:20 | 07:37 | 05:08 | 02:51 | 07:28 | 00:40 | 07:34 | 10:50 | 04:30 |
| idle time constrained [hh:mm] | 03:24 | 02:36 | 01:48 | 05:00 | 03:48 | 08:18 | 03:48 | 05:06 | 07:30 | 05:06 | 02:54 | 07:18 | 00:36 | 06:24 | 09:06 | 04:12 |
| Final SOC unconstrained [%] | 99 | 98 | 97 | 100 | 100 | 100 | 100 | 100 | 100 | 100 | 78 | 100 | 100 | 100 | 100 | 100 |
| Final SOC constrained [%] | 96 | 92 | 94 | 99 | 100 | 100 | 100 | 100 | 100 | 100 | 78 | 100 | 100 | 100 | 100 | 100 |

**Figure 4.2:** Illustration of the power-scheduling action of the local control: the top graph displays the connection and charging times for all EVs, represented by dotted and solid lines, respectively. The bottom table compares the resulting idle times and final SOCs across both scenarios. The EVs connected to the same chargers are represented with the same colour.

## 4.2 Aggregation of multiple EV clusters

This second study focuses on examining the interaction between the VA controller and the CA controller. The simulation test case involves four EV clusters connected to two different transformers integrated with wind turbines as part of a small Virtual Power Plant (VPP). Fig. 4.3 illustrates the layout of the VPP, showing

the location of the clusters, the wind turbines and the transformers. Similarly to the single cluster analysis, the study compares two scenarios: Scenario 1, an unconstrained scenario where the CA does not provide coordination among clusters and power modulation is not applied; and Scenario 2, where the CA coordinates the consumption of each cluster, and the VAs coordinates charging sessions within the clusters through priority-based sharing and scheduling of the power. The aim of the study is to assess the performance of the distributed control architecture in performing RES power matching, RES power smoothing, and peak shaving to avoid transformer overloading, all while ensuring efficient EV charging across the clusters.

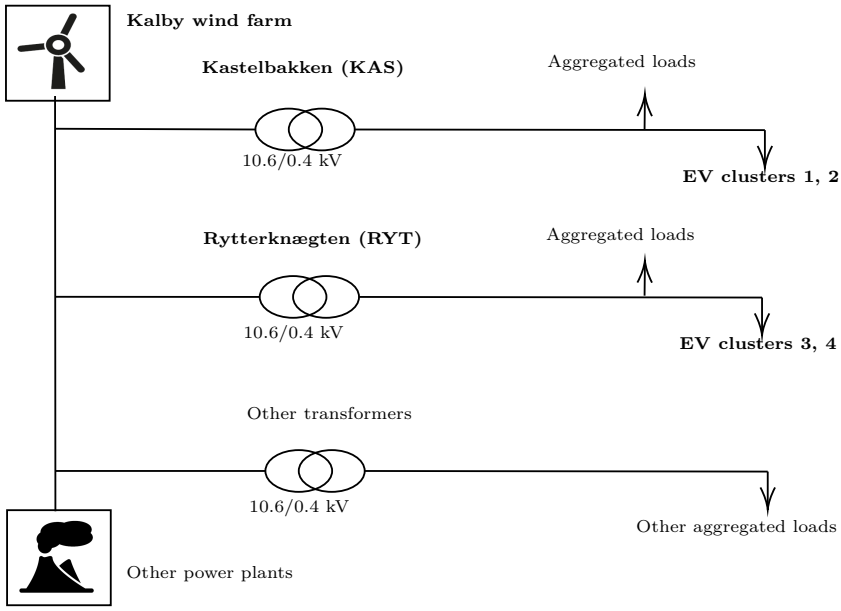


**Figure 4.3:** Simplified grid layout for the system

In Scenario 2, the CA sends dynamic power references ($P_{CA}^{ref,1}$, $P_{CA}^{ref,2}$, $P_{CA}^{ref,3}$, $P_{CA}^{ref,4}$) to the clusters according to two objectives: maximising wind power consumption and managing transformer congestion. When the transformer loadings are below a specified threshold, the sum of the power references for the four clusters $\sum_{n=1}^{n=4} P_{CA}^{ref,n}$ is set to align with wind power output, distributing the load among the clusters based on the number of chargers. If the loading of one of the transformers exceeds 75%, the CA activates a droop control mechanism for the clusters fed

| EV cluster | Number of Chargers | Scenario 1 | Scenario 2 |
|---|---|---|---|
| 1 (8 EVs) | 4 Chargers | 44 kW | 21 kW |
| 2 (32 EVs) | 16 Chargers | 176 kW | 86 kW |
| 3 (16 EVs) | 8 Chargers | 88 kW | 43 kW |
| 4 (12 EVs) | 6 Chargers | 66 kW | 32 kW |

**Table 4.1:** Characteristics of each cluster in both scenarios: number of EVs, number of chargers, maximum power consumption in Scenario 1 and connection capacities in Scenario 2 for each cluster.

by such transformer, gradually reducing their aggregated power reference until it reaches zero at 80% transformer loading, preventing further congestion. For example, if the Kastelbakken transformer is overloaded, the CA reduces the aggregated power reference of Cluster 1 and Cluster 2 ($P_{CA}^{ref,1} + P_{CA}^{ref,2}$). For each cluster, the related $P_{CA}^{ref,n}$ acts as an upper boundary for the smart charging power and can range from the value of the connection capacity of the cluster to 0 kWh. When the $P_{CA}^{ref,n}$ becomes too low and not all the connected EVs can charge at least with their minimum power, the EVs with the lowest priorities gradually disconnect.

The grid layout used in the simulation is based on a portion of the power system on the island of Bornholm, Denmark. The Kalby wind farm and two transformers, Kastelbakken and Rytterknægten, are part of this grid. Both transformers have a rated apparent power of 500 kVA and operate at 10.6/0.4 kV. The simulation inputs include one-second resolution data for wind power production and transformer loading, as shown in Fig. 4.4. The transformers experience two daily peaks, with loading exceeding 80% even without the presence of the clusters. The behaviour of the 68 EVs connecting to the clusters was modelled using data from the previous study, which consisted of behaviour from 16 EVs provided by Nissan EVs Telematics. The inputs for this simulation include the arrival time, SOC at connection time and disconnection time. Additional characteristics, such as battery capacities and phase configuration, were generated using the same criteria from the earlier study. Table 4.1 provides a detailed description of the EV clusters in both scenarios, including the number of EVs, number of chargers, and connection capacities for each cluster.

### 4.2.1 Performance of the system

Figure 4.5 provides the time history of the dynamic power references $P_{CA}^{ref,n}$ (in blue) and the power consumption $P_{PCC,n}^{meas}$ (in red) for the four clusters. From 0 to 6 am, the transformers work within their 75% threshold, and the wind power

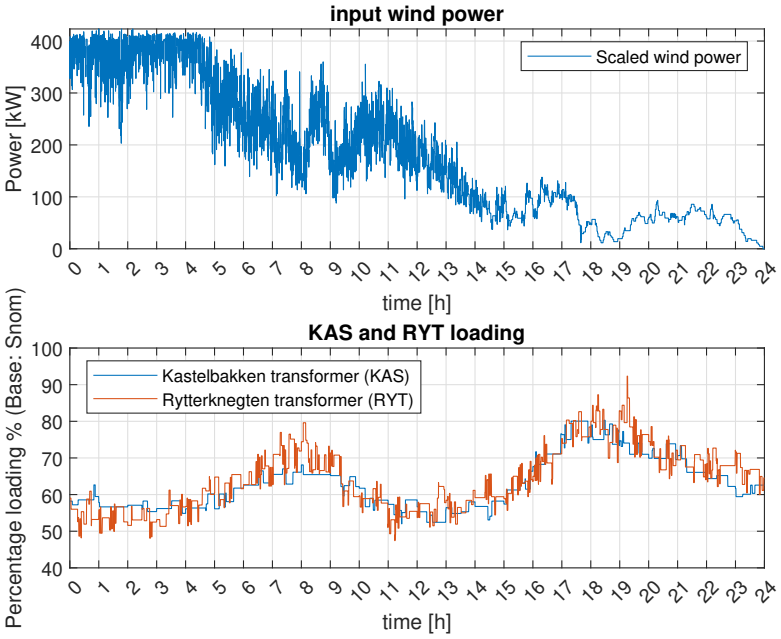


**Figure 4.4:** Top graph: Scaled wind power output of Kalby wind farm. Bottom graph: transformer loading for Kastelbakken (in blue) and Rytterknægten (in orange)

production is larger than the aggregated connection capacity of the clusters. Therefore, the power reference equals the connection capacity for all the clusters. Later in the day, the wind power production decreases and the CA lower the power references $P_{CA}^{ref,n}$ for all the clusters. The different clusters coordinate to follow the wind power production until the transformers become overloaded. Then the power references $P_{CA}^{ref,n}$ are further reduced, and eventually, the clusters gradually halt the charging sessions. Towards the end of the day, because of the EVs leaving the clusters, the allowed power cannot be utilised, leaving the VPP available to other loads in the grid.

Fig. 4.6 shows, in the top and center graphs, the impact of the power consumption of the clusters on transformer loading. Both graphs display the original loading data (in blue), the loading from Scenario 1 (in orange), and the additional loading from Scenario 2 (in green). In Scenario 1, where there is no power cur-

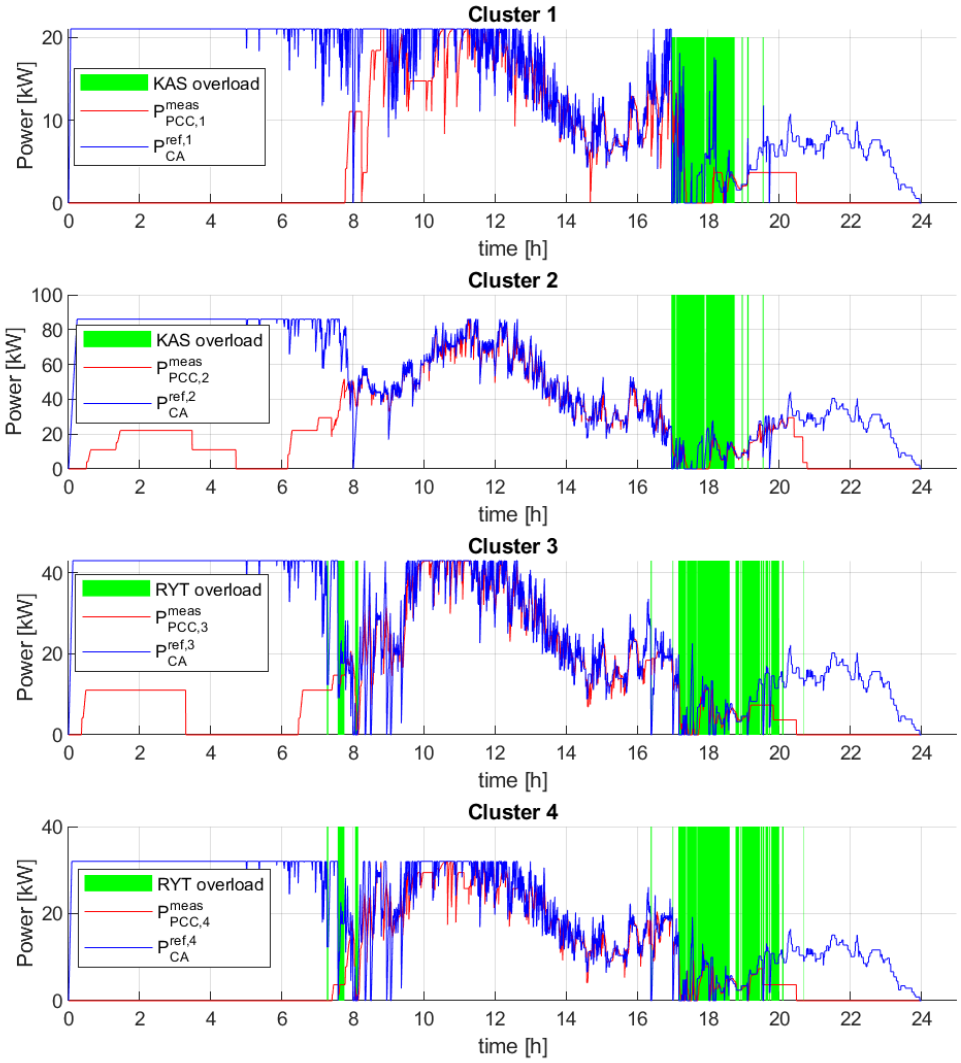


**Figure 4.5:** Time-histories of the aggregated power consumption of the four EV clusters. Cluster 1 and Cluster 2 are connected to the transformer Kastelbakken (KAS), while Cluster 3 and Cluster 4 are connected to Rytterknægten (RYT)

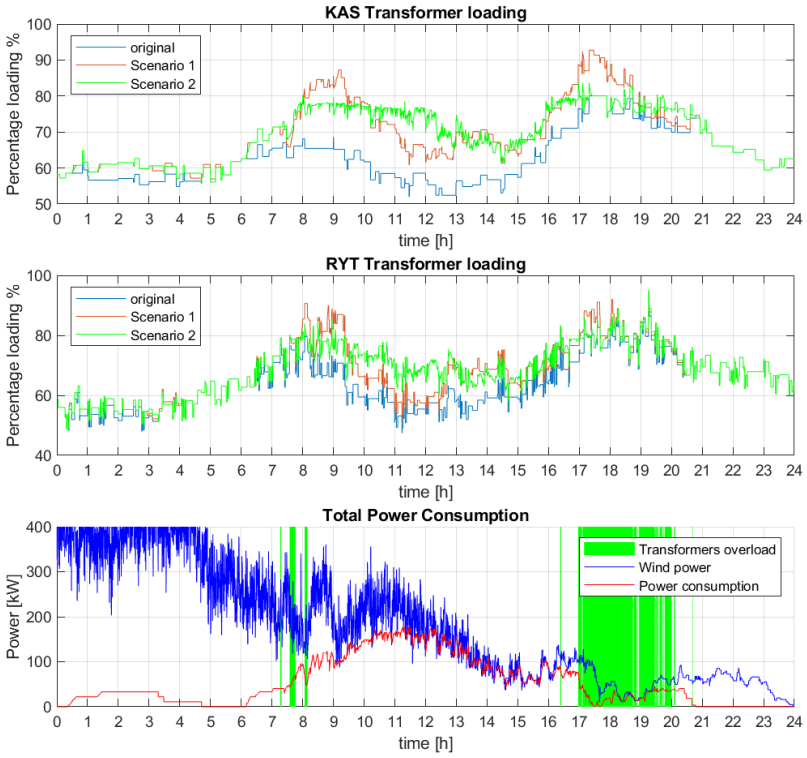


**Figure 4.6:** Overall virtual power plant outputs. Top graph: Kastelbakken feeder loading. Middle graph: Rytterknægten feeder loading. Bottom graph: VPP power flow.

tailment, the clusters negatively affect transformer loading, exacerbating overloads with peaks exceeding 80% and creating pronounced valleys. However, in Scenario 2, the power curtailment from the CA effectively reduces these peak loads, redistributing power consumption to less congested hours. This results in transformer loading remaining below the 80% threshold and a more stable overall transformer loading profile throughout the day. The peak shaving effect is especially evident in the Kastelbakken transformer between 10:00 and 13:00. Moreover, the bottom graph in Fig. 4.6 shows the total wind power production in blue, the total

power consumption of the four EV clusters in red, and the periods when either transformer is overloaded, represented by the green areas. The graph shows that, during the first half of the simulation, the wind power production is higher than the aggregated connection capacity of the clusters, which is 182 kW. However, from 12:00 the wind power production falls within the aggregated connection capacity of the system, and the system accurately follows the power production. After 16:00 the EVs start disconnecting or getting fully charged, causing a deviation between power consumption and production. From 17:00 to 20:00 the system reduces the power consumption to protect the transformers. Overall, the results illustrated in Fig. 4.5 and Fig. 4.6 demonstrate that the double-layer control action of the CA and VAs can effectively coordinate power consumption across clusters to align with wind power production based on the number of connected EVs. Furthermore, when the transformer approaches its overloading threshold, the CA can reduce the power reference of the affected clusters, potentially leading to full load shedding. The VAs will then automatically disconnect EVs as needed to ensure compliance with the set-points provided by the CA.

Additionally, Table 4.2 showcases some performance indicators of the VPP in the constrained scenario. The table shows that during the simulation, the wind turbines produce a total of 4.36 MWh, the cluster consumes 1.34 MWh and therefore the VPP exports 3.07 MWh. Due to the disproportion between production and consumption, the VPP imports only 92 kWh. The final two indicators in the table are the average root mean square (RMS) of wind power production and the average RMS of the VPP output, both calculated using their respective fitting curves over a 24-hour period. The RMS of wind power production provides a qualitative estimate of its fluctuations, while the RMS of the VPP output allows for a comparable assessment of the oscillations in the power exported by the VPP. The difference between the two values is only marginal, suggesting that the energy stored in the clusters had little effect on mitigating wind power variability. This limited impact is attributed to the disproportion between the wind power production and the power consumption of the clusters. Specifically, during most of the simulation, the wind power production either exceeded the aggregated connection capacity of the four clusters, or the clusters were unable to match the power production due to a lack of available EVs or because they were engaged in managing the loading of the transformers.

Fig. 4.7 presents two scatter plots outlining the charging fulfilment of the EVs based on the initial SOC. The left plot shows the distribution of energy charged across all EVs, while the right plot displays the final SOC distribution. Two linear fitting curve illustrate the general trend of the distribution for three-phase EVs and single-phase EVs. The left plot reveals that the system prioritises charging EVs with a lower initial SOC regardless of whether single-phase or three-phase, while

| Index | Value |
|---|---|
| Total energy produced [MWh] | 4.36 |
| Total energy used [MWh] | 1.34 |
| Energy imported [MWh] | 0.092 |
| Energy exported [MWh] | 3.07 |
| Average RMSE wind power production | 33.22 |
| Average RMSE VPP | 33.05 |

**Table 4.2:** Performance indicators for the virtual power plant

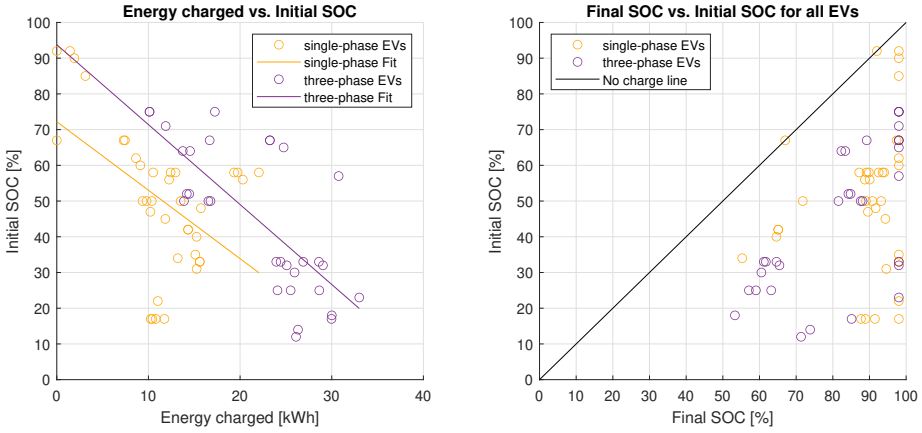


**Figure 4.7:** Graphical representation of the overall charging fulfilment of the 68 EVs. Left graph: distribution of the energy charged based on the initial SOC. Two linear fitting curves illustrate the general trend of the distribution. Right graph: distribution of the final SOC relative to the initial SOC.

delaying those with a higher initial SOC. Specifically, EVs with lower initial SOC receive more energy, while those with higher SOC charge less. It is also evident that single-phase EVs charge less energy overall compared to three-phase EVs. However, the right plot shows that, despite receiving less energy on average, single-phase EVs reach a higher final SOC than their three-phase counterparts. This discrepancy is due to the single-phase EVs having generally smaller battery capacities in the simulations. The results demonstrate effective prioritisation, as EVs connecting

with an initial SOC below 45% charge at least 10.7 kWh (for single-phase) and 15 kWh (for three-phase). Only two EVs (both single-phase) are not charged at all, but they started with high initial SOCs of 68% and 92%. These results outline the suitability of the distributed architecture to achieve correct priority-based power scheduling and power sharing, even during the coordination of different clusters for FTM flexibility services.

## 4.3 Summary of the findings

This section summarises the findings from the two computational analyses described in the previous sections.

The study in **Paper [P3]**, summarised in Section 4.1, investigated the feasibility of power-scheduling and power-sharing functionalities according to priority using local communication in a distributed architecture. Overall, the local control of the VAs proved suitable for the effective coordination of the charging sessions within a cluster, guaranteeing normal operation of the cluster under a reduced connection capacity without incurring overshoots and with only marginal differences in the charging fulfilment and idle time of the EVs.

The study in **Paper [P4]** and summarised in Section 4.2, investigated the coordination between the global and local control for providing FTM services. The results demonstrate that the distributed architecture ensures a high level of controllability across clusters. The simulation outputs show that the global control layer of the system effectively coordinates the power consumption of the four clusters to simultaneously perform RES power matching and peak shaving to prevent transformer overloading. Meanwhile, the local control in each cluster accurately follows the power set-point provided by the global control layer, managing the different charging sessions through power-sharing and power-scheduling functionalities based on priorities. Overall, the distributed control architecture proved to be a technically feasible solution for both FTM and BTM flexibility services, while reducing communication and computational demands compared to a centralised control system.

As expected, due to AC-DC conversion efficiency of the on-board chargers, more energy was necessary to achieve the same energy accumulated within the batteries, suggesting that power-scheduling should be preferred over power-sharing, and that individual power-sharing should be limited in controlling architectures. Additionally, having chargers with higher power capacity would further improve the charging efficiency. These changes would overall result in shorter charging sessions.

During the study some important aspect needing further improvement were found: Firstly, the SOC-based prioritisation system is not feasible in real life be-

cause the chargers cannot read the SOC from the EVs with the current protocols. Manually adding details of battery capacity or current SOC might not be user-friendly and discourage users from providing their inputs. Moreover, using the SOC to prioritise the charging sessions results in prioritising cars with low SOC, which is unrelated to the current energy needs of users. Secondly, scheduling the charging session only among the different plugs of each charger is not an optimal power-scheduling strategy. Although the parking lot still has idle time as a buffer for the cars to charge, the idle time is not evenly distributed over the chargers, generating a loss of charging opportunity. If an EV with very low SOC is connected to one plug of the charger, the other plug will be locked from charging for a long time. These considerations led to improvements in the control architecture, resulting in Version 2.

CHAPTER 5

# Experimental validation of the system

This chapter focuses on the experimental testing of the distributed architecture. The developed system architecture relies on prototype chargers produced by the company Circle Consult, a stakeholder of the ACDC project. Section 5.1 presents the experimental setup and the devices utilised for performing the test. These tests are run on Version 2 of the system, which is the improved design of the architecture, solving the limitations found during the computational analysis. The tests conducted include power-sharing (Section 5.2), power-scheduling (Section 5.3), RES power matching (Section 5.4), and peak shaving (Section 5.5). The final set of tests covers frequency regulation, both with equal and different priorities (Section 5.6). The results for power-sharing, peak shaving, and RES power matching are derived from **Paper [P5]**, power-scheduling from **Paper [P6]**, and frequency regulation from **Paper [P7]**. Each paper provides a more detailed technical description of the control algorithms and their respective results. Finally, Section 5.7 summarises the results and provides some discussion points for future work.

## 5.1 Experimental setup and test cases

For the purpose of the experiments, the system is integrated into a microgrid at the Energy System Integration Lab – SYSLAB on Risø campus, as shown in Figure 5.1. The microgrid is primarily powered by renewable energy sources (RES) and is connected to the external grid through a 200 kVA transformer. The setup consists of the following components (from left to right in the figure): a connection to the

external grid, the transformer, a 5 kW PV system, an emulated 20 kW PV system, a 10 kW wind turbine, a controllable load, and two chargers (C1 and C2), connected to the PCC. The connection capacity at the PCC is limited to 53 A (36.6 kW), which is lower than the combined maximum capacity of the two chargers, of 64 A (44 kW). The emulated PV system consists of a power source that can mimic PV power production in real-time, but its rated power can be manually changed. It is used to reproduce PV power production in case RES production during the testing day is absent or very limited. The controllable load simulates varying grid loads, providing a way to test the performance of the system under different conditions. In the experiments, four EVs are used, one for each charger plug. The test includes two Renault ZOEs and two Nissan LEAFs: both models can charge with a maximum current of 32 A. However, ZOEs have three-phase charging capabilities, charging with a power of 22 kW, while the LEAFs are single-phase and have a maximum power consumption of 7.36 kW.

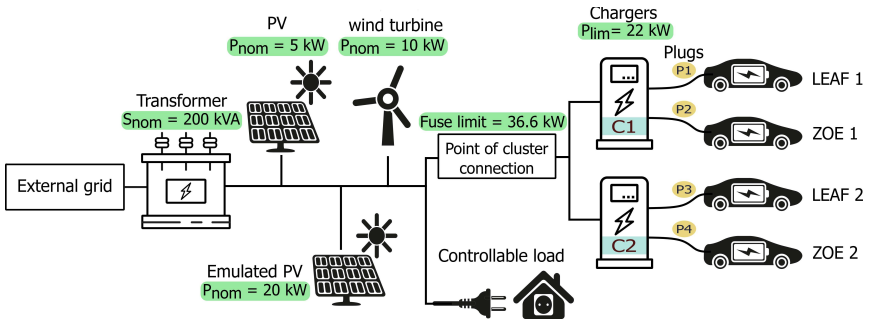


**Figure 5.1:** Electrical system setup and representation of the devices involved.

## 5.2 Test power-sharing

This test is performed to validate the suitability of the control architecture for power-sharing among the charging EVs. During the first test, the four EVs were connected sequentially, in the order: ZOE 1, ZOE 2, LEAF 1 and LEAF 2. Fig. 5.2 shows the power consumption over time for each EV. When ZOE 1 was connected to C1, it started charging with a maximum current of 32 A because the connection capacity was not reached, and no power-sharing was needed. Upon the connection of ZOE 2 to charger C2, the system activated its power-sharing functionalities to prevent exceeding the connection capacity at the PCC of 53 A. This resulted in the CA providing to both EVs an equal current of 26.5 A, theoretically corresponding

to 18.3 kW each. However, the graph shows that both EVs consumed only 17 kW. When LEAF 1 was connected to C1, the VA in C1 had to share its maximum current capacity of 32 A equally among the two EVs. Therefore, each EV charged at 16 A. These set-points correspond to 11 kW for ZOE 1 and 3.7 kW for LEAF 1. The CA redistributed the remaining current (21 A) to ZOE 2, corresponding to 14.5 kW. While the LEAF 1 adjusted its power consumption precisely to 3.7 kW, both ZOEs undershot their set-points: ZOE 1 charged at 10 kW instead of 11 kW and ZOE 2 charged at 13.7 kW instead of 14.5 kW. Subsequently, LEAF 2 was connected to C2, requiring the CA to redistribute the current capacity at the PCC between C1 and C2 again. Each EV was thus allowed a current of 13.25 A, corresponding to 3 kW for the LEAFs and 9.1 kW for the ZOEs. However, the ZOEs again undershot, consuming only 8 kW each. Finally, both ZOEs were disconnected and the two LEAFs shared the connection capacity of the PCC equally, consuming 6.1 kW each. The test concluded with the disconnection of all the EVs.

The test demonstrates that the distributed control architecture is capable of performing power-sharing functions effectively and in a timely manner. Both the CA and VA ensured that no overloads occurred, either at the PCC connection capacity or at the individual chargers. Furthermore, the study reveals key insights into the physical capabilities of both the chargers and the EVs.

One important finding relates to the power factor characteristics of the EVs. The undershoot observed in the power consumption of the two ZOEs compared to their set-points is linked to the consumption of reactive power during power modulation. As documented in [91], power modulation impacts reactive power generation in all EV models charging with alternating current (AC). The paper reveals that this production varies significantly among different EV models, confirming that second-generation Renault ZOEs consume a high amount of reactive power compared to other EVs. Additionally, this effect is more pronounced at lower charging power levels. In AC chargers, since the output of the chargers corresponds to an allowed current for the EVs, the actual active power they consume depends on the power factor characteristic of their on-board charger.

Another key insight relates to the physical limitations of the chargers in handling power-sharing when both three-phase and single-phase EVs are connected. Specifically, in the presented experimental setup, the 53 A limitation applies to each phase individually. As a result, when a single-phase EV is charging, the other connected three-phase EVs must reduce their consumption across all phases to avoid exceeding the capacity of the system on the most heavily loaded phase. In the test scenario, for instance, when all EVs were connected, only one phase reached full capacity (53 A), while the other two phases operated at half capacity (26.5 A). Therefore, in presence of single-phase EVs, the controller must limit the overall power shared among the EVs to ensure that no phase exceeds its current

capacity. Phase imbalances during EV charging are problematic not only for the power-sharing capabilities of charging clusters but also for grid operators (GOs), who must ensure that phase imbalances on every grid node remain within tolerance levels. This issue can be mitigated by rotating the wiring of each plug, so that an equal number of plugs have each of the three phases as their primary phase. This rotation reduces the likelihood of multiple single-phase EVs charging on the same phase, thereby minimizing the risk of phase imbalances.

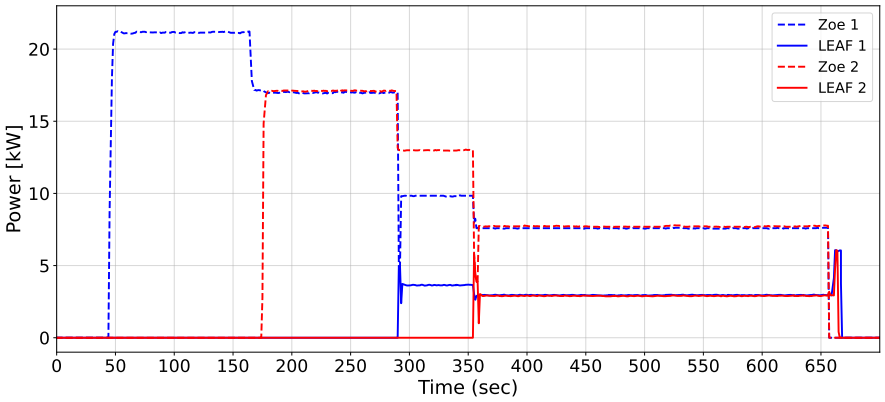


**Figure 5.2:** Power-sharing test: active power of EVs

## 5.3 Test power-scheduling

This test is performed to validate the suitability of the local control to perform power-scheduling among the charging sessions based on the $\rho_{int}$ set by the users. To demonstrate the functionality, during the test, the constant power reference set by the CA is 16 A, and the power-sharing functionality within the VAs is removed, forcing the system to only perform power-scheduling among the EVs. Additionally, to maximize switching events during the test, both EVs were connected with equal user priorities , and the queuing time before switching was reduced to 30 seconds. As a result, once one EV begins charging, its $\rho_{int}$ diminishes relative to the other, prompting the VAs to pause its session and resume charging for the idle EV. The short queuing time was specifically chosen to increase the number of switches during the testing period. However, in practical applications, a longer queuing time would be preferable to avoid excessive switching between EVs.

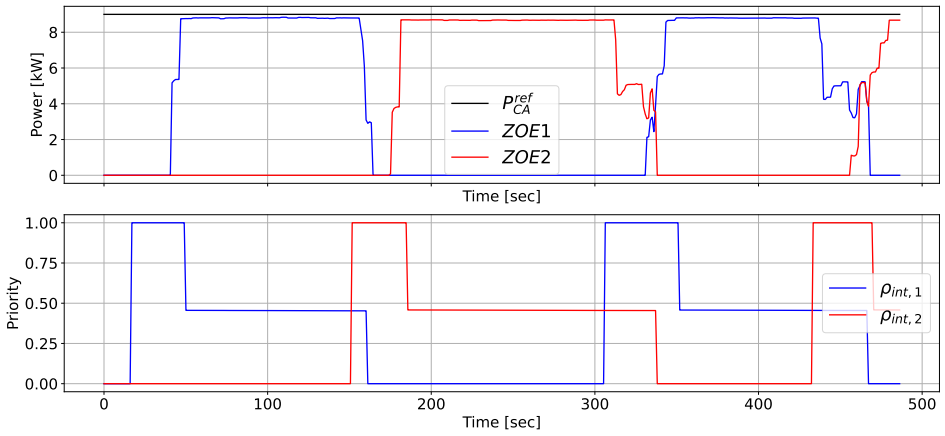


**Figure 5.3:** Power-scheduling test: active power of the EVs (top graph) and internal priority $\rho_{int}$ for the two EVs

Fig. 5.3 shows a time history of the power consumption from the two ZOEs employed for the test. The two ZOEs are connected almost at the same time, with ZOE 1 being the first one to be scheduled. The bottom graph illustrates the $\rho_{int}$ function within the VAs signalling, with a value of 1, the start of an EV charging session to the other VAs. This allows all the other VAs to either refrain from taking action or to disconnect or reduce their power consumption to accommodate the new charging session. As the charging session progresses, the $\rho_{int}$ decreases and, when the priority value of the ZOE 1 becomes lower than the priority of ZOE 2, the scheduling system activates, pausing the session of ZOE 1 and starting the session of ZOE 2. The switching repeats other two times before the end of the test. The graph highlights that the charging EV lowers the power consumption to an intermediate step before halting the charging session completely. This is possibly because of an interference of the anti-overshoot functionality embedded in the VAs, which lowers the power consumption of the EV before the other can connect. This intermediate step is not desired and leads to two overshoots of the power reference from the CA during the last two switches of the charging sessions. The anti-overshoot functionality of the VAs is important to prevent the system from over-shooting the power reference during the first stages of power-sharing when a new charging session starts or resumes. However, this functionality should have been deactivated alongside the power-sharing function, as having one without the other can interfere with power-scheduling and cause overshoots. During the last two switches,

the system overshoots the power reference of 0.9 kW and 1.8 kW respectively, the overshoots last respectively 1.05 s and 5.25 s, not being a risk for standardised type C breakers, used at the PCC. A more comprehensive analysis of the overshoot can be found in **Paper [P6]**. While further investigation is required and the test needs to be rerun to ensure optimal control tuning, the power-scheduling functionality of the local control layer has demonstrated technical feasibility. Future work will revisit the test to refine and enhance the power-scheduling capabilities of the architecture.

A crucial key limitation was found during the tests of the system, which concerns the EVs. In detail, it was found that not all the EVs have the capacity to restart a charging after the charging session was interrupted by the charger, without the direct physical interaction of the user with the EV through key or by opening the doors. As with the reaction time of the EVs and the reactive power production, the behaviour of different EVs models can vary significantly and the outputs of the tests with unknown models can be unpredictable. These findings further highlight the urgency of standardization of the interaction between EVs and EVSEs, discussed in the previous chapter. Solving this problem is of utmost importance for future development of smart charging infrastructure.

## 5.4 Test RES following

This test was performed to validate the capabilities of the control architecture to coordinate power consumption of the chargers to match RES power production. The controller aims to match power production without disconnecting the EVs when power is too low. During the test, the system received real-time measurements of RES production, supplemented by the PV emulator to compensate for the insufficient RES power generation caused by unfavorable weather conditions. During the test, ZOE 1 and ZOE 2 and C1 were used.

Figure 5.4 shows a time-history of the RES power production and EV power consumption during the test. Similarly to the first test, the two EVs are connected subsequently. Before activating the RES following mode, the first EV and the second EVs were connected subsequently. The first drop in the graph corresponds to the reduction in power consumption by the first EV to make room for the second EV as it began its charging session, ensuring that the combined load did not exceed the current capacity of the charger. Once both EVs were connected, the RES following mode was activated, and the system started power-sharing to align with RES production. During the test, the RES power experienced two 10 kW drops, due to the gradual curtailment of the PV emulator. Despite a notable undershoot in power consumption——attributed to the consumption of reactive power from the

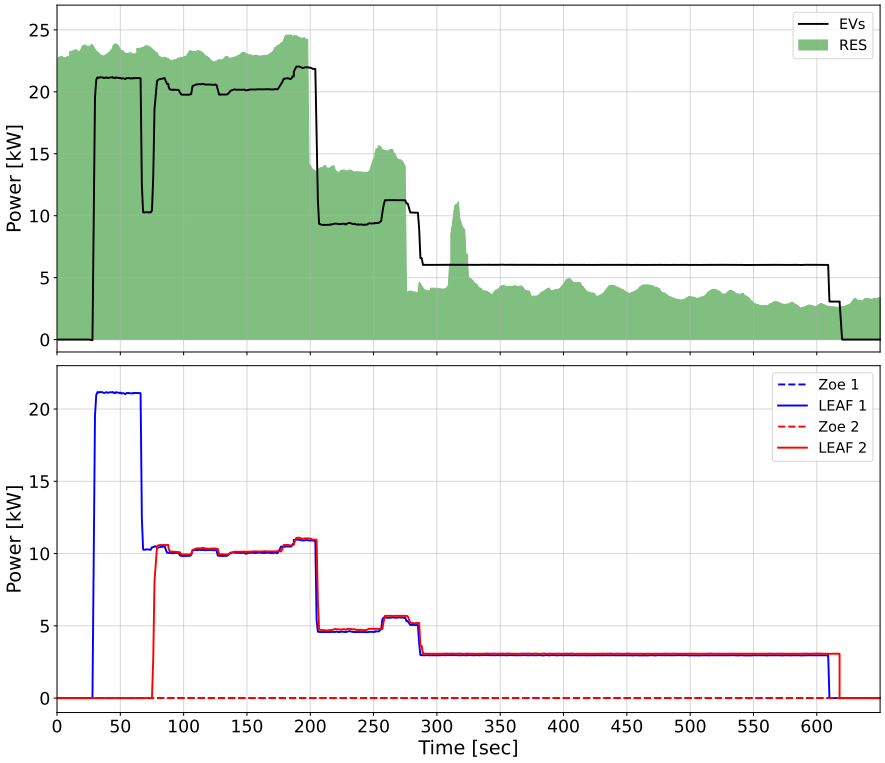


**Figure 5.4:** RES power matching test: aggregated active power of the cluster and RES production

EVs—the system successfully adjusted the power consumption to match the fluctuating RES input. It also ensured that the EVs maintained at least the minimum charging level when RES power was insufficient, as seen in the latter half of the test, where RES production hovered around 4 kW, and the EVs still consumed approximately 6 kW. The RES generation experienced a brief spike, lasting around 10 seconds, which was not followed by an increase in EV power consumption. This lack of responsiveness was associated primarily due to the PI controllers in the VAs becoming ”wound up” at the low saturation limit. In detail, when RES input dropped below the minimum charging threshold of the EVs, the PI controllers continuously generated set-points to match RES production. However, since the EVs could not charge below their minimum power level, a persistent negative error

accumulated in the integral term of the PI controller, driving the output to its negative saturation point. Once this limit was reached, the integral term gradually lowered its value, regardless of the output of the PI controller. As a result, when RES conditions improved, the PI controller was slow to respond, requiring time to unwind the stored error in the integral term.

To address this issue, a later version of the VAs incorporated an anti-windup mechanism in the PI controllers. This modification limited the buildup of the integral term when the controller reached its saturation point, allowing the VAs to respond more quickly to changes in input without becoming stuck at their output limits.

Overall, the test demonstrated the effectiveness of the distributed control architecture in coordinating the charging of two EVs connected to a single charger, ensuring power-sharing in line with RES production.

## 5.5 Test peak shaving

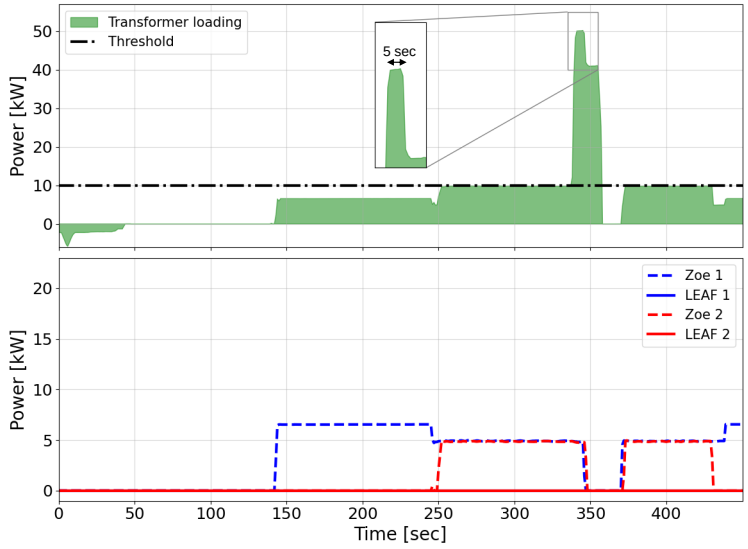


**Figure 5.5:** Transformer protection test. Top graph: transformer loading and threshold for power curtailment. Bottom graph: active power of the EVs

This test was performed to validate the capabilities of the system to pause the cluster consumption in the event of transformer overloading. For the scope of the demonstration, the two LEAFs were connected to C1 and C2, and the transformer loading limit was set to 10 kW. Fig. 5.5 shows the time history of the test: in the top graph, the power consumption of the two EVs is illustrated, while the bottom graph shows the transformer limit with the red dotted line and the power exported or imported during the test. The power exported is indicated with negative values, while the power imported is indicated with positive values. The graph starts by showing the disconnection of RES production happening at 2100 s. Afterwards, the two EVs are connected to the chargers, sharing the available 10 kW to prevent transformer overload. At 2370s an external controllable load of 40 kW was connected, resulting in a spike in the transformer loading, which reached 50 kW. Within 5 s the system reacted by halting the charging sessions of both the EVs. When the operating conditions of the transformer were restored, the charging sessions restarted automatically. This demonstration shows that the distributed control architecture can disconnect EVs in a timely manner to perform transformer protection.

## 5.6 Priority-based frequency regulation

This section describes the performance of the system in providing frequency regulation to the grid while coordinating the charging sessions of EVs according to priority. Two tests were performed: in the first, all the EVs have the same priority, and therefore, their involvement in regulating the frequency is equal; in the second, the user inputs are set according to different charging urgency, and thus, the control system gives the EVs different power shares and different degrees of involvement. It is important to note that fulfilling the energy request and respecting the duration of the charging session are not the focus of the investigation. The CA receives frequency measurements $f_{meas}$ from the meter at the PCC. In the CA, there is an integrated droop control which translates these inputs into power reference $P_{CA}^{ref}$. The CA broadcasts $P_{CA}^{ref}$ to the VAs. The VAs have the same controlling algorithm described in Section 3.3. A more detailed description of the controller and its mathematical formulation is found in **Paper [P7]**.

In the tests, the two ZOEs were connected to C1 and C2. A virtual connection capacity of 32 A is chosen for the test, and a maximum current of 16 A is applied to each plug. In the test with equal priorities, the same user inputs were chosen for the two charging sessions, and the power range allocated to frequency regulation was set to $\pm 2.5$ kW. Consequently, the aggregated power set-points of the EVs varied between 12.5 kW and 17.5 kW for a frequency range of 49.9 Hz to 50.1 Hz. In contrast, in the test with different priorities, the internal priorities $\rho_{int}$ were

set to 0.7 and 0.3, respectively, and the power range for frequency regulation was increased to ±3 kW. As a result, the aggregated power set-points ranged from 13 kW to 19 kW for the same frequency range of 49.9 Hz to 50.1 Hz.

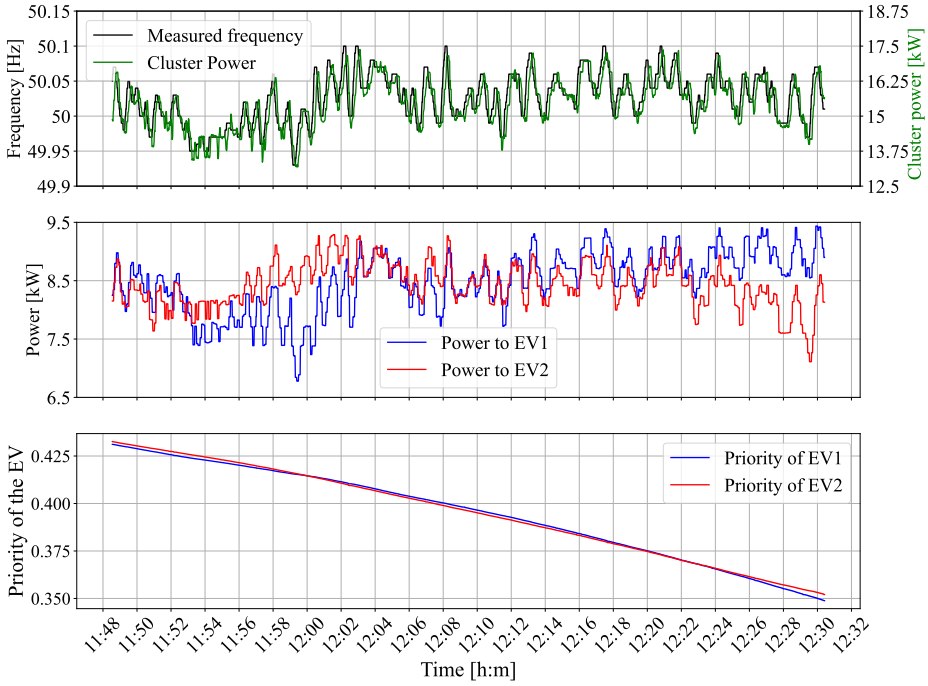


**Figure 5.6:** Time history of the frequency test with equal priorities $\rho_{int}$: frequency and power measured (top graph), power dispatched to each vehicle (middle graph), priority of the EVs (bottom graph).

### 5.6.1 Test frequency regulation with equal priorities

Figure 5.6 presents a time-history of the test, highlighting the key parameters: the top graph displays the measured frequency and power throughout the test, the middle graph shows the power consumption of each EV, and the bottom graph illustrates the priority trends, $\rho_{int}$, for the two EVs over the course of the test. The top graph features a double y-axis, with both y-axes aligned to emphasize the precision of the controller. The top graph shows fast and accurate coordination

of the CA and VAs control actions to adjust the aggregated power consumption of the EVs. The system shows a general undershoot of the power consumption compared to the frequency-related set-points. The graph also shows the system delays in following the power set-points. These delays are due to multiple factors: the communication delays due to the different intermediate nodes between the communication path that goes from the PCC to the CA and the VAs, the reaction time of the PI controllers within the VAs, and the reaction times of the EVs. The middle graph shows that the EVs have equal power adjustment with some relative divergence, where at times, the first EV is consuming more and other times, the second EV is consuming more. These divergences could be considered negligible or the result of random interactions between the controllers and the EVs. However, it cannot be ruled out that, despite efforts to match their initial conditions, the two EVs may have differed in temperature, state of health of the battery, or other factors that were not accounted for before the test. These factors could be further investigated in future work. The bottom graph displays the trends of $\rho_{int}$ for the two EVs, starting around 0.43 and decreasing to 0.35. These $\rho_{int}$ values mirror the power consumption patterns of the two EVs, with the EV that charges the fastest showing a more rapid decline in $\rho_{int}$. Consequently, since EV1 consumes the most power by the end of the experiment, it concludes with the lowest $\rho_{int}$.

### 5.6.2 Test frequency regulation with different priorities

Similarly for the test with equal priority, in Fig. 5.7 the time history of the frequency regulation performances is provided. Although the graph shows very similar behaviour to the one in the first test, there is a more significant delay and additional oscillation of the power measured at the PCC compared to the reference power. The second graph shows that one of the EVs is constantly charging to the maximum power, showing almost no participation to frequency regulation, while the second EV is the only one involved in the frequency regulation. Such changed working conditions in the controlling action might result in a need for different controller tuning, which will be addressed in future work. The priority trends for both EVs ran nearly parallel throughout the charging session, with their priorities decreasing as they approached the completion of their requested energy.

Finally, Fig.5.8 presents a normalized cross-correlation on the left to visualize the delays, and a histogram on the right showing the error distribution between the $P_{PCC}^{meas}$ and the expected power consumption of the cluster, highlighting both the delay and the precision of the control action. In the left graph, the y-axis illustrates the normalized cross-correlation coefficient and the x-axis the value of lag in seconds. The lag represents the displacement between the two time-series

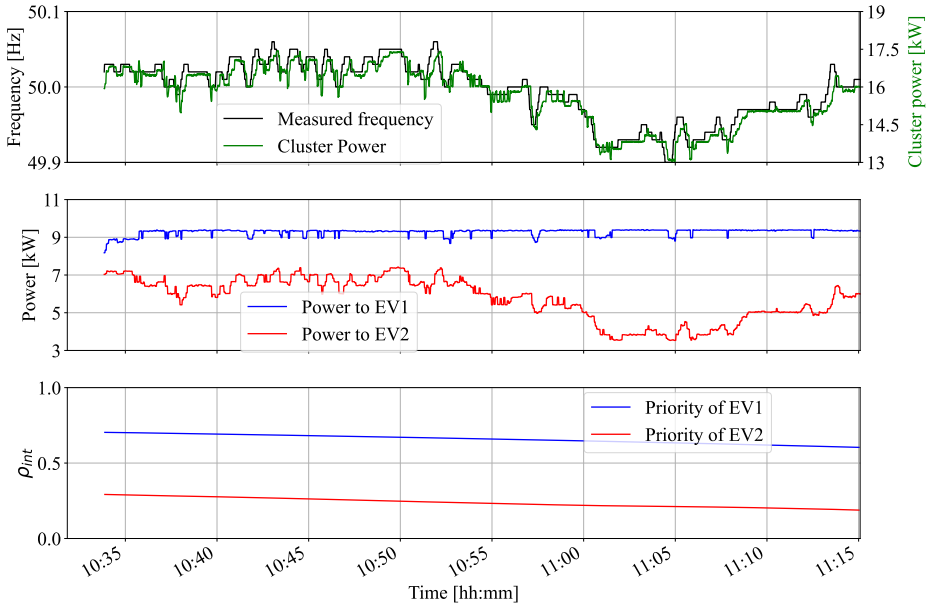


**Figure 5.7:** Time history of the frequency test with different priorities $\rho_{int}$: frequency and power measured (top graph), power dispatched to each vehicle (middle graph), priority of the EVs (bottom graph).

for which each cross-correlation coefficient is calculated. The normalized cross-correlation peaks at 0.98 at a lag value of 8.48 seconds. Such a result indicates that the two curves have a very high degree of similarity but the measured power curve is delayed by 8.48 seconds compared with the expected power curve. The skewness of the right graph confirms the undershoot of the control action of the system, which is, on average, 0.17 kW. Generally, the error ranges from -1.08 kW to 0.48 kW.

These results demonstrate the fast and accurate response of the control action for frequency regulation, as well as the technical feasibility of the control architecture to handle more complex tasks that combine frequency regulation (FTM) with charging prioritization (BTM).

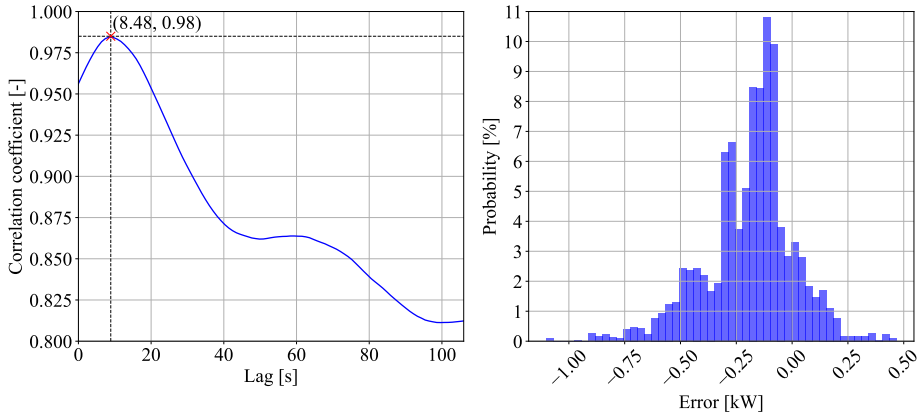


**Figure 5.8:** Normalized cross-correlation of the frequency with the power measured during the experimental validation (left graph); Histogram of the error distribution between expected power and measured power during the experimental validation (right graph).

## 5.7 Summary of the results

This section summarizes the findings from the experimental validation of the control system described earlier. The experiments aimed to confirm the technical feasibility of the functionalities previously simulated in computational analyses, though they were tested on a smaller scale due to limited access to chargers and EVs. These functionalities included power-sharing, RES power matching, peak shaving (as detailed in **Paper [P5]**), power-scheduling (**Paper [P6]**), and priority-based frequency regulation (**Paper [P7]**).

Overall, the system effectively managed all tested functionalities. The CA successfully provided a dynamic power reference for distribution among chargers, while the VAs autonomously coordinated to meet power demands based on priority. The system demonstrated both speed and accuracy, with a response time of under 5 seconds for disconnecting EVs in transformer overload situations and an average reaction time of 8.5 seconds during frequency regulation tests involving two ZOEs. Precision was mostly maintained, though reactive power consumption by EVs affected set-point accuracy.

However, some challenges were identified, particularly regarding controller tuning and interactions. For instance, in the RES power matching test, the PI con-

troller experienced ”windup” issues, and during power-scheduling tests, the anti-overshooting feature of the VA interfered with the switching of charging sessions, causing minor overshoots. These challenges were tied not to the architecture itself, but rather to the need for better tuning of the controllers, which have since been addressed in the current EV cluster at the Risø Campus. Future work will focus on longer-duration tests (over several days) to assess the combined functionality of power-scheduling, power-sharing, and prioritization for a variety of FTM services, such as RES following and transformer protection, as simulated in **Paper** [**P4**].

The experimental campaign also provided key insights into real-world EV-EVSE interactions. The power-sharing experiment indicated that single-phase EVs could significantly limit the control range of other EVs in the cluster due to phase imbalances and current limitations on each phase at the PCC breakers. Specifically, to prevent tripping, the controller needs to protect the most heavily loaded phase, even if this results in underutilization of the remaining phases. A mitigation strategy could involve either a passive or combined passive-active approach. The passive approach entails rotating the wiring of chargers to balance phase distribution within the cluster. An active approach would complement this by mapping the phase configuration within the controller, allowing optimization of the control action based on the primary phase of each charger.

Another limitation affecting the accuracy of the control action is the variability in EV behavior. The tests revealed significant differences between EVs in terms of reactive power consumption, response delays, and their ability to resume charging automatically after a controller-induced pause. While reactive power issues and response delays require careful consideration to optimize control strategies and maintain grid stability, they are not critical to the feasibility of smart charging functionalities or the proposed architecture. However, the inability of some EVs to automatically resume charging poses a major challenge to the technical feasibility of power-scheduling strategies in commercial applications. This unpredictability in EV behavior warrants further investigation, requiring solutions either from a control system perspective or through standardization of EV functionalities.

CHAPTER 6

# Conclusion

## 6.1 Summary

Automated EV smart charging technologies have the potential to become essential components of future smart grids. These technologies enable dynamic control of EV charging processes, offering flexible storage capacity to the grid and enhancing the security and stability of electricity supply. This is especially important as energy production increasingly relies on RES, which are less controllable than traditional energy sources, and energy demand from EVs becomes increasingly significant for the grid.

This thesis explores the potential of EV clusters to function autonomously as controllable loads, providing flexibility services to GOs while ensuring a seamless charging experience for EV users. The focus of the thesis can be grouped in two perspectives: the first is the design of an analytical framework to simplify the planning and sizing of smart EV clusters, with an eye on the future development of flexibility markets and the standardization of EV-based flexibility services. The second is the design of an autonomous distributed control architecture to harness the flexibility potential of EV clusters and provide controllability both on a large scale, to GOs and aggregators, and on a small scale, to CPOs and EV users. The designed control architecture involves a two-layer control, consisting of a cloud-based control unit for the global control and an autonomous control unit embedded within the charger, for local control. The control architecture was developed and implemented in a workplace parking lot at Risø campus. The project demonstrated the feasibility of the system and assessed its potential capabilities.

The first part of the thesis focuses on the integration of smart EV clusters as controllable loads for providing grid services. The opening chapter provides an overview of the deployment status of smart EV infrastructure, identifying techno-

logical, economic, and policy barriers to their integration as providers of flexibility services. These barriers create uncertainty around the flexibility potential of EV clusters and their profitability as controllable loads, which hinders investment in smart EV infrastructure. To address this uncertainty, the thesis proposed an analytical framework designed to quantify the flexibility potential of EV clusters. This data analysis tool enables CPOs to leverage their extensive metering data to summarize the flexibility potential of clusters across a variety of services using a few simple metrics. The method was applied to a computational sensitivity analysis of an existing workplace EV cluster, evaluating how various cluster characteristics and user behaviours influence its flexibility potential. The sensitivity analysis revealed that user energy requests, EV battery sizes, and connection patterns are the most critical factors when sizing an EV cluster and selecting a suitable strategy. These factors significantly influence both the amount and timing of flexibility, with clusters offering more flexibility at the beginning of work shifts and less throughout the day due to fewer new connections. The study identifies scheduling-based smart charging strategies as means for mitigating the effects of insufficient connection capacity in clusters. These strategies are also essential for fully utilizing the power capacity of chargers, especially when the chargers have high power capacity. The analysis also showed that the number of EVs alone does not significantly impact flexibility potential. Instead, connection patterns and energy requests have a much greater influence, affecting the timing and amount of flexibility over a given time period.

The second part of the thesis focused on the development of the autonomous distributed control architecture for EV clusters. In the different chapters, the thesis covered the design concept and implementation, development stages, computational analysis, and experimental validation of the system. The computational analysis was first applied to a single-cluster configuration for local services, then to an aggregation of clusters coordinating their consumption to match wind turbine power production and reduce load to prevent transformer overloading. In the simulations, the distributed control architecture effectively managed charging sessions across both control layers: the cloud-based control successfully coordinated power consumption among clusters by dispatching dynamic power set-points, ensuring peak shaving and RES power matching; simultaneously, the chargers autonomously scheduled and modulated each charging session based on user-defined charging urgency, matching the dynamic set-points from the cloud-based control. The last chapter of the thesis described the experimental demonstration of the simulated smart charging functionalities on a smaller scale. Overall, the test validated the technical feasibility of the distributed control architecture for power-sharing, power-scheduling, RES power matching, peak shaving, and priority-based frequency regulation. The experimental campaign, conducted with Renault ZOEs

and Nissan Leafs, demonstrated effective and consistent performance, with the cluster achieving full reaction to a new power measurement within 8.5 seconds. However, the system encountered some control limitations, primarily resulting in undershoots in EV power consumption compared to the set-points. Certain issues, such as phase imbalances caused by single-phase EVs and reactive power production during EV modulation, can be mitigated, and solutions were proposed. Other limitations, particularly related to the incompatibility of some EV models with scheduling strategies, underscore the need for policies promoting the standardization of onboard charging technologies.

## 6.2 Perspectives for future research

The first part of the thesis proposed an analytical framework for the quantification of flexibility potential of EV clusters. On this regard, two key areas for future research have been identified. First, the method could be enhanced by incorporating indexes that account for the individual flexibility of each charging session. This is particularly relevant for the TFI, as time flexibility can vary significantly between EVs. Using a single parameter to represent this could be misleading, as the analysis showed. Understanding this variation could help compare the scheduling effectiveness of different charging strategies and offer insights into user behaviour. Second, further research should investigate the optimal flexibility capacity for EV clusters, focusing on how cluster size and electrical layout affect CAPEX and potential OPEX savings from flexibility services based on market pricing forecasts. These insights could enhance the planning of smart charging clusters and improve returns on investment for CPOs and aggregators.

The second part of the thesis introduced a novel autonomous distributed control architecture as a promising solution for large-scale control of smart EV clusters, enabling both BTM and FTM services. However, field tests were limited to a single cluster with a maximum of four EVs, and conducted over a short time period. Future research should expand these tests to larger-scale scenarios, involving multiple clusters and more EVs to fully assess the potential of the architecture.

Future research should further refine the control strategy by investigating the interaction between global and local control output update rates, local control tuning, and the behavior of a diverse range of EV models. During the tests, significant differences in control accuracy, reaction times, and delays were observed among various EV models. Notably, some vehicles were unable to automatically restart charging after being paused by the controller, requiring manual intervention, such as opening the door, which posed a major limitation for power-scheduling functionalities. Additionally, variations in on-board charging technologies led to differing

behaviours related to reactive power production and phase consumption. These inconsistencies introduced unpredictability, limiting the controllability and response time of the system, and must be considered in commercial applications.

Finally, a valuable next step in researching this novel architecture would be a techno-economic comparison between the distributed control architecture and conventional centralized systems. While the distributed approach offers scalability and reduces the computational load on a single cloud entity, potentially lowering operational costs, its increased design and control complexity may lead to higher per-charger costs. A comparison of the two approaches could offer deeper insights into the practical feasibility and cost-effectiveness of distributed control architectures.

# Bibliography


[1] *The Paris Agreement*. URL: https://unfccc.int/process-and-meetings/the-paris-agreement/the-paris-agreement.

[2] I. E. Agency. *World energy outlook 2023*. OECD/IEA Paris, 2023.

[3] C. Crozier, T. Morstyn, and M. McCulloch. "The opportunity for smart charging to mitigate the impact of electric vehicles on transmission and distribution systems." In: *Applied Energy* 268 (2020), page 114973. DOI: 10.1016/j.apenergy.2020.114973.

[4] T. Mai, M. M. Hand, S. F. Baldwin, et al. "Renewable electricity futures for the United States." In: *IEEE Transactions on Sustainable Energy* 5 (2013), pages 372–378.

[5] H. Kondziella and T. Bruckner. "Flexibility requirements of renewable energy based electricity systems - A review of research results and methodologies." In: *Renewable and Sustainable Energy Reviews* 53 (2016), pages 10–22. DOI: 10.1016/j.rser.2015.07.199.

[6] L. Calearo, M. Marinelli, and C. Ziras. "A review of data sources for electric vehicle integration studies." In: *Renewable and Sustainable Energy Reviews* 151 (2021), page 111518.

[7] M. Muratori. "Impact of uncoordinated plug-in electric vehicle charging on residential power demand." In: *Nature Energy* 3 (2018), pages 193–201. DOI: 10.1038/s41560-017-0074-z.

[8] L. Calearo, A. Thingvad, K. Suzuki, and M. Marinelli. "Grid Loading Due to EV Charging Profiles Based on Pseudo-Real Driving Pattern and User Behavior." In: *IEEE Transactions on Transportation Electrification* 5 (3 2019), pages 683–694. DOI: 10.1109/TTE.2019.2921854.

[9] C. Binding, D. Gantenbein, B. Jansen, et al. "Electric vehicle fleet integration in the Danish EDISON project - A virtual power plant on the island of Bornholm." In: *IEEE PES General Meeting, PES 2010* (2010), pages 1–8. DOI: 10.1109/PES.2010.5589605.

[10] T. Unterluggauer, F. Hipolito, P. B. Andersen, J. Rich, and M. Marinelli. "Conditional Connection Agreements for EV Charging: Review, Design, and Implementation of Solutions for the Low Voltage Distribution Grid." In: *Under review* (2024). DOI: https://dx.doi.org/10.2139/ssrn.4734703.

[11] M. Z. Degefa, I. B. Sperstad, and H. Sæle. "Comprehensive classifications and characterizations of power system flexibility resources." In: *Electric Power Systems Research* 194 (2021), page 107022. DOI: 10.1016/j.epsr.2021.107022.

[12] M. Resch, J. Buhler, B. Schachler, and A. Sumper. "Techno-Economic Assessment of Flexibility Options Versus Grid Expansion in Distribution Grids." In: *IEEE Transactions on Power Systems* 36 (2021), pages 3830–3839. DOI: 10.1109/TPWRS.2021.3055457.

[13] F. Gonzalez-Venegas, M. Petit, and Y. Perez. "Electric Vehicles as flexibility providers for distribution systems. A techno-economic review." In: (2019).

[14] L. Shi, Y. Hao, S. Lv, L. Cipcigan, and J. Liang. "A comprehensive charging network planning scheme for promoting EV charging infrastructure considering the Chicken-Eggs dilemma." In: *Research in Transportation Economics* 88 (2021), page 100837. DOI: 10.1016/j.retrec.2020.100837.

[15] N. Sadeghianpourhamami, N. Refa, M. Strobbe, and C. Develder. "Quantitive analysis of electric vehicle flexibility: A data-driven approach." In: *International Journal of Electrical Power & Energy Systems* 95 (2018), pages 451–462.

[16] *Spirii optimises charging with Load Management.* 2021. URL: https://spirii.com/knowlegde/load-management/.

[17] *What is Dynamic Load Management in EV charging?* 2021. URL: https://www.virta.global/blog/what-is-dynamic-load-management.

[18] F. G. Venegas, M. Petit, and Y. Perez. "Plug-in behavior of electric vehicles users: Insights from a large-scale trial and impacts for grid integration studies." In: *eTransportation* 10 (2021), page 100131. DOI: 10.1016/j.etran.2021.100131.

[19] F. G. Venegas, M. Petit, and Y. Perez. "Active integration of electric vehicles into distribution grids: barriers and frameworks for flexibility services." In: *Renewable and Sustainable Energy Reviews* 145 (2021), page 111060.

[20] R. Fachrizal, M. Shepero, D. van der Meer, J. Munkhammar, and J. Widén. "Smart charging of electric vehicles considering photovoltaic power production and electricity consumption: A review." In: *eTransportation* 4 (2020), page 100056. DOI: https://doi.org/10.1016/j.etran.2020.100056.

[21] X. Su, H. Yue, and X. Chen. "Cost minimization control for electric vehicle car parks with vehicle to grid technology." In: *Systems Science & Control Engineering* 8 (2020), pages 422–433.

[22] M. H. Tveit, K. Sevdari, M. Marinelli, and L. Calearo. "Behind-the-meter residential electric vehicle smart charging strategies: Danish cases." In: *2022 International Conference on Renewable Energies and Smart Technologies*. IEEE. 2022.

[23] M. Müller, Y. Blume, and J. Reinhard. "Impact of behind-the-meter optimised bidirectional electric vehicles on the distribution grid load." In: *Energy* 255 (2022), page 124537. DOI: https://doi.org/10.1016/j.energy.2022.124537.

[24] E. Sortomme, M. M. Hindi, S. D. J. MacPherson, and S. S. Venkata. "Coordinated Charging of Plug-In Hybrid Electric Vehicles to Minimize Distribution System Losses." In: *IEEE Transactions on Smart Grid* 2 (2011), pages 198–205. DOI: 10.1109/TSG.2010.2090913.

[25] K. Prakash, M. Ali, M. Siddique, et al. "Bi-level planning and scheduling of electric vehicle charging stations for peak shaving and congestion management in low voltage distribution networks." In: *Computers and Electrical Engineering* 102 (2022), page 108235.

[26] K. Knezović, S. Martinenas, P. B. Andersen, A. Zecchino, and M. Marinelli. "Enhancing the role of electric vehicles in the power grid: field validation of multiple ancillary services." In: *IEEE Transactions on Transportation Electrification* 3 (2016), pages 201–209.

[27] J. Nájera, H. Mendonça, R. M. de Castro, and J. R. Arribas. "Strategies comparison for voltage unbalance mitigation in LV distribution networks using EV chargers." In: *Electronics* 8 (2019), page 289.

[28] M. Soleimani and M. Kezunovic. "Mitigating transformer loss of life and reducing the hazard of failure by the smart EV charging." In: *IEEE Transactions on Industry Applications* 56 (2020), pages 5974–5983.

[29] E. Yao, V. W. S. Wong, and R. Schober. "Robust Frequency Regulation Capacity Scheduling Algorithm for Electric Vehicles." In: *IEEE Transactions on Smart Grid* 8 (2017), pages 984–997. DOI: 10.1109/TSG.2016.2530660.

[30] S. Falahati, S. A. Taher, and M. Shahidehpour. "A new smart charging method for EVs for frequency control of smart grid." In: *International Journal of Electrical Power & Energy Systems* 83 (2016), pages 458–469. DOI: https://doi.org/10.1016/j.ijepes.2016.04.039.

[31] F. Mwasilu, J. J. Justo, E.-K. Kim, T. D. Do, and J.-W. Jung. "Electric vehicles and smart grid interaction: A review on vehicle to grid and renewable energy sources integration." In: *Renewable and Sustainable Energy Reviews* 34 (2014), pages 501–516. DOI: https://doi.org/10.1016/j.rser.2014.03.031.

[32] K. Sevdari, L. Calearo, P. B. Andersen, and M. Marinelli. "Ancillary services and electric vehicles: An overview from charging clusters and chargers technology perspectives." In: *Renewable and Sustainable Energy Reviews* 167 (2022), page 112666.

[33] E. Netbeheer, Enpuls, ElaadNL, and MAXEM. *Charge Management of Electric Vehicles At Home*. Technical report. ElaadNL, 2020.

[34] K. Sevdari. "Control and clustering of electric vehicle chargers for the provision of grid services." PhD thesis. DTU Wind and Energy Systems, 2023.

[35] H. S. Das, M. M. Rahman, S. Li, and C. W. Tan. "Electric vehicles standards, charging infrastructure, and impact on grid integration: A technological review." In: *Renewable and Sustainable Energy Reviews* 120 (2020).

[36] European commission. *Regulation (EU) 2019/943 on the internal market for electricity*. 2019.

[37] T. Pallesen and P. H. Jacobsen. "Solving infrastructural concerns through a market reorganization: A case study of a Danish smart grid demonstration." In: *Energy Research and Social Science* 41 (2018), pages 80–88. DOI: 10.1016/j.erss.2018.04.005.

[38] H. Stian, A. Heidi, G. Hanne, and D. Espen. *Market based flexibility procurement for Nordic DSOs*. Technical report. 2021.

[39] C. Heinrich, C. Ziras, A. L. Syrri, and H. W. Bindner. "EcoGrid 2.0: A large-scale field trial of a local flexibility market." In: *Applied Energy* 261 (2020), page 114399.

[40] A. Gadea, M. Marinelli, and A. Zecchino. "A market framework for enabling electric vehicles flexibility procurement at the distribution level considering grid constraints." In: Institute of Electrical and Electronics Engineers Inc., 2018. ISBN: 9781910963104. DOI: 10.23919/PSCC.2018.8443012.

[41] J. Ostergaard, C. Ziras, H. W. Bindner, et al. "Energy Security through Demand-Side Flexibility: The Case of Denmark." In: *IEEE Power and Energy Magazine* 19 (2 2021), pages 46–55. DOI: 10.1109/MPE.2020.3043615.

[42] L. Calearo. “Grid integration of electric vehicles: battery degradation and user needs.” PhD thesis. DTU Wind and Energy Systems, 2022.

[43] Transport & Environment. *How implementing the Clean Energy Package can foster electromobility.* Technical report. 2020.

[44] K. Knezović, M. Marinelli, A. Zecchino, P. B. Andersen, and C. Traeholt. “Supporting involvement of electric vehicles in distribution grids: Lowering the barriers for a proactive integration.” In: *Energy* 134 (2017), pages 458–468. DOI: 10.1016/j.energy.2017.06.075.

[45] L. Sørensen, K. B. Lindberg, I. Sartori, and I. Andresen. “Analysis of residential EV energy flexibility potential based on real-world charging reports and smart meter data.” In: *Energy and Buildings* 241 (2021), page 110923. DOI: 10.1016/j.enbuild.2021.110923.

[46] J. Engelhardt. “Reconfigurable Batteries in Electric Vehicle Fast Chargers: Towards Renewable-Powered Mobility.” PhD thesis. DTU Wind and Energy Systems, 2022.

[47] M. K. Gerritsma, T. A. Al Skaif, H. A. Fidder, and W. G. van Sark. “Flexibility of electric vehicle demand: Analysis of measured charging data and simulation for the future.” In: *World Electric Vehicle Journal* 10 (2019), pages 1–22. DOI: 10.3390/wevj10010014.

[48] M. A. van den Berg, I. Lampropoulos, and T. A. AlSkaif. “Impact of electric vehicles charging demand on distribution transformers in an office area and determination of flexibility potential.” In: *Sustainable Energy, Grids and Networks* 26 (2021), page 100452. DOI: 10.1016/j.segan.2021.100452.

[49] J. Rominger, M. Loesch, and ... “Utilization of Electric Vehicle Charging Flexibility to Lower Peak Load by Controlled Charging (G2V and V2G).” In: *FAC Workshop on Control of Smart Grid and Renewable Energy Systems (CSGRES 2019).* 2019, pages 1–6.

[50] E. C. Kara, J. S. Macdonald, D. Black, M. Bérges, G. Hug, and S. Kiliccote. “Estimating the benefits of electric vehicle smart charging at non-residential locations: A data-driven approach.” In: *Applied Energy* (2015 2015). DOI: 10.1016/j.apenergy.2015.05.072.

[51] P. H. Divshali and C. Evens. “Behaviour analysis of electrical vehicle flexibility based on large-scale charging data.” In: *2019 IEEE Milan PowerTech, PowerTech 2019* (2019). DOI: 10.1109/PTC.2019.8810590.

[52] M. Hijjo and A.-L. Klingler. “Modeling and Simulation of Electric Vehicle Flexibility to Support the Local Network.” In: *2021 International Conference on Smart Energy Systems and Technologies (SEST)*. 2021, pages 1–6. DOI: 10.1109/SEST50973.2021.9543258.

[53] M. Voß, M. Wilhelm, and S. Albayrak. “Application independent flexibility assessment and forecasting for controlled EV charging.” In: *SMARTGREENS 2018 - Proceedings of the 7th International Conference on Smart Cities and Green ICT Systems* 2018-March (2018), pages 108–119. DOI: 10.5220/0006795601080119.

[54] J. Zhang, L. Che, X. Wan, and M. Shahidehpour. “Distributed Hierarchical Coordination of Networked Charging Stations based on Peer-to-peer Trading and EV Charging Flexibility Quantification.” In: *IEEE Transactions on Power Systems* (2021), pages 1–1. DOI: 10.1109/TPWRS.2021.3123351.

[55] C. Gschwendtner, C. Knoeri, and A. Stephan. “Mind the goal: Trade-offs between flexibility goals for controlled electric vehicle charging strategies.” In: *Iscience* 26 (2023).

[56] J. B. Gutierrez-Lopez and D. Möst. “Characterising the flexibility of electric vehicle charging strategies: a systematic review and assessment.” In: *Transport Reviews* 43 (2023), pages 1237–1262.

[57] Å. L. Sørensen, B. B. Morsund, I. Andresen, I. Sartori, and K. B. Lindberg. “Energy profiles and electricity flexibility potential in apartment buildings with electric vehicles–A Norwegian case study.” In: *Energy and Buildings* 305 (2024), page 113878.

[58] N. K. Panda and S. H. Tindemans. “Efficient quantification and representation of aggregate flexibility in Electric Vehicles.” In: *Electric Power Systems Research* 235 (2024), page 110811.

[59] F. Al Taha, T. Vincent, and E. Bitar. “An efficient method for quantifying the aggregate flexibility of plug-in electric vehicle populations.” In: *IEEE Transactions on Smart Grid* (2024).

[60] E. UK. *connecting your fleet - A guide for businesses in Greater London*. URL: https://www.energy-uk.org.uk/publication.html?task=file.download&id=7673.

[61] L. Calearo, C. Ziras, K. Sevdari, and M. Marinelli. “Comparison of Smart Charging and Battery Energy Storage System for a PV Prosumer with an EV.” In: (2021), pages 1–6.

[62] O. Frendo, J. Graf, N. Gaertner, and H. Stuckenschmidt. “Data-driven smart charging for heterogeneous electric vehicle fleets.” In: *Energy and AI* 1 (2020), page 100005.

[63] M. Nour, S. Said, A. Ali, and C. Farkas. “Smart charging of electric vehicles according to electricity price.” In: (2019), pages 158–163.

[64] T. Alghamdi, D. Said, and H. Mouftah. “Decentralized electric vehicle supply stations (D-EVSSs): A realistic scenario for smart cities.” In: *IEEE Access* 7 (2019), pages 91327–91338.

[65] Z. Lee, G. Lee, T. Lee, C. Jin, and R. Lee. “Adaptive charging networks: A framework for smart electric vehicle charging.” In: *IEEE Transactions on Smart Grid* 12 (2021), pages 305–317.

[66] F. Tuchnitz, N. Ebell, J. Schlund, and M. Pruckner. “Development and evaluation of a smart charging strategy for an electric vehicle fleet based on reinforcement learning.” In: *Applied Energy* 285 (2021), page 116380.

[67] B. Vaidya and H. Mouftah. “Smart electric vehicle charging management for smart cities.” In: *IET Smart Cities* 2 (2020), pages 22–29.

[68] S. Hussain, C. Lai, and U. Eicker. “Flexibility: Literature review on concepts, modeling, and provision method in smart grid.” In: *Sustainable Energy, Grids and Networks* 34 (2023), page 100717.

[69] H. Khalkhali and S. Hosseinian. “Multi-class EV charging and performance-based regulation service in a residential smart parking lot.” In: *Sustainable Energy, Grids and Networks* 23 (2020), page 100354.

[70] M. K. Gerritsma, T. A. AlSkaif, H. A. Fidder, and W. G. van Sark. “Flexibility of electric vehicle demand: Analysis of measured charging data and simulation for the future.” In: *World Electric Vehicle Journal* 10 (2019), page 14.

[71] J. Park, Y. Sim, G. Lee, and D. Cho. “A fuzzy logic based electric vehicle scheduling in smart charging network.” In: *2019 16th IEEE Annual Consumer Communications and Networking Conference (CCNC)* (2019), pages 1–6.

[72] D. Chekired and L. Khoukhi. “Smart grid solution for charging and discharging services based on cloud computing scheduling.” In: *IEEE Transactions on Industrial Informatics* 14 (2017), pages 1220–1231.

[73] C. Diaz-Londono, L. Colangelo, F. Ruiz, and D. Patino. “Optimal strategy to exploit the flexibility of an electric vehicle charging station.” In: *Energies* 12 (2019), page 3834.

[74] J. Zhang, L. Che, and X. Wan. "Distributed hierarchical coordination of networked charging stations based on peer-to-peer trading and EV charging flexibility quantification." In: *IEEE Transactions on Smart Grid* 12 (2021), pages 3205–3217.

[75] O. Frendo, N. Gaertner, and H. Stuckenschmidt. "Open Source Algorithm for Smart Charging of Electric Vehicle Fleets." In: *IEEE Transactions on Industrial Informatics* 17 (2021), pages 6014–6022. DOI: 10.1109/TII.2020.3038144.

[76] M. Marinelli, S. Martinenas, K. Knezović, and P. B. Andersen. "Validating a centralized approach to primary frequency control with series-produced electric vehicles." In: *Journal of Energy Storage* 7 (2016), pages 63–73. DOI: 10.1016/j.est.2016.05.008.

[77] N. B. Arias, S. Hashemi, P. B. Andersen, C. Træholt, and R. Romero. "V2G enabled EVs providing frequency containment reserves: Field results." In: *2018 IEEE international conference on industrial technology (ICIT)* (2018), pages 1814–1819.

[78] J. García-Villalobos, I. Zamora, J. I. S. Martín, F. J. Asensio, and V. Aperribay. "Plug-in electric vehicles in electric distribution networks: A review of smart charging approaches." In: *Renewable and Sustainable Energy Reviews* 38 (2014), pages 717–731. DOI: 10.1016/j.rser.2014.07.040.

[79] R. F. Atallah, C. M. Assi, W. Fawaz, M. H. K. Tushar, and M. J. Khabbaz. "Optimal Supercharge Scheduling of Electric Vehicles: Centralized Versus Decentralized Methods." In: *IEEE Transactions on Vehicular Technology* 67 (9 2018), pages 7896–7909. DOI: 10.1109/TVT.2018.2842128.

[80] *AWS pricing*. Accessed on the 18th of September 2024. URL: https://aws.amazon.com/pricing/.

[81] *Oracle pricing*. Accessed on the 18th of September 2024. URL: https://www.oracle.com/cloud/pricing/.

[82] C. Ziras, A. M. Prostejovsky, H. W. Bindner, and M. Marinelli. "Decentralized and discretized control for storage systems offering primary frequency control." In: *Electric Power Systems Research* 177 (March 2019), page 106000. DOI: 10.1016/j.epsr.2019.106000.

[83] L. Gan, U. Topcu, and S. H. Low. "Optimal decentralized protocol for electric vehicle charging." In: *IEEE Transactions on Power Systems* 28 (2013), pages 940–951. DOI: 10.1109/TPWRS.2012.2210288.

[84] P. Richardson, D. Flynn, and A. Keane. "Local versus centralized charging strategies for electric vehicles in low voltage distribution systems." In: *IEEE Transactions on Smart Grid* 3 (2012), pages 1020–1028. DOI: 10.1109/TSG.2012.2185523.

[85] Statnett SF. *Distributed balancing of the power grid*. Technical report. 2021, pages 1–48.

[86] X. Han, K. Heussen, O. Gehrke, H. W. Bindner, and B. Kroposki. "Taxonomy for Evaluation of Distributed Control Strategies for Distributed Energy Resources." In: *IEEE Transactions on Smart Grid* 9 (5 2018), pages 5185–5195. DOI: 10.1109/TSG.2017.2682924.

[87] S. Faddel and O. A. Mohammed. "Automated distributed electric vehicle controller for residential demand side management." In: *IEEE Transactions on Industry Applications* 55 (2018), pages 16–25.

[88] C.-H. Lo and N. Ansari. "Decentralized controls and communications for autonomous distribution networks in smart grid." In: *IEEE transactions on smart grid* 4 (2012), pages 66–77.

[89] X. Han, K. Heussen, O. Gehrke, H. W. Bindner, and B. Kroposki. "Taxonomy for Evaluation of Distributed Control Strategies for Distributed Energy Resources." In: *IEEE Transactions on Smart Grid* 9 (2018), pages 5185–5195. DOI: 10.1109/TSG.2017.2682924.

[90] *DS/EN 61851-1:2019. Electric vehicle conductive charging system - Part 1: General requirements*. 2019.

[91] K. Sevdari, L. Calearo, B. H. Bakken, P. B. Andersen, and M. Marinelli. "Experimental validation of onboard electric vehicle chargers to improve the efficiency of smart charging operation." In: *Sustainable Energy Technologies and Assessments* 60 (2023), page 103512. DOI: https://doi.org/10.1016/j.seta.2023.103512.

PART II

# Collection of papers

# PAPER [P1]

## Barriers and Solutions for EVs Integration in the Distribution Grid

Authors:

Simone Striani, Kristian Sevdari, Lisa Calearo, Peter Bach Andersen, Mattia Marinelli

Published in:

*Proceedings of the 2021 56th International Universities Power Engineering Conference (UPEC)*

DOI:

10.1109/UPEC50034.2021.9548235.

# Barriers and Solutions for EVs Integration in the Distribution Grid

Simone Striani, Kristian Sevdari, Lisa Calearo, Peter Bach Andersen, Mattia Marinelli
*Department of Electrical Engineering*
*Technical University of Denmark*
Roskilde, Denmark
{sistri; krisse; lica; matm; pba}@elektro.dtu.dk

2021 56th International Universities Power Engineering Conference (UPEC) | 978-1-6654-4389-0/21/$31.00 ©2021 IEEE | DOI: 10.1109/UPEC50034.2021.9548235

***Abstract*—The mass penetration of electric vehicles (EVs) could develop grid stability problems due to the increase of peak loads created by coincident charging factors. Smart charging is the control of the EV charging loads and has long been identified as a potential solution. Smart charging could also contribute to grid stability by mitigating the intermittent nature of renewable energy generation. This paper describes the current status of EV flexibility services at the distribution level. The analysis of the smart charging status is done considering the technological, economic and regulatory frameworks, and presenting what the different barriers of each of these aspects are. Additionally, the paper introduces the ACDC project (Autonomously Controlled Distributed Charger), which aims at developing an EV clustering method based on distributed smart charging control logic for flexibility services. For divulgation purposes, the scheduled test case scenario of the parking lot at the Technical University of Denmark is described. The paper concludes on some of the most relevant actions to overcome the most imminent barriers and to push further the roll-out of EV charging infrastructure towards the target EV penetration planned by policymakers.**

***Index Terms*—Electric Vehicle, Distribution Grid, Smart Charging, Flexibility**

## I. Introduction

In order to achieve draw-down of $CO_2$ emissions, the governments are trying to hinder the reliance on fossil fuels for energy production and transportation, in favor of sustainable technologies. On the energy production front, this means promoting renewable energy systems (RES), while regarding the transportation sector, this consists of speeding up the electrification of private and public transportation systems through the roll-out of electric vehicle (EV) technologies. The global scheduled roll-out of EVs aims at reaching 50 million EVs by 2025 and 140 million by 2030 [1]. Charging large EV fleets can result in stability and security challenges in the distribution grid, associated with grid components not being properly dimensioned to stand the resulting increased power required [2]. However, thanks to smart charging, EVs have the potential of adapting their power consumption to the current needs of the distribution grid. The provision of such distribution grid services could delay, or even set aside, the necessity for costly grid updates [3].

Many demonstration projects [4] are currently working on the feasibility of different grid services through smart charging, providing test cases to gain experimental data. EV clusters can be deployed both behind the meter (BTM) and in front of the meter (FTM) [5]. BTM services are services provided to the users and they consist of load coordination among different EVs, buildings (residential, commercial or industrial) and eventual distributed energy resources (DER) at the connection point. FTM services are provided to the Distribution System Operators (DSOs). In this case the EVs can be coordinated in groups by aggregators and provide their flexibility directly to the grid. Smart charging could contribute to the supply adequacy and quality, reduction of peak loads and transformer congestion, reduction of curtailment and allowance for higher usage of low-cost RES electricity [6], [7]. The challenges associated with the integration of EVs in the power system can be categorized in technological, economics, and policy related [8]. The objective of this paper is to identify and list the most relevant challenges in each of these categories, and to conclude by suggesting a set of actions that could be taken for overcoming such obstacles. Furthermore, this paper introduces the ACDC (Autonomously Controlled Distributed Charger) project providing an overview of its demonstration layout.

Firstly, section II provides a conceptual basis including the definition of different EV flexibility services. Secondly, section III describes the status of technological maturity of EV smart chargers. Section IV, provides a description of the economic framework for flexibility while in section V there is a description of the regulatory status of EV infrastructures. Finally, section VI introduces the ACDC project and section VII concludes with some general recommendations deduced from the literature review in each of the described field.

## II. Smart Charging as grid flexibility service

This section describes in more details the different smart charging configurations and explains what are the flexibility services. The section ends with a description of the properties of flexibility services useful for the following sections.

### A. Smart charging

In Fig.1 the possible smart charging configurations are illustrated. The unidirectional power flow (V1G) chargers allow the car to adjust its rate of charging. Additionally, the vehicle-to-grid (V2G) technology allows to inject power back to the grid. These configurations are FTM because the charger interacts directly with the grid and can be directly controlled by the DSO or aggregator.

978-1-6654-4389-0/21/$31.00 © 2021 IEEE

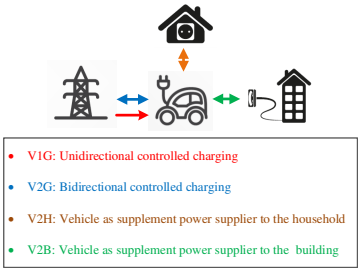


Fig. 1. Illustration of different smart charging configurations adapted from [9].

The other two are vehicle-to-home (V2H) and vehicle-to-building (V2B), both BTM configurations: in these last two configurations the car is connected to a house or a building and it adjusts its consumption to generate services for the household/building (V2H/V2B).

### B. Possible flexibility services from EVs

In the power grid, flexibility services are power regulations performed by either supply or demand, with the scope of maximising the security and stability of energy supply. Fig. 2 describes the main services that can be provided with EVs. Such services can be categorized in system flexibility and local flexibility. The first category consists of services that target the system as a whole, including the transmission and the production side of the grid. The local flexibility, which is the main focus of this paper, consists of DSO services (also called FTM services) and BTM services. The DSO services are directly managed and controlled by the DSO through contracts with aggregators or directly with the user. They aim at reducing voltage unbalances (voltage magnitude regulation, phase voltage unbalance reduction), solving the grid instabilities related with the capacity of transformers and lines cables (congestion prevention, capacity management), optimizing the loads to reduce losses (loss reduction) and increase the power quality by active or reactive power injection (power quality correction). Smart chargers available today are still not capable of power quality correction, although studies showed that it could need little development effort and be profitable [10].

BTM services aim at minimizing the electricity cost by importing the least possible energy from the grid and schedule charging at times where the cost of electricity is lower.

In order to clearly define the quantity and the quality of a flexibility service, we follow the definition of theoretical and practical attributes given by the authors in [11]. Theoretical attributes are the attributes that characterize the ideal load modulation set point. Practical attributes are additional attributes introduced due to the unideality of the systems (e.g. delays, tolerances, etc.), and they describe the actual performance with which the charger can follow those set-points. These attributes are described below.

**Theoretical Attributes:**

- *Direction*: Unidirectional or Bidirectional power adjustment capabilities (V1G or V2G).
- *Power Capacity*: Maximum active power possible.
- *Starting time*: Starting time of the service.
- *Duration*: Duration of the service.
- *Location*: Location of the electric vehicle supply equipment (EVSE) or EV related to the grid topology.

**Practical Attributes:**

- *Accuracy*: Maximum allowed tolerance between required and delivered power response.
- *Precision*: Maximum allowed tolerance between the power setpoint and the actual power erogation.
- *Activation Time*: Time between setpoint reception and flexibility activation.
- *Ramp-up time*: Time that it takes for the charger to adapt to a higher set-point.
- *Ramp-down time*: Time that it takes for the charger to adapt to a lower set-point.

These attributes need to be assessed to be within standardized tolerances, and to be transparently communicated among the stakeholders for the provision of flexibility services. Such communication is crucial for the establishment of quality and therefore value of the different products provided.

## III. Current Technology and Infrastructures

### A. Electric Vehicle Supply Equipment

Nowadays smart charging technologies have reached market roll-out in Europe. The overview of the commercially available chargers carried out in [12] concludes that, in 2020, more than 50% of the available EVSE presented smart charging functionalities. The most common functionalities reported in the paper are load modulation (dynamic load management and limitation of power setpoints) and power sharing with the household/building. Here, some of the capabilities of the top-end smart chargers available today are described:

- *BTM functionalities*: These capabilities refer to the ability to coordinate the charging between the vehicles and the household/building demand and eventual DER production. The charging can be coordinated via power sharing, scheduling and charging prioritization (using state-of-charge (SOC), driving plan or pattern).
- *Inter-connectivity*: In order to provide the above-mentioned distribution services and BTM functionalities, smart chargers are able to have multiple communication channels: they are connected locally with the building energy meter, but also they are connected to the internet, from which they could be coordinated by aggregators in order to provide flexibility. Moreover, their status is usually available via the internet or Bluetooth so that the user can interact remotely with the EV, the charger and easily plan his trip.
- *System recognition*: ID number of the individual EVSE, or alternatively of the EV, must be defined to ensure that the proper user is procured and remunerated for the delivered flexibility. Further information

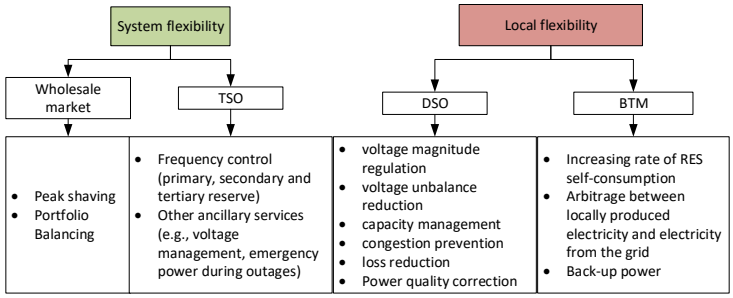


Fig. 2. Description of the different flexibility services that EVs can provide.

should also be made accessible by the EV manufacturers, which is, e.g., currently not the case for the SOC data. Naturally, user privacy must be ensured by regulations so that all collected data are treated as confidential and kept private.

It is important to notice that the capabilities listed describe the top-end chargers available, and therefore the characteristics are not representative of the average of the chargers in the market and even less of the chargers currently deployed. Indeed the majority of the chargers in European cities are not capable of any smart function, thus also called ”dumb” chargers.

### *B. Control architecture*

The coordination and control of different clusters of smart chargers need to be performed effectively by the DSO, user or aggregator. Different control architectures have been proposed and investigated in the literature [13]. They can be categorized into centralized, decentralized or distributed control architectures. The centralized architectures rely on a central intelligence called Cloud Aggregator (CA), which controls directly all the chargers. In the decentralized approach, the intelligence is called Virtual Aggregator (VA). The VA resides in each charger and is therefore sensitive to local measurements. Since the centralized control relies on a single server, it is prone to disconnection errors and delays. On the other hand, the decentralized system is very robust, although its controlling capacity is less efficient due to the limited data it receives from the system. Finally, the distributed control approach combines the benefits from both architectures. It is able to coordinate between local control and global control because it communicates both with VA and CA.

### *C. Grid observability and smart metering*

One of the most important factors in the prompt development of charging infrastructures is the development of smart metering and grid observability. Direct measurements from EVSE or other local metering systems could provide the DSO with more knowledge about the grid, making it capable of judging if flexibility procurement or grid reinforcement are necessary.

Countries where the adoption of smart chargers is combined with experimental demonstration campaigns are leading the way towards the generation of invaluable lessons on user behaviours, the correct planning of charging infrastructures as well as economic and policies suggestion for aggregators, DSOs and governments [14].

In the majority of the countries where smart meters are deployed, all units are certified and installed by the DSO, which is also responsible for data collection and management.

It is of particular importance to clearly define the requirements on the specific measurement parameters, such as the sampling rate, which must be chosen as a trade-off between the information speed on the one hand, and the installation and data management cost on the other.

The European Clean Energy Act requires that all member states assess the cost-benefit of smart meters and ensure that at least 80% of consumers are equipped with smart meters by 2024, if the cost-benefit analysis is positive [15]. It is also stated that smart meters functionalities should include remote reading with two-way communication and a sampling rate not greater than 15-min. Yet, there are no international standards that would ensure these functionalities, so the status across Europe considerably varies.

However, several European countries have plans for a wide-scale roll-out of smart meters supported by the national regulatory framework. Yet, there is still a relatively large share of countries that has not started their deployment due to negative or inconclusive results of the cost-benefit analysis [2].

As a result, many of the consumers still buy ”dumb chargers” because they are cheaper and countries do not incentivize the purchase of smart options. The additional cost of retrofitting the older EVSEs once EV smart charging becomes a common practice should be considered.

The EV chargers and models need to show their internal parameters to DSOs and aggregators to be managed correctly in the flexibility service. There is still a lack of experimental data on the practical attributes of the EV capabilities, and authors in [16] state that there might be a difference in EVs response accuracy based on the external conditions.

Smart meters characteristics and functions need to be standardized as their varying performances is observed to be one of the major barriers towards flexibility procurement.

### D. Information and communication technologies

Information and communication technology (ICT) ensures advanced metering, control and transactional communication among different stakeholders: EVs, EVSEs, DSOs, TSOs, market operators/players and the end-user. ICTs are crucial to provide grid monitoring for the actual research and development of flexibility services. EV-related communication protocols can be divided into front-end and back-end protocols, and they are respectively between the EV and EVSE and between the EVSE and a third party, such as an aggregator. Nowadays, the vast majority of contemporary EVs are compliant with IEC 61851 or SAE J1772 standard, according to which the EV charging current can be limited between the minimum charging current of 6 A and the maximum one, which is the EVSE rated current (10 A, 16 A, 32 A, etc.). One of the present limits of the existing protocols is the lack of communication of fundamental EV information, such as battery size and SOC. Moreover, there are not protocols that support entirely V2G functions. Standard ISO/IEC 15118 covers communication between EVSE and EV, as well as among all stakeholders involved in the supply process [17]. It takes into account the data encryption for both confidentiality and data integrity purposes and it is currently being revised to include V2G functionalities if used together with OCCP 2.0 or IEC 63110 (between EVSE and aggregator or charge point operator).

## IV. Economic framework for flexibility

The economic framework for flexibility services is a central barrier hindering the development of a flexibility value chain. The economic and regulatory frameworks are hugely interconnected. This section will illustrate different economic tools currently under development for creating flexibility value on the DSO perspective that are proposed by the literature [18].

### A. Grid codes

This approach proposes to update grid codes for grid connection of flexible loads or DER with the scope of imposing flexibility requirements. There are discussions on what should be strategical requirements to facilitate the development of market-based flexibility services.

### B. Connection agreements

These are agreements between DSOs and consumers for flexibility provision. There are two main types of smart connection contracts: interruptible contracts and variable capacity contracts (VCCs) [8]. Interruptible contracts entitle the DSOs to control EV charging energy consumption based on the grid conditions. This type maximizes grid stability at the expense of user comfort and acceptance. In VCCs, the DSOs provide scheduled or dynamic max power allowance for charging necessities and related dynamic prices.

### C. Electricity tariffs

This mechanism generates an indirect provision of flexibility because it encourages end-users to adapt their consumption. Network tariffs are paid by the consumers, together with other taxes. They consist of roughly 25% of the electricity bill and resemble the planning and operational costs of the network. There are different kinds of tariff structures/components: energy component (€/kWh), capacity component (€/kW), grid connection component (€). Currently, not all countries are deploying network tariffs to encourage the use of flexibility. Although some of the above-mentioned tariffs are still under development, every country should update the electricity tariff to include at least two components: the capacity and an energy one [11].

The ToU (Time-of-Use) tariff is a simple price mechanism to incentivize off-peak consumption that could result in reduced congestion. However, with high-penetration scenarios the charging synchronization of large fleets during off-peak hours is a potential risk.

A tariff structure trending in current research is the Distribution Locational Marginal Prices (DLMPs), where the cost of electricity is dependent on the particular nodes of the distribution grid. There are different variations of such tariff, which can include local constraints such as voltage, losses, power quality, etc. These structures, although promising, raise some important concerns regarding the difficulty of implementation as well as inequality and transparency issues.

Dynamic capacity tariffs could be a very efficient framework. These tariffs would force consumers to adapt their maximum consumption to the grid conditions for a given period of time. The drawbacks of the capacity tariffs are that they could hinder the development of fast-charging stations.

### D. Flexibility markets

In recent years some markets for different EV flexibility services were developed (for example, system balancing and energy management) and started being used by aggregators. EV flexibility markets at the distribution level are still far from sufficient, since there is not a market structure and digital infrastructure [19]. Regulators should incentivize the creation of a larger number of smaller local flexibility markets based on nodal pricing systems [20]. With a Market-based approach, DSOs explicitly procure flexibility services from a market. The penetration of the EV-based services in flexibility markets will increase the value of such services and allow their trading among different stakeholders. Again, there are various viable approaches: Long or Medium-term bilateral contracts or short terms Market Platforms. The role of the DSO is to define the flexibility requirements, which can be offered by different aggregators or prosumers.

Market frameworks have a strong potential to generate value for all stakeholders [21] and are the preferred approach by regulators.

## V. Regulation

### A. Redefining the role of DSOs

Before the beginning of the transition towards renewable energy resources the grid was easier to operate. This is because it had a virtually radial shape with the consumers at the center and the producers at the outer radiuses. The

flow was unidirectional and the loads and production were easier to forecast and control. Therefore the DSO approach to congestion and voltage issues was simply reinforcing the grid when needed (the so-called "fit-and-forget" approach). The economic and regulatory frameworks were therefore built around this model and the DSOs were remunerated based on the capital expenditures (CAPEX) for grid renovation.

Nowadays, the evolution towards smart grids requires a shift towards a TOTEX-based (total expenditure) framework, where the DSOs need to minimize their OPEX (operational expenditure) as well as the CAPEX. This need is at the moment only partially met and there is still need for a reform of the regulatory framework to push the DSOs to manage their expenditures proactively and to deploy the value of load flexibility [22].

### B. Standardization of EV connections

Because of its technological novelty, there are often some administrative problems related to V2G technology. In more details, V2G chargers installation imply additional and often redundant administrative procedures that discourage their adoption by the user. The cause of these obstacles is that connection requirements, classification and standardization of V2G connections are not fully developed yet. Regulators, system operators, EV and EVSE manufacturers need to work on the standardization of interconnection requirements in order to reduce the administrative processes and ensure safety for both end-user and the system itself. On the other hand, V1G, V2H and V2B are more technologically mature and their connections have already been standardized in the previous years [17].

### C. Interaction between actors

As previously stated, there are different approaches for DSOs to provide flexibility: Grid codes based, contract based and market based approaches. The grid codes based approach requires the DSOs to stipulate direct obligations for flexibility provisions or contract arrangements directly with the EV user so that they can directly control the EV charging process. The market-based approaches require an additional interaction between DSOs and TSO. The interaction between DSOs and EV users often requires the mediation of aggregators, which can cluster different EVs and manage their flexibility into tradeable services packages.

The interaction between DSOs and TSOs is considered a key aspect in the European Clean Energy Package as the penetration of RES and DER increases. This is because the distribution network and the transmission network often have different needs that could be in contrast. Often the needs of the transmission network need to be prioritized compared to the ones of the distribution network.

## VI. The ACDC Project

Some of the aspects discussed in this paper are analysed by the ACDC project. The ACDC (Autonomously Controlled Distributed Charger) is a Danish project that aims at developing a clustering method for autonomous smart charging with distributed control architecture and a virtual aggregator. The cluster contains a set of EV chargers controlled to provide FTM and BTM grid services. The global grid status is communicated via a Cloud Aggregator, through which FTM services can be provided. Furthermore, the local coordination between the chargers for BTM services is handled by the virtual aggregator. The development of the clustering method is ongoing, although a more detailed description of the control logic is available in [23] together with the simulation results of a V2H scenario with 2 EVs. As part of the demonstration campaign, the designed technology will be installed in one of the parking lots of the Risø research campus of the Danish Technical University (DTU). A satellite picture of the parking lot is shown in Fig. 3. The scope is to validate the charging performances in a V2B office case. The parking lot will host 8 smart chargers with 2 type-2 plugs each. Each plug can support a maximum charge rate of 11 kW from a 3 phase charger. The parking lot could potentially charge with a max power of 88 kW. However, the grid capacity of the parking is limited to 43 kW (63 A, 3 phase). The parking lot will serve to develop and demonstrate ACDC's distributed charging control logic for BTM and FTM services under limited grid capacity.

Fig. 3. Satellite picture of the parking lot location. The red dots indicate the chargers.

## VII. Conclusion

An overview of the current development status of the EV integration in the distribution grid was provided. Many authors believe that smart chargers could potentially be an important component of the future smart grid. Smart charging could drastically reduce the drawbacks related to EV integration and, at the same time, solve the increasing grid instability problems due to other sources, like DER. However, there are still many barriers before the smart charging technology is fully mature. In this paper, the authors described the current status of EV flexibility services at the distribution level, including the technological, economic and regulation perspectives. Moreover, the

TABLE I
FUTURE STEPS NEEDED TO PUSH THE DEVELOPMENT OF ROBUST EV INFRASTRUCTURES FOR DISTRIBUTION GRID SERVICES IN EACH OF THE FIELDS ANALYZED

| **Technical** | **Economic framework** | **Regulatory framework** |
|---|---|---|
| Further R&D on smart charging capabilities. | Keep or introduce temporary incentives for cars, shared mobility and Mobility-as-a-service | Enhance active management requirement to DSOs |
| Standardize and ensure interoperability between different EVs and EVSE. | Research on business models for aggregators and charge point operators | Standardize cost-benefit analysis for smart meters |
| Develop and test ICT and standards (especially V2G) | Develop and test new Network tariff structures | Ensure a clear classification and standardization of V2G connection requirements for V2G prosumers |
| User interactivity and interconnectivity | Strategical location for different types of chargers to ensure trust in EV infrastructures investors | Create incentives for smart chargers purchase |
| Continue the demonstration project campaigns to gather data. | Establish local flexibility platforms with increasingly competitive approaches. | Define DSO-TSO priorities and the interaction between every stakeholder |
| Increase grid observability | Continuous revision and improvement of economic framework of flexibility based on the lessons learned | Set ambitious targets ($CO_2$ reduction, targets for different transport types) |

authors introduced the ACDC project and a test case of its demonstration campaign to explain part of the ongoing research and development on clustering methods for smart charging functionalities. In conclusion, recommendations on possible steps to be followed in each of the analyzed perspectives are summarized in table I: From a technical point of view, the bottleneck for the roll-out of smart charging is the related ICT: Development of the existing standards and protocols is needed to ensure EVSE-EV interoperability, user-EVSE interactivity and grid observability. From an economic point of view, the focus should be on two aspects: developing market platforms to provide trading of services and developing business models to assure profitability for investors of EV infrastructures, as well as aggregators and prosumers. Finally, the regulatory framework should set ambitious targets and stimulate technical and economic value-chain development. This can be done by standardizing and including the different technologies, defining their available products and regulating the interaction between stakeholders along the value chain.

## ACKNOWLEDGMENT

The work in this paper is supported by the research projects ACDC (EUDP grant number: 64019-0541) and FUSE (EUDP grant number: 64020-1092).

## REFERENCES

[1] International Energy Agency, "Global ev outlook: Entering the decade of electric drive," tech. rep., 2020.

[2] K. Knezović, M. Marinelli, A. Zecchino, P. B. Andersen, and C. Traeholt, "Supporting involvement of electric vehicles in distribution grids: Lowering the barriers for a proactive integration," *Energy*, vol. 134, pp. 458–468, 2017.

[3] L. Calearo, A. Thingvad, H. H. Ipsen, and M. Marinelli, "Economic value and user remuneration for ev based distribution grid services," *Proceedings of 2019 IEEE PES Innovative Smart Grid Technologies Europe, ISGT-Europe 2019*, 9 2019.

[4] M. Marinelli et al., "Electric vehicles demonstration projects-an overview across europe," *UPEC 2020 - 2020 55th International Universities Power Engineering Conference, Proceedings*, 9 2020.

[5] International Renewable Energy Agency, "Behind-the-meter batteries: innovation landscape brief," tech. rep., 2019.

[6] P. Hanemann, M. Behnert, and T. Bruckner, "Effects of electric vehicle charging strategies on the german power system," *Applied Energy*, vol. 203, pp. 608–622, 2017.

[7] M. V. D. Berg, I. Lampropoulos, and T. AlSkaif, "Impact of electric vehicles charging demand on distribution transformers in an office area and determination of flexibility potential," *Sustainable Energy, Grids and Networks*, vol. 26, p. 100452, 2021.

[8] F. G. Venegas, M. Petit, and Y. Perez, "Active integration of electric vehicles into distribution grids: Barriers and frameworks for flexibility services," *Renewable and Sustainable Energy Reviews*, vol. 145, p. 111060, 7 2021.

[9] The International Renewable Energy Agency, "Innovation outlook: Smart charging for electric vehicles," tech. rep., 2019.

[10] S. Martinenas, K. Knezovic, and M. Marinelli, "Management of power quality issues in low voltage networks using electric vehicles: Experimental validation," *IEEE Transactions on Power Delivery*, vol. 32, pp. 971–979, 4 2017.

[11] K. Knezović, M. Marinelli, P. Codani, and Y. Perez, "Distribution grid services and flexibility provision by electric vehicles: A review of options," *Proceedings of the Universities Power Engineering Conference*, vol. 2015-November, 2015.

[12] K. Sevdari, "Electric vehicle chagers market outlook," tech. rep., 2020.

[13] X. Han et al., "Taxonomy for Evaluation of Distributed Control Strategies for Distributed Energy Resources," *IEEE Transactions on Smart Grid*, 2018.

[14] C. Hecht, S. Das, C. Bussar, and D. U. Sauer, "Representative, empirical, real-world charging station usage characteristics and data in germany," *eTransportation*, vol. 6, 11 2020.

[15] European commission, "Regulation (eu) 2019/943 on the internal market for electricity," 2019.

[16] K. Knezovic, S. Martinenas, P. B. Andersen, A. Zecchino, and M. Marinelli, "Enhancing the role of electric vehicles in the power grid: Field validation of multiple ancillary services," *IEEE Transactions on Transportation Electrification*, vol. 3, pp. 201–209, 3 2017.

[17] H. S. Das, M. M. Rahman, S. Li, and C. W. Tan, "Electric vehicles standards, charging infrastructure, and impact on grid integration: A technological review," *Renewable and Sustainable Energy Reviews*, vol. 120, 3 2020.

[18] Council of European Energy Regulators, "Flexibility use at distribution level," tech. rep., 2017.

[19] T. Pallesen and P. H. Jacobsen, "Solving infrastructural concerns through a market reorganization: A case study of a danish smart grid demonstration," *Energy Research and Social Science*, vol. 41, pp. 80–88, 7 2018.

[20] J. Ostergaard et al., "Energy security through demand-side flexibility: The case of denmark," *IEEE Power and Energy Magazine*, vol. 19, pp. 46–55, 3 2021.

[21] A. Gadea, M. Marinelli, and A. Zecchino, "A market framework for enabling electric vehicles flexibility procurement at the distribution level considering grid constraints," *20th Power Systems Computation Conference, PSCC 2018*, 8 2018.

[22] Transport & Environment, "How implementing the clean energy package can foster electromobility," tech. rep., 2020.

[23] K. Sevdari, L. Calearo, S. Striani, L. Rønnow, P. B. Andersen, and M. Marinelli, "Autonomously distributed control of electric vehicle chargers for grid services," 2021, under-review.

PAPER [P2]

# Flexibility Potential Quantification of Electric Vehicle Charging Clusters

Authors:

Simone Striani, Tim Unterluggauer, Peter Bach Andersen, Mattia Marinelli

Under review in:

*Sustainable Energy, Grids and Networks*

# Flexibility Potential Quantification of Electric Vehicle Charging Clusters

Simone Striani, Tim Unterluggauer, Peter Bach Andersen, Mattia Marinelli
*Department of Wind and Energy Systems*
*Technical University of Denmark*
Roskilde, Denmark
{sistri; timun; pba; matm}@dtu.dk

***Abstract*—A significant obstacle to providing flexibility services with electric vehicles (EVs) is the uncertainty surrounding the profitability and flexibility potential of charging clusters when utilised as a flexible load. Currently, there is a lack of comprehensive and easily applicable methods for quantifying flexibility in the literature. This paper introduces an evaluation tool and a set of flexibility indexes to assess the capability of charging clusters to deliver flexibility services. The method is designed to evaluate and quantify the flexibility potential of charging clusters in terms of short-term and long-term power adjustments and charge scheduling. Through sensitivity analysis, we examine how connection capacity, EV battery capacities, power capabilities, and the number of daily charging sessions influence the flexibility potential of charging clusters. Our findings highlight a direct relationship between the grid connection capacity of clusters and their ability to perform short-term power adjustments. Moreover, while larger batteries tend to reduce energy and time flexibility, their increased storage capability facilitates managing and scheduling a larger energy volume. Furthermore, for the days analysed, the flexibility potential showed minimal sensitivity to the number of daily charging sessions. Instead, the amount of energy requested and connection patterns emerge as key determinants of overall flexibility. In summary, this research provides valuable insights that can inform the design, monitoring, and assessment of EV charging clusters when evaluating their suitability for various flexibility services.**

## List of Abbreviations

| | |
|---|---|
| **APFI** | Average Power Flexibility Index |
| **BTM** | Behind the meter |
| **CAPEX** | Capital expenditures |
| **CPO** | Charge point operator |
| **DER** | Distributed energy resource |
| **EFI** | Energy Flexibility Index |
| **FTM** | In front of the meter |
| **HEF** | Hourly energy flexibility |
| **MPFI** | Minimum Power Flexibility Index |
| **OPEX** | Operational expenditures |
| **RES** | Renewable Energy Sources |
| **SoC** | State of charge |
| **TFI** | Time Flexibility Index |

## I. Introduction

The push to electrify the transport sector as a means of reducing carbon emissions has spurred extensive research into challenges related to the adoption of electric vehicles (EVs), including the planning of charging infrastructure [1] and the integration of EVs into power systems [2]. Although EVs can strain the power distribution grid [3], they also present opportunities for various stakeholders by acting as flexible loads and providing flexibility services [2]. These flexibility services can be classified as behind the meter (BTM) or in front of the meter (FTM), with FTM services being further classified as local or system-wide [2]. BTM services offer benefits to EV users [4] or charging site owners [5] by lowering grid connection and charging costs or improving the self-consumption of distributed energy resources (DERs) [6, 7]. Local FTM services support the power distribution network by addressing issues such as grid losses [8], peak shaving [9], congestion management [10], voltage imbalances [11], and reducing transformer loss-of-life [12]. System-wide FTM services contribute to the stability of the transmission system, providing frequency control [13, 14] and facilitating the integration of variable renewable energy sources [15].

### A. Motivation and objectives

Charging infrastructure, especially in Denmark, is often implemented in the form of charging clusters, where multiple outlets share a single grid connection. These clusters typically use load-sharing management systems to optimise power distribution, thereby reducing grid connection costs [16]. Although smart charging systems can potentially enable additional flexibility services, their exploitation faces several challenges, including technical, economic, and policy-related issues as outlined in [17]. Furthermore, a significant obstacle to offering these services is the uncertainty regarding the flexibility potential and profitability of EV charging clusters.

This paper addresses the challenge of quantifying the flexibility potential of EV charging clusters by examining the influencing factors. We introduce an evaluation tool and a set of flexibility indexes to assess the capability of charging clusters for BTM and FTM flexibility services. This tool is intended to support charge point operators (CPOs) and aggregators in estimating the effectiveness of providing these flexibility services to users and grid operators. Additionally,

we perform a sensitivity analysis to evaluate how various factors, such as connection capacity, battery capacity, power capabilities, and the number of charging events, affect the flexibility potential of charging clusters.

### B. State of the art in flexibility quantification

Despite the importance of understanding the flexibility potential of EVs, its quantification remains complex and underexplored. Existing literature offers various approaches, often focusing on a single dimension. The works in [18–20] examine time-based flexibility, with [18] focusing on public charging in residential areas and [19, 20] on office locations. Research [21] investigates non-residential charging in California, defining flexibility as the ratio of idle to total connection time. Studies such as [22–24] quantify flexibility in terms of power or energy. For example, [22] examines public and workplace charging in Helsinki under Finnish regulations, while [23, 24] focuses on German data. Paper [25] analyses the EV flexibility potential of residential apartment complexes, defining flexibility as idle capacity, which is the product of idle time and maximum charging power.

More recent work tries to quantify flexibility from multiple perspectives, considering different dimensions. The paper [26] introduces a distributed coordination strategy between charging clusters and the distribution system operator, using three indexes to quantify the contribution of flexibility: 1) a deviation index, 2) a charging target violation index, and 3) a mileage index. The first index assesses the deviation of the State of Charge (SoC) from the baseline, the second index quantifies the satisfaction loss when the departure SoC deviates from the baseline, and the third index reflects battery degradation costs [27]. The research in [28] introduces four different flexibility metrics addressing 1) total load shift, 2) increase in midday load, 3) peak reduction, and 4) flatness of the load curve. These metrics are used to quantify the impact of different charging strategies and plug-in behaviours on flexibility provision. Similarly, [29] addresses EV flexibility with respect to different charging strategies but provides a systematic review and assessment. The review focuses on four dimensions of flexibility: 1) temporal, 2) durational, 3) quantitative, and 4) locational flexibility. The authors conclude that the flexibility of charging strategies is underexploited and that the different dimensions are not equally leveraged. The research presented in [30] stresses that the quantification of EV flexibility also hinges on the respective stakeholder and introduces a comprehensive Norwegian case study to quantify the potential flexibility of EVs in apartment buildings. This work assesses a multitude of power and energy flexibility KPIs, including peak power reduction, self-consumption, and efficiency. Finally, the studies [31, 32] quantify the aggregated flexibility of EVs through extensive mathematical modelling. Although both papers provide novel approaches to quantifying the flexibility for a fleet of EVs, their applicability remains questionable due to complexity and data availability concerns.

In conclusion, most of the literature approaches the topic of quantifying EV flexibility from a single dimension, namely power, time, or energy. When addressed individually, these definitions do not provide a comprehensive perspective on flexibility by covering all perspectives. Furthermore, existing flexibility definitions fail to include the trade-offs between BTM and FTM flexibility goals. For instance, power flexibility might help understand how power demand could be modulated, but it doesn't necessarily reveal the time cost for the users. Additionally, due to limited connection capacity and the need for power sharing, there is no straightforward relationship between the power modulation rate and the decrease in idle time [33].

### C. Contributions

This paper contributes to the EV flexibility quantification literature by introducing a straightforward yet comprehensive set of criteria to assess the flexibility potential of EV charging clusters. The proposed approach offers a promising alternative to existing methods, which often fail to evaluate the trade-offs between competing flexibility services or are complex to apply. Additionally, through sensitivity analysis, the paper provides concrete insights into EV cluster dimensioning and its suitability for various flexibility services based on current or projected characteristics. Finally, the paper illustrates the applicability of the proposed criteria by analysing a real-world workplace charging cluster in Copenhagen, Denmark, using actual data from the chargers deployed.

This paper is organized as follows: Section II outlines the methodology used in this study, including the flexibility indexes and the simulation model; Section III details and analyzes the key findings; Finally, Section IV summarises the conclusions drawn from the study, discusses its limitations, and suggests directions for future research.

## II. Methodology

This section outlines the methodology of this study, focusing on the design of the proposed flexibility metrics and the computational analysis conducted for an EV cluster located in Denmark. Subsection II-A discusses the power, energy, and time constraints of a charging cluster, as well as two charging strategies, which inform the definition of four qualitative flexibility indexes and one quantitive criterion in Subsection II-B. Subsection II-C demonstrates the practical application of these indexes, while Subsection II-D elaborates on the model design, including input parameters and output metrics. Finally, Subsection II-D addresses the underlying assumptions and limitations of the model.

### A. Charging cluster constraints

To quantify the flexibility potential of a charging cluster, it is essential to establish lower and upper boundaries and a potential solution space based on its electrical dimensions and connection patterns. Exemplified for an illustrative charging cluster in Fig. 1, we describe those attributes in more detail in the following.

To start with, we need to introduce the physical upper and lower boundaries of the charging cluster, which are as follows:

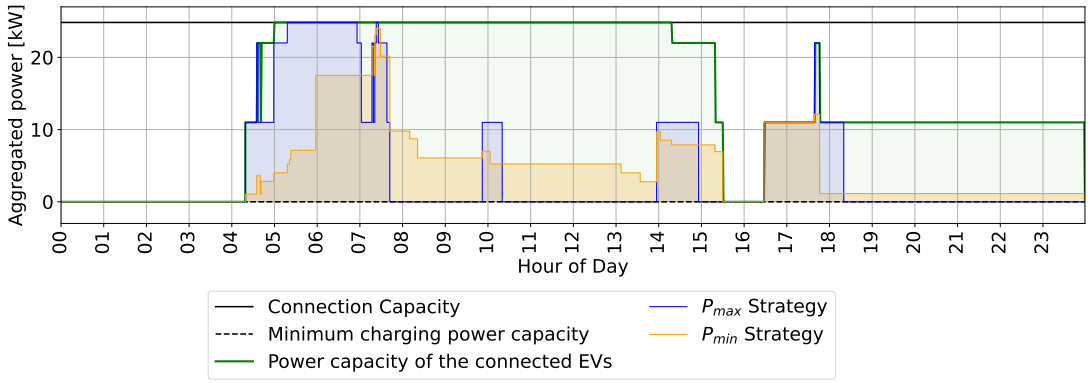


Fig. 1: Example of the aggregated power time-series for a generic charging cluster. The graph illustrates the boundaries influencing the power consumption of the EVs over time.

- **Grid connection capacity of the EV cluster:** Illustrated as the solid black line in Fig. 1, the grid connection capacity defines the maximum power the charging cluster can deliver. Often, the grid connection is lower than the combined outlet capacity of the charging cluster to minimise grid connection costs and accelerate charging infrastructure deployment [16].

- **Minimum charging power capacity:** Vehicle-to-grid charging systems could potentially inject power into the grid and discharge the EVs, expanding the minimum charging power capacity to negative values. However, since this technology is not yet fully available for commercial applications, this study considers only unidirectional charging. Consequently, the lower power limit of the charging cluster is set to 0 kW, as indicated by the dashed black line in Fig. 1.

While the boundaries mentioned above consider the technical limitations of the charging cluster, its flexibility potential further depends on the connected EVs and their charging behaviour. In the following, we describe the theoretical maximum power and energy capabilities of the charging cluster in more detail:

- **Maximum power capacity of connected EVs:** When the grid connection capacity is not fully utilised, the power delivered to each EV is constrained by either the maximum power capacity of the chargers or the EV itself. Consequently, the total potential power demand of the charging cluster will vary over time and can be defined for timestep t as $\sum_{i=1}^{n} p_{\max,i}(t)$, where $n$ represent the number of EVs charging, and $p_{\max,i}$ is the maximum power capacity of each charger and EV. This variable power capacity limit, illustrated by the green line in Fig. 1, is particularly relevant in charging clusters with low rates of concurrent charging.

- **Maximum energy potential of the EV cluster:** The area encompassed by the boundaries given by the grid connection capacity, the minimum charging power capacity, and the power capacity of the connected EVs represents the maximum energy potential $E_{pot}$. It is represented by the green area in the Fig. 1. In abstract terms, the energy potential of the cluster is the energy that the charging cluster could potentially charge to EVs with infinite energy storage within the boundaries of the power capacity of the chargers, connection pattern and connection capacity of the cluster (i.e., all EVs charge at full power for the entire duration of their connection time).

However, the current boundaries do not consider the limited battery capacity of the EVs. Once an EV is fully charged or has reached the energy level requested by the user, it will stop charging. Afterwards, the EV will remain idle until its scheduled disconnection time. Fig. 1 illustrates two charging strategies used to highlight the aforementioned limited energy capacity and are needed to derive the quantitative flexibility criteria within this paper. These strategies will be referred to as $P_{max}$ *Strategy*, represented in blue in Fig. 1, and $P_{min}$ *Strategy*, depicted in yellow. The design of $P_{max}$ *Strategy* aims to charge the EVs as quickly as possible (i.e., by providing maximum power). In contrast, $P_{min}$ *Strategy* is designed to charge the EVs as slowly as the connection duration of each EV allows (i.e. the charging demand is spread equally over the whole duration of being plugged).

1) ***$P_{max}$ Strategy*:** The $P_{max}$ *Strategy* is the charging strategy currently commercialised in most charging clusters. It calculates the charging power of the $i$-th EV at time $t$ as:

$$P_{\mathrm{EV}_i}(t) = \begin{cases} \frac{CC}{n} & \text{if } \sum_{i=1}^{n} P_{\mathrm{EV}_i}(t) \geq CC \\ P_{\mathrm{max},i}(t) & \text{if } \sum_{i=1}^{n} P_{\mathrm{EV}_i}(t) < CC, \end{cases} \quad (1)$$

where $CC$ represents the grid connection capacity in kW, $n$ is the number of EVs charging at time $t$, and $P_{\mathrm{max},i}(t)$ is the maximum power that the $i$-th charger and EV allow. The formula describes that if the connection capacity has been reached, all the chargers will avoid overshooting it by modulating their charging power equally (i.e., by load sharing). In contrast, if the connection capacity is not reached, each charger will maximise the charging power.

2) ***$P_{min}$ Strategy*:** On the other hand, the $P_{min}$ *Strategy* calculates the charging power of the $i$-th EV at time $t$ as:

$$P_{\mathrm{EV}_i}(t) = \begin{cases} \frac{CC}{n} & \text{if } \sum_{i=1}^{n} P_{\mathrm{EV}_i}(t) \geq CC \\ \frac{E_{\mathrm{requested,i}}}{t_{\mathrm{disconn,i}} - t_{\mathrm{conn,i}}} & \text{if } \sum_{i=1}^{n} P_{\mathrm{EV}_i}(t) < CC. \end{cases} \quad (2)$$

In addition to the connection time $t_{conn,i}$, the strategy requires inputs from the user of the $i$-th EV, namely the total energy requested $E_{requested,i}$ and the expected time of disconnection $t_{disconn,i}$, to calculate the charging power.

It is important to note that, unless scheduling functionalities are considered, compliance with the IEC 61851-1 standard requires the EVs to have a minimum allowable current of 6 A [34]. For single-phase and three-phase EVs charging with a Type 2 plug, this translates to minimum power capacities of 1.38 kW and 4.15 kW, respectively. This paper does not focus on any specific EV charging technology; therefore, we recommend tailoring the $P_{min}$ *Strategy* and $P_{max}$ *Strategy* to the capabilities of the charging technology under consideration when deploying this evaluation tool.

### *B. Flexibility evaluation criteria*

This section outlines the criteria developed in this study to evaluate the flexibility potential of an EV charging cluster. To begin with, we introduce four flexibility indexes designed to provide a qualitative assessment of the flexibility potential of an EV cluster. A flexible cluster is defined as a cluster that can deliver flexibility services without compromising user charging requirements (e.g. when EVs maintain idle time). Conversely, an inflexible cluster cannot provide flexibility services without negatively impacting the fulfilment of the user's charging demand. In the following flexibility indexes, an infinitely flexible cluster is assigned a score of 1, while a fully inflexible cluster is assigned a score of 0. Within the context of the previously defined cluster constraints, the four indexes for a generic charging cluster are as follows:

*1) **Energy Flexibility Index (EFI)**:* From the energy perspective, the energy flexibility index is defined as:

$$EFI = 1 - \frac{E_{ch}}{E_{pot}}. \quad (3)$$

In the formula, $E_{ch}$ is the aggregated energy demand, defined as the total energy delivered to all the EVs connected during the time period under analysis (e.g. the blue area depicted in Fig. 1). The EFI is relevant to understand the suitability of the charging cluster to delay energy in time.

*2) **Power Flexibility Indexes (MPFI and APFI)**:* Concerning the power domain, we distinguish two different indexes. On the one hand, the Minimum Power Flexibility Index is defined as:

$$MPFI = 1 - \frac{P_{max,avg}}{CC}, \quad (4)$$

where $P_{max,avg}$ is the average daily maximum that the aggregated power of the charging cluster reaches over a given period, and $CC$ is the connection capacity. The MPFI estimates the remaining power flexibility during peak utilisation of the charging cluster.

On the other hand, the Average Power Flexibility Index is:

$$APFI = 1 - \frac{P_{mean,ch}}{CC}, \quad (5)$$

where $P_{mean,ch}$ is the average charging power dispatched by the charging cluster, considering only the time periods during which at least one EV is charging. The MPFI and APFI are important for understanding the ability of the charging cluster to make short-term power adjustments under peak demand conditions and average operating conditions, respectively. A significant difference between the MPFI and APFI indicates a highly variable utilization rate throughout the day.

*3) **Time Flexibility Index (TFI)**:* Lastly, in the time domain, the time flexibility index is defined as:

$$TFI = \frac{t_{idle,avg}}{t_{tot,avg}}. \quad (6)$$

While $t_{idle,avg}$ represents the average idle time of the EVs connected to the charging cluster when fully charged, $t_{tot,avg}$ depicts the average total connection time of the EVs. The TFI estimates how much the charging session can be shifted in time without influencing the charging fulfilment. The TFI is, therefore, relevant for BTM services and charge scheduling.

Finally, we propose the quantitative indicator to assess the flexibility potential of the EV cluster over the time period under analysis as follows:

*4) **Hourly energy flexibility (HEF)**:* In the previous subsection, we defined the $P_{max}$ *Strategy* and $P_{min}$ *Strategy* as the ultimate upper and lower boundaries of the EV cluster, respectively. By comparing the energy accumulated over time between these two strategies, we can quantify the hourly flexibility, which represents the amount of energy that can be deferred each hour without compromising charging fulfilment. The hourly energy flexibility is defined as:

$$HEF = \Delta E = \int_{t}^{t+1} \Delta P(t) dt, \quad (7)$$

where $t$ and $t+1$ denote the interval between the beginning and the end of each hour of the day, and $\Delta P(t)$ is the difference in power consumption between the charging strategies at time $t$. Understanding the profile of HEF is crucial for identifying when and how much energy flexibility is available.

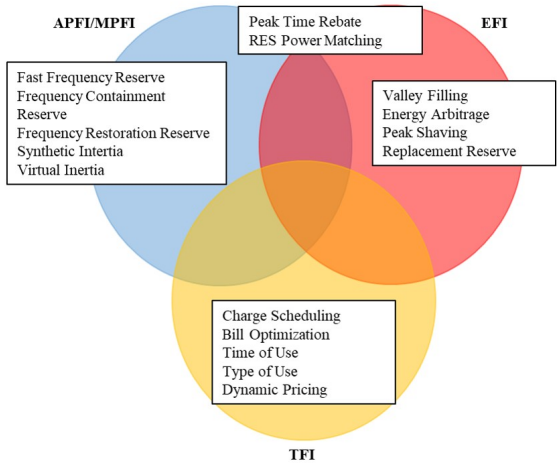


Fig. 2: Venn diagram illustrating the relationship between the flexibility indexes and types of flexibility services (see Table A1). Services requiring short-term power adjustment are associated with the APFI and MPFI (blue domain), while services requiring long-term flexibility services are linked to the EFI (red domain). Additionally, BTM flexibility services correspond to the TFI (yellow domain). The diagram helps to visualise the overlap and distinct areas of flexibility services related to each index.

### C. Application of flexibility indexes

Fig. 2 shows a Venn diagram illustrating a set of flexibility services assigned to each of the four qualitative flexibility indexes proposed in this paper. As previously mentioned, the power-related flexibility indexes MPFI and APFI aim to measure the capability of the charging cluster to perform short-term power adjustments. Examples of such adjustments include synthetic inertia, virtual inertia or any fast frequency services. In contrast, the EFI evaluates the ability of the charging cluster to sustain power adjustments over time. Examples of such services include congestion management and valley filling. Lastly, within this framework, the TFI measures the capacity of the charging cluster to perform BTM services. Longer idle times increase the ability to shift charging to more cost-effective periods. This capability is used in practices such as bill optimization and Time of Use based charging strategies. The definition and requirements of such flexibility services can be found in Table A1 in the appendix. The allocation of the given flexibility services in the different domains of the Venn diagram is based on the standardised activation time, duration, and technical requirements for such flexibility services. It is important to note that the mutual influence of one index on the other could depend on the charging strategy used.

Furthermore, the flow chart and corresponding table presented in Fig. 3 illustrate the application of the flexibility indexes for analysing an EV charging cluster. This framework demonstrates how a CPO can utilize these indexes to plan the design or upgrade an EV cluster to maximize its flexibility according to the desired types of services. The analysis focuses on the most relevant combinations of flexibility indexes, resulting in six distinct cases. To keep the overview concise, cases with high MPFI are omitted, as they are considered less critical compared to those with high MPFI. Additionally, two paths in the flowchart are excluded because they are not deemed realistic. These paths correspond to scenarios where only one flexibility index significantly deviates from the others (i.e., low TFI and high TFI). The framework offers suggestions for improving the flexibility potential or charging fulfilment for each case. While some improvements are optional, achieving a balanced flexibility score across the different indexes is considered ideal.

### D. Computational demonstration of the method

To demonstrate the method for quantifying the flexibility of an EV cluster, a simplified model of a workplace charging cluster located in Copenhagen, Denmark, has been developed. The cluster includes 10 chargers, each with a capacity of 22 kW, while the overall grid connection capacity is limited to 82 kW. Fig. 4 illustrates the model along with its inputs and outputs. The model operates with a time resolution of one minute and uses real charging session data provided by the CPO Spirii for the year 2022.

The model utilizes two primary types of inputs. First, it incorporates user behaviour data from the charging sessions, including connection and disconnection times, as well as energy demand, to establish the connection patterns within the charging cluster. Second, it integrates information about the cluster's electrical layout, such as connection capacity and individual charger power, to identify the cluster's constraints, as detailed in Subsection II-A. Using these inputs, the model derives the $P_{max}$ *Strategy* and the $P_{min}$ *Strategy*. Initially, the model employs equations 1 and 2 to calculate the power required for each EV at each timestep under both strategies. Next, it integrates the charging power for each EV over time to determine the total energy charged. Each EV will cease charging once its energy demand $E_{requested,i}$ is fulfilled. The end-time of each charging session is then calculated, along with the idle time for each EV. Finally, the model computes the total power consumption and the total energy charged for the entire charging cluster.

The model outputs include the flexibility index scores and the HEF. Additionally, it provides time series data on aggregated power, charging patterns, and connection patterns of the EVs. This data is used to analyze the results in the subsequent section.

### E. Assumptions and limitations of the simulation

During the design of the simulation model to demonstrate the flexibility quantification method, several assumptions were made to simplify the analysis and address the lack of more detailed EV charging data.

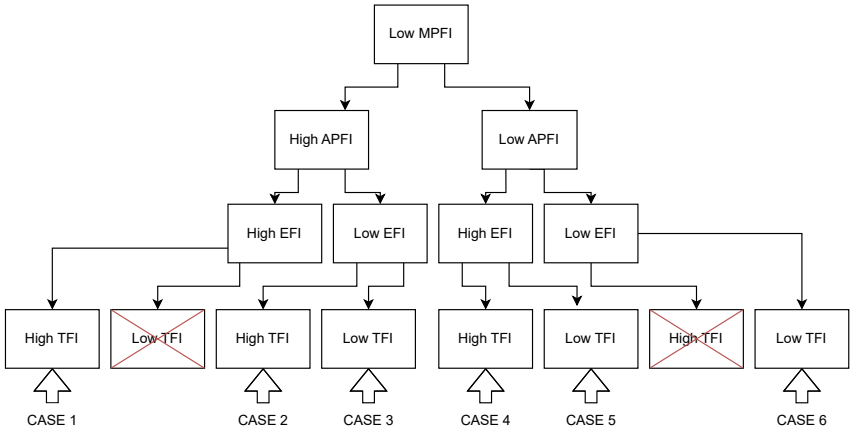


| CASE | Description |
|---|---|
| 1 | The EV cluster shows high rates of concurrent charging at certain times (low MPFI), but all the other indexes indicate a high potential for both BTM and FTM flexibility services. Implementing a smart charging strategy could improve energy and time management or support a range of flexibility services. Lowering the grid connection capacity could reduce capital expenditure (CAPEX) if the EV cluster is still in the planning phase. |
| 2 | In addition to peak concurrent charging conditions (low MPFI), the power capacity of the chargers may also limit the performance of the EV cluster. High APFI and low EFI suggest that the system has a limited ability to delay energy accumulation over time. Given the high TFI, the EV cluster could be expanded by adding more chargers, potentially in combination with adding charging prioritisation strategies. Alternatively, reducing the connection capacity could lower CAPEX if the EV cluster is still in the planning phase. |
| 3 | The EV cluster demonstrates limited flexibility potential: it experiences high utilisation rates at certain times (low MPFI), but charging sessions are otherwise infrequent and isolated (high APFI). The EVs are only connected for short durations (low TFI), a pattern commonly observed in EV clusters at shopping malls or highway charging stations, which are only heavily used during specific times of the day. |
| 4 | The cluster exhibits high levels of concurrent charging overall. However, by implementing a smart charging strategy, there is potential to delay energy consumption in time for both BTM and FTM services, as indicated by high EFI and TFI. |
| 5 | The cluster shows high levels of concurrent charging overall. However, the combination of high EFI and low TFI indicates an opportunity to implement a smart charging strategy. This could lead to more optimal scheduling of charging sessions and improved overall charging fulfilment. |
| 6 | The highly utilized charging cluster faces high rates of concurrent charging, with frequent load sharing and minimal potential to delay energy consumption. The EVs have limited idle time. To address this, increasing the grid connection capacity and implementing a smart charging strategy is recommended. |

Fig. 3: Overview of key flexibility index combinations requiring adjustments to enhance flexibility potential or charging fulfilment. The figure outlines six primary cases and recommends specific actions for each scenario.

The first limitation relates to the real-life implementation of the $P_{min}$ *Strategy*. In the model, connection and disconnection times, along with the energy demand recorded for each charging event, are used to derive the $P_{min}$ *Strategy*. While the simulation, therefore, relies on historical data, in practice, the planned departure time and energy demand would need to be provided by the user, with the control strategy executed in real-time. Although requiring user input might hinder large-scale implementation, it was deemed necessary to quantify the flexibility potential in this work.

Next, a notable limitation is the lack of detailed modelling of the EV battery and onboard charger dynamics. Previous research has shown that the modulation of charging power can significantly affect the charging efficiency of EVs [35]. In particular, reducing the charging power often leads to lower efficiency, where the energy stored in the battery may be less than the energy delivered by the chargers. Our model does not explicitly account for this relationship, which may result in a slight overestimation of energy accumulation in the $P_{min}$ *Strategy*, and consequently, the flexibility potential of the EV cluster. This slight overestimation could be mitigated by charge scheduling rather than relying on power modulation. Although the assumption of constant efficiency is not entirely accurate in real-world scenarios, it was considered acceptable given the primary objectives of this study.

Another limitation stems from the assumption that all EVs

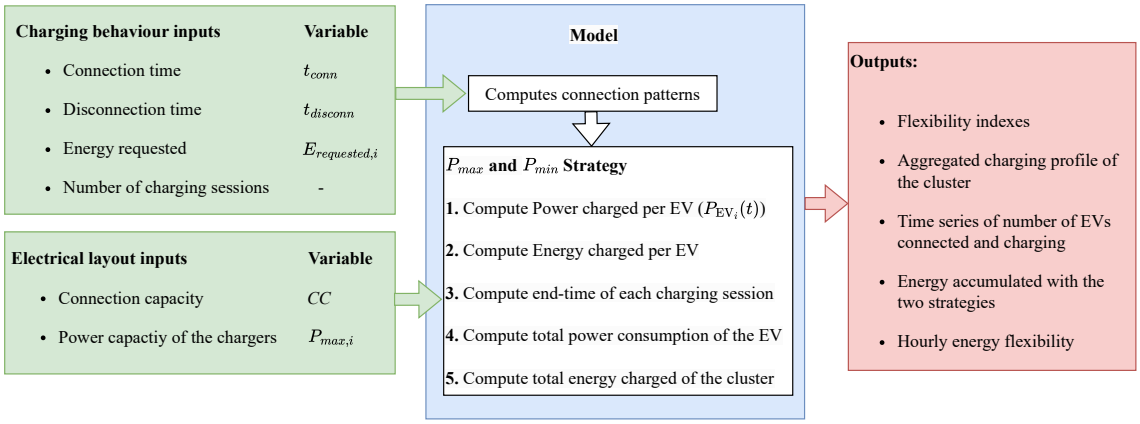


Fig. 4: Flowchart of the model, illustrating the inputs (in green), the intermediate calculations of the model (in blue), and the outputs (in red).

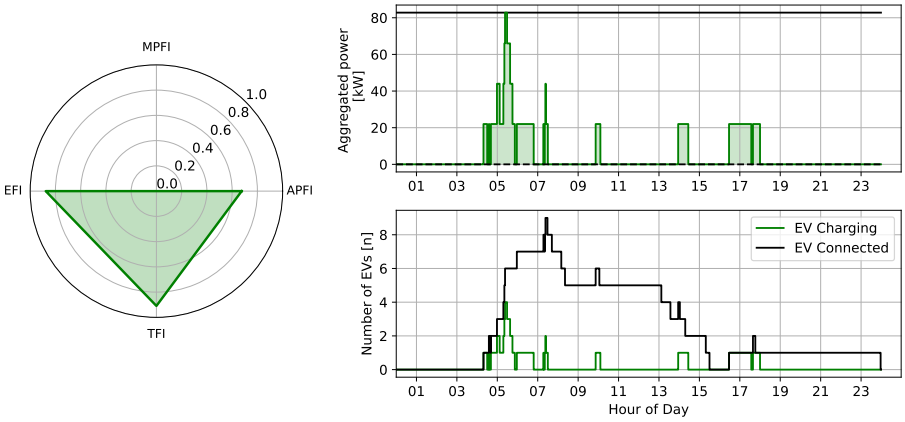


Fig. 5: Analysis of the EV charging cluster performance on August 31, 2022, using the original $P_{min}$ *strategy*. The figure includes a radar graph on the left showing flexibility index results, a plot of the aggregated power demand of the EV cluster at the top right, and a chart of the number of EVs connected and charging at the bottom right.

have constant and equal charging power, regardless of their SoC or model. In reality, the variation in charging power across different SoCs and EV models could affect the dynamics within a charging cluster, a factor not addressed in the current study. This assumption was deemed necessary in the absence of information about the charging power during the charging sessions or the EV models and their SoC during the charging sessions. Although incorporating power measurement data from each charger could enhance the accuracy of the model, this level of detail is deemed beyond the scope of the current study.

It is important to notice that these simulations primarily focus on demonstrating the application of the proposed flexibility quantification method and the associated flexibility indexes, serving as a proof of concept. The computational analysis and the simplified EV cluster model are only used to illustrate their practical utility and exemplify their potential use in real-life scenarios. While the results provide a broad understanding of how various parameters affect flexibility potential, the paper does not aim to comprehensively analyse the charging cluster data. For a more thorough evaluation of cluster performance, a detailed analysis with high-accuracy models and larger datasets—ideally covering multiple years—is recommended.

## III. Results and Discussion

This section presents the results of applying the proposed flexibility criteria to the modelled EV cluster. Subsection III-A provides an analysis of the EV cluster with default charging

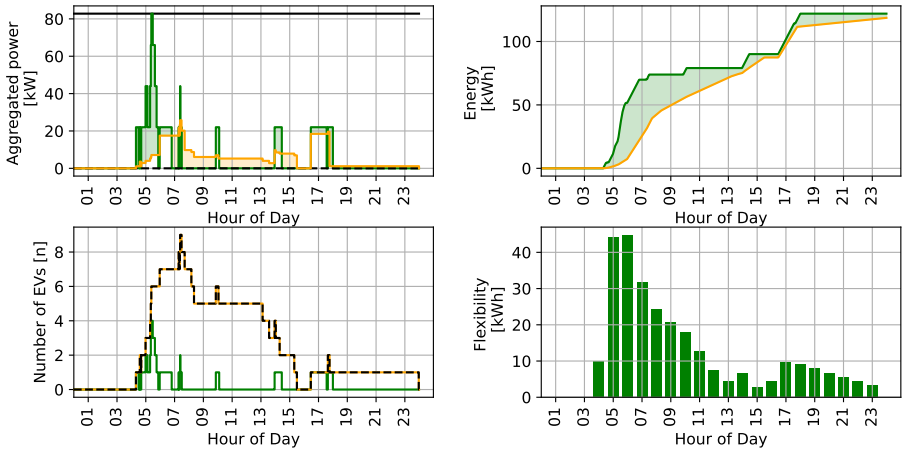


Fig. 6: Comparison of the flexibility potential of the EV charging cluster on August 31, 2022, using two different charging strategies: $P_{max}$ *Strategy* and $P_{min}$ *Strategy*. The figure includes the aggregated power time series in the top-left, the number of EVs connected and charging in the bottom-left, the accumulated energy demand in the top-right, and the HEF in the bottom-right.

behaviour (i.e., $P_{max}$ *Strategy*), utilising the original data input. This analysis evaluates the performance of the cluster using the proposed flexibility indexes and draws conclusions regarding the optimal dimensioning of its electrical layout. Next, Subsection III-B addresses the HEF of the charging cluster by additionally considering $P_{min}$ *Strategy*. Finally, through a sensitivity analysis, the study investigates the impact of different charging cluster characteristics on both qualitative and quantitative flexibility criteria. The results of the flexibility indexes, along with the HEF metrics, are analysed to offer insights into the performance of the charging cluster under varying conditions. Specifically, the study examines the effects of connection capacity in Subsection III-C, EV battery capacity in Subsection III-D, charger capacity in Subsection III-E, and the number of charging events in Subsection III-F.

### *A. Qualitative flexibility potential assessment of the cluster*

This section presents an analysis of the EV charging cluster using original input data from August 31, 2022, the day with the highest number of charging sessions in the historical dataset (15 sessions). Fig. 5 provides a radar plot (left) displaying the performance of the EV cluster across various flexibility indexes for this day. The top-right plot illustrates the aggregated power demand, while the bottom-right plot shows the number of EVs connected and actively charging. The MPFI is 0, indicating a lack of flexibility during peak hours due to intensive concurrent charging in the early hours of the day. In contrast, the APFI is 0.67, which, when combined with the MPFI, suggests significant variability in utilisation throughout the day. The aggregated power demand and the number of EVs charging plots reveal that peak utilization occurs at 5:00 AM, when four EVs are charging simultaneously, drawing a total of 82 kW. The high EFI of 0.88 indicates that the charging of all EVs can be substantially delayed without compromising their charging needs. This is further supported by the high TFI of 0.91 and by the bottom-right graph, which shows that, on average, EVs remain idle 91% of their connection time. This suggests a considerable flexibility potential within the cluster. Implementing a smart charging strategy could leverage this idle time to enhance power flexibility during peak periods.

Overall, the results reveal that the EV cluster under analysis is significantly over-dimensioned for the current user behaviour, particularly considering that the selected day represents the highest utilization rate in 2022. This suggests that the CAPEX invested in sizing the connection capacity may be excessive. However, as EV adoption increases and the utilization rate of the cluster rises in future years, the current capacity could become more appropriate. In the short term, adopting an effective charging strategy could reduce operational expenditures (OPEX) by maximising the flexibility potential of the cluster.

### *B. Quantitative flexibility potential assessment of the cluster*

In the following, we apply our flexibility quantification method to assess the flexibility potential of the analysed EV charging cluster. Fig. 6 provides a detailed illustration of our analysis for August 31, 2022. The top-left panel of the figure displays the aggregated power of the EV charging cluster over the course of the day, while the bottom-left panel shows the number of EVs that are charging and connected. The top-right panel presents the total accumulated energy, and the bottom-right panel illustrates the HEF throughout the day. Each graph encompasses the results for both the original scenario, which

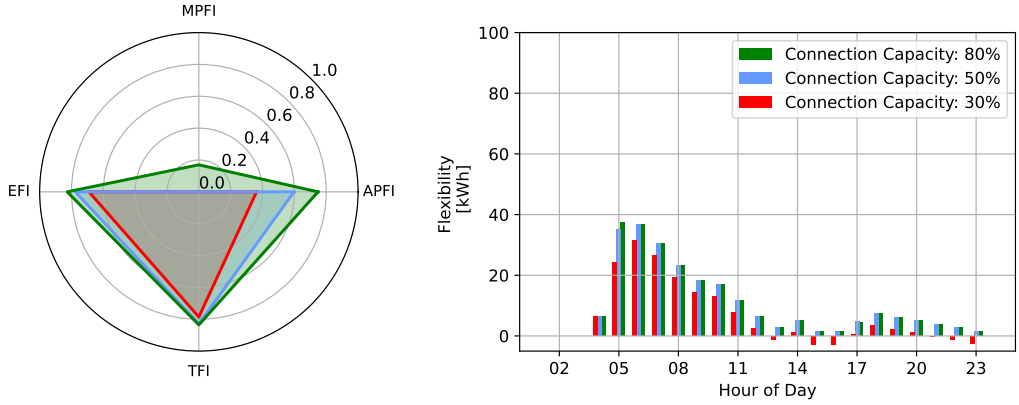


Fig. 7: Impact of the grid connection capacity on the charging cluster performance. The colours green, blue, and red represent scenarios in which the connection capacity is 80%, 50%, and 30% of the original grid connection (82 kW), respectively. On the left, flexibility indexes are evaluated, while the HEF is depicted on the right.

utilises $P_{max}$ *Strategy* (shown in green), and the $P_{min}$ *Strategy* scenario (shown in yellow).

Compared to the original $P_{max}$ *Strategy*, the $P_{min}$ *Strategy* decreases the aggregated power consumption by prolonging the charging duration of all EVs and maintaining a minimum power level throughout the entire charging period. This effect is illustrated in the bottom-left plot, where the number of EVs charging under the $P_{min}$ *Strategy* matches the number of EVs connected, as indicated by the black dotted line. Consequently, the $P_{min}$ *Strategy* results in a lower and more stable aggregated power consumption throughout the day. Specifically, it reduces the peak aggregated power consumption during high-demand hours from 82 kW to 25 kW and shifts the peak consumption period from approximately 5:30 AM to 7:30 AM.

Lastly, the accumulated energy graph shows that in both strategies, the EVs charge a total of 124 kWh. However, there is a substantial difference in the rate at which energy is accumulated between the two strategies. This difference is directly proportional to the number of EVs charging at any given time. The HEF graph confirms this trend, revealing two peaks: one at 45 kW at 6:00 AM and another at 9.8 kW at 5:00 PM. The average HEF of the EV cluster is 14 kWh. This trend is crucial as it highlights the significant impact of user behaviour, which is influenced by the type and location of the EV cluster, on the timing and amount of flexibility the cluster can provide. In this particular workplace EV cluster, the timing of flexibility appears to depend on the shifts of the workers parking their EVs and plugging them into the chargers.

In the following, we analyse the sensitivity of the flexibility criteria with respect to the aforementioned parameter.

### C. Impact of connection capacity

In the first analysis, the sensitivity of the flexibility potential of the EV cluster on August 31, 2022, is evaluated by varying the grid connection capacity. Three scenarios are considered, wherein the connection capacity is set to 30%, 50%, and 80% of the original grid connection of 82 kW, respectively. Each scenario utilises chargers with a power capacity of 11 kW. Fig. 7 displays the results of this analysis. The left graph illustrates the performance of the EV cluster across the different flexibility indexes, while the right plot depicts the corresponding HEF for each scenario. A detailed summary of the sensitivity analysis outcomes is further presented in Table I. The MPFI ranges from 0 in the first two cases to 0.17 in the last scenario, showing that the connection capacity during peak utilization rate is not reached only in the last scenario. The APFI is also low, with a significant variation, ranging from 0.36 to 0.75 as the connection capacity increases. The variation in EFI is less pronounced but still notable, ranging from 0.69 to 0.83, while the TFI shows the least variation, ranging from 0.79 to 0.84.

TABLE I: Flexibility criteria results for various connection capacities. The connection capacity, expressed as a percentage, is based on the original grid connection of 82 kW.

| **Grid connection capacity [%]** | **30** | **50** | **80** |
|---|---|---|---|
| MPFI | 0.00 | 0.00 | 0.17 |
| APFI | 0.36 | 0.60 | 0.75 |
| EFI | 0.69 | 0.78 | 0.83 |
| TFI | 0.79 | 0.83 | 0.84 |
| Maximum HEF [kWh] | 31.37 | 36.83 | 37.45 |
| Average HEF [kWh] | 10.95 | 11.40 | 11.51 |

The HEF increases with increasing connection capacity. Specifically, the maximum HEF rises from approximately 31 kWh to 37 kWh, while its average increases from roughly 11 kWh to 11.5 kWh. As illustrated in Fig. 7, at 30% connection capacity, the HEF exhibits several instances of negative values, signifying missed charging opportunities attributable to suboptimal energy management within the $P_{max}$ *Strategy*.

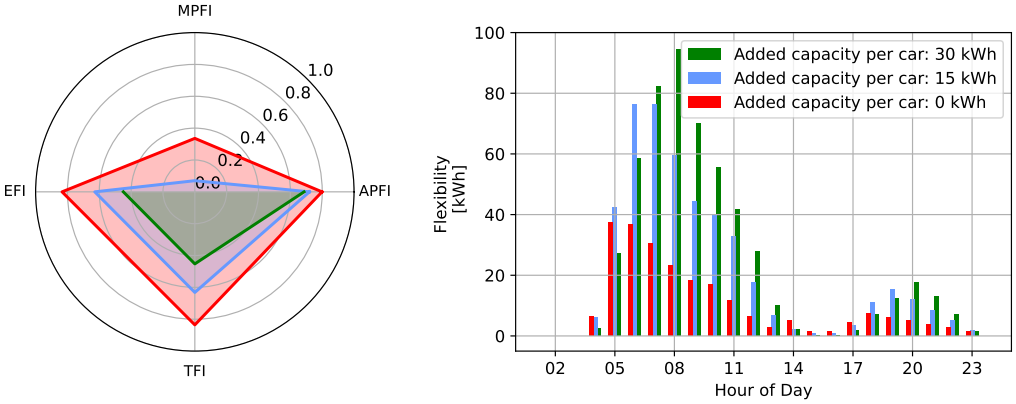


Fig. 8: Impact of the battery size on the charging cluster performance. The colours green, blue, and red represent scenarios with an additional battery capacity of 30, 15, and 0 kWh, respectively. The flexibility indexes are assessed on the left, whereas the HEF is assessed on the right.

Specifically, the total energy accumulated by the end of the day with the $P_{min}$ *Strategy* exceeds that of the $P_{max}$ *Strategy*. This discrepancy arises because, upon reaching the connection capacity limit, the $P_{max}$ *Strategy* allocates power uniformly across all EVs, irrespective of their departure schedules. Consequently, some EVs may depart before achieving full charge. Such a result highlights the need for strategies capable of scheduling charging sessions in EV clusters with limited connection capacity.

Overall, these results indicate that connection capacity significantly affects the suitability of the EV cluster for power-based flexibility services under the given conditions. In contrast, its impact on time and energy flexibility is only marginal. Despite the average idle time of all EVs being 60%, the HEF reveals that at least one EV did not complete its charging session before the disconnection time. In future work, we will consider modifying the time flexibility index to account for the time flexibility of EVs with the lowest idle time.

### D. Impact of battery capacity

Next, the flexibility potential of the EV cluster on August 31, 2022, is examined by varying the battery capacities across different scenarios. In the first scenario, the power capacity of the chargers remains unchanged. In the second scenario, the battery capacity is increased by 15 kWh, and in the third scenario, it is increased by 30 kWh. Although the exact battery capacities of the EVs are not known, it is assumed that the energy requested by users reflects the battery capacity. Accordingly, the additional energy is added to the energy requested under the original conditions. The connection capacity is set at 82 kW, with each charger having a power capacity of 11 kW. This sensitivity analysis is essential for understanding how the flexibility potential of EV clusters may evolve with future generations of EVs, given the anticipated increase in battery capacity.

TABLE II: Flexibility criteria results for various battery capacities. The table shows the additional capacity beyond the initial energy capacity, which is assumed to be equal to the charging demand of the EVs.

| **Additional battery capacity [kWh]** | **0** | **15** | **30** |
|---|---|---|---|
| MPFI | 0.34 | 0.07 | 0.00 |
| APFI | 0.80 | 0.72 | 0.69 |
| EFI | 0.83 | 0.63 | 0.45 |
| TFI | 0.84 | 0.63 | 0.45 |
| Maximum HEF [kWh] | 37.4 | 76.5 | 94.5 |
| Average HEF [kWh] | 11.5 | 23.1 | 26.7 |

Fig. 8 and Table II illustrate the results following the same format as the previous sensitivity analysis. Overall, the results show a decline in all flexibility indexes as battery capacities increase. This is because, as the energy demand increases, the ability to defer charging diminishes when connection time and charger power capacity are held constant. The most affected indexes are the EFI, which drops from 0.83 to 0.45, and the TFI, which decreases from 0.84 to 0.45. Additionally, the MPFI falls from 0.34 in Scenario 1 to 0 in Scenario 3, indicating a higher peak power demand. Conversely, the APFI is less impacted due to charger capacity constraints and the relatively consistent number of EVs charging concurrently each hour, aside from the initial peak. An interesting observation from Fig. 8 is that while the EFI decreases with increasing battery capacity, the HEF that can be achieved by delaying charging actually increases. This finding underscores that the HEF is significantly influenced by the storage capacity available in the cluster and the duration of each EV's charging session. Indeed, Scenario 3 demonstrates the highest HEF observed in this study, with a peak of 94.5 kWh and an average of 26.7 kWh. Moreover, as battery capacities grow, the peak utilization rate—and consequently, the peak HEF—shifts to later times.

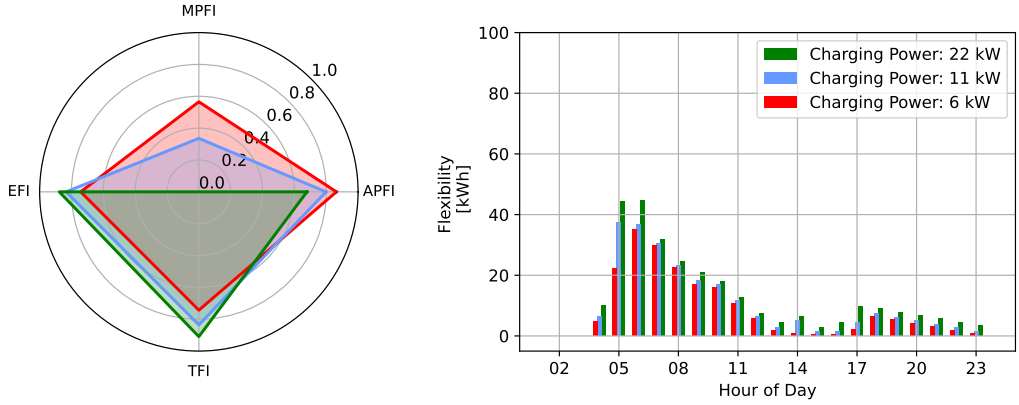


Fig. 9: Impact of the charging power on the charging cluster performance. The colours green, blue, and red represent scenarios where the charging power is set to 22 kW, 11 kW, and 6 kW, respectively. Flexibility indexes are evaluated on the left, while HEF is depicted on the right.

Specifically, the HEF peaks at 5:00 AM in Scenario 1 and at 8:00 AM in Scenario 3.

Overall, these results demonstrate that battery capacity is the most crucial parameter influencing the energy and time flexibility of a charging cluster. Specifically, when the connection capacity is sufficiently high, larger battery capacities increase the amount of energy consumption that can be deferred each hour. Furthermore, as the idle time of the EVs decreases, the peak in utilization rate and energy flexibility shift to later times. Finally, this sensitivity analysis underscores the complementarity between qualitative and quantitative measurements of flexibility criteria. While the qualitative measure of energy flexibility potential indicated by the EFI decreases due to reduced room within the constraints of the cluster to schedule energy delivery over time, the total amount of flexible energy increases significantly, enhancing the HEF.

### *E. Impact of charging power*

In this sensitivity analysis, the flexibility potential of the EV cluster on August 31, 2022, is evaluated by varying the charging power capacities of the chargers and EVs. The simulated charging capacities are 6 kW in Scenario 1, 11 kW in Scenario 2, and 22 kW in Scenario 3 (same as base case), which reflect the range of existing AC power capacities available for slow charging. The connection capacity is kept at 82 kW.

Fig. 9 and Table III present the results of the analysis. The radar graph in Fig. 9 demonstrates that increasing the EV charging capacity diminishes the flexibility scores for the power indexes MPFI and APFI, with MPFI being the most affected, decreasing to 0 in the final scenario. Conversely, the EFI and TFI scores exhibit an inverse relationship to these power indexes. Higher EV charging capacity facilitates faster charging, thus enhancing the potential to adjust charging schedules to meet grid operators' and users' needs. However, this benefit is accompanied by an increased peak power demand, particularly in the absence of a smart charging strategy. The HEF results indicate that higher power capacities correlate with a higher HEF, with peak values ranging from roughly 35 kWh in Scenario 1 to approximately 45 kWh in Scenario 3, and average values ranging from 9.6 kWh in Scenario 1 to 14 kWh in Scenario 3. Additionally, as the power capacity of the chargers increases, the peak HEF shifts to earlier times, moving from 6:00 AM in Scenario 1 to approximately 5:00 AM in Scenario 3.

TABLE III: Flexibility criteria results for different charging power capabilities.

| **Charging power [kW]** | **6** | **11** | **22** |
|---|---|---|---|
| MPFI | 0.57 | 0.34 | 0.00 |
| APFI | 0.86 | 0.80 | 0.68 |
| EFI | 0.74 | 0.83 | 0.88 |
| TFI | 0.74 | 0.84 | 0.91 |
| Maximum HEF [kWh] | 35.2 | 37.5 | 44.7 |
| Average HEF [kWh] | 9.6 | 11.5 | 14.0 |

### *F. Impact of number of charging events*

The last sensitivity analysis of this study examines how the number of charging events affects flexibility potential. Three different days were selected for this analysis: Scenario 1 represents August 31, 2022, when 15 charging sessions were recorded; Scenario 2 represents February 16, 2022, with 10 recorded charging sessions; and Scenario 3 represents January 18, 2022, which saw five recorded charging sessions. The connection capacity is kept at 82 kW, and the charger power capacity is 11 kW.

Fig. 10 and Table IV showcase the results of the analysis. In general, the results from the flexibility indexes and the HEF indicate that the number of daily charging sessions is not

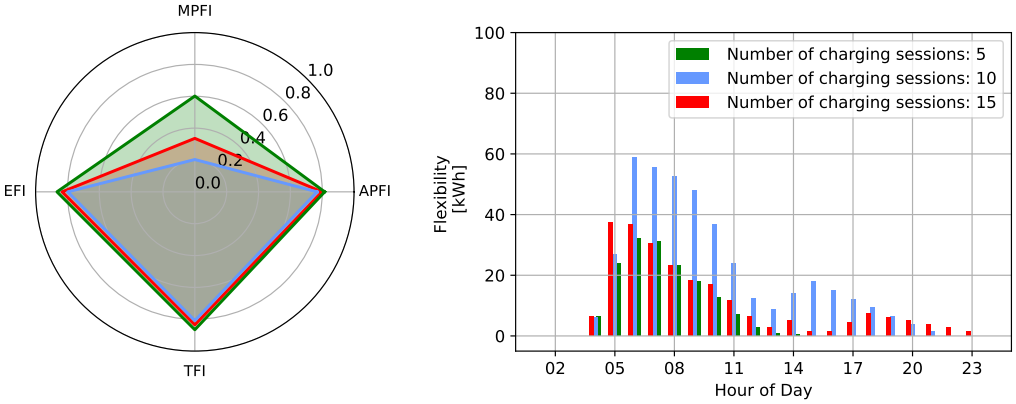


Fig. 10: Impact of the number of charging sessions on the charging cluster performance. The colours green, blue, and red represent scenarios where 5, 10, and 15 charging sessions are considered, respectively. On the left, flexibility indexes are evaluated, while the HEF is shown on the right.

TABLE IV: Flexibility criteria results for different numbers of charging sessions. The analysis is based on simulations from different days, each varying in the total number of recorded charging events.

| **Number of charging events** | **5** | **10** | **15** |
|---|---|---|---|
| MPFI | 0.34 | 0.20 | 0.60 |
| APFI | 0.80 | 0.77 | 0.82 |
| EFI | 0.83 | 0.80 | 0.87 |
| TFI | 0.84 | 0.81 | 0.87 |
| Maximum HEF [kWh] | 37.5 | 58.9 | 32.2 |
| Average HEF [kWh] | 11.5 | 22.8 | 14.4 |

the primary factor influencing the flexibility potential. Instead, the total energy requested by the EVs and the connection patterns play a more significant role. Notably, Scenario 2, where 10 EVs charge a total of 150 kWh, scores the lowest across all flexibility indexes, despite having fewer charging sessions compared to Scenario 3, where 15 EVs charge a total of 112 kWh. Overall, the radar graph shows only a marginal impact on the flexibility indexes, except for the MPFI, which decreases from 0.6 to 0.2. The HEF graph further highlights the predominant influence of the energy requested, with the HEF averaging 22.8 kWh and reaching a maximum of 58.9 kWh in Scenario 2. In comparison, Scenario 3 averages 14.4 kWh with a peak of 32.2 kWh. Additionally, the graph reveals a different distribution of flexibility based on connection patterns.

## IV. Conclusion

This paper introduces an evaluation tool and a set of flexibility criteria to assess the flexibility potential of EV charging clusters. The evaluation tool is demonstrated using an existing workplace charging cluster located in Copenhagen, Denmark, leveraging real historical data. The method is designed to quantify the suitability of a charging cluster to provide both BTM and FTM flexibility services. Specifically, the criteria are defined to evaluate short-term and long-term power adjustment capabilities, as well as charge scheduling capabilities. The proposed method consists of five flexibility criteria: four flexibility indexes to provide a qualitative assessment of the flexibility potential and one quantitative metric. The five criteria are defined as follows:

- Minimum Power Flexibility Index (MPFI): Quantifies the power flexibility potential during peak utilization of the charging cluster.
- Average Power Flexibility Index (APFI): Represents the average power flexibility potential throughout the charging process.
- Energy Flexibility Index (EFI): Assesses the ability of the charging cluster to strategically delay the charging requested by users.
- Time Flexibility Index (TFI): Evaluates the ability of the cluster to manage EV charging while simultaneously offering additional services.
- Hourly Energy Flexibility (HEF): Provides an hourly measurement of the maximum amount of energy that can be deferred by employing a smart charging strategy.

Among these, the MPFI and APFI focus on power-based flexibility services, while the EFI relates to energy-based services and the TFI is primarily associated with BTM services. Conversely, the HEF provides an energy-based measurement that quantifies the extent and timing of energy deferral capabilities. When employed within a pseudo-real simulation environment, this method facilitates the evaluation of the suitability of the cluster for diverse flexibility services under operational conditions. It also supports the design of new charging clusters and the monitoring and optimisation of existing systems.

Furthermore, a sensitivity analysis was performed to exam-

ine how different determinants affect the flexibility potential of charging clusters. The characteristics considered encompass hardware layout (such as the grid connection capacity and charger/car power capacity), software technology (including control strategies and the utilisation of user inputs), and user behaviour (encompassing charging patterns and EV characteristics). Although the primary objective of this study was not to analyse the specific charging cluster but rather to illustrate the flexibility criteria, it was observed that the analysed cluster was highly oversized relative to its utilisation rate in 2022. The sensitivity analysis further revealed that:

- A reduction in grid connection capacity significantly reduces the suitability of the charging cluster for power-based flexibility services, while its effects on energy flexibility are marginal. Although the average idle time of all the EVs was only marginally affected, a substantial reduction in connection capacity necessitates priority-based charging scheduling.
- Storage capacity/energy requested is the most influential factor for energy and time flexibility, while its impact on power flexibility is less pronounced. Higher energy requests allow for greater energy flexibility gains through smart charging strategies and shift the timing of energy availability throughout the day.
- Increasing the power capabilities of the chargers enhances the ability of the cluster to schedule energy consumption over time but also raises peak power consumption. This results in higher power peaks and longer average idle times.
- The number of charging sessions has a limited impact on the flexibility potential of the cluster. Instead, the total energy charged/requested and user connection patterns are more critical determinants for evaluating flexibility potential.
- Optimizing the charging strategy by adjusting power levels and scheduling charging sessions improves flexibility potential across all scenarios examined. Effective charging strategies are essential for maximizing flexibility and improving charging efficiency in clusters with poorly designed electrical layouts.

These findings underscore the importance of selecting appropriate charging strategies, particularly during periods of high concurrent charging, to optimise flexibility and meet the needs of both grid operators and users.

### A. Future work

The study identifies two key areas for further research. To begin with, the current evaluation indexes (MPFI, APFI, EFI and TFI) assess the performance of the entire EV cluster but do not account for the individual performance of each EV. Future research should develop metrics that evaluate the charging efficiency and flexibility of each EV separately, as this will enable a more precise optimization of the charging control strategy. The current metrics are averaged across all EVs, which overlooks the fact that each EV may have different charging needs and flexibility. For example, new metrics could address factors such as minimum idle time and lost charging opportunities for individual EVs.

Second, future studies should investigate the optimal flexibility capacity for clusters under various conditions. This involves analysing how the size of the electrical layout of a charging cluster impacts CAPEX and the potential reduction in OPEX due to flexibility services. Additionally, the accessibility of EV clusters to flexibility markets, along with the standardization and pricing of these services, will play a crucial role. Gaining insights into these aspects could improve the planning and management of smarter charging clusters and enhance returns on investment for CPOs and aggregators.

## Acknowledgment

The work in this paper is supported by the research projects ACDC (EUDP grant number: 64019-0541) and FUSE (EUDP grant number: 64020-1092).

## References

[1] T. Unterluggauer, J. Rich, P. B. Andersen, and S. Hashemi, "Electric vehicle charging infrastructure planning for integrated transportation and power distribution networks: A review," *ETransportation*, p. 100163, 2022.

[2] F. G. Venegas, M. Petit, and Y. Perez, "Active integration of electric vehicles into distribution grids: barriers and frameworks for flexibility services," *Renewable and Sustainable Energy Reviews*, vol. 145, p. 111060, 2021.

[3] T. Unterluggauer, F. Hipolito, J. Rich, M. Marinelli, and P. B. Andersen, "Impact of cost-based smart electric vehicle charging on urban low voltage power distribution networks," *Sustainable Energy, Grids and Networks*, vol. 35, p. 101085, 2023.

[4] R. Fachrizal, M. Shepero, D. van der Meer, J. Munkhammar, and J. Widén, "Smart charging of electric vehicles considering photovoltaic power production and electricity consumption: A review," *eTransportation*, vol. 4, p. 100056, 2020.

[5] X. Su, H. Yue, and X. Chen, "Cost minimization control for electric vehicle car parks with vehicle to grid technology," *Systems Science & Control Engineering*, vol. 8, no. 1, pp. 422–433, 2020.

[6] M. H. Tveit, K. Sevdari, M. Marinelli, and L. Calearo, "Behind-the-meter residential electric vehicle smart charging strategies: Danish cases," in *2022 International Conference on Renewable Energies and Smart Technologies*. IEEE, 2022.

[7] M. Müller, Y. Blume, and J. Reinhard, "Impact of behind-the-meter optimised bidirectional electric vehicles on the distribution grid load," *Energy*, vol. 255, p. 124537, 2022.

[8] E. Sortomme, M. M. Hindi, S. D. J. MacPherson, and S. S. Venkata, "Coordinated charging of plug-in hybrid electric vehicles to minimize distribution system losses," *IEEE Transactions on Smart Grid*, vol. 2, no. 1, pp. 198–205, 2011.

[9] K. Prakash, M. Ali, M. Siddique, A. Karmaker, C. Macana, D. Dong, and H. Pota, "Bi-level planning and scheduling of electric vehicle charging stations for peak shaving and congestion management in low voltage distribution networks," *Computers and Electrical Engineering*, vol. 102, p. 108235, 2022.

[10] K. Knezović, S. Martinenas, P. B. Andersen, A. Zecchino, and M. Marinelli, "Enhancing the role of electric vehicles in the power grid: field validation of multiple ancillary services," *IEEE Transactions on Transportation Electrification*, vol. 3, no. 1, pp. 201–209, 2016.

[11] J. Nájera, H. Mendonça, R. M. de Castro, and J. R. Arribas, "Strategies comparison for voltage unbalance mitigation in lv distribution networks using ev chargers," *Electronics*, vol. 8, no. 3, p. 289, 2019.

[12] M. Soleimani and M. Kezunovic, "Mitigating transformer loss of life and reducing the hazard of failure by the smart ev charging," *IEEE Transactions on Industry Applications*, vol. 56, no. 5, pp. 5974–5983, 2020.

[13] E. Yao, V. W. S. Wong, and R. Schober, "Robust frequency regulation capacity scheduling algorithm for electric vehicles," *IEEE Transactions on Smart Grid*, vol. 8, no. 2, pp. 984–997, 2017.

[14] S. Falahati, S. A. Taher, and M. Shahidehpour, "A new smart charging method for evs for frequency control of smart grid," *International Journal of Electrical Power & Energy Systems*, vol. 83, pp. 458–469, 2016.

[15] F. Mwasilu, J. J. Justo, E.-K. Kim, T. D. Do, and J.-W. Jung, "Electric vehicles and smart grid interaction: A review on vehicle to grid and renewable energy sources integration," *Renewable and Sustainable Energy Reviews*, vol. 34, pp. 501–516, 2014.

[16] T. Unterluggauer, F. Hipolito, P. B. Andersen, J. Rich, and M. Marinelli, "Conditional connection agreements for ev charging: Review, design, and implementation of solutions for the low voltage distribution grid," *Under review*, 2024.

[17] K. Sevdari, L. Calearo, P. B. Andersen, and M. Marinelli, "Ancillary services and electric vehicles: An overview from charging clusters and chargers technology perspectives," *Renewable and Sustainable Energy Reviews*, vol. 167, p. 112666, 2022.

[18] M. K. Gerritsma, T. A. Al Skaif, H. A. Fidder, and W. G. van Sark, "Flexibility of electric vehicle demand: Analysis of measured charging data and simulation for the future," *World Electric Vehicle Journal*, vol. 10, no. 1, pp. 1–22, 2019.

[19] M. A. van den Berg, I. Lampropoulos, and T. A. AlSkaif, "Impact of electric vehicles charging demand on distribution transformers in an office area and determination of flexibility potential," *Sustainable Energy, Grids and Networks*, vol. 26, p. 100452, 2021.

[20] J. Rominger, M. Loesch, and ..., "Utilization of Electric Vehicle Charging Flexibility to Lower Peak Load by Controlled Charging (G2V and V2G)," in *FAC Workshop on Control of Smart Grid and Renewable Energy Systems (CSGRES 2019)*, no. Csgres, 2019, pp. 1–6.

[21] E. C. Kara, J. S. Macdonald, D. Black, M. Bérges, G. Hug, and S. Kiliccote, "Estimating the benefits of electric vehicle smart charging at non-residential locations: A data-driven approach," *Applied Energy*, 2015.

[22] P. H. Divshali and C. Evens, "Behaviour analysis of electrical vehicle flexibility based on large-scale charging data," *2019 IEEE Milan PowerTech, PowerTech 2019*, no. 731297, 2019.

[23] M. Hijjo and A.-L. Klingler, "Modeling and simulation of electric vehicle flexibility to support the local network," in *2021 International Conference on Smart Energy Systems and Technologies (SEST)*, 2021, pp. 1–6.

[24] M. Voß, M. Wilhelm, and S. Albayrak, "Application independent flexibility assessment and forecasting for controlled EV charging," *SMARTGREENS 2018 - Proceedings of the 7th International Conference on Smart Cities and Green ICT Systems*, vol. 2018-March, no. Smartgreens 2018, pp. 108–119, 2018.

[25] L. Sørensen, K. B. Lindberg, I. Sartori, and I. Andresen, "Analysis of residential EV energy flexibility potential based on real-world charging reports and smart meter data," *Energy and Buildings*, vol. 241, p. 110923, 2021.

[26] J. Zhang, L. Che, X. Wan, and M. Shahidehpour, "Distributed hierarchical coordination of networked charging stations based on peer-to-peer trading and ev charging flexibility quantification," *IEEE Transactions on Power Systems*, pp. 1–1, 2021.

[27] M. Cañigueral and J. Meléndez, "Flexibility management of electric vehicles based on user profiles: The arnhem case study," *International Journal of Electrical Power & Energy Systems*, vol. 133, p. 107195, 2021.

[28] C. Gschwendtner, C. Knoeri, and A. Stephan, "Mind the goal: Trade-offs between flexibility goals for controlled electric vehicle charging strategies," *Iscience*, vol. 26, no. 2, 2023.

[29] J. B. Gutierrez-Lopez and D. Möst, "Characterising the flexibility of electric vehicle charging strategies: a systematic review and assessment," *Transport Reviews*, vol. 43, no. 6, pp. 1237–1262, 2023.

[30] Å. L. Sørensen, B. B. Morsund, I. Andresen, I. Sartori, and K. B. Lindberg, "Energy profiles and electricity flexibility potential in apartment buildings with electric vehicles–a norwegian case study," *Energy and Buildings*, vol. 305, p. 113878, 2024.

[31] N. K. Panda and S. H. Tindemans, "Efficient quantification and representation of aggregate flexibility in electric vehicles," *Electric Power Systems Research*, vol. 235, p. 110811, 2024.

[32] F. Al Taha, T. Vincent, and E. Bitar, "An efficient method for quantifying the aggregate flexibility of plug-in electric vehicle populations," *IEEE Transactions on Smart Grid*, 2024.

[33] K. Sevdari, L. Calearo, S. Striani, P. B. Andersen, M. Marinelli, and L. Rønnow, "Autonomously distributed

control of electric vehicle chargers for grid services," in *2021 IEEE PES Innovative Smart Grid Technologies Europe (ISGT Europe)*. IEEE, 2021, pp. 1–5.

[34] K. Sevdari, L. Calearo, B. H. Bakken, P. B. Andersen, and M. Marinelli, "Experimental validation of onboard electric vehicle chargers to improve the efficiency of smart charging operation," *Sustainable Energy Technologies and Assessments*, vol. 60, p. 103512, 2023.

[35] L. Calearo, C. Ziras, K. Sevdari, and M. Marinelli, "Comparison of smart charging and battery energy storage system for a pv prosumer with an ev," pp. 1–6, 2021.

# Appendix

TABLE A1: Classification of potential EV flexibility services for FTM applications (Own illustration based on the work in [17]).

| **Frequency services** | |
|---|---|
| *Services* | *Description* |
| 1. Fast frequency reserve | 1. Power injection starts within 2 seconds and lasts for several minutes; assists in reducing the *Rate of change of frequency*. |
| 2. Frequency containment reserve | 2. Power injection begins within 30 seconds and is fully activated within 2-5 minutes; aids in containing deviations from the nominal frequency. |
| 3. Frequency restoration reserve | 3. Activated within 5-15 minutes and sustained until frequency is restored; assists in bringing the system frequency back to its nominal value. |
| 4. Replacement reserve | 4. Power delivered within 15 minutes to 1 hour; ensures sufficient active power reserves following a disruption and replaces the Frequency restoration reserve. |
| 5. Synthetic inertia | 5. Immediate response ($<$1 second) to frequency changes; emulates the behaviour of traditional rotating generators. |
| 6. Virtual inertia | 6. Instantaneous response to frequency changes through the use of power electronics and advanced control technologies. |
| **Grid stability** | |
| *Services* | *Description* |
| 1. Emergency power | 1. Activated during emergencies to provide critical infrastructure with power; typically involves non-scheduled power plants that can start up quickly. |
| 2. Energy arbitrage | 2. Involves charging when prices are low (off-peak) and discharging when prices are high (peak). |
| 3. RES power smoothing | 3. Aims to reduce the variability of power output from renewable energy sources, which helps to mitigate issues like power flickering. |
| 4. Black start capability | 4. Helps the power grid to restart after a total or partial blackout by supplying power until interconnected system is established again. |
| 5. Anti-islanding | 5. Prevents local generators from continuing to supply power during a wider network outage, ensuring the safety of repair crews and preventing the spread of faults. |
| 6. Low voltage ride through | 6. Requires power generation systems to maintain operation despite dips in grid voltage; contributing to overall grid stability. |
| 7. Fault ride through | 7. Requires power generation systems to maintain operation during grid faults or abnormal operating conditions, such as short circuits. |
| 8. Valley filling | 8. Involves charging energy storage systems during off-peak periods (when demand is low) and discharging them during peak times; helps to alleviate load peaks. |
| 9. Peak shaving | 9. Entails reducing or curtailing demand during peak times to relieve stress on the grid. |
| **Congestion management** | |
| *Services* | *Description* |
| 1. Time of use | 1. Involves varying electricity prices based on the time of the day to encourage consumers to shift their electricity use to periods of lower demand. |
| 2. Type of use | 2. Featured different rates depending on the type of electricity usage, with additional fees based on grid carbon intensity. |
| 3. Dynamic pricing | 3. Encompasses the adjustment of electricity prices in real-time according to supply and demand; requires advanced metering infrastructure and sophisticated rate design. |
| 4. Extreme day pricing | 4. Refers to significantly increased electricity prices on days with expected extremes, often in response to weather events; it aims to incentivize consumers to shift their usage away from these peak periods. |
| 5. Peak time rebate | 5. Offers discounts or rebates to customers who reduce their electricity usage during peak demand periods. |
| 6. RES power matching | 6. Involves scheduling the operation of Renewable Energy Sources (RES) to align with demand profiles, helping to mitigate the issues caused by the intermittency of RES. |
| 7. Phase balancing | 7. Aims to distribute electrical loads evenly across all phases in a three-phase power system to improve efficiency and reduce losses. |
| 8. DER power matching | 8. Matches supply with demand in systems with DERs, often through demand response programs or adjustments to DER output. |

PAPER [P3]

# Autonomously Distributed Control of EV Parking Lot Management for Optimal Grid Integration

Authors:

Simone Striani, Kristian Sevdari, Peter Bach Andersen, Mattia Marinelli, Yuki Kobayashi, Kenta Suzuki

Published in:

*2022 International Conference on Renewable Energies and Smart Technologies (REST)*

DOI:

10.1109/REST54687.2022.10022907.

# Autonomously Distributed Control of EV Parking Lot Management for Optimal Grid Integration

Simone Striani, Kristian Sevdari,
Peter Bach Andersen, Mattia Marinelli
*Department of Wind and Energy Systems*
*Technical University of Denmark*
Roskilde, Denmark
{sistri; krisse; petb; matm}@dtu.dk

Yuki Kobayashi, Kenta Suzuki
*EV System Laboratory*
*Nissan Motor Co., Ltd.*
Yokosuka, Japan
{yuki-kobayashi; ke-suzuki}@mail.nissan.co.jp

***Abstract*—This paper proposes an autonomous distributed control design for coordinating the charging process of parking lots for electric vehicles (EVs). The focus of this paper is to investigate the performance of the modeled architecture. The model simulates for 24 hours an office parking lot scenario with real input data from 16 EVs. The primary objective is to quantify the fulfillment of the demand and the guaranteed amount of energy for each user. The secondary objective is to analyze the effects of restricting the power capacity of the parking lot from 88 kW to 43 kW. In the constrained charging scenario, the system guarantees a minimum energy of 12.2 kWh (roughly 61 km) to each car connected for at least 5 hours and 54 minutes. In the unconstrained charging scenario 12 EVs reach maximum state-of-charge (SOC), while 11 EVs reach it in the constrained one. Demand fulfillment is only marginally different between the two scenarios because the final SOC values of the EVs are nearly the same. On the other hand, constraining connection capacity reduces significantly the idle state of six chargers.**

***Index Terms*—Electric Vehicle, Distribution Grid, Smart Charging, Flexibility**

## I. Introduction

Electric grids must withstand the increased volatility of energy production and energy demand. On the production side, this is because electricity production will gradually shift towards renewable energy sources (RES), which are less predictable and controllable. On the demand side, this is because electric vehicles (EVs) will gradually become the main private means of transportation [1]. The charging of large EV fleets will increase the amplitude of peak energy demand due to concurrent charging in peak hours [2], [3]. Smart charging is a technology that allows EVs to become flexible loads for the grid and deliver flexibility services to the distribution and transmission system [4] . Consequently, this technology has the potential to mitigate the negative impacts of the penetration of RES and EVs [5]. As a results, the mass roll-out of smart chargers offers the opportunity to reduce or delay expensive grid upgrades [6]. Smart charging is a novel technology, therefore extensive experimental data on its optimal features and development is needed [7]. For instance, it needs to be further technically developed, standardized, and exhaustively tested before its full roll-out. Many technical aspects of the technology need to be further developed: the chargers technical characteristics and the information and communication technology (ICT) need to be standardized so that interoperability is ensured between chargers, EVs, smart meters and grid components [8]. The smart charging technology can be investigated through experimental campaigns and mathematical modeling of charging clusters. Demonstration campaigns are the starting point for the generation of data to be used for the further development of the technology [9]. Grid observability of already deployed chargers is the key to the development of smart charging on a large scale; therefore, deployed chargers should be coupled with smart meters to generate real usage data in different scenarios [10]. The design of mathematical models is the starting point for understanding the interaction between the clusters and the vehicles for behind-the-meter (BTM) services, and between the clusters and the grid for front-of-the-meter (FTM) services [11]. In short, BTM services are a series of power and energy services that can be used to fulfill specific user's needs. They are generally provided to users or the building connected to the parking lot by the system. Examples of BTM services are energy arbitrage, power sharing and power scheduling between EVs. FTM services are other power and energy services meant to benefit the grid and to ensure its optimal performances. They are managed by its operators (such as DSOs and TSOs). Some FTM services are congestion management, peak-shaving and voltage unbalance reduction. A more complete description of the grid services can be found in [11]. This paper focuses on the technical side of the development of smart charging, through the modelling of a smart charger based on a distributed control architecture. The focus is on BTM services and on illustrating the design and performance of such a control architecture. The rest of the paper is structured as follows. Section II describes the objective of the research in more detail; Section III describes the methodology adopted for the study; Section IV introduces the results of the case study simulation; Section V provides conclusions and future work.

## II. Objectives of the research

This work is part of the modelling and demonstration activities of the ACDC project (Autonomously Controlled Distributed Chargers). The project aims to develop a clustering method for smart chargers in which different parking lots can be monitored and governed with a distributed control architecture. Such an architecture consists of two control intelligences: the cloud aggregator (CA) and the virtual aggregator (VA). The former is responsible for the coordination of different parking lots for the provision of flexibility services FTM and grid integration. The latter is

responsible for the coordination of the different chargers within a parking lot for BTM services. The user can interact with the system to check charging schedule and monitoring the charging session. The CA will guarantee full controllability by grid operators for the provision of flexibility services on the market. The VA will guarantee maximization of user comfort and minimization of charging point operators' (CPO) expenses.

This study will focus on the local control architecture, describing the VA and illustrating the performance of the parking lot components, in terms of fulfillment of the users' charging sessions. Therefore, the control architecture needs to ensure that each user of the parking lot has a certain minimum amount of energy available at the end of the charging session. The parking lot model performs power scheduling and power sharing among the connected EVs throughout the day. The research objectives of this paper are:

- Analysing the performance of power scheduling and power sharing functions in order to lower the point of common coupling (PCC) connection capacity.
- Giving an overview of the EV charging sessions in order to measure the capacity of the parking lot to fulfill the users' demand.
- Measuring the flexibility available in the parking lot in terms of chargers' idle time and surplus energy available.

## III. Methodology

This section describes the methodology implemented in this paper. The model developed uses as a starting point the model previously built in [12].

### A. Comparison of control architecture strategies

There are several types of control architectures. They can be classified as centralized, decentralized, or distributed [13]. The centralized control architecture consists of one central control element that collects information from the grid and decides the power set-points for the power demand / supply of every device remotely. In the decentralized control architecture, the central (common) control objective is pursued independently by local control elements independently; therefore, local control elements only use local measurements and actuators. The distributed control architecture, instead, contains both a central controller (in this case the CA) and a local controller (in this case the VA). The central controller coordinates charging clusters on a higher level. For example, CA receives information from the grid and dispatches set-points to the local controller. At the lower level, local controllers process and distribute the set-points among the different devices with local communication. The advantages and drawbacks of centralized control, distributed control, and decentralized control are described in [14]. Although previous smart charging strategies rely on a centralized control approach [15], this study exploits the distributed control approach. The dual nature of the communication, both local and cloud-based, is worth being explored for several reasons: with this strategy, the charger would be capable of working even if the communication with the grid is interrupted, or if one of the chargers stops working; moreover, the local communications between the controlling units is faster and more robust [16].

### B. Global system architecture

Fig. 1 provides an overall illustration of the control architecture applied to a number of N clusters. The CA and the VA are, respectively, two intelligences that control the parking lot power demand both according to the status of the grid and to the preferences of the EV users.

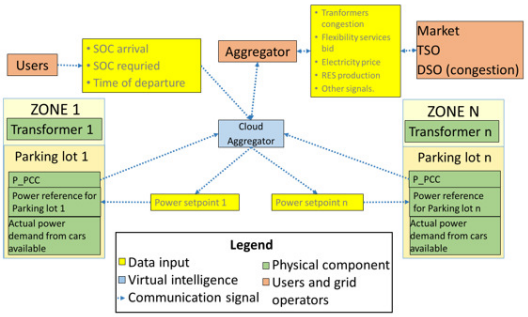


Fig. 1. Global system architecture and communication paths between different actors.

The CA is the global intelligence, and it has two main functions: the first is receiving signals from the grid, such as RES production, electricity price, and grid congestion. The CA translates these inputs into power set-points and sends them to the VA of each cluster. The second function is to receive user inputs (via the mobile app) and to distribute them to the VAs. The users' inputs are the state of charge (SOC) at the time of plug-in, the battery capacity and the scheduled time of departure. The VA is the local intelligence and broadcasts power set-points received from the CA to all the chargers of its cluster. Based on user preferences, the VA gives instructions to the chargers, such as charging priority and power scheduling based on SOC. Lastly, the smart meter feedbacks the power consumed to the CA, so that the CA can continuously redistribute the power among the parking lots according to the availability of cars and local grid conditions.

### C. Local system architecture

Fig. 2 provides a simplified illustration of the model for a single cluster. Each charger is composed of the VA (divided into primary and secondary functions) and the charger controller. The parking lot contains N chargers. In the parking lot, there is a smart meter connected to the point of common coupling (PCC). The primary function of the VA (shortly VA_primary) is the constant power set point reception from the cloud and consequent constant adjustment of the total demand of the parking lot. VA_primary is active only in one of the chargers, to avoid redundancy in communication. However, in case of its malfunctioning, other chargers can automatically replace it with their VA. The secondary function of the VA (shortly VA_secondary) is to schedule and share charging power among the EVs, and it is active in all the N chargers. A description of the power and information flow follows: On the left, the

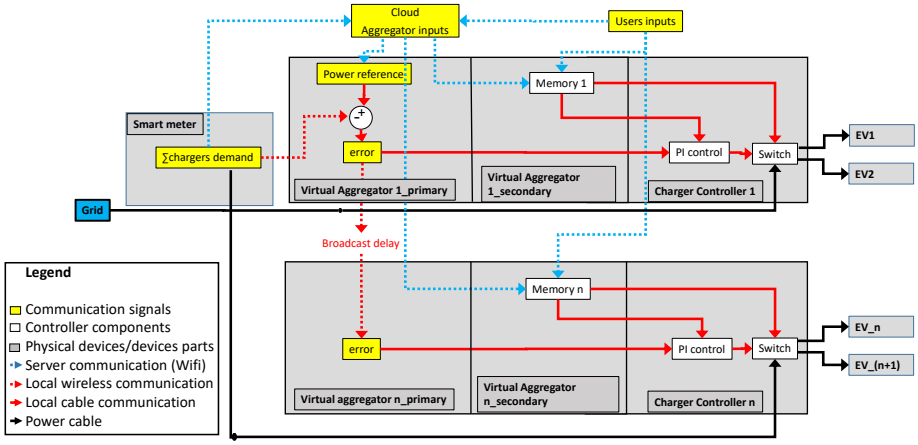


Fig. 2. Local system architectures and communication between different components of the parking lot.

smart meter records the power flowing from the grid to the chargers. The smart meter sends the consumption measurements through wired communication to VA1_primary, part of charger 1. VA1_primary also receives set-points from the CA via Wi-Fi or Ethernet communication. Such set-points are the result of the CA processing data from the grid. VA1_primary compares the difference between the set-points of the CA and the actual measurement of the smart meter and calculates an error value. VA1_primary broadcasts the error value to all the chargers via cable (for charger 1) and via wireless communication (for chargers 2 to N). The users communicate their inputs via the mobile app to the CA. The CA sends them to the secondary function of each VA, via Wi-Fi communication. Each VA_secondary stores the information from the charger meter and communicates with the PI control and with the switch according to the EV priorities. The power coming from the grid flows through the smart meter to the switches. The switches deliver alternately the power to one of the connected EVs based on the schedule calculated by each VA_secondary. Each VA_secondary would automatically calculate the current SOC based on scheduled charging and user input. The total power demand is continuously recorded by the smart meter.

### D. Case Study

For the scope of this paper, the model is tailored to a parking lot scenario. The simulated scenario is a workplace parking lot of the Risø research campus of Technical University of Denmark. The parking lot will house 8 smart chargers with double type-2 plugs for each charger. Each charger can simultaneously charge only one car, even if two cars are plugged in. Each plug can support a maximum current of 16 A (11 kW charging 3 phase or 3.68 kW charging 1 phase). In the unconstrained scenario, the maximum power capacity of the parking lot is therefore 88 kW, while in the constrained charging scenario a fuse limit of 43 kW is chosen. In the latter scenario, the chargers will perform power scheduling and sharing to avoid overloading the fuse. When constructed, the parking lot will be suitable for experimental analysis to validate the results of the simulation and expand the findings to a larger scale.

### E. Model assumption and inputs

The model is designed in Matlab/Simulink. The simulation has a total time of 24h, with a variable time-step. The inputs of the model are EV parking behavior data from a real office parking lot and are summarized in Table I. The table shows in the same color the EVs connected to the same charger. The data are provided by a Nissan EV telematics and consist of a dataset containing arrival time, SOC at the beginning of the session, and planned departure time from 16 EV users in a time range of 24 hours with a time resolution of one second. In addition, the simulation incorporates EV models and relative battery capacity. They represent a sample of the most common EVs found in the DTU university campus. Such info is

TABLE I
INPUTS OF THE MODEL FOR THE SIMULATION.

| EV num | Model | Charging Phases | Battery_capacity [kWh] | Initial SOC [%] | Connection time [hh:mm] |
|---|---|---|---|---|---|
| EV1 | Tesla Model 3 | 3 | 75 | 25% | 08:47-18:08 |
| EV2 | Peugeot iOn | 1 | 14.5 | 17% | 09:31-12:29<br>14:41-18:00 |
| EV3 | Tesla P85D | 3 | 85 | 33% | 08:24-08:52<br>10:40-17:40 |
| EV4 | Nissan LEAF | 1 | 24 | 50% | 08:31-17:12 |
| EV5 | Nissan LEAF | 1 | 62 | 58% | 08:36-20:29 |
| EV6 | Nissan e-NV200 | 1 | 24 | 67% | 08:24-19:25 |
| EV7 | Renault Zoe | 3 | 44 | 50% | 07:47-12:15<br>12:53-16:06<br>16:24-17:18 |
| EV8 | Volkswagen E-golf | 1 | 36 | 58% | 08:15-18:10 |
| EV9 | Tesla Model 3 | 3 | 75 | 67% | 07:56-18:03 |
| EV10 | Nissan LEAF | 1 | 24 | 92% | 10:40-16:23 |
| EV11 | Nissan LEAF | 1 | 62 | 42% | 07:25-17:01 |
| EV12 | Nissan e-NV200 | 1 | 24 | 33% | 07:35-19:55 |
| EV13 | Renault Zoe | 3 | 44 | 33% | 00:21-04:00 |
| EV14 | Renault Zoe | 3 | 44 | 75% | 08:31-17:12 |
| EV15 | Tesla Model 3 | 3 | 75 | 67% | 08:55-22:16 |
| EV16 | Renault Zoe | 3 | 44 | 17% | 06:28-09:15<br>11:41-17:06 |

inputted in the model directly to characterize the EVs, their arrival and departure time. Based on these information the VA schedules their charging time and power. The switch performs scheduling by prioritizing the EVs with lower SOC with schedules of 30% SOC each. The EV models contain a simplified battery model and AC-DC converter efficiency which decreases linearly from 90% at full charge (11 kW for 3 phase charging or 3.68 kW for 1 phase charging) to 80% at minimum charge (4.15 kW for 3 phase charging or 1.38 kW for 1 phase charging) [17]. At the end of each iteration, the power consumed by each charger is recorded on the smart meter. The smart meter will calculate the total power demand of the last iteration for the next iteration cycle. More information about the model's signal discretization and communication delays can be found in [12].

## IV. Results

Figure 3 displays the connection and charging time of EVs throughout the day. The y-axis shows the EV number, while the x-axis shows the time in hours. For each EV the dotted line represents the connected time while the continuous line is the actual charging time. The lines of EVs connected to the same charger are shown in the same color. Fig.3 gives a detailed overview of the charging schedule of each EV, and the alternate switching between two EVs plugged on each charger. Further, some EVs reach their maximum SOC and stop charging before leaving. The surplus energy is used to charge the rest of EVs faster. However, the same energy surplus can be used for FTM flexibility services if the other EVs are already charging with maximum capacity.

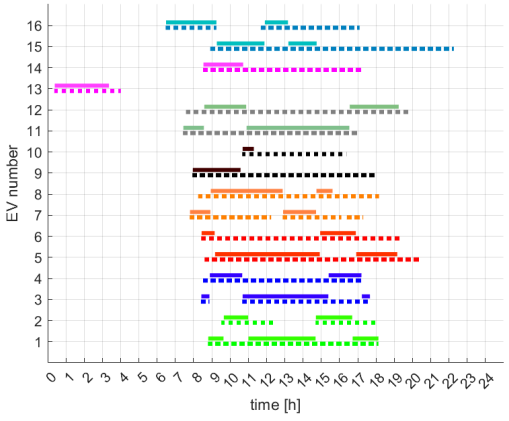


Fig. 3. Connection and charging time history of the simulation.

Fig. 4 provides the overall results of the parking lot simulation during the 24 hours period. The top graph illustrates a time history of the charging power in the constrained charging and unconstrained charging cases for comparison. The bottom graph shows the time history of the number of EVs charging and the number of EVs connected in the constrained charging case. In the unconstrained charging case the peak demand due to concurrent charging is 66 kW. However, the bottom graph suggests that 43 kW is an acceptable limit because most of the EVs are fully charged and stop charging long before they leave the parking lot. In fact, after 11:30 am, only 6 cars are charging at the same time.

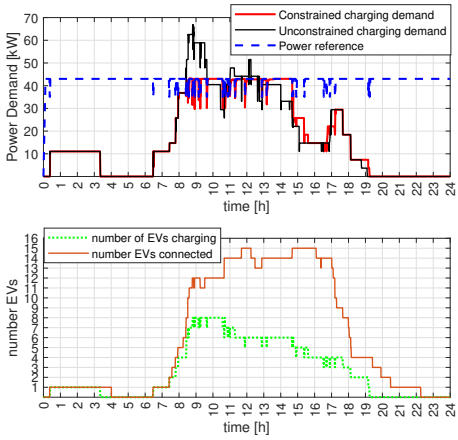


Fig. 4. Overall time history of the total power demand with unconstrained and constrained charging (top). Time history of number of EVs connected and charging (bottom)

Table II shows the performance of the charging sessions for the parking lot. In detail, the results are similar for both scenarios: 11 EVs are fully charged by the end of their charging session in the constrained scenario, one less than the unconstrained one. Otherwise, the results are very similar. EV11 has the lowest SOC of 78% in both scenarios. However, EV11 charges in both scenarios to its maximum power while connected, showing that constrained charging does not affect its demand fulfillment. EV11 is a single phase EV with a high battery capacity of 62 kWh and it manages to charge 25 kWh (roughly 125 km). Regarding EVs that do not reach 100% SOC: the minimum amount of energy guaranteed by the parking lot is 12.2 kWh if an EV is parked for at least 5 hours and 54 minutes. Therefore, assuming that EVs drive an average of 5 km per kWh, the parking lot is capable of guaranteeing approximately 61 km of driving autonomy during the simulated day. In addition, six of the eight chargers reach idle state for an average of 4 hours and 19 minutes per charger because their plugged EVs are fully charged. This idle time shows that, in this simulation, the fuse limit could be even lower than 43 kW without a significant effect on vehicle demand fulfillment. However, such time buffer can be used for FTM flexibility services.

Lastly, the parking lot erogates power for 19 hours and 24 minutes over 24 hours. In such time, the total energy output in the constrained charging scenario is 414 kWh, whereas in the unconstrained charging scenario it would instead be 413 kWh. This confirms that the charging bottleneck is the power limit of each charger (11 kW, for 3 phase charging, and 3.68 kW, 1 phase charging) and not the fuse limit. The actual energy stored in the EV batteries is 368 kWh and 373 kWh in the constrained and uncon-

TABLE II
TABLE SHOWING THE MOST RELEVANT SIMULATION OUTPUT PER CAR AND PER CHARGER

| | | Charger 1 | | Charger 2 | | Charger 3 | | Charger 4 | | Charger 5 | | Charger 6 | | Charger 7 | | Charger 8 | |
|---|---|---|---|---|---|---|---|---|---|---|---|---|---|---|---|---|---|
| Idle time constrained | [hh:mm] | 00:00 | | 00:00 | | 01:18 | | 02:32 | | 06:46 | | 00:39 | | 07:04 | | 07:30 | |
| Idle time unconstrained | [hh:mm] | 00:00 | | 00:00 | | 01:41 | | 03:28 | | 06:55 | | 00:47 | | 08:08 | | 09:30 | |
| | | EV1 | EV2 | EV3 | EV4 | EV5 | EV6 | EV7 | EV8 | EV9 | EV10 | EV11 | EV12 | EV13 | EV14 | EV15 | EV16 |
| Charging mode | # | 3 phase | 1 phase | 3 phase | 1 phase | 1 phase | 1 phase | 3 phase | 1 phase | 3 phase | 1 phase | 1 phase | 1 phase | 3 phase | 3 phase | 3 phase | 3 phase |
| Available_time | [hh:mm] | 09:18 | 05:54 | 07:24 | 08:36 | 11:48 | 00:00 | 06:42 | 09:54 | 10:06 | 05:42 | 9.6 | 12:18 | 03:36 | 08:36 | 13:18 | 08:12 |
| EV_charging_time | [hh:mm] | 05:54 | 03:18 | 05:36 | 03:36 | 08:00 | 02:42 | 02:54 | 04:48 | 02:36 | 00:36 | 6.7 | 05:00 | 03:00 | 02:12 | 04:12 | 04:00 |
| EV_tot_energy_charged_AC (constrained) | [kWh] | 59.5 | 12.2 | 58.5 | 13 | 29.2 | 8.9 | 25.6 | 17.1 | 28.1 | 2.2 | 25 | 18 | 32.4 | 13.3 | 29.4 | 41.4 |
| Final SOC unconstrained | [ %] | 99 | 98 | 97 | 100 | 100 | 100 | 100 | 100 | 100 | 100 | 78 | 100 | 100 | 100 | 100 | 100 |
| Final SOC constrained | [ %] | 96 | 92 | 94 | 99 | 100 | 100 | 100 | 100 | 100 | 100 | 78 | 100 | 100 | 100 | 100 | 100 |

strained charging scenarios, respectively. This difference is due to the lower AC-DC conversion efficiency of the cars when modulating the charging power. These losses can be minimized by prioritizing power scheduling over power sharing. However, such losses may still be acceptable considering that the system reduces the overloading of the grid and the need to upgrade the connection capacity of the parking lot and components of the distribution grid.

## V. Conclusion and Future Work

This paper illustrates an autonomous distributed control and logic design for coordinating the charge of EVs in a parking lot. The modeled architecture is applied to a 24 hours simulation of an office parking lot scenario with real input data from 16 EVs. Two scenarios are compared: constrained charging (43 kW fuse limit) and unconstrained charging (88 kW is the maximum power that can be supplied by the chargers). The local performance of the parking lot follows: 11 EVs reach maximum SOC in the constrained scenario, one less than the unconstrained one. Otherwise the demand fullfillment performances are similar. EV11 reaches only 78% SOC in both scenarios due to its slow charging capacity. The parking lot guarantees a minimum of 12.2 kWh (roughly 61 km) to each car and has a significant amount of idle time from 6 chargers. This is because most EVs are fully charged before the charging session ends, and the resulting energy buffer can be used for FTM flexibility services or to further reduce the fuse limit. Overall, the architecture schedules the charging of all EVs correctly, starting from the ones with lower SOC. Having two plugs per charger, of which one is functioning at a time, is a convenient way to have more EVs connected without needing a high connection capacity. Prioritizing power scheduling over power sharing and limiting the modulation of the charging power is also important not to lose efficiency in AC-DC energy conversion of the EV. In the future, the model will also be used to investigate phase balancing, by automatically switching 3 phase EVs to 1 phase. Furthermore, the simulated EV parking lot scenario will be constructed and used to validate the results.

## Acknowledgment

The work in this paper is supported by the research projects ACDC (EUDP grant number: 64019-0541) and FUSE (EUDP grant number: 64020-1092). Website: www.acdc-bornholm.eu and www.fuse-project.dk

## References

[1] International Energy Agency, "Global ev outlook: Entering the decade of electric drive," tech. rep., 2020.

[2] M. Muratori, "Impact of uncoordinated plug-in electric vehicle charging on residential power demand," *Nature Energy*, vol. 3, pp. 193–201, 3 2018.

[3] L. Calearo, A. Thingvad, K. Suzuki, and M. Marinelli, "Grid loading due to ev charging profiles based on pseudo-real driving pattern and user behavior," *IEEE Transactions on Transportation Electrification*, vol. 5, pp. 683–694, 2019.

[4] M. Z. Degefa, I. B. Sperstad, and H. Sæle, "Comprehensive classifications and characterizations of power system flexibility resources," *Electric Power Systems Research*, vol. 194, no. January, p. 107022, 2021.

[5] C. Crozier, T. Morstyn, and M. McCulloch, "The opportunity for smart charging to mitigate the impact of electric vehicles on transmission and distribution systems," *Applied Energy*, vol. 268, no. March, p. 114973, 2020.

[6] M. Resch, J. Buhler, B. Schachler, and A. Sumper, "Techno-Economic Assessment of Flexibility Options Versus Grid Expansion in Distribution Grids," *IEEE Transactions on Power Systems*, vol. 36, no. 5, pp. 3830–3839, 2021.

[7] F. G. Venegas, M. Petit, and Y. Perez, "Active integration of electric vehicles into distribution grids: Barriers and frameworks for flexibility services," *Renewable and Sustainable Energy Reviews*, vol. 145, p. 111060, 7 2021.

[8] H. S. Das, M. M. Rahman, S. Li, and C. W. Tan, "Electric vehicles standards, charging infrastructure, and impact on grid integration: A technological review," *Renewable and Sustainable Energy Reviews*, vol. 120, 3 2020.

[9] M. Marinelli et al., "Electric vehicles demonstration projects - an overview across europe," *2020 55th International Universities Power Engineering Conference (UPEC)*, pp. 1–6, 2020.

[10] L. Calearo, M. Marinelli, and C. Ziras, "A review of data sources for electric vehicle integration studies," *Renewable and Sustainable Energy Reviews*, vol. 151, no. December 2020, 2021.

[11] S. Striani, K. Sevdari, L. Calearo, P. B. Andersen, and M. Marinelli, "Barriers and solutions for evs integration in the distribution grid," *UPEC 2021 56th International Universities Power Engineering Conference*, 2021.

[12] K. Sevdari, L. Calearo, S. Striani, P. B. Andersen, M. Marinelli, and L. Rønnow, "Autonomously distributed control of electric vehicle chargers for grid services," in *2021 IEEE PES Innovative Smart Grid Technologies Europe (ISGT Europe)*, pp. 1–5, IEEE, 2021.

[13] J. García-Villalobos, I. Zamora, J. I. S. Martín, F. J. Asensio, and V. Aperribay, "Plug-in electric vehicles in electric distribution networks: A review of smart charging approaches," *Renewable and Sustainable Energy Reviews*, vol. 38, pp. 717–731, 2014.

[14] X. Han, K. Heussen, O. Gehrke, H. W. Bindner, and B. Kroposki, "Taxonomy for evaluation of distributed control strategies for distributed energy resources," *IEEE Transactions on Smart Grid*, vol. 9, pp. 5185–5195, 9 2018.

[15] K. Sevdari, L. Calearo, P. Bach, and M. Marinelli, "Ancillary services and electric vehicles : an overview from charging clusters and chargers technology perspectives," *Renewable & Sustainable Energy Reviews*, vol. under-review, 2022.

[16] "Automated distributed electric vehicle controller for residential demand side management," *IEEE Industry Applications Society Annual Meeting, IAS*.

[17] L. Calearo, C. Ziras, K. Sevdari, and M. Marinelli, "Comparison of smart charging and battery energy storage system for a pv prosumer with an ev," in *2021 IEEE PES Innovative Smart Grid Technologies Europe (ISGT Europe)*, pp. 1–6, IEEE, 2021.

PAPER [P4]

# Wind Based Charging via Autonomously Controlled EV Chargers under Grid Constraints

Authors:

Simone Striani, Kristian Sevdari, Mattia Marinelli, Vasileios Lampropoulos Yuki Kobayashi, Kenta Suzuki

Published in:

*Proceedings of the 2022 57th International Universities Power Engineering Conference (UPEC)*

DOI:

10.1109/UPEC55022.2022.9917883.

# Wind Based Charging via Autonomously Controlled EV Chargers under Grid Constraints

Simone Striani, Kristian Sevdari, Mattia Marinelli
*Department of Wind and Energy Systems*
*Technical University of Denmark*
Roskilde, Denmark
{sistri; krisse; matm}@dtu.dk

Vasileios Lampropoulos
*Nordic RCC*
*Energinet*
Copenhagen, Denmark
vas@nordic-rcc.net

Yuki Kobayashi, Kenta Suzuki
*EV System Laboratory*
*Nissan Motor Co., Ltd.*
Yokosuka, Japan
{yuki-kobayashi; ke-suzuki}@mail.nissan.co.jp

2022 57th International Universities Power Engineering Conference (UPEC) | 978-1-6654-5505-3/22/$31.00 ©2022 IEEE | DOI: 10.1109/UPEC55022.2022.9917883

***Abstract*—Smart charging has a strong potential to mitigate the challenges in security of supply caused by the increasing reliance on renewable energy sources (RESs) and electric vehicles (EVs). This paper describes the performances of an autonomous distributed control for coordinating the charge of four parking lots as part of a virtual power plant. The virtual power plant consists of a wind farm and four parking lots located in different areas of the grid and connected to two different feeders. The control architecture is applied to a 24-hour simulation with input data from a wind park, the loading data of two feeders, and user behavior from 68 EVs. The objectives of the architecture are: maximization of the wind power usage to charge the EVs; minimization of feeders overloading; minimization of energy imported from the grid; assurance of sufficient charging fulfillment; wind power variability mitigation. Under simulated conditions, the control architecture keeps the feeder loading below 80% by reducing the power allowance to the parking lot during peak demand. Nonetheless the four parking lots guarantee an energy charged of 10.7 kWh for all EVs starting the charging session with less than 60% state of charge (SOC). The total energy produced by the wind power plant is 4.36 MWh, of which 1.34 MWh is used to charge EVs. The remaining 3.07 MWh is exported to the grid, and only 92 kWh is imported from the grid for charging. Further investigation is needed regarding the wind power variability mitigation, as its reduction is only marginal under simulated conditions.**

***Index Terms*—Electric Vehicle, Distribution Grid, Virtual Power Plant, Smart Charging, Flexibility**

## I. Introduction

The power system is experiencing two major energy transitions: the transition to renewable energy sources (RESs) as the main source of energy and the transition to electric vehicles as the main mean of transportation. Therefore, in the near future, the power system will experience increased fluctuation both in energy demand and energy supply [1]. On the one hand, the energy supply will fluctuate more due to the intermittent nature of RES. On the other hand, the energy demand will have larger peaks and valleys due to concurrent charging of EVs at certain times of the day [2]. The overloading of feeders and lines may lead Distribution System Operators (DSOs) to reinforce the already existing infrastructure or deploy power system flexibility solutions to delay expensive upgrades of the grid [3]. Such flexibility can be provided from EVs, through smart charging. Smart charging is defined as the adaptation of the charging process of the EVs according to both the power system condition and the needs of the vehicle users [4]. Smart charging can be used to deliver flexibility services to the distribution and transmission system. Consequently, this technology has the potential to mitigate the negative impacts coming from both RES and EV penetration [5]. As a results, the mass roll-out of smart chargers offers the opportunity to reduce or delay expensive grid upgrades [3]. Flexibility services provided by EVs can be divided into two categories, namely behind-the-meter (BTM) and in-front-of-the-meter (FTM) [6]. BTM services benefit users and focus on coordinating the EVs consumption with other loads (e.g. buildings) and distributed energy resources (DER) behind the point of common coupling (PCC). FTM services benefit the grid, and are managed by the DSOs and TSOs in order to ensure stability and security of supply. In [7], it is thoroughly explained what are BTM and FTM services. These types of grid services include prioritizing charging during off-peak times to assist in reducing peak loads, alleviating feeder congestion through charging power adjustments, and reducing wind power curtailment through the utilization of excess wind power production for the charging process [8].

This paper investigates the application of smart charging in a virtual power plant (VPP) scenario. VPPs are a type of clustering model that attempts to manage geographically scattered electrical generation and demand as if they were one entity for the system operator [9]. The mission of a VPP is to network DERs in order to monitor, forecast, and trade their power [10]. Inside a VPP, EVs are able to provide wind power production matching [11]. In this context autonomous control of electric vehicles is deployed within multiple parking lots for the provision of FTM services [12]. This study focuses on the global control architecture and on its application to a simulated virtual power plant scenario. In the virtual power plant, the architecture adjusts the power set points for each EV clusters to achieve the following scopes:

- Maximize wind energy usage for charging EVs.
- Provision of an energy buffer to store wind energy in times of low demand.
- Provision of congestion management for the feeders to

which parking lots are connected.

- Assurance of a sufficient amount of energy to all the cars connected to the parking lots.
- Provision of wind power variability mitigation through charging modulation

The rest of the paper is structured as follows. Section II describes the objective of the research in more detail; Section III describes the methodology adopted for the study; Section IV introduces the results of the case study simulation; Section V provides conclusions and future work.

## II. Methodology

This section describes the methodology implemented in this paper. The model developed uses as a starting point the model previously built in [13] and further developed in [14].

### A. System architecture

The system architecture used in this study relies on a distributed control approach [15]. The communication happens both on local level and on global level with a cloud-based solution. Figure 1 provides an overview of the control architecture. In the figure the grey shaded areas represents a number of N generic location in the distribution grid. The electricity in each area is distributed to all the connected buildings, and to the parking lots. The cloud-based global control is performed by the Cloud Aggregator (CA). The local control architecture is performed by the Virtual Aggregator (VA), present in all the N parking lots. The functions of the CA are the following: signal reception and processing, controllability and power set point dispatch. The CA receives signals from the grid, such as RES production from the surrounding RES power plants, and grid congestion. The CA provides controllability to different actors (Aggregator, DSOs and TSO) according to other signals (for example electricity price, or market bids). In addition, the CA provides information to parking lot users about which parking lots are available via mobile app. Users can also input through the app different requests to schedule and set their charging session priority. The users' inputs are the state of charge (SOC) at the time of plug-in, the battery capacity and the scheduled time of departure. The CA processes these inputs and dispatches to the VA both power set points and user requests. The VA receives inputs from the CA and from the smart meter of the parking lot. On the one hand, the VA stores the user's information and schedules the charging sessions accordingly. Based on user preferences, the VA gives instructions to the chargers, such as charging priority and power scheduling based on SOC and energy charged. On the other hand, the VA of each parking lot matches the power reference given by the CA with the actual consumption recorded from the smart meter. In case there are buildings connected to the same smart meter, the VA will additionally perform power sharing between the buildings and the parking lot. For each time step, the VA broadcasts new power set points to all the chargers of its cluster. The global control ends each iteration with a feedback loop from the smart meter to the CA. The smart meter updates the CA on the power consumed in the previous iteration. Therefore, the CA collects power

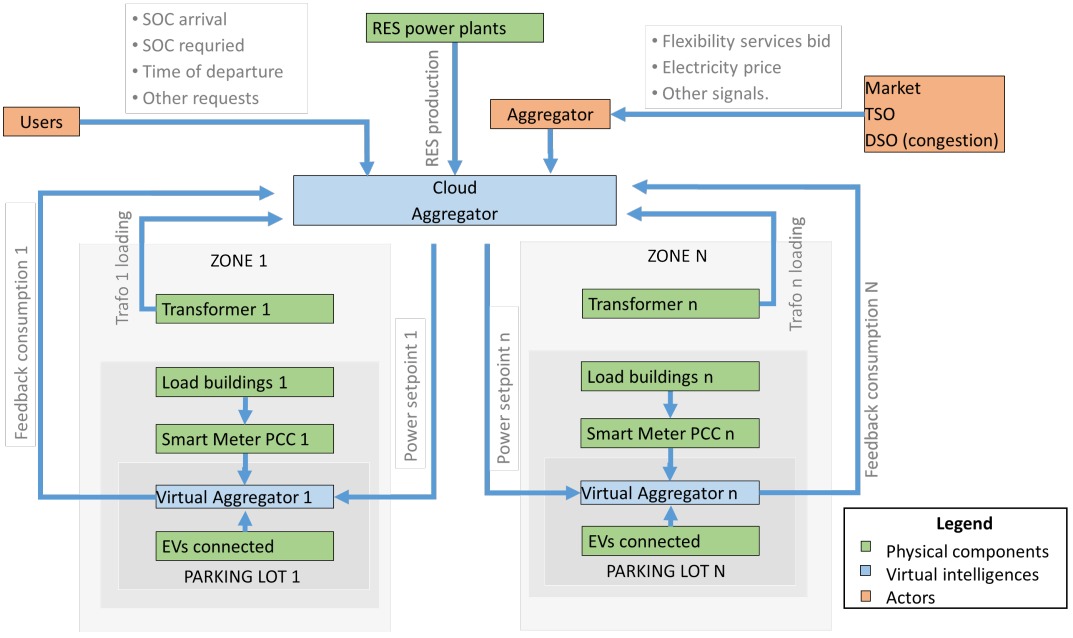


Fig. 1. Global system architecture and communication paths between different actors.

consumption data from the N parking lots and redistributes the power among the parking lots according to the availability of cars and local grid conditions. For a more detailed description of the local system architecture, this article refers to [14].

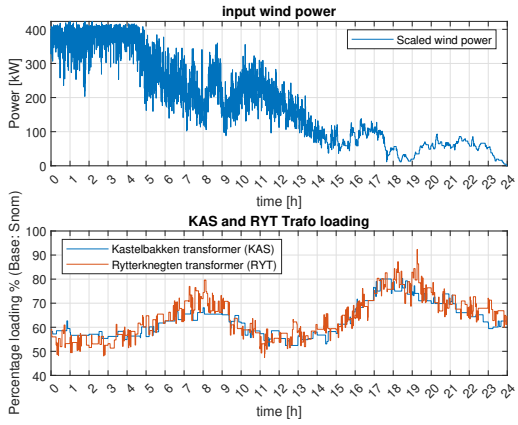


Fig. 2. Top graph: Scaled wind power output of Kalby wind farm. Bottom graph: feeder loading for Kastelbakken (in blue) and Rytterknægten (in orange)

### B. Model Inputs

For the scope of this paper, the model is tailored to the power system deployed on the island of Bornholm in Denmark. The time domain of the simulation is 24 hours. The inputs of the simulation are SCADA secondly power production data from Kalby wind farm consisting of three wind turbines with a rated power of 2 MW [16]. Power production is scaled by a factor of 10 before it is used as input for the simulation to match the parking lot load. The grid structure is also tailored to part of the transmission and distribution system of the island. The parking lots are connected to the 10.6 kV feeders with a rated apparent power of 500 kVA, called Kastelbakken and Rytterknægten, respectively. The model receives secondly loading data of both feeders recorded on the 20th of January 2020. Figure. 2 shows the original data on wind power production and feeder loading. Notice that the feeders have two daily peaks each, during which they eventually reach values higher than 80%, which is the system's threshold for disconnecting the parking lots. This is because a safety margin of 20-30% feeders loading should always be kept in order to manage sudden spikes in demand. The EV behavior consists of pseudoreal data of 68 EVs generated from recorded data of 16 EVs by Nissan EV telematics. The dataset contains arrival time, SOC at the beginning of the session, and planned departure time from EV users. The dataset has a time range of 24 hours with a time resolution of one second. The EV models and relative battery capacity are added by the authors. They represent a sample of the most common EVs found in the DTU university campus.

### C. Simulation model and assumptions

The model is created in Matlab/Simulink. The simulation runs with a variable time step, setting the minimum time step at 0.1 s. More information about the model's signal discretization and communication delays can be found in [13]. Figure 3 shows the layout of the grid to which the system is applied. The system architecture controls four parking lots, two connected to Kastelbakken feeder and two connected to Rytterknægten feeder. The parking lots connected to Kastelbakken feeder house 8 and 32 EV plugs, respectively. The ones connected to the Rytterknægten feeder house 16 and 12 EV plugs, respectively. Each of the chargers in the parking lots is equipped with type-2 plugs. Each charger has two plugs, but can simultaneously charge only one car. Each plug can support a maximum current of 16 A (11 kW charging three-phase or 3.68 kW if charging single-phase). Each charger contains a switch, deployed to charge alternately both cars plugged according to a schedule decided automatically by the system. The schedule prioritizes EVs according to two criteria: the first is the SOC inputted by the user at the beginning of the charging session; the second is how much energy the EV charged during the current session. The priority lowers linearly as the SOC and energy charged increase. When two EVs on the same charger reach the same priority, the switch start giving power to the idle EV. One charging window lasts circa 5 kWh, but it varies marginally according to SOC and battery capacity. The VA continuously keeps track of the priority order of the cars in order to gradually disconnect the cars with the lowest priorities as the power allowance decreases. In case the feeder reaches a loading of 80% or higher all the EVs of the parking lot are disconnected. The EV models contain a simplified battery model and AC-DC converter efficiency which decreases linearly from 90% at full charge (11 kW for three-phase charging or 3.68 kW for single-phase charging) to 80% at minimum charge (4.15 kW for three-phase charging or 1.38 kW for single-phase charging) [17].

Table I contains the maximum power capacities for all parking lots in both constrained and unconstrained scenarios. Notice that in the unconstrained scenario, the system does not perform any power curtailment, and the maximum capacity of each parking lot is given by the power limit of the chargers, which is 11 kW. In the constrained charging scenario, the chargers adjust the power consumption to the power allowance with a PI controller. The CA instead adjusts the power set points given to all parking lot with a droop controller based on the percentage loading of the feeders.

| Parking lot | Unconstrained scenario | Constrained scenario |
|---|---|---|
| 1 (8 EVs) | 44 kW | 21 kW |
| 2 (32 EVs) | 176 kW | 86 kW |
| 3 (16 EVs) | 88 kW | 43 kW |
| 4 (12 EVs) | 66 kW | 32 kW |

TABLE I
MAXIMUM POWER FOR EACH PARKING LOT IN EACH SCENARIO

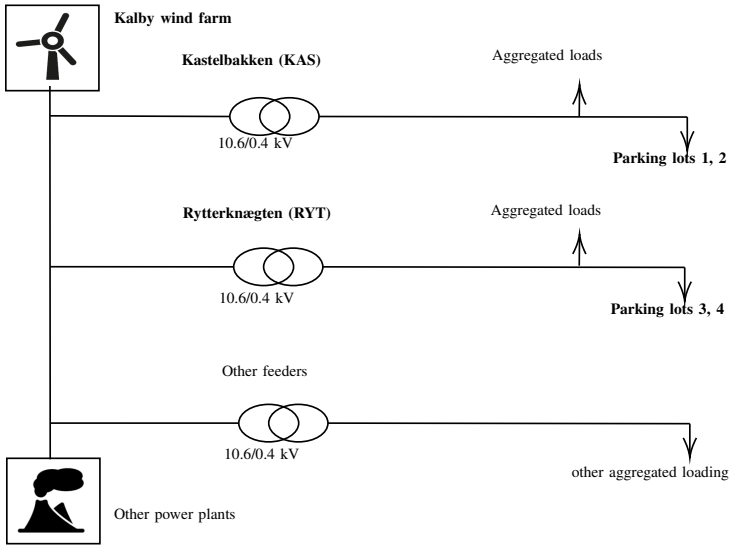


Fig. 3. Simplified grid layout for the system

## III. Results

Figure 4 provides the overall results of the simulation for parking lot 2, taken as example, during the 24 hours period. The top graph illustrates a time history of the charging power in the constrained charging and unconstrained charging cases for comparison. The graph shows in blue the dynamic power reference adjusting to the wind power and to the feeders congestion. The dynamic power reference acts as an upper boundary for the smart charging power. The power reference is controlled by the CA based on the available wind power and on transformer congestion. As expected, in both constrained and unconstrained charging scenarios, the power demand of the parking lot is lower then the power reference when there are not enough EVs available to use such power. The bottom graph shows the number of EVs connected and charging in the constrained charging scenario. When the power reference becomes too low and not all the connected EVs can charge at least with their minimum power, the EVs with the lowest priorities get gradually disconnected. From 0 to 6 am, the feeder is not loaded, therefore, the power reference equals the fuse limit. Later in the day, when the feeder becomes overloaded, the power reference is reduced, and eventually the parking lots are disconnected for safety reasons. Towards the end of the day, because of EVs leaving the parking lot, the power allowed cannot be used. As a consequence, the virtual power plant either distributes the power to other parking lots or exports it to the grid.

Figure 5 shows the distribution of energy charged for all the EVs based on their initial SOC. The graph describes that for both single-phase and three-phase EVs the system prioritizes the EVs with lower SOC and delays the charging of EVs

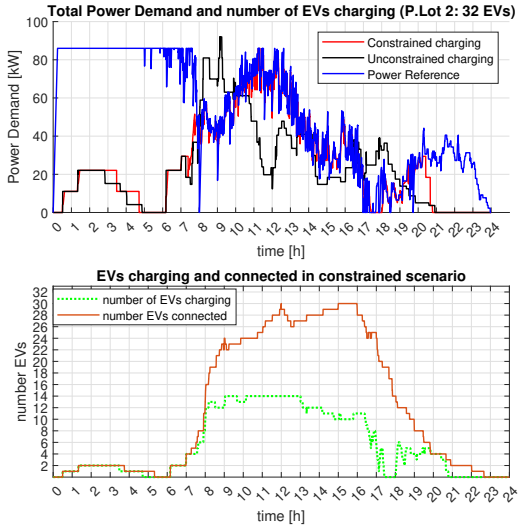


Fig. 4. Parking lot 2: Power demand in constrained and unconstrained scenarios (above); Connection and charging history (below).

with high initial SOC. In detail, single-phase EVs with an initial SOC lower than 60% manage to charge at least 10.7 kWh. This means that in the current conditions the 4 parking lots guarantee a driving autonomy of 53.5 km, assuming that the EVs can drive 5 km per kWh. With the current logic, the system charges three-phase EVs roughly three times more

than single-phase EVs. This ratio could be decreased in order to guarantee a higher guaranteed energy charged to all EVs. However, this could potentially create discontent in three-phase EV users of the parking lot.

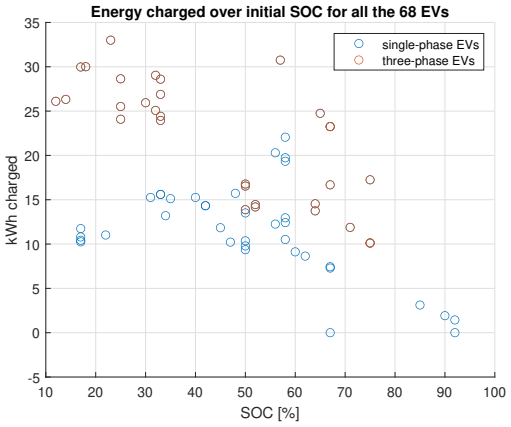


Fig. 5. Distribution of energy charged over initial SOC

Figure 6 describes the influence of parking lots on feeders and the power output of the virtual power plant during the simulated 24 hours. Both feeders (top and middle graphs) reach high-level loading (above 90%) in the unconstrained charging scenario. In the constrained charging scenario, the control architecture manages to maintain the feeder loading below the designed threshold of 80%. Notice that there are some peaks above 80%, however those peaks are present in the original data and are not due to the influence of the parking lots. The bottom graph shows the net power production of the virtual power plant, which is defined as:

$$P_{net} = P_{wind} - P_{charging} \tag{1}$$

Where $P_{wind}$ is the power produced by the wind farm and $P_{charging}$ is the power used by the four parking lots. The bottom graph shows also a fitting curve in order to visualize the average net power without the wind power fluctuation. In the current layout, the wind power produced is almost always higher than the power used by the parking lots. As a consequence, the virtual power plant is always exporting power to the grid. Table II presents the evaluation indices for the virtual power plant in the constrained EV charging scenario. The total energy produced during the day is 4.36 MWh of which 1.34 MWh is used to charge the EVs. The remaining 3.07 MWh is exported to the grid. A very small amount of energy (92 kWh) is imported from the grid to charge when the wind production is very low and the parking lots are full. Lastly, the average root-mean-square error provides an assessment of the wind power variability mitigation performed by the parking lots.

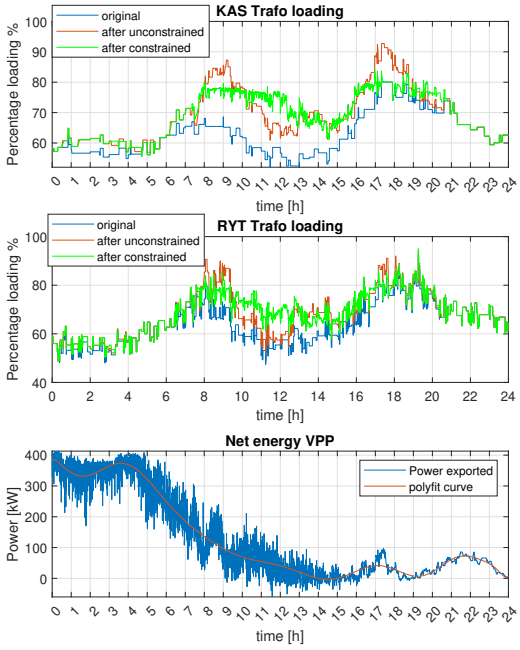


Fig. 6. Overall virtual power plant graphs outputs. Top graph: Kastelbakken feeder loading. Middle graph: Rytterknægten feeder loading. Bottom graph: VPP power flow.

| Index | Value |
|---|---|
| Total energy produced [MWh] | 4.36 |
| Total energy used [MWh] | 1.34 |
| Energy imported [MWh] | 0.092 |
| Energy exported [MWh] | 3.07 |
| Average RMSE wind power production | 33.22 |
| Average RMSE VPP | 33.05 |

TABLE II
INDEXES OF EVALUATION FOR THE VIRTUAL POWER PLANT

There are two values of average root-mean square error (RMSE): the first represents the average oscillation of the wind power production; the second represents the average oscillation of the net VPP power. In the first case, the error is calculated between the fitting curve of the wind power production and the actual wind power production. In the second case, the error is calculated between the fitting curve of the net VPP power (showed in Fig. 6) and the actual net VPP power exported. Both values of RMSE are then averaged over the 24 hours. The two values are only marginally different, and therefore show an insufficient capacity of the system to mitigate wind power variability in the simulated conditions. The reason for such behavior might lie in the relative dimensions of the components of the system: wind

farm, parking lots and feeders. In detail, on the one hand, the wind power capacity might be too large compared to the capacity of the parking lot. On the other hand, the high loading of the feeders is the main driver of the power adjustments of the parking lot during peak hours. Further investigation is needed to investigate the capacity of the system to perform wind power variability mitigation.

## IV. Conclusion and future work

This paper illustrates the performances of an autonomous distributed control for coordinating the charge of four parking lots as part of a virtual power plant. The virtual power plant consists of a wind farm and four parking lots located in different parts of the grid and connected to two different feeders. The system is investigated via a 24-hour simulation including input data of a wind park, loading data of two feeders, and user behaviour from 68 EVs. Two scenarios are compared: unconstrained charging and constrained charging. In the first scenario, the EVs always charge at their maximum power. In the second scenario, the architecture controls the parking lots demand with the following scopes: maximization of the wind power usage to charge the EVs; minimization of feeders overloading; minimization of energy imported from the grid; assurance of sufficient charging fulfillment; wind power variability mitigation. In the unconstrained charging scenario, the feeders loading reached peaks of 95%, which in a real case scenario would remove any safety margin used to handle sudden spikes or changes in the demand. In the constrained charging scenario, the control architecture kept the loading of both feeders under the requested value of 80%, by reducing the power allowance given to the parking lots during peak demand. On the local level, the control logic prioritized EVs with lower SOC and disconnected the EVs with lower priority when the feeders were highly loaded. In the simulated conditions, the guaranteed amount of energy for EVs with SOC lower than 60% was 10.7 kWh. Therefore, assuming a driving consumption of 1 kWh per 5 km, the 4 parking lots guaranteed a driving autonomy of 53.5 km after the charging session. The remaining power that could not be allocated to the EVs, either due to fulfillment of their charging requirements or due to lack of EV availability, was injected to the grid. Regarding the performances of the virtual power plant, the total energy produced during the day was 4.36 MWh of which 1.34 MWh was used for charging the EVs. The remaining 3.07 MWh was exported to the grid. A very small amount of energy (92 kWh) was imported from the grid for charging. The system showed only marginal capacity to mitigate wind power production variability in the simulated conditions. Some hypothetical reasons were formulated: for example the power capacity of the parking lots compared to the wind farm power capacity; the high loading of the feeders being a major constraint to the power allowance trends of the parking lots. In the future, wind power variability mitigation studies are going to be addressed. Furthermore, different VPP layouts and dimensions will be investigated in order to find the optimal ratio between EV storage and power production.


## Acknowledgment

The work in this paper is supported by the research projects ACDC (EUDP grant number: 64019-0541) and FUSE (EUDP grant number: 64020-1092). Website: www.acdc-bornholm.eu and www.fuse-project.dk


## References


[1] H. Kondziella and T. Bruckner, "Flexibility requirements of renewable energy based electricity systems - A review of research results and methodologies," *Renewable and Sustainable Energy Reviews*, vol. 53, pp. 10–22, 2016.

[2] L. Calearo, A. Thingvad, K. Suzuki, and M. Marinelli, "Grid loading due to ev charging profiles based on pseudo-real driving pattern and user behavior," *IEEE Transactions on Transportation Electrification*, vol. 5, 2019.

[3] M. Resch, J. Buhler, B. Schachler, and A. Sumper, "Techno-Economic Assessment of Flexibility Options Versus Grid Expansion in Distribution Grids," *IEEE Transactions on Power Systems*, vol. 36, no. 5, pp. 3830–3839, 2021.

[4] "Innovation outlook smart charging for electric vehicles summary for policy makers," tech. rep., IRENA, 2019.

[5] C. Crozier, T. Morstyn, and M. McCulloch, "The opportunity for smart charging to mitigate the impact of electric vehicles on transmission and distribution systems," *Applied Energy*, vol. 268, no. March, p. 114973, 2020.

[6] F. G. Venegas, M. Petit, and Y. Perez, "Active integration of electric vehicles into distribution grids: Barriers and frameworks for flexibility services," *Renewable and Sustainable Energy Reviews*, vol. 145, 2021.

[7] S. Striani, K. Sevdari, L. Calearo, P. Andersen, and M. Marinelli, "Barriers and solutions for evs integration in the distribution grid," *2021 56th International Universities Power Engineering Conference (UPEC)*, 2021.

[8] M. B. Anwar, M. Muratori, P. Jadun, E. Hale, B. Bush, P. Denholm, O. Ma, and K. Podkaminer, "Assessing the value of electric vehicle managed charging: a review of methodologies and results," *Energy & Environmental Science*, 2022.

[9] H. Saboori, M. Mohammadi, and R. Taghe, "Virtual power plant (vpp), definition, concept, components and types," pp. 1–4, 2011.

[10] N. Kraftwerke, "Virtual power plant: How to network distributed energy resources." https://www.next-kraftwerke.com/vpp/virtual-power-plant. Accessed 16 December 2021.

[11] C. Binding, D. Gantenbein, B. Jansen, O. Sundström, P. B. Andersen, F. Marra, B. Poulsen, and C. Træholt, "Electric vehicle fleet integration in the Danish EDISON project - A virtual power plant on the island of Bornholm," *IEEE PES General Meeting, PES 2010*, 2010.

[12] K. Sevdari, L. Calearo, P. B. Andersen, and M. Marinelli, "Ancillary services and electric vehicles: an overview from charging clusters and chargers technology perspectives," *Renewable and Sustainable Energy Reviews*.

[13] K. Sevdari, L. Calearo, S. Striani, P. B. Andersen, M. Marinelli, and L. Rønnow, "Autonomously distributed control of electric vehicle chargers for grid services," in *2021 IEEE PES Innovative Smart Grid Technologies Europe (ISGT Europe)*, pp. 1–5, IEEE, 2021.

[14] S. Striani, K. Sevdari, Y. Kobayashi, K. Suzuki, P. B. Andersen, and M. Marinelli, "Autonomously distributed control of ev parking lot management for optimal grid integration," *International Conference on Renewable Energies and Smart Technologies (IC-REST)*, 2022, under-review.

[15] X. Han, K. Heussen, O. Gehrke, H. W. Bindner, and B. Kroposki, "Taxonomy for evaluation of distributed control strategies for distributed energy resources," *IEEE Transactions on Smart Grid*, vol. 9, pp. 5185–5195, 9 2018.

[16] M. Ledro, L. Calearo, J. M. Zepter, T. Gabderakhmanova, and M. Marinelli, "Influence of realistic ev fleet response with power and energy controllers in an ev-wind virtual power plant," *Sustainable Energy, Grids and Networks*, vol. 31, p. 100704, 2022.

[17] L. Calearo, C. Ziras, K. Sevdari, and M. Marinelli, "Comparison of smart charging and battery energy storage system for a pv prosumer with an ev," in *2021 IEEE PES Innovative Smart Grid Technologies Europe (ISGT Europe)*, pp. 1–6, IEEE, 2021.

PAPER [P5]

# Laboratory Validation of Electric Vehicle Smart Charging Strategies

Authors:

Anna Malkova, Simone Striani, Jan Martin Zepter, Mattia Marinelli, Lisa Calearo

Published in:

*Proceedings of the 2023 58th International Universities Power Engineering Conference (UPEC)*

DOI:

10.1109/upec57427.2023.10294673.

# Laboratory Validation of Electric Vehicle Smart Charging Strategies

Anna Malkova, Simone Striani,
Jan Martin Zepter, Mattia Marinelli
*Department of Wind and Energy Systems*
*Technical University of Denmark*
Roskilde, Denmark
{anmalk; sistri; jmwze; matm}@dtu.dk

Lisa Calearo
*Ramboll Danmark A/S*
Copenhagen S, Denmark
licl@ramboll.com

2023 58th International Universities Power Engineering Conference (UPEC) | 979-8-3503-1683-4/23/$31.00 ©2023 IEEE | DOI: 10.1109/UPEC57427.2023.10294673

***Abstract*—Electric vehicles (EVs) are the connecting point of the transportation and electricity sectors and are an important milestone towards the decarbonization goal. Smart charging of EVs is considered a key enabler for the broad deployment of EVs. Acting as flexible demand, smart charging releases stress on the grid infrastructure and enables potential flexibility to the renewable energy sources (RES), thereby enhancing the power system. This paper presents results from experimental tests with two smart charger prototypes developed within the ACDC project. The autonomously and distributed controlled chargers connecting four EVs are integrated into the Energy System Integration Lab (SYSLAB) of the Technical University of Denmark. The conducted tests aim at different flexibility services, namely power sharing, RES following, and transformer protection. The developed chargers fulfil the assigned tasks and are able to provide ancillary services to the grid and RES.**

***Index Terms*—Smart chargers, Electric vehicles, Flexibility, Renewable energy sources**

## I. Introduction

The energy transition from fossil fuels is one of the main tasks addressed by governments to reach the $CO_2$ drawdown. Yet, several tasks need to be solved for achieving a smooth transition, such as the extended deployment of renewable energy sources (RES), electrification of the transport and heat applications, and efficient use of energy [1]. The deployment of both large-scale and domestic RES increases the vulnerability of the network due to their intermittent generation. Increased controllability and predictability of RES and more flexible participation in the electricity market can be achieved using energy storage technologies [2] such as stationary battery storage, electric vehicles (EVs) batteries and others.

At the same time, according to transport electrification trends by 2030, the number of EVs will also grow and reach 200 million globally [3] and 0.8 million in Denmark [4] in particular. As the number of EVs increases, their uncontrolled charging impact on the energy infrastructure will also increase. This could create challenges, e.g., network congestion, generation capacity expansion, and reduction of transformers' lifespan, among others [5]. Nevertheless, EVs have a potential of flexibility reserve for the power system with a sufficiently large battery capacity (global average of EV battery capacity is 65.8 kWh [6]) and high availability to charge (e.g. more than 90% of daytime in Denmark [7]). Ref. [8] suggests that by aggregating EVs and deploying smart charging strategies, it will be possible to limit, or even avoid, the aforementioned problems in the electrical grid, as well as reduce investment in essential stationary storage systems. Smart charging is defined in [9] as an adaptation of EVs charging process to meet power systems conditions and EV users' needs. Smart charging can be implemented with respect to different objectives (technical, financial), control approaches (centralized, distributed, decentralized) and scaling factors (residential buildings, parking lots, regional level) [10]. According to [11] ancillary services for the grid provided by smart charging can be divided into frequency and flexibility services. Further, the authors in [12] distinguish local flexibility services between front-of-the-meter (FTM) and behind-the-meter (BTM). FTM services, such as prevention of transformer and load peaks congestion, voltage control, loss reduction, and power quality enhancement, are dispatched by the distribution system operator for grid needs. In turn, BTM services aim to reduce the energy bill using price signals and increasing the rate of self-consumption (if distributed RES are applied) while also serving as a backup power battery.

Despite extensive research on the modelling of smart charging strategies, their experimental implementation and testing in real systems are still limited and only little literature exists on this topic. Frendo et al. [13], for instance, developed a smart charging algorithm for EVs parked at a workplace, which was validated through a one-year field test. However, the algorithm was designed solely with the objective of improving customer satisfaction and did not take into account grid services or RES. On the other hand, in [14] a centralized smart charging approach was explored, aiming to provide multiple ancillary services, but the study was limited to a single EV and did not consider any RES integration.

This paper presents the results of a field demonstration of two chargers providing a broader spectrum of smart charging strategies. The demonstration has been performed in the Energy System Integration Lab (SYSLAB) located in DTU Risø Campus, Denmark. The smart charging logic implementation is based on previous models described in [15] and [16]. The

979-8-3503-1683-4/ 23/$31.00 ©2023 IEEE

smart charging strategy embedded in the chargers is developed on a rule-based method and considers a distributed approach (according to the classification of the authors in [17]) with the combination of both the FTM and BTM services. The goal of the ACDC project is to implement smart distributed charging control in workplace parking lots. Four control objectives are demonstrated in this article:

- Power sharing
- RES following
- Transformer protection (TRAFO)
- Cloud aggregator communication failure

All four modes are working together, reacting to the dynamic conditions and requirements of the system. However, during the demonstration, the tests have been conducted on the individual modes to explicitly showcase the performances of each mode separately.

The rest of the paper is structured as follows. Section II describes the smart charging control architecture description; Section III presents the actual electrical experimental setup; Section IV specifies the system limitations; Section V describes the control objectives in a more detailed way; Section VI introduces the results of the smart charging experiments; and Section VII provides the conclusions and future work prospects.

## II. Control Architecture Description

In this section, the communication and control architectures of the laboratory setup are presented.

### A. Communication architecture

The communication scheme can be observed in Figure 1. Initial information necessary for smart charging implementation includes wind-produced power, PV-produced power, transformer loading, fuse limit at the point of the charging cluster connection, and EV connection status. This information is sent every 1 s to the central cloud server, which is implemented through Amazon Web Services (AWS). Subsequently, AWS broadcasts such information to the virtual aggregators (VA) of the chargers. The VAs are the controllers of each plug. When the first EV is connected the corresponding VA becomes the primary VA and dispatches power for all connected EVs (on Figure 1 the EV1 is connected first and hence VA1 becomes the primary VA). The AWS also stores the latest status of each VA: EV connection status, current, and charging phases.

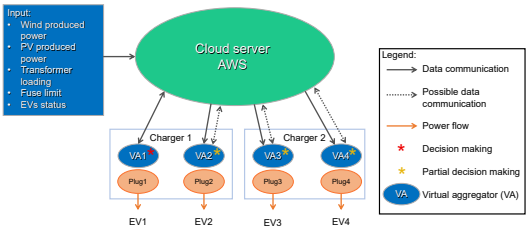


Fig. 1: Communication scheme

Information from the AWS to the charger and vice versa is transmitted via mobile Internet using SIM cards placed on the chargers' control boards. The information flows in the following order:

- Input information from measurement boards and chargers arrives at the AWS cloud server.
- The AWS broadcasts this information to the primary VA.
- Primary VA processes the received information and sends control outputs to the AWS.
- The AWS then dispatches those signals to the other VAs.

If there is a fault event and the primary VA goes offline, the next available and operating VA (i.e., an EV is connected) will take on its role (shown through dashed arrows in Figure 1).

### B. Control architecture

The control scheme (Figure 2) shows the control loop and the key roles of the actors in the system. The responsibility of the AWS is shown in light green and the VAs in blue. The primary VA (VA1) receives the system data and EVs connection status from AWS, executes the power allocation and produces power references for each plug. The main logic behind power allocation is to provide maximum available power while sharing it equally between connected cars and following the designated mode of operation. The charging power is measured at the chargers' connection points and transmitted via the AWS to the VA1. Then these two $Pmeas$ go through the processing inside the VA1 and transform into measurements of each plug. The transformation happens according to the EVs status and the power sharing principle. For example, if all four EVs are connected then the measurements from the chargers $Pmeas_{ch1,ch2}$ convert into four plug measurements: $Pmeas_{1,2,3,4} = [\frac{Pmeas_{ch1}}{2}; \frac{Pmeas_{ch1}}{2}; \frac{Pmeas_{ch2}}{2}; \frac{Pmeas_{ch2}}{2}]$. If only one EV is connected to a charger, the respective $Pmeas_{ch}$ is allocated to that EV. After summation of $Pref_{1,2,3,4}$ and $Pmeas_{1,2,3,4}$ in VA1, the four errors are produced. All errors except the error of VA1 are redirected to other VAs through AWS. Error 1 of the VA1 is transferred internally. Then the PI controller inside each VA reacts to the received error and controls the power flow to the plug.

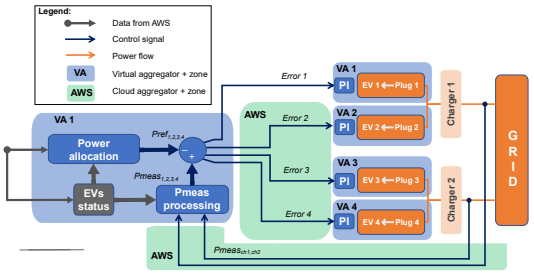


Fig. 2: Control scheme

## III. Experimental Setup

The experimental microgrid is predominantly powered by RES connected to an external grid through a 200 kVA trans-

former. The system is composed of the following components (from left to right in Figure 3): external grid connection, transformer, 5 kW PV system, 20 kW emulated PV, 10 kW Aircon wind turbine, controllable load, PCC with two three-phase chargers (C1 and C2). Each charger has 2 plugs: C1 has Plug 1 (P1) and Plug 2 (P2); C2 has Plug 3 (P3) and Plug 4 (P4).

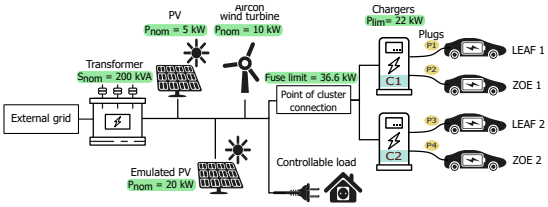


Fig. 3: Electrical system setup

The emulated PV is established using an external transformer to the system and a controllable back-to-back inverter. This is used to reproduce the PV power production in case RES during the testing day are absent or very limited. The controllable load simulates varying grid loading to test the smart charging logic's capabilities under varying conditions.

The maximum charging power is 22 kW (32 A) per charger. This means that if two vehicles are connected to the same charger, each EV can charge with maximum 11 kW. The fuse limit at the PCC is set to 36.6 kW (53 A). This means that if four cars are connected to the chargers (two per charger) the total maximum charging power is 36.6 kW and not 44 kW.

During the experiments, four electric vehicles (EVs) are considered - one for each plug of the chargers. To create more variability, two Renault ZOE with three-phase charging capability and two Nissan LEAF with single-phase charging capability are chosen. The allocation of the EVs to their respective plugs is shown in Figure 3 and their charging characteristics are displayed in Table I.

TABLE I: EVs charging parameters

| Parameter / EV | Renault ZOE | Nissan LEAF |
|---|---|---|
| Battery capacity, kWh | 41 | 62 |
| Charging power capacity, kW | 22 (7.36 per phase) | 7.36 |
| Maximum charging current, A | 32 | 32 |
| Number of possible phases for charging | 3 | 1 |

## IV. Limitations of the Setup

Some features of the current implementation of chargers require further development and thereby pose limitations on the demonstration installation.

### A. Ghost phases limitation:

Due to the absence of an internal electrical meter, the chargers do not yet recognize single-phase cars and therefore treat all connected cars as three-phase ones. Indeed, the chargers are still prototypes and their PI controllers dispatch the set point current to all three phases of the plugs, even if the connected car is one phase. The power consumed by a single-phase car is only one-third of the power set point of the charger.

### B. Reactive power limitation:

The actual control signal is a current, not an active power. The part of the current goes to the system elements' magnetization, and therefore to the reactive power, which is not measurable yet. The choice to utilize active power in this article is based on its convenience regarding comprehension and visualization.

Also, in cases where the setpoint current for three-phase ZOE decreases, the share of reactive power in it increases. As a result, the decrease in the current setpoint is not proportionate to the decrease in active power. Therefore, in demonstration modes with small or zero setpoints, the single-phase LEAFs were used, where this issue does not appear.

## V. Definition of Control Objectives

Smart charging can be designed to achieve various control objectives aimed at enhancing grid stability, lowering charging expenses, facilitating renewable energy integration, extending battery lifespan, and improving user convenience. Those objectives can be applied independently or in combination as long as they do not conflict with each other. In the following sections, the implemented control objectives are described by providing first the concept and then the demonstration methodology.

### A. Power sharing mode

Power sharing is the ability of smart chargers to distribute limited available power (station connection limit, fuse limit or other) proportionally between the outlets and chargers (if there are several) and thus between the EVs at the charging station.

Maximizing the number of EVs charging at a single connection point is crucial. Charging station operators can benefit from charging more EVs within the available power limit to reduce the need for grid expansion capital expenditure, prolong the lifespan of existing infrastructure, and increase revenue by accommodating more customers. Although power sharing results in a lower charging power per EV, this may not pose an issue during extended EV connection periods, such as at workplace parking lots or overnight at homes. In this way, it can be ensured that in those hours all EVs will be charged with the desired energy even with lower charging power.

Both chargers and all four cars are used to demonstrate power sharing. Firstly, ZOE 1 is connected to C1, then ZOE 2 to C2 to show power sharing between chargers. Afterwards, the remaining LEAF 1 and LEAF 2 are sequentially connected to C1 and C2 allowing observation of the chargers' ability to distribute power within one charger and keep power sharing between chargers.

### B. RES following mode

This test demonstrates the architecture's capability to match charging power according to RES power production.

EV charging coordinated with local RES production offers several advantages depending on the intended goals and the power supplied by RES such as increased self-sufficiency of the system with local RES, mitigation of RES variability, and avoidance of RES curtailment, among others.

In order to match EV charging power with the RES production test two EVs were used (only ZOEs due to the *Ghost phases* limitation), and each of them was connected to a separate charger. Moreover, an additional emulated PV production of 20 kW was added due to weather conditions affecting real PV panel capacity. This in turn improved the demonstration proof of concept as created more variable RES output power which the chargers had to adjust to.

### C. TRAFO protection mode

The TRAFO protection mode is aiming at adjusting the charging power of the chargers to avoid transformer overloading.

The transformer is usually considered a bottleneck in future smart grids, where the electricity demand and the penetration of renewables are forecasted to increase. The increase in power flowing and production volatility could in the future overload the transformers, resulting in damages, shorter life spans and overall increased costs.

During the TRAFO protection test, the transformer limit was set manually using the AWS cloud system and two EVs connected to both chargers were used (only LEAFs due to the *Reactive power* limitation). Then local system consumption was increased applying the auxiliary load of the laboratory to see the system reaction to this demand spike.

### D. Cloud aggregator (AWS) communication failure mode

The last test was performed to investigate the chargers' capability to remain operational in case of communication loss with the cloud aggregator.

The ability to remain up and running despite various disruptions (cyber-attacks, equipment failure, or just a short-term loss of communication) is essential for maintaining the stability of the power system. After all, when charging stops, an imbalance will be created in the network, which will increase the risk of even greater consequences, such as protection tripping, cascade failure, and over-voltages, among others.

In this test, only one EV (LEAF 1) connected to C1 was used. To reproduce the communication failure simulation the SIM card with mobile 3G Internet was physically removed.

## VI. Results

In this section, the results of the demonstration experiment are presented in chronological order. In total, the tests ran for 55 minutes, which is displayed on the x-axis of the results graphs in seconds.

### A. Power sharing test

The test performance can be seen from Figure 4 with the following test description. A colour difference on the graph corresponds to different chargers (blue - C1; red - C2) and a line style - to car brand (solid - ZOE; dashed - LEAF).

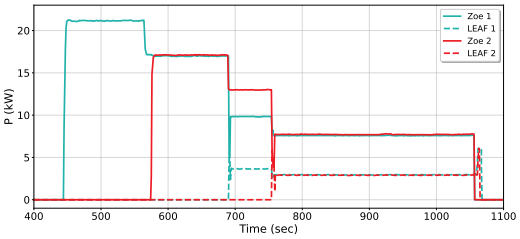


Fig. 4: Power sharing test: active power of EVs

The first EV – three-phase Renault ZOE 1 - plugged to C1 at 440 s and started charging with three phases with almost maximum power of 21 kW. At 560 s a second EV – ZOE 2 - is connected to C2 and the ZOE 1 started to decrease its consumption to give space for power to the second EV to avoid overshooting the PCC limit. 10 s later (570 s) both cars were charging at the same power of 17 kW which is almost the $P_{max}$ of PCC – they are sharing the limited power between chargers.

At 690 s, a third EV – Nissan LEAF 1 capable of charging with single-phase - is connected to C1, in response, both ZOEs decreased their consumption, and after 5 s LEAF 1 started charging 4 kW on one phase. Then, at 750 s the fourth EV – LEAF 2 connected and started to charge. It is clear that the cars were not charging with their maximum power. This is due to the *ghost phases* limitation. If the charging power of single-phase cars is multiplied by 3 the charging power of all EVs is actually close to the $P_{max}$ limit of PCC (36.6 kW):

$$P_{EVs} = 3\,\text{kW} \cdot 3\,\text{phases} \cdot 2\ \text{EVs (LEAFs)} + \\ +8\,\text{kW} \cdot 2\ \text{EVs (ZOEs)} = 34\,\text{kW}$$

The output power is less than the maximum due to the *reactive power* limitation.

Moreover, the power consumption of each charger is not greater than 17 kW – the chargers limit is also respected. With this knowledge, there is a clear observation of power sharing between chargers' plugs and between chargers themselves.

### B. RES following test

A demonstration of the architecture capability to match the charging power according to RES power production is shown in Figure 5.

The first EV - ZOE 1 is connected to C1 at 1380 s and started to charge with maximum power. The RES production is above the $P_{max}$ limit of the charger and that is why the consumption of the EV is constant. The second EV - ZOE 2 is plugged in at 1425 s and started to charge after the power

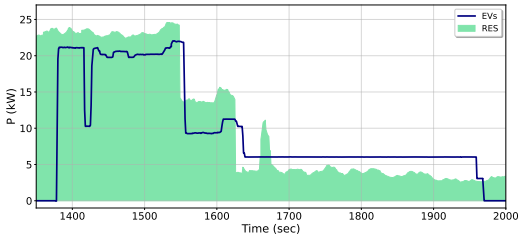


Fig. 5: RES following test: total EVs active power and RES production

sharing procedure with the first EV. The charging power of the EVs follows the RES production with a small time delay of 5-7 s. A small discrepancy of 1.0-2.5 kW between RES production and EVs' total power consumption is again due to reactive power consumption, which increases as the power curtailment of the car increases. At 1550 s there is a steep decline in RES power production from 25 to 14 kW. The EVs reacted to that change with the above-mentioned delay within which the system was importing power from the grid to support the power balance. At 1625 s RES power again declined to 4 kW, which is now not enough to charge EVs with minimum power. So, both cars have reduced their consumption to a minimum and remained in a state of waiting for better conditions of RES production. The time sensitivity of the charger communication and control was not enough to detect and follow the RES production spike at 1675 s. At 1960 s the EVs are disconnected.

### C. TRAFO protection test

A demonstration of the capability of the architecture to adjust its charging power in order to avoid transformer overloading is presented in Figure 6.

The transformer loading limit is set to 10 kW. At 2100 s RES production was shut down and led to an interruption of power export (no negative values of $P_{Trafo}$) in Figure 6. The LEAF 1 is connected and started to charge at around 2200 s. At 2300 s LEAF 2 is connected and since the chargers consider the EVs to charge with three phases, the first LEAF leaves space for the second diminishing the charging power. Then they both are charging at 5 kW – sharing power and without exceeding the established transformer limit.

At 2370 s an external controllable load of 40 kW is connected. The transformer has a power import spike of 50 kW. After a few seconds, the TRAFO protection mode was deployed: the EVs reacted to the transformer overloading and stopped charging to mitigate the power congestion (shown in purple circles in Figure 6).

At 2410 s the external load is disconnected, thus relieving congestion of the transformer and, with an 8 s delay, the EVs started to charge again, reaching the transformer limit.

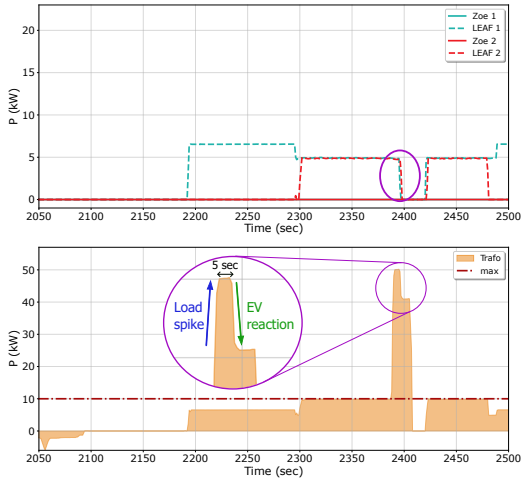


Fig. 6: Active power of EVs (top plot) and at transformer (bottom plot) in the TRAFO protection test

### D. Cloud aggregator (AWS) communication failure test

In this last demonstration phase, the SIM card from C1 was removed, in order to demonstrate the capability of the charger to remain operational in the absence of communication. The SIM card was responsible for communicating with the cloud aggregator via mobile Internet. The LEAF 1, still connected to C1 from the previous test, was charging with 6.5 kW (Figure 7). After removing the SIM card the LEAF 1 is charging with the same power, while the charger is waiting to reconnect.

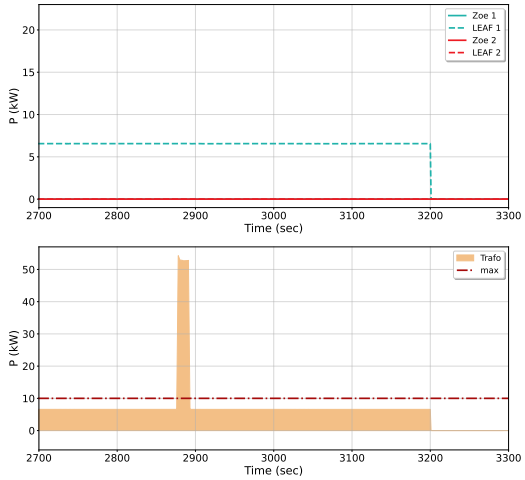


Fig. 7: Active power of EVs (top plot) and at transformer (bottom plot) in the AWS failure test

In order to show that now the charger does not have communication, the TRAFO protection mode was repeated. At 2870 s an external load of 45 kW was connected and overloaded the transformer by around 40 kW. However, this time the EV did not react to the transformer overload and did not decrease its consumption. The EV kept charging at 6.5 kW until it was plugged out at 3200 s.

Thereby, the charger demonstrated the ability to charge the EV even in the absence of communication, prioritizing the EV charging needs.

## VII. Conclusions

This paper describes the experimental performance of two smart charger prototypes towards several flexibility services. The experimental system was built in DTU SYSLAB, a grid-tied microgrid laboratory, for the public demonstration of the ACDC project. The communication and control architectures have a distributed approach and are implemented in an AWS cloud with a 3G mobile Internet connection. The setup consisted of different RES, a grid connecting transformer, an auxiliary load, and two smart chargers connecting four EVs. Four smart charging control objectives (modes) are illustrated in detail: power sharing capability, RES following mode, TRAFO protection deployment, and cloud aggregator (AWS) communication failure. In the first mode, smart chargers efficiently distribute power among connected cars, considering both charger-to-charger and plug-to-plug scenarios. They adjust the charging power of already connected EVs when another vehicle is plugged in to avoid exceeding the limit. This solution optimizes the use of existing grid infrastructure and facilitates greater EV adoption by accommodating more vehicles. In the second mode, chargers demonstrate their ability to follow the RES power production, aligning the EVs' charging power with the RES curve. When RES production is insufficient, EVs charge at minimal power to minimize energy import from the grid. This mode offers multiple benefits, including reduced grid feeder load, optimized RES utilization, and RES variability mitigation. Enhancing the system architecture's communication bottlenecks analysis can further improve response time. The third mode aims to protect the transformer from overloading. The chargers react to the exceeded transformer loading limit and stop the charging. After the overload is removed, they return to normal operation. The final mode showcases chargers' capability to remain operational during communication loss by maintaining the last power set point. This mode enables the system to handle unforeseen circumstances and maintain consistent performance. In summary, the experimental tests confirmed the viability of coordinated smart charging among multiple chargers with varied control objectives.

Future work aims to address the setup limitations by installing an electrical meter in each charging station. This will enable the distinction between three-phase and single-phase EVs and the measurement of reactive power to ensure correct control independent of EV performance. Additionally, the control logic will be expanded to incorporate user preferences, prioritization, and charging scheduling.

## Acknowledgment

The work in this paper has been supported by the research project ACDC (EUDP grant nr: 64019-0541) www.acdc-bornholm.eu and by the research project EV4EU (Horizon Europe grant no. 101056765 ) https://ev4eu.eu/

## References

[1] IRENA, "World energy transitions outlook 2022: 1.5° c pathway," 2022.

[2] K. Dykes, J. King, N. DiOrio, R. King, V. Gevorgian, D. Corbus, N. Blair, K. Anderson, G. Stark, C. Turchi, and P. Moriarty, "Opportunities for Research and Development of Hybrid Power Plants," may 2020. [Online]. Available: https://www.osti.gov/servlets/purl/1659803/

[3] "Global EV Outlook 2022 – Analysis - IEA." [Online]. Available: https://www.iea.org/reports/global-ev-outlook-2022

[4] M. S. Kany, B. V. Mathiesen, I. R. Skov, A. D. Korberg, J. Z. Thellufsen, H. Lund, P. Sorknæs, and M. Chang, "Energy efficient decarbonisation strategy for the Danish transport sector by 2045," *Smart Energy*, vol. 5, feb 2022.

[5] S. Tirunagari, M. Gu, and L. Meegahapola, "Reaping the Benefits of Smart Electric Vehicle Charging and Vehicle-to-Grid Technologies: Regulatory, Policy and Technical Aspects," *IEEE Access*, vol. 10, pp. 114 657–114 672, nov 2022.

[6] "Electric vehicle database," https://ev-database.org/cheatsheet/useable-battery-capacity-electric-car, 2023.

[7] A. Thingvad, "The Role of Electric Vehicles in Global Power Systems," 2021.

[8] M. Taljegard, V. Walter, L. Göransson, M. Odenberger, and F. Johnsson, "Impact of electric vehicles on the cost-competitiveness of generation and storage technologies in the electricity system," *Environmental Research Letters*, vol. 14, no. 12, p. 124087, dec 2019. [Online]. Available: https://iopscience.iop.org/article/10.1088/1748-9326/ab5e6bhttps://iopscience.iop.org/article/10.1088/1748-9326/ab5e6b/meta

[9] I. I. L. Brief, "Electric-vehicle smart charging," 2019.

[10] R. Fachrizal, M. Shepero, D. van der Meer, J. Munkhammar, and J. Widén, "Smart charging of electric vehicles considering photovoltaic power production and electricity consumption: A review," *eTransportation*, vol. 4, p. 100056, may 2020.

[11] K. Sevdari, L. Calearo, P. B. Andersen, and M. Marinelli, "Ancillary services and electric vehicles: An overview from charging clusters and chargers technology perspectives," *Renewable and Sustainable Energy Reviews*, vol. 167, p. 112666, oct 2022.

[12] S. Striani, K. Sevdari, L. Calearo, P. B. Andersen, and M. Marinelli, "Barriers and Solutions for EVs Integration in the Distribution Grid," *2021 56th International Universities Power Engineering Conference: Powering Net Zero Emissions, UPEC 2021 - Proceedings*, aug 2021. [Online]. Available: https://orbit.dtu.dk/en/publications/barriers-and-solutions-for-evs-integration-in-the-distribution-gr

[13] O. Frendo, N. Gaertner, and H. Stuckenschmidt, "Open Source Algorithm for Smart Charging of Electric Vehicle Fleets," *IEEE Transactions on Industrial Informatics*, vol. 17, no. 9, pp. 6014–6022, sep 2021.

[14] K. Knezovic, S. Martinenas, P. B. Andersen, A. Zecchino, and M. Marinelli, "Enhancing the Role of Electric Vehicles in the Power Grid: Field Validation of Multiple Ancillary Services," *IEEE Transactions on Transportation Electrification*, vol. 3, no. 1, pp. 201–209, mar 2017.

[15] K. Sevdari, L. Calearo, S. Striani, P. B. Andersen, M. Marinelli, and L. Ronnow, "Autonomously Distributed Control of Electric Vehicle Chargers for Grid Services," *Proceedings of 2021 IEEE PES Innovative Smart Grid Technologies Europe: Smart Grids: Toward a Carbon-Free Future, ISGT Europe 2021*, 2021.

[16] S. Striani, K. Sevdari, M. Marinelli, V. Lampropoulos, Y. Kobayashi, and K. Suzuki, "Wind Based Charging via Autonomously Controlled EV Chargers under Grid Constraints," pp. 1–6, nov 2022.

[17] X. Han, K. Heussen, O. Gehrke, H. W. Bindner, and B. Kroposki, "Taxonomy for Evaluation of Distributed Control Strategies for Distributed Energy Resources," *IEEE Transactions on Smart Grid*, vol. 9, no. 5, pp. 5185–5195, sep 2018.

# PAPER [P6]

## Implementation of priority-based scheduling for electric vehicles through local distributed control

Authors:

Kristoffer Laust Pedersen, Simone Striani, Jan Engelhardt, Mattia Marinelli

Under review:

*Proceedings of the 2024 IEEE PES Innovative Smart Grid Technologies Europe (ISGT Europe)*

# Implementation of priority-based scheduling for electric vehicles through local distributed control

Kristoffer Laust Pedersen, Simone Striani, Jan Engelhardt, Mattia Marinelli
*Department of Wind and Energy Systems*
*Technical University of Denmark*
Roskilde, Denmark
{klape; sistri; janen; matm}@dtu.dk

***Abstract*—Distributed load management systems can become a crucial enabler for the widespread adoption of electric vehicles (EVs). The present paper experimentally demonstrates a priority-based scheduling algorithm that enables all chargers of an EV parking lot to coordinate their charging processes in a distributed manner. The distributed approach reduces control delays and maintains consistent management complexity, regardless of the number of chargers. A system is developed in which each electric vehicle supply equipment (EVSE) makes local decisions individually, sharing only their priorities with the other EVSEs of the cluster. The approach controls the total cluster consumption to a connection capacity while prioritizing the charging of EVs with the highest urgency. The scheduling algorithm is implemented in a real-life charging cluster, and its working principle is demonstrated through field tests. The system successfully shows the scheduling of two EVs to charge on a shared connection of 9 kW. The common capacity of the cluster showed a utilization ratio of 0.86 without critically overloading the grid connection.**

***Index Terms*—charging clusters, electric vehicles, experimental validation, load management, user-centric.**

## I. Introduction

The worldwide adoption of electric vehicles (EVs) continues at an unprecedented rate [1], generating a need for a robust and futureproof charging infrastructure [2]. Most EV charging will occur in residential areas and workplaces, where each cluster has similar user behavior [3]. With no control of the charging, power consumption will eventually exceed the installed grid capacity, as the areas have high arrival coincidence [4]. Accommodating the added loading without expensive grid reinforcements requires load management, such as smart charging. On the other hand, user behaviour at workplaces and homes is also significant as destination chargers [5], where parking time exceeds the necessary charging time, generating flexibility. An opportunity to perform load management without compromising the users arises with the flexibility, allowing time-shifting of the power consumption of individual EVs.

This paper will address the control of multiple electric vehicle supply equipment (EVSE) installed in a cluster with the same point of common coupling (PCC) at the grid connection. This paper introduces a novel distributed scheduling approach, where the charging processes are scheduled alternatingly in case the available cluster power capacity is reached. As opposed to common power-sharing approaches, scheduling promises higher efficiencies since the converter technology in EVs shows increasing efficiency for higher power values [6]. Moreover, the proposed distributed control is inherently different from common smart charging approaches, which employ principal/agent [7] or central architectures [8]. While such approaches have been predominantly used in the past years, they rely on increased data traffic, are prone to single-point failure, and may have scaling challenges as EVs increase rapidly [9]–[11].

979-8-3503-9042-1/24/$31.00 ©2024 IEEE

The paper presents a fully implemented distributed energy resource control system where the main contributions are:

- Development of a scalable distributed control architecture tailored for managing large-scale clusters of EVSEs
- Design and implementation of an EVSE state machine for scheduling EV charging sessions for improved efficiency
- Experimental validation through field testing, demonstrating the effectiveness of the proposed system in dynamically managing EV charging infrastructure

This paper is organised as follows: Section II describes the generic architecture of communication and decision-making; Section III presents the implementation of the architecture in terms of equipment and test procedures; Section IV presents and discusses the test results; Finally, Section V offers conclusions derived from the test, limitations, and future work.

## II. Methodology

This paper uses a distributed decision-making approach to include the user inputs in the control architecture. The design of the developed system is first described in terms of the entities and their communications signals and, later, the specific decision-making process done at each EVSE.

### A. Control architecture

The developed distributed control architecture is described in Fig. 1, where two layers of decision-making entities control the cluster consumption.

A virtual aggregator (VA) is introduced directly into the EVSE hardware to ensure fast and reliable reactions. Each $\mathrm{VA_i}$ ($i \in 2 \cdot N$) aggregates information and takes decisions for $\mathrm{EVSE_i}$, serving a maximum of one EV ($\mathrm{EV_i}$) at a time. The primary output of each VA is the maximum power consumption reference sent to the connected EV, $P_{i,ref}$.

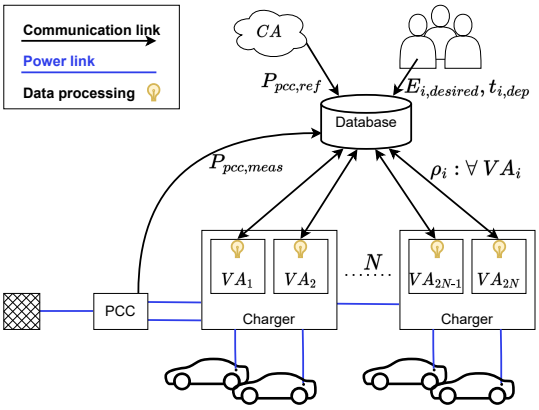


Fig. 1: Architecture of the control. Each VA controls a single EVSE charging outlet based on the data gathered in the shared local database.

To enable collaborative decision-making, the VAs require data inputs from other entities and horizontal communication among the VAs of the cluster. By realizing that flexibility arises from a gap between the user's needs and the individual power capacity ($P_{i,\max}$), we introduce the novel approach. The architecture, therefore, relies on user requests in the form of energy ($E_{i,desired}$) and expected departure time ($t_{i,dep}$) communicated directly to $VA_i$ at the start of a session. The control assumes that the user request is negotiated with a hereby dependent variable energy price. The dependency should reflect possible congestions at the PCC or EVSE level to ensure that the cluster can meet the demand of all users [12]. Based on the user inputs, the VA continuously computes the concealed priority to charge $\rho_c$:

$$\rho_c = \frac{E_{i,desired} - E_{i,charged}}{(t_{i,dep} - t_{now}) \cdot P_{i,\max}} \quad \in [0, 1) \tag{1}$$

$\rho_c$ is normalized with ($P_{i,\max}$), providing higher priority if power capabilities are low. This value is shared with the other VAs as the broadcasted $\rho_i$ for each $VA_i$ to facilitate horizontal communication:

$$\rho_i = \begin{cases} 1 & \text{when initiating charging} \\ \rho_c & \text{when steadily charging} \\ 0 & \text{otherwise} \end{cases} \tag{2}$$

Three distinct values of $\rho$ bear significance as information for all VAs of the cluster.

- $\rho = 1$ when a VA needs to initiate charging, requesting other VAs to allocate capacity and avoiding PCC overloading.
- $\rho_m$ the lowest non-zero $\rho$ in the cluster. $\rho_m$ is thus the priority marginally justifying charging during PCC congestions.
- $\rho = 0$ when a VA has no urge to participate in consuming power, either as no EV needs power or the PCC is congested, and it's $\rho_c < \rho_m$.

Further inputs of PCC reference and measured power are necessary for the VA. The measurement of power $P_{pcc,meas}$ is local and broadcasted through the shared database to the VAs. The Cloud Aggregator (CA) is the higher level of decision-making, taking decisions based on outside signals, and provides the cluster reference power $P_{pcc,ref}$, which is fixed at the cluster limit for this paper.

### B. State machine of virtual aggregator

Based on the data inputs outlined for the architecture and specific local measurements at the charger, each VA will transit through the state machine in Fig. 2, where the following section will reference the states by their number as {x}.

Each VA will transit from Idle {0} to the Starting point {1} whenever a user has provided the user inputs for an already connected EV. At this point, it will evaluate whether the cluster's current state allows for entry, in which case it will proceed to the initiation sequence {4-6}. Otherwise, it will transit to the Queue {2-3} where it will wait for a predefined time interval $t_{wait}$ after $\rho_c$ has increased above $\rho_m$. In the initiation sequence, the VA awaits a drop in the PCC power measurements {4} before it allows charging with the minimum power {5} and increases steadily from there {6}. When the single EV's constant consumption is reached, it will steadily charge {7-8}. When a VA already charging {7-8} finds another VA initiating {4-6} with $\rho = 1$, it will make space {9-10}. Only the marginally charging VA with $\rho_m$ will be in {10}, generating the necessary space for the entering VA. While lowering power consumption, it will continuously evaluate if the power level is considered inefficient $P_{i,ref} < \frac{P_{i,\max}}{2}$, in which case it will be queuing itself.

For all the states where charging occurs, the charging will naturally arrive at Session ended {11} whenever the user's desired energy $E_{desired}$ is reached.

The state of the VA is the primary factor for defining the power reference $P_{i,ref}$. For the states where charging is not allowed {0-4} and {11} $P_{i,ref} = 0$. The charging will always initiate in {5} with minimum power $P_{\min}$ and gradually increase as more power becomes available in the PCC {6}. In the steady control states, the VAs will either singlehandedly {8} or as a function of its relative share of $\rho$ {7} perform PI-control of the $P_{pcc,meas}$ towards $P_{pcc,ref}$ for the most congested of the three phases.

While making space as the marginal consumer {8} the control setpoint will be with a margin of $P_{\min}$ towards $P_{pcc,ref}$, while those in {9} will keep $P_{i,ref}$ constant.

## III. Case Study

The control architecture described above is tested in a real-life application with EVs and the European AC charging protocol for communication with the EV. The equipment used and test procedure will now be described before the results of the tests are discussed.

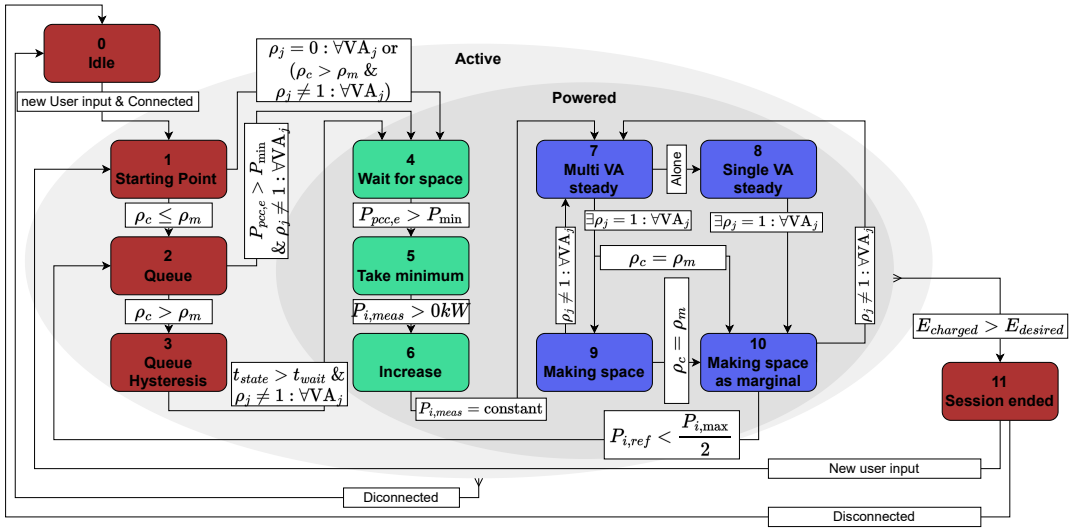


Fig. 2: State machine for the VAs. Subscript $i$ refers to the specific $\mathrm{VA_i}$, and $j$ evaluates all VAs of the cluster. $P_{pcc,e} = P_{pcc,ref} - P_{pcc,meas}$.

### A. Laboratory equipment

A fully distributed real-time power control loop has been implemented where measurements, decisions and actuation have been made with physically distinct nodes according to Fig. 1.

The chargers, developed for the ACDC project [13], utilize the IEC 62196 Type 2 charging protocol described in IEC 61851-1:2019 [14], and have a 32 A 5-cord connection thus a maximum of 7.3 kW on each three phases. The control range of the charger to each EV is lower bound by the protocol to $P_{\min} = 1.38kW$ and upper bound by equally sharing its grid connection capacity of $\frac{7.3}{2\text{plugs}} = 3.66kW$ per plug per phase. Each EVSE is externally controlled with a single datapoint of allowed power $(P_{i,ref})$ [W] per phase, which the EVSE relays to the EV through the type 2 protocol pilot signal. When using this hardware and protocol, the reference is limited to $P_{i,ref} \in \{0\} \cup [1.38, 3.66]kW$.

Connected to the chargers are two Renault Zoes, each eqipped with a 22 kW onboard charger and a 41 kW h battery.

The chargers connect to the main grid through the PCC equipped with a smart meter (DEIF Multi-instrument MIC-2 MKII) publishing the power consumption $(P_{pcc,meas})$ in 1-second intervals to the MQTT broker energydata.dk. A separate script requests the data of the MQTT broker, which is both logged and pushed to the local database. The local control database is implemented with Whiteboard, a custom-made local server accessible by all system entities. This database contains parameter and value pair instances for all the inputs of the VAs.

To implement the novel algorithms of the distributed control, the controller algorithms (VA and CA) are deployed on three separate beaglebone® black industrial microcontrollers. The controllers have a wired ethernet connection to obtain outside data and communicate $P_{i,ref}$ setpoints to chargers and $\rho_i$ to the local control database for the other VAs. The CA and VA log the current state of all variables internally at the end of each code scan.

To enable user interaction, the chargers have a publicly available website. The website allows users to enter identification and session-specific data: name, EV type, plug ID, requested energy $(E_{i,desired})$ and time of departure $(t_{i,dep})$. The website stores the data in a database and makes the session data of the last entry for each plug available on the local control database.

### B. Test procedure

A test is set up to demonstrate the scheduling of two EVs. The test was part of the live demonstration of the EV4EU [15] and ACDC [13], [16] projects in Risø September 2023 showcasing multiple features.

To demonstrate the scheduling, the CA broadcasts a constant $P_{pcc,ref} = 9\,\mathrm{kW}$, as this enables a single EV to occupy the total PCC capacity. During the demonstration, the queuing time of the VA was set as $t_{wait} = 30\,\mathrm{s}$. This design parameter was set to demonstrate the switching functionality and should be considered more prolonged for actual implementations to avoid too frequent switches. The EVs are connected with an initial state of charge (SOC) = $40\,\%$ to $50\,\%$ and the user inputs of Table I.

The inputs have been chosen to provide a similar priority of $\rho \approx 0.5$ for both, demonstrating scheduling.

TABLE I: Input data from the users.

| Entry time | Plug number | $E_{desired}$ [kWh] | $t_{arr}$ [HH:mm] | $t_{dep}$ [HH:mm] |
|---|---|---|---|---|
| 13:23:15 | 1 | 20 | 13:23 | 17:23 |
| 13:25:28 | 2 | 20 | 13:25 | 17:24 |

### C. Key performance indicators

The control of a cluster seeks to meet the user needs under the grid limitations. A set of key performance indicators (KPIs) is defined to assess the system's utilization of the PCC power capacity whilst minimizing implications of potential overloadings.

*1) PCC energy utilization ratio:* A KPI for the system is the ability to utilize the available power when the PCC is congested. The energy utilization ratio (UR) evaluates the ability to utilize the power over a period of time [17]. It evaluates the energy delivered to EVs relative to the potential common energy flow $P_{pcc,ref}$. For the cluster, it is found as follows:

$$\mathrm{UR}_{pcc} = \frac{\int \min\left[P_{pcc}(t)\ ,\ P_{pcc,ref}\right] dt}{\int P_{pcc,ref} dt} \tag{3}$$

$P_{pcc,ref}$ is included as a minimum boundary in the calculation not to reward overloading.

*2) PCC overloading:* Any overloadings should be further quantified as the system controls consumption towards the upper limit of $P_{pcc,ref}$. For the PCC of a cluster, a type C circuit breaker applies, and KPIs are inherited. The analytical parameters of an overload are comprised of $I_{ol}$, the peak normalized current, and $t_{ol}$, the total period with current over nominal. The current overloading can be converted to a power for each phase as $P_{ol} = I_{ol} \cdot V_{nom,LN}$, by assuming unity power factor and nominal voltage. A controller of currents could be implemented with the same algorithm to comply strictly with the current limitations.

## IV. Results and Discussion

The results of the scheduling demonstration as described in Section III-B will be presented.

In Fig. 3, a time-history of 7 min of the public priority and power consumption of each EVSE is visualized. Within this period, three switches occur, initiated by the non-charging VA when it sets $\rho = 1$. The VA starts consuming power only after it has observed enough capacity at PCC to begin charging. After it has taken over the power, the priority stabilizes at $\rho \approx 0.5$ and is thus the new marginally charging VA.

The $\mathrm{UR}_{\mathrm{pcc}}$ is found over the 7 min to be 0.858. The blue and orange area of Fig. 4 indicates the steady state and switching 'non-utilized energy' accounting for 0.017 and 0.132 each. The system-integrated steady state margin for the PI controller affects the steady state, ensuring steady powers with the 1 A resolution of setpoints to the EVs. On the other hand, the switching impact is affected by three parameters. First, the magnitude of the margin $P_{\min}$ generated by the marginal VA and is directly related to the type 2 plug protocol of minimum

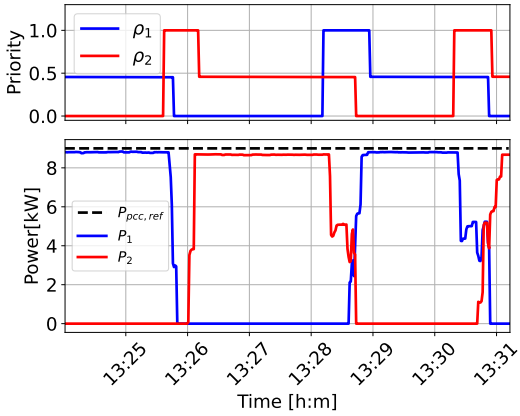


Fig. 3: Representative time window of broadcasted priority and power consumption of two VAs scheduling over time. $\mathrm{VA}_1$ is already charging as $\mathrm{VA}_2$ receives user inputs at 13:25:28 and starts charging. Scheduling continues from this point with switches every $\approx 2$ min.

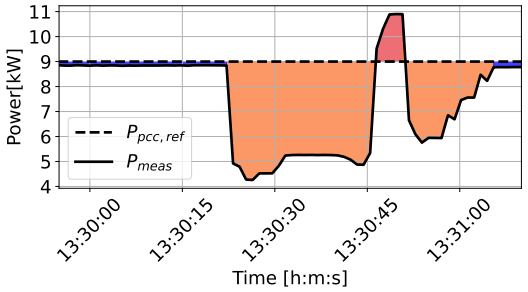


Fig. 4: Cluster reference and consumption measured at the PCC for a single switching period. The consumption follows with a margin the reference during steady charging but drops to make space (orange area) and overloads (red area) during a switch

6 A. Secondly, there are delays in the control system, including the reaction time of the EVs, as one VA cannot allow charging before it has been observed that capacity has been made available for it. Thirdly, the design parameter of $t_{wait}$ impacts the time ratio between steady charging and switching and can allow longer charging periods with priorities drifting further apart.

An advantage of the distributed architecture is the short control path from PCC measurement to reactions of the EV. For this experiment, this advantage is obscured by the inherent delays of the proprietary implementation, as the switches have a 15 s interval from the charging EV modulates down until the new VA starts to consume power. Indeed, the EV down-regulating reaction time of 0 s to 5 s and non-standard defined

startup time is part of this delay and is inherent in the startup of the onboard charger. Further, the VA is implemented with a 5 s fixed asynchronous update frequency, which impedes its reaction time. The mentioned delays generate a nondeterministic behaviour, which is apparent in the analysis of the two first switches of Fig. 3, The first switch (13:25:40) makes a complete stop of power consumption, whereas the switch back from $VA_2$ to $VA_1$ (13:28:15) has a smoother cluster power consumption.

With the given delays of a proprietary installation, the $UR_{pcc}$ thus shows quite good for a control architecture where the down-modulation of one VA should be observed on the PCC measurements before another VA can communicate a start. On the other hand, the requirement to immediately ramp up the reference to 6 A will inevitably impact the $UR_{pcc}$ negatively.

During the experiment, the cluster overloaded the PCC during two switching events. As shown in Fig. 4 (highlighted in red), this overloading occurred when a new EV initiated charging simultaneous to the already charging EV overcompensating the low overall power consumption. The observed overload peaks of 1.1 and 1.2 times the rated 9 kW, lasting 1.05 s and 5.25 s respectively, fall well within type C breaker standards, demonstrating the system's ability to schedule the two EVs within PCC limitations.

Future work on the control system should address the database as a critical single point of failure. Either bypassing the database with individual distributed communication or incorporating a fallback state in Fig. 2 to handle communication failures.

## V. Conclusion

This paper proposed a distributed control architecture for coordinating EV charging based on user needs. The system facilitates higher charging efficiency by alternately allocating available cluster power to individual chargers.

The method was implemented in an EV charging cluster and experimentally demonstrated, achieving an utilization rate of 0.86 of the cluster power capacity, while managing occasional overloads within acceptable limits. The distributed control demonstrated strong potential for further research in scheduling control schemes, especially with larger fleets over extended periods. While dependent on pricing models, the system also offers an underlying technical framework for future pricing studies. These studies could explore users' willingness to be flexible and investigate the relationship between departure time, energy requests, and session pricing.

On the technical side, future enhancements may require communication from VAs in the queue to express priority in a separate range, ensuring priorities are followed for reinitiation of charging. The next steps include scaling the system to larger EVSE clusters and extending the testing period, positioning this approach as a significant advancement toward efficient and scalable EV charging solutions.


## Acknowledgment

The work in this paper is supported by the research projects ACDC (EUDP grant number: 64019-0541) www.acdc-bornholm.eu and by the research project EV4EU (Horizon Europe grant no. 101056765 ) ev4eu.eu.


## References


[1] *Iea Global-Ev-Data-Explorer*. https://www.iea.org/data-and-statistics/data-tools/global-ev-data-explorer. URL: https : / / www . iea.org/data-and-statistics/data-tools/global-ev-data-explorer.

[2] L. Noel, G. Zarazua De Rubens, J. Kester, and B. K. Sovacool. "Understanding the Socio-Technical Nexus of Nordic Electric Vehicle (EV) Barriers: A Qualitative Discussion of Range, Price, Charging and Knowledge". In: *Energy Policy* 138 (2020), page 111292. DOI: 10.1016/j.enpol.2020.111292.

[3] T. Unterluggauer, K. Rauma, P. Järventausta, and C. Rehtanz. "Short-term Load Forecasting at Electric Vehicle Charging Sites Using a Multivariate Multi-step Long Short-term Memory: A Case Study from Finland". In: *IET Electrical Systems in Transportation* 11 (2021), pages 405–419. DOI: 10.1049/els2.12028.

[4] L. Calearo, A. Thingvad, K. Suzuki, and M. Marinelli. "Grid Loading Due to EV Charging Profiles Based on Pseudo-Real Driving Pattern and User Behavior". In: *IEEE Transactions on Transportation Electrification* 5 (2019), pages 683–694. DOI: 10.1109/TTE.2019.2921854.

[5] A. Thingvad, P. B. Andersen, T. Unterluggauer, C. Træholt, and M. Marinelli. "Electrification of Personal Vehicle Travels in Cities - Quantifying the Public Charging Demand". In: *eTransportation* 9 (2021), page 100125. DOI: 10.1016/j.etran.2021.100125.

[6] K. Sevdari, L. Calearo, B. H. Bakken, P. B. Andersen, and M. Marinelli. "Experimental Validation of Onboard Electric Vehicle Chargers to Improve the Efficiency of Smart Charging Operation". In: *SSRN Electronic Journal* (2023). DOI: 10.2139/ssrn.4460277.

[7] X. Cao, S. Striani, J. Engelhardt, C. Ziras, and M. Marinelli. "A Semi-Distributed Charging Strategy for Electric Vehicle Clusters". In: *Energy Reports* 9 (2023), pages 362–367. DOI: 10.1016/j.egyr.2023.10.014.

[8] J. García-Villalobos, I. Zamora, J. San Martín, F. Asensio, and V. Aperribay. "Plug-in Electric Vehicles in Electric Distribution Networks: A Review of Smart Charging Approaches". In: *Renewable and Sustainable Energy Reviews* 38 (2014), pages 717–731. DOI: 10.1016 /j.rser.2014.07.040.

[9] X. Han, K. Heussen, O. Gehrke, H. W. Bindner, and B. Kroposki. "Taxonomy for Evaluation of Distributed Control Strategies for Distributed Energy Resources". In: *IEEE Transactions on Smart Grid* 9 (2018), pages 5185–5195. DOI: 10.1109/TSG.2017.2682924.

[10] P. Richardson, D. Flynn, and A. Keane. "Local Versus Centralized Charging Strategies for Electric Vehicles in Low Voltage Distribution Systems". In: *IEEE Transactions on Smart Grid* 3 (2012), pages 1020–1028. DOI: 10.1109/TSG.2012.2185523.

[11] W. Liu, W. Gu, X. Yuan, and K. Zhang. "Fully Distributed Control to Coordinate Charging Efficiencies for Energy Storage Systems". In: *Journal of Modern Power Systems and Clean Energy* 6 (2018), pages 1015–1024. DOI: 10.1007/s40565-017-0373-1.

[12] A. Alsabbagh and C. Ma. "Distributed Charging Management of Electric Vehicles Considering Different Customer Behaviors". In: *IEEE Transactions on Industrial Informatics* 16 (2020), pages 5119–5127. DOI: 10.1109/TII.2019.2952254.

[13] *ACDC Project*. URL: https://www.acdc-bornholm.eu/home.

[14] *IEC_61851-1:2019. Electric Vehicle Conductive Charging System - Part 1: General Requirements*. 2019.

[15] *EV4EU*. URL: https://ev4eu.eu/.

[16] A. Malkova, S. Striani, J. M. Zepter, M. Marinelli, and L. Calearo. "Laboratory Validation of Electric Vehicle Smart Charging Strategies". In: *IEEE* (58th International Universities Power Engineering Conference (UPEC) 2023). DOI: 10.1109/upec57427.2023.10294673.

[17] M. Hockman, T. Logenthiran, and J. Sheng. "Optimizing Renewable Energy Utilization Ratio with Model Predictive Control". In: *IECON 2023- 49th Annual Conference of the IEEE Industrial Electronics Society*. IECON 2023- 49th Annual Conference of the IEEE Industrial Electronics Society. Singapore, Singapore: IEEE, 16/2023, pages 1–8. ISBN: 9798350331820. DOI: 10.1109/IECON51785.2023.10312337.

PAPER [P7]

# Experimental Investigation of a Distributed Architecture for EV Chargers Performing Frequency Control

Authors:

Simone Striani, Kristoffer Laust Pedersen, Jan Engelhardt, Mattia Marinelli

Published in:

*World Electric Vehicle Journal*

DOI:

110.3390/wevj15080361.

World Electric Vehicle Journal

MDPI

*Article*

# Experimental Investigation of a Distributed Architecture for EV Chargers Performing Frequency Control

**Simone Striani*, Kristoffer Laust Pedersen, Jan Engelhardt and Mattia Marinelli***

Department of Wind and Energy Systems, Technical University of Denmark, 4000 Roskilde, Denmark; klape@dtu.dk (K.P.); janen@dtu.dk (J.E.)
* Correspondence: sistri@dtu.dk (S.S.); matm@dtu.dk (M.M.)

**Abstract:** The demand for electric vehicle supply equipment (EVSE) is increasing because of the rapid shift toward electric transport. Introducing EVSE on a large scale into the power grid can increase power demand volatility, negatively affecting frequency stability. A viable solution to this challenge is the development of smart charging technologies capable of performing frequency regulation. This paper presents an experimental proof of concept for a new frequency regulation method for EVSE utilizing a distributed control architecture. The architecture dynamically adjusts the contribution of electric vehicles (EVs) to frequency regulation response based on the charging urgency assigned by the EV users. The method is demonstrated with two Renault ZOEs responding to frequency fluctuation with a combined power range of 6 kW in the frequency range of 50.1 to 49.9 Hz. The results confirm consistent power sharing and effective frequency regulation, with the system controlling the engagement of the EVs in frequency regulation based on priority. The delay and accuracy analyses reveal a fast and accurate response, with the cross-correlation indicating an 8.48 s delay and an average undershoot of 0.17 kW. In the conclusions, the paper discusses prospective improvements and outlines future research directions for integrating EVs as service providers.

**Keywords:** electric vehicle supply equipment; smart charging; frequency regulation; ancillary services; experimental validation; distributed control



**Citation:** Striani, S.; Pedersen, K.; Engelhardt, J.; Marinelli, M. Experimental Investigation of a Distributed Architecture for EV Chargers Performing Frequency Control. *World Electr. Veh. J.* **2024**, *1*, 0. https://doi.org/

Received: 28 June 2024
Revised: 4 August 2024
Accepted: 8 August 2024
Published:



## 1. Introduction

Smart EV charging technologies leverage the storage capabilities of EVs to make them controllable demand-side resources, crucial for the development of smart grids [1]. These technologies offer flexibility services beneficial to distribution and transmission system operators [2] and delay expensive grid upgrades required because of the growing demand from electric transportation [3]. Moreover, EVs can contribute to grid stability by offsetting power fluctuations from renewable energy sources [4]. This study presents an experimental demonstration for frequency regulation using smart chargers under a distributed control system, where each EV adjusts its charging power in response to grid frequency changes based on user input. Traditionally, frequency stability has relied on conventional power plants known for their quick responsiveness and high inertia [5]. However, the rise of renewable energy sources challenges this stability by reducing overall system inertia [6]. Commercializing frequency regulation through frequency flexibility markets allows power producers and consumers to offer balancing power services [7]. With their substantial storage capacity, EV fleets can significantly contribute to frequency regulation [8], offering benefits to the transmission system, charging point operators, and EV users [9]. These advantages include enhanced grid stability, potential revenue, and reduced charging costs [10].

Distributed architectures are mostly unexplored for smart charging applications. Previous research in EV charging infrastructure has predominantly focused on centralized control architectures involving a single central unit managing each charger. Centralized control offers operational transparency and optimal performance, yet it faces challenges with

scalability, vulnerability to cyber-attacks, and privacy issues [11]. Decentralized control operates through local units, offering scalability and robustness with simpler communication and direct user control, but it lacks optimal performance because of the absence of global coordination [12]. Distributed control systems integrate centralized and decentralized approaches, using central and local components for comprehensive grid management. This hybrid approach harnesses the strengths of both systems, providing precise, scalable, and robust control solutions [13,14].

The experimental evidence of the technical feasibility of frequency regulation via EVSE provided in this study contributes to the research literature on the topic, where most existing studies rely on computational analyses and focus on its economic potential. In addition, current research on frequency regulation focuses on centralized and decentralized systems, often via vehicle-to-grid (V2G) approaches [15], despite most existing EVs only being capable of unidirectional charging. Indeed, although V2G technology has high economic potential, there remains a lack of standardization [16], as well as technological and regulatory readiness, for its full deployment [17]. Thingvad et al. [18] analyzed the economic viability of employing a fleet of 10 EVs for frequency regulation in the Danish grid, comparing the potential of unidirectional and V2G systems. Their findings indicated that while bidirectional systems can generate higher revenue for aggregators and EV owners, they also incur more significant energy losses and necessitate additional equipment. The authors proposed a novel scheduling strategy leveraging historical frequency data to optimize capacity and revenue for market actors. Regarding computational analysis, the research literature presents different methods for frequency regulation. Yao et al. [19] proposed a robust optimization framework for scheduling EV frequency regulation capacity under a performance-based compensation scheme to maximize user revenue. The study in [20] introduced a fuzzy control-based smart charging method for EVs, demonstrating its effectiveness in reducing frequency deviations in simulation tests. Orihara et al. [21] explored a decentralized V2G system contributing to frequency regulation and battery state-of-charge (SOC) synchronization, highlighting its potential for future research comparing it with centralized systems. Other authors explored the coordination of EV charging with large-scale heat pumps [22] or with local energy storage [23] for frequency regulation, both addressing battery degradation issues. Meng et al. [24] developed a strategy for dynamic frequency control using EV clusters, taking into account the travel behavior of EVs, focusing on stabilizing frequency fluctuations and improving economic operation. Experimental studies primarily conducted by the Technical University of Denmark with a centralized control architecture have provided insights into the practical application of frequency regulation. Marinelli et al. [25] tested the performance of commercial EVs in primary frequency control with a centralized control architecture, suggesting improvements for system response. A field test with a V2G EV fleet performing frequency normal reserve under a centralized control scheme was proposed in [26]. The experimental investigation, conducted over five years, provided significant insights into battery degradation. The study concluded that battery degradation from power cycling of the EVs is minimal compared to the calendar degradation.

This paper contributes to research on frequency regulation via EVSE with the following key innovations: Firstly, the paper introduces a distributed architecture approach to smart EV charging, offering a promising alternative to the commonly studied centralized and decentralized systems. Secondly, the designed system allows individual users to engage in frequency regulation to varying degrees based on their charging needs. Charging prioritization is unavailable in deployed chargers and is fundamental to smart charging development. Lastly, the paper provides a proof-of-concept demonstrating the technical feasibility of frequency regulation using EV chargers. This contribution is of utmost importance in the absence of literature presenting empirical evidence of frequency regulation using unidirectional EV chargers with distributed control architecture. Overall, this paper proves the technical feasibility of frequency regulation through an EV charging system

with a lean yet robust system architecture, a first step toward integrating unidirectional EV clusters in frequency markets.

The remainder of this paper is organized as follows: Section 2 presents a theoretical overview of the control concept, including the control and communication system design. Section 3 details the physical implementation of the control concept, providing a clear guide for other researchers who wish to replicate the results. Section 4 presents and discusses the key findings. Finally, Section 5 offers conclusions and outlines perspectives on future work.

## 2. Methods

This chapter outlines the control concept deployed in this study. Section 2.1 presents a general introduction to the system components and the computational intelligence in the cloud server, named cloud aggregator (CA), and in the charger, named virtual aggregator (VA). This section then provides a mathematical description of CA control in Section 2.2 and VA control in Section 2.3.

### *2.1. Description of the Control Concept: CA, VA, and Priority*

The distributed control concept includes double-layer control: The control of the cluster as a whole is performed by the CA, a computational intelligence located in a cloud server. The autonomous control of each charger is managed by the VA embedded within each charger [27]. Figure 1 illustrates the communication architecture with a simplified block diagram. The cluster of chargers connects to the grid at the point of common coupling (PCC), where a smart meter reads their consumption and grid conditions. The meter provides frequency and consumed power measurements at the PCC and sends them to the CA and the VAs. A user interface allows users to input the energy requested and the departure time for the charging session. The inputs are directly communicated to the VA of the respective charger and are fundamental for the power-sharing among the VAs.

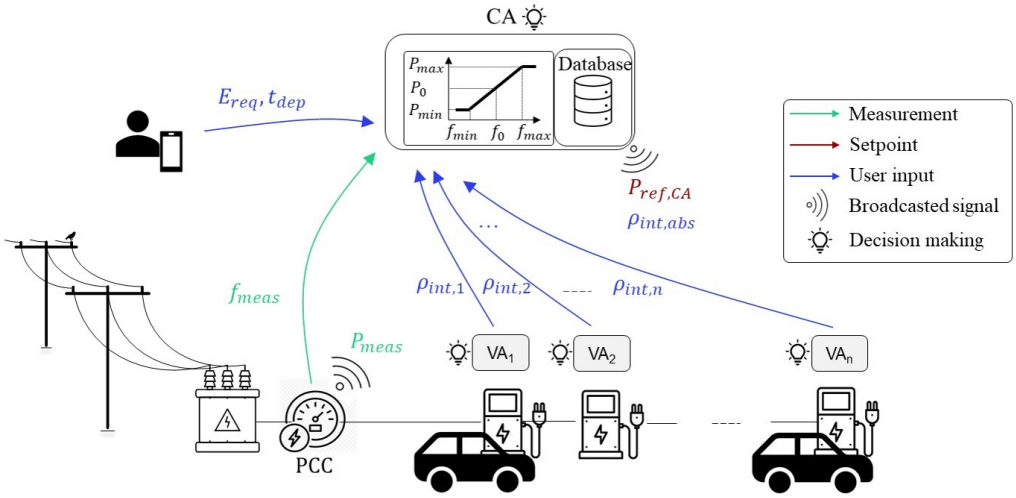


**Figure 1.** Simplified block diagram of the proposed distributed control architecture applied to a general parking lot with a number "n" of chargers.

### *2.2. Controller in the CA*

The CA is the global intelligence, and it has three main functions. Firstly, it receives frequency measurements $f_{meas}$ from the meter. Secondly, it translates these inputs into

power set points ($P_{CA}^{ref}$) based on the droop control characteristic. Thirdly, it broadcasts the power set points to the VAs of the cluster. The droop control in the CA is defined as

$$P_{CA}^{ref} = P_0 + k_{droop} \cdot (f_0 - f_{\text{measured}}) \tag{1}$$

The power range allocated to frequency regulation, denoted as $P_{bid}$, is set to $\pm 3$ kW in our demonstration. $P_{bid}$ defines $P_{max}$ and $P_{min}$, where $P_0$ is the power set point at 50 Hz ($f_0$). $P_{max}$ and $P_{min}$ determine the controllable range of $P_{CA}^{ref}$. The droop control coefficient $k_{droop}$ is calculated as $(P_{max} - P_{min})/\Delta f$. Each iteration of the CA ends with the broadcast of $P_{CA}^{ref}$ to the VAs.

### 2.3. Controller in the VA

The $P_{CA}^{ref}$ is retrieved by the VAs together with the power measurement $P_{meas}$ from the meter at the PCC. Each VA also stores the user inputs received by the user interface. The user inputs are the energy requested by the user $E_{req}$ and the departure time $t_{dep}$. The inputs are used to calculate the internal priority $\rho_{int}$ of each VA as

$$\rho_{int} = \frac{E_{req} - E_{charged}}{(t_{dep} - t_0) \cdot P_{rated,EVSE}} \tag{2}$$

In the formula, $E_{charged}$ is the energy charged by the EV, measured by the plug during the charging session, $t_0$ is the current time, and $P_{rated,EVSE}$ is the rated power of the plug. $\rho_{int}$ is a value between 0 and 1.

$\rho_{int}$ is an intermediate step for the calculation of the relative priority $\rho_r$, which is a control parameter of the VA. Indeed, each VA shares its $\rho_{int}$ with all the VAs through the CA. Then, each VA calculates its relative priority $\rho_r$ as:

$$\rho_r = \frac{\rho_{int}}{\sum_{i=1}^{N_{EVs}} \rho_{int,i}} \tag{3}$$

where $\sum_{i=1}^{N_{EVs}} \rho_{int,i}$ (denoted as $\rho_{int,abs}$ in the figure) represents the summation of the internal priorities of all the chargers. While $\rho_{int}$ is shared among the VAs, $\rho_r$ is not shared among the chargers.

Knowing the power error for the whole cluster ($P_{error,PCC} = P_{CA}^{ref} - P_{meas}$) and $\rho_r$, each VA can calculate the power reference as

$$P_{ref,i} = \begin{cases} P_{ref,i-1} + P_{error,PCC} \cdot \rho_r & P_{error,PCC} > 0 \\ P_{ref,i-1} + P_{error,PCC} \cdot (1 - \rho_r) & P_{error,PCC} < 0 \end{cases} \tag{4}$$

In the formula, $i$ corresponds to the current iteration of the controller, and $i-1$ corresponds to the previous iteration. Equation (4), applied in two different scenarios based on the sign of $P_{error,PCC}$, outlines the operation of a PI controller with integral gain $K_i$ set to 1. The proportional gain $K_p$ varies, being directly proportional to $\rho_r$ when $P_{error,PCC} > 0$ and to $(1 - \rho_r)$ when $P_{error,PCC} < 0$. This control approach ensures that EVs with higher priority will more readily increase their power demand in response to positive errors while reducing it less when the error is negative. In contrast, lower-priority EVs will have a smaller increase in power demand for positive errors and a larger decrease for negative errors. This strategy guarantees that EVs maintain their allocated share of power consumption dynamically, adapting to continuous changes in error, which may result from frequency fluctuations. Each VA calculates its power reference $P_{ref,i}$ and communicates it to its charging plug. The control loop completes with feedback on power and frequency measurements provided by the meter at the PCC to the VAs and the CA.

## 3. Physical Implementation

This subsection describes the physical implementation of the architecture concept. Section 3.1 details the hardware and software used in the test. Section 3.2 describes the test case chosen for the demonstration. This chapter provides a clear guide for other researchers who wish to replicate the results.

### *3.1. Hardware and Software Used*

The VAs and the CA reside in "Beaglebone® black industrial" microcontrollers, shown in Figure 2. The microcontrollers have an ARM Cortex-A8 1 GHz processor with a RAM of 512 MB and an embedded flash memory of 4 GB. The microcontrollers run on Debian OS, and all the control algorithms are built in Python 3.8. Each charger has a dedicated external microcontroller, where the control algorithm is executed. This arrangement is due to a non-disclosure agreement with Circle Consult, the manufacturer and operator of the chargers, limiting direct control integration. Consequently, only the final power set points can be communicated to the chargers. The CA also has a dedicated microcontroller. These microcontrollers run on Debian OS and are connected to the network via wired Ethernet to facilitate data exchange. During the tests, the CA and the VA operate with an update rate of 4 and 2 s, respectively. Therefore, they execute their scripts (which consist of reading inputs, computing outputs, and sending outputs) at their respective intervals. Regarding network connectivity, the chargers are linked to the internet through a 4G connection, while other devices utilize the university Wi-Fi, which is secured by a firewall. The firewall restrictions on direct communication necessitate a server database as a mediator for data exchange across the two network interfaces. This server, acting as a central hub, facilitates the flow of information among devices without retaining a historical record of data values, only storing the most recent updates. In other words, the server database mediates all the communication paths in Figure 1.

The charging system incorporates a web interface, which allows for the input and management of user data and session-related parameters $E_{req}, t_{dep}$.

The VAs on the Beaglebone microcontrollers use Amazon Web Services as an interface to transmit their final power set point to the microcontrollers integrated with the chargers.

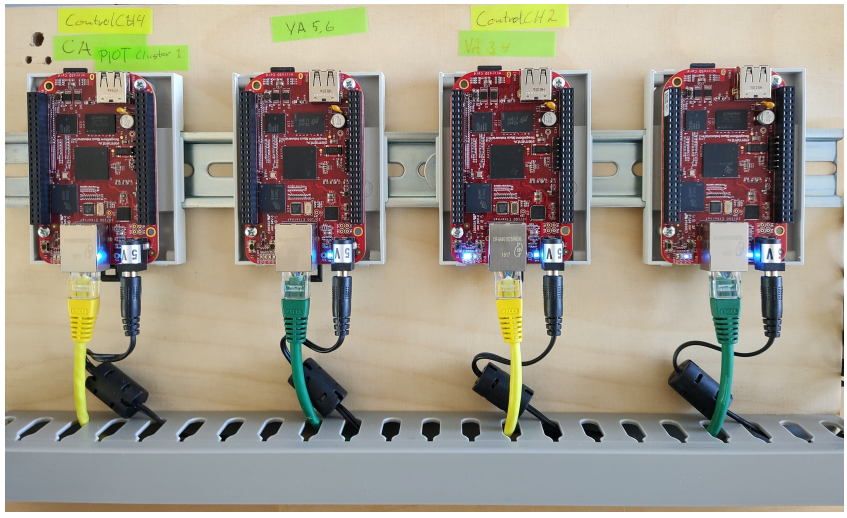


**Figure 2.** Beaglebone® black industrial microcontrollers used for testing the control architecture.

The microcontrollers integrated with the chargers convert the power set point received from the external microcontrollers into a current set point, which they then relay to the

charger actuators. The PCC is equipped with a smart meter (DEIF Multi-instrument MIC-2 MKII), which publishes, among other parameters, the power consumption and frequency measured in 1 s intervals to the MQTT data broker energidata.dk. The charger utilizes type 2 charging protocol as outlined in IEC 61851-1:2019 [28], featuring a 32 A 5-wire connection capable of delivering up to 22 kW of 3-phase power. However, the maximum power consumption per plug is limited to 11 kW, setting the operational control range between 3.68 kW and 11 kW for charging electric vehicles.

### *3.2. Test Case*

In the tests, two Renault Zoes were employed for the frequency regulation, as shown in Figure 3. These Renault Zoes have a 22 kW onboard charger and a 41 kWh battery. For both EVs, the user inputs are assumed to be 8.1 kWh for EV1 and 19 kWh for EV2, resulting in internal priorities $\rho_{int}$ of 0.7 and 0.3, respectively. The length of the charging session inputted is 3 h for both vehicles. It is important to note that fulfilling the energy request and respecting the duration of the charging session are not the focus of the investigation. The user inputs are chosen to establish the priorities mentioned above. The expected results are that the high-priority EV charges more than the EV with lower priority while performing frequency regulation. The $P_{bid}$ is chosen to be $\pm 3$ kW, meaning that the power that can be used for regulation is 6 kW. The droop control is set up to be in the range of 13 kW to 19 kW for a frequency range of 49.9 Hz to 50.1 Hz.


**Figure 3.** Experimental setup implemented: The figure shows the two Renault Zoes and the charger used in the test. The test is conducted in the DTU Energy System Integration Lab (SYSLAB).

## 4. Results and Discussion

This chapter details the performance of the distributed architecture observed during the test. Section 4.1 delves into the time history of frequency, power consumption, SOC, and priority ($\rho_{int}$), aiming to illustrate the general trends and behaviors observed. Section 4.2 presents the analysis of the system's delay and accuracy in responding to frequency changes. Section 4.3 describes the benefits of the system for the transmission system operators, charging point operators, and users. Finally, Section 4.4 discusses some identified limitations affecting the system's reaction time.

### 4.1. System Behavior Observed

In Figure 4, the time history of the frequency regulation performances is provided. The top graph shows the time history of the frequency measurements and the power consumed by the cluster; the graph has a double y-axis showing the frequency range on the left side and the power measured range on the right side. The scales of the dual y-axis are calibrated to highlight any potential overshoots or undershoots in the measured cluster power compared to the expected power from the droop controller. The graph shows a correct match of power and frequency, with some additional oscillation and a general undershoot of the power measured at the PCC compared to the expected power. Such oscillations around the power set point might be due to non-optimal interaction between the control tuning, the VAs set point update rate, and the reaction time of the EVs. The undershoot of the power adjustment could be related to the production of reactive power of the EVs at low charging power. In detail, because the charger output is the maximum allowed current for the EVs, the active power consumed by the EVs depends on the power factor characteristic of the onboard charger. This phenomenon has been reported in previous studies on the modulation of EVs [29]. The Renault Zoe is optimized to charge at its rated power (22 kW), while the reactive power increases when charging at low active power. Both phenomena—the oscillations and the undershoot of the power measured—should be further analyzed in future work. The bottom graph shows the individual dynamic power consumed by each EV during the test. The graph shows that EV1 charges at higher power because of the higher priority. EV2 has lower priority and, therefore, lower charging power. Furthermore, the charging power of EV1 saturates at an upper limit. As a result, the aggregated cluster response in the upper direction in case of frequency increases can only be provided by EV2. This behavior can potentially slow down the reaction time in this direction of service provision since only EV2 is reacting to frequency increases. This is particularly true because the design of the PI control, defined in the Equation (4), allocates a smaller share of the up-regulation power to the low-priority EV. Future work will address this behavior by adjusting the PI control near the upper and lower power limits of the plug.

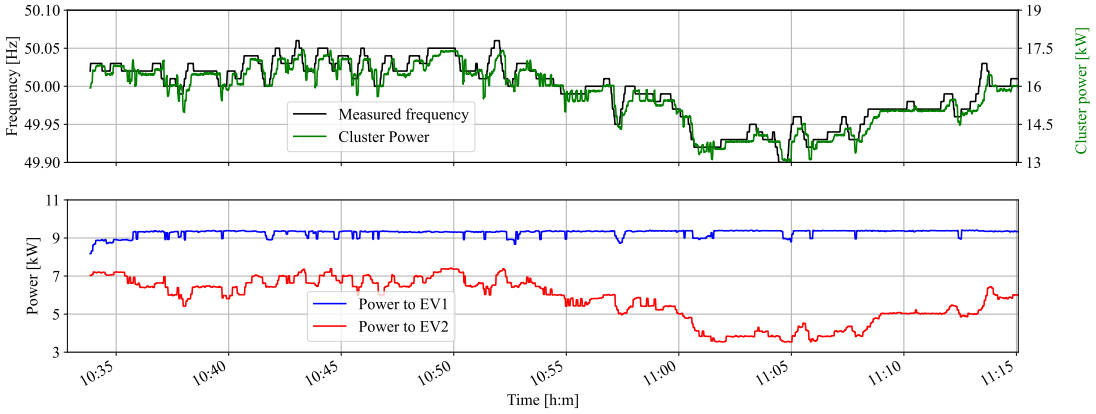


**Figure 4.** Representative time window of the experimental validation of frequency regulation using distributed control architecture: frequency and power measured (**top**); power dispatched to each EV (**bottom**).

Figure 5 illustrates the development of the SOC in the top graph and their priorities over time for two EVs in the bottom graph. At the start of the test, the SOCs for EV1 and EV2 were 17 % and 14 %, respectively. The SOC of EV1 increased faster because of its higher power allocation than EV2. At the end of the test, the SOCs were 48 % and 33 % for

EV1 and EV2, respectively. The priority trends for both EVs ran nearly parallel throughout the charging session, with their priorities decreasing as they approached the completion of their requested energy.

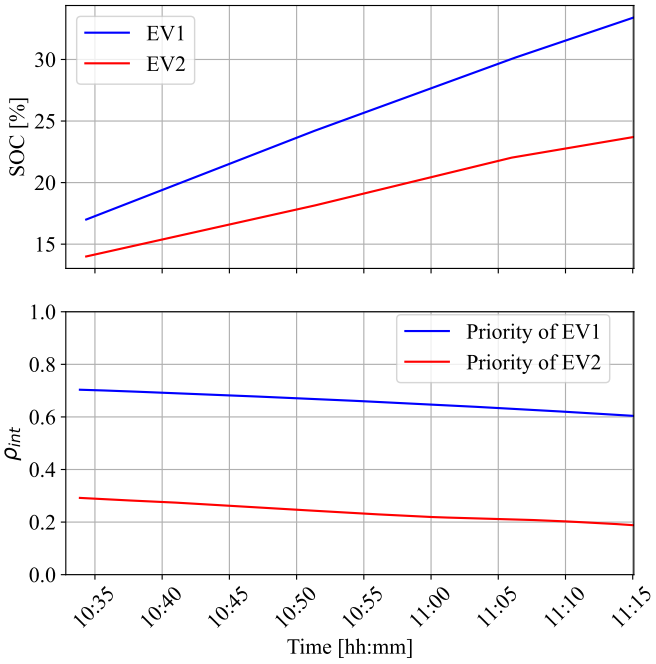


**Figure 5.** Trends of SOC (**top**) and internal priority (**bottom**) for the two EVs during the experimental validation.

A comparison of the bottom graph in Figure 4 and the graphs in Figure 5 reveals the impact of the longer period of underfrequency occurring from 10:50 until the end of the test. Because of its lower priority, EV2 reduced its power consumption, while EV1 maintained charging at maximum power. Consequently, the rate of SOC increase and the rate of priority decrease for EV2 slowed down. In contrast, the priority and SOC trends for EV1 remained unaffected, as EV1 maintained constant power.

### *4.2. Response Delay and Accuracy*

Figure 6 shows a normalized cross-correlation of the power measured at the PCC ($P_{meas}$) and power expected from the droop control ($P_{exp}$) to visualize the delays. The normalized cross-correlation is computed using the Pearson formula for each value of lag between the two curves:

$$r(k) = \frac{\sum_i (P_{meas}i - P_{meas}^{avg}i) \cdot (P_{exp,i+k} - P_{exp,i+k}^{avg})}{\sigma_{P_{meas}} \cdot \sigma_{P_{exp}} \cdot N} \quad (5)$$

In the formula, $k$ is the value of lag, and $\sigma_{P_{meas}}$ and $\sigma_{P_{exp}}$ are the standard deviations of the power measurement and expected power, respectively. $N$ is the length of the time series. In the graph, the y-axis shows the normalized cross-correlation coefficient, and the x-axis shows the lag in seconds. The lag represents the displacement between the two time series for which each cross-correlation coefficient is calculated. The normalized cross-correlation peaks at 0.98 at a lag value of 8.48 s of the measured power curve with the expected power curve. Such a result, although semi-quantitative, tells us that the two curves have a very

high degree of similarity. The delay depends on different factors. Together with the delays in communication and actuation of the control signals, an important factor is the reaction time of the EVs. In our case, the two car models are identical. However, reaction time can be drastically different depending on brand and model.

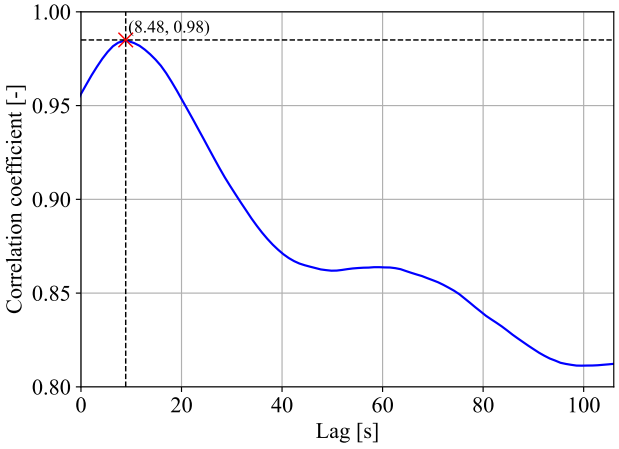


**Figure 6.** Normalized cross-correlation of the frequency with the power measured during the experimental validation.

Finally, Figure 7 illustrates a histogram of the error distribution between the measured power and the expected power during the test. For this analysis, the measured power was shifted by approximately 8.48 s to highlight the controller's precision and minimize the influence of the controller delay on the calculation. The analysis confirms the previously identified undershoot of the measured power in response to the frequency signal in Figure 4, with an average undershoot of 0.17 kW during the test. Additionally, the error ranges from −1.08 kW to 0.48 kW. The error values fall within the range of −0.73 kW to 0.29 kW for the 98th percentile, indicating a 2 % probability of an error exceeding 0.29 kW or subceeding −0.73 kW.

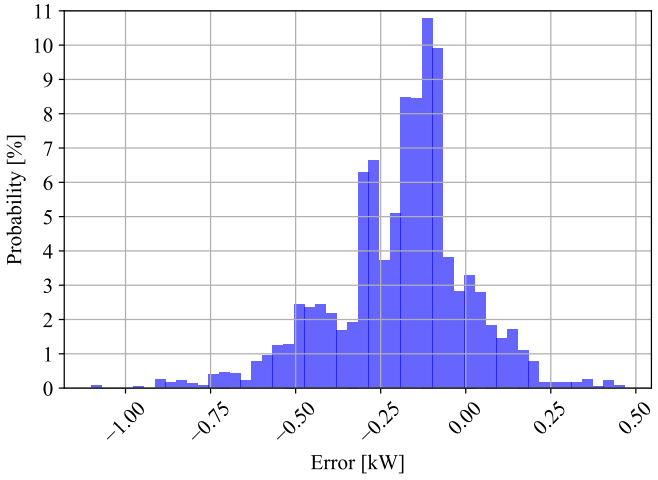


**Figure 7.** Histogram of the error distribution between expected and measured power during the experimental validation.

### 4.3. Discussion of the Results

The results demonstrate a fast and accurate system response to frequency changes, including effective coordination among individual EVs based on their priority. Large-scale adoption of this system by charging point operators can generate significant value for all stakeholders in the EVSE business, as well as for EV users. The transmission system operator can purchase flexibility services from charging point operators, improving grid stability. Charging point operators will profit from trading frequency services and can develop business models incentivizing users to participate in frequency regulation by offering cheaper charging prices. Thanks to the robust prioritization mechanism, users can lower their charging costs without compromising their charging requirements. The additional power cycling incurred by the EVs is not expected to increase battery degradation significantly [26]. Lowering charging prices will, in turn, incentivize the purchase of more EVs.

### 4.4. Limitations of the Results

In our physical implementation, we identified several limiting factors that contribute to additional delays in the control action, offering areas for improvement: Firstly, the database server, necessitated by firewall constraints, is an intermediary node in most control communications, thereby adding delays in communicating set points. Bypassing this node can potentially streamline the communication process. Similarly, compliance with the non-disclosure agreement necessitated locating the VAs externally from the chargers, creating an additional intermediate node for all control communication. Incorporating the control logic of the VAs directly into the chargers can shorten the control communication pathway. Lastly, improving the current one-second sampling rate of the DEIF meter can accelerate system response to new set points and decrease reaction times.

## 5. Conclusions

This paper presents an experimental demonstration of frequency regulation provided by an EV charging infrastructure with a novel distributed control architecture. This architecture integrates global intelligence for cluster control and local intelligence within each charger's microcontroller for autonomous localized control. The control concept combines power modulation of EVs in response to frequency fluctuations and prioritization of charging sessions according to charging urgency. The proof of concept is conducted using two Renault ZOEs with different priorities. During the experimental demonstration, the EV charging power and engagement in frequency regulation varied according to their priorities, while the system as a whole responded accurately to frequency fluctuations. A cross-correlation analysis revealed a peak of similarity between the expected power and power measured at 8.48 s. The error between expected and measured power ranged from −1.08 kW to 0.48 kW, with an average system undershoot of 0.17 kW. The accuracy and delay analysis show potential suitability for frequency services, although further studies are needed. Consistent with previous studies, the paper identifies the EVs as the likely cause of undershooting power set points and suggests future investigations to enhance the reliability of EVs as service providers. Finally, the study outlines system improvements and future research directions for integrating EVs into the power system.

**Author Contributions:** Conceptualization, S.S., J.E. and M.M.; Methodology, S.S.; Software, S.S. and K.P.; Validation, S.S.; Investigation, S.S. and K.P.; Resources, K.P. and M.M.; Data curation, S.S.; Writing—original draft, S.S.; Writing—review & editing, S.S., J.E., K.K. and M.M.; Supervision, J.E. and M.M.; Project administration, M.M.; Funding acquisition, M.M. All authors have read and agreed to the published version of the manuscript.

**Funding:** The work in this paper is supported by the research project ACDC (EUDP grant number: 64019-0541) and by the research project EV4EU (Horizon Europe grant no. 101056765) https://ev4eu.eu, accessed on 10 August 2024.

**Data Availability Statement:** The original contributions presented in the study are included in the article, further inquiries can be directed to the corresponding authors.

**Conflicts of Interest:** The funders had no role in the design of the study; in the collection, analyses, or interpretation of data; in the writing of the manuscript; or in the decision to publish the results

## References


1. Vishnu, G.; Kaliyaperumal, D.; Jayaprakash, R.; Karthick, A.; Kumar Chinnaiyan, V.; Ghosh, A. Review of Challenges and Opportunities in the Integration of Electric Vehicles to the Grid. *World Electr. Veh. J.* **2023**, *14*, 259. https://doi.org/10.3390/wevj14090259.
2. Crozier C.; Morstyn T.; McCulloch M. The opportunity for smart charging to mitigate the impact of electric vehicles on transmission and distribution systems. *Appl. Energy* **2020**, *268*, 114973. https://doi.org/10.1016/j.apenergy.2020.114973.
3. Gunkel, P.A.; Bergaentzlé, C.; Jensen, I.G.; Scheller, F. From passive to active: Flexibility from electric vehicles in the context of transmission system development. *Appl. Energy* **2020**, *277*, 115526. https://doi.org/10.1016/j.apenergy.2020.115526.
4. Muratori M.; Marcus A.; Arent D; Bazilian M.; Cazzola P.; Dede E.; Farrell J.; Gearhart C.; Greene D.; Jenn A. The rise of electric vehicles—2020 status and future expectations. *Prog. Energy* **2021**, *3*, 022002. https://doi.org/10.1088/2516-1083/abe0ad.
5. Ulbig, A.; Borsche, T.S.; Andersson, G.; Zurich, E. Impact of Low Rotational Inertia on Power System Stability and Operation. *Ifac Proc. Vol.* **2014**, *47*, 7290–7297
6. Fernández-Guillamón, A.; Gómez-Lázaro, E.; Muljadi, E.; Ángel Molina-García. Power systems with high renewable energy sources: A review of inertia and frequency control strategies over time. *Renew. Sustain. Energy Rev.* **2019**, *115*, 109369. https://doi.org/10.1016/j.rser.2019.109369.
7. Borne, O.; Korte, K.; Perez, Y.; Petit, M.; Purkus, A. Barriers to entry in frequency-regulation services markets: Review of the status quo and options for improvements. *Renew. Sustain. Energy Rev.* **2018**, *81*, 605-614. https://doi.org/10.1016/j.rser.2017.08.052.
8. González, L.G.; Siavichay, E.; Espinoza, J.L. Impact of EV fast charging stations on the power distribution network of a Latin American intermediate city. *Renew. Sustain. Energy Rev.* **2019**, *107*, 309–318. https://doi.org/10.1016/j.rser.2019.03.017.
9. Liu, H.; Qi, J.; Wang, J.; Li, P.; Li, C.; Wei, H. EV Dispatch Control for Supplementary Frequency Regulation Considering the Expectation of EV Owners. *IEEE Trans. Smart Grid* **2018**, *9*, 3763–3772. https://doi.org/10.1109/TSG.2016.2641481.
10. Sevdari, K.; Calearo, L.; Andersen, P.B.; Marinelli, M. Ancillary services and electric vehicles: An overview from charging clusters and chargers technology perspectives. *Renew. Sustain. Energy Rev.* **2022**, *167*, 112666. https://doi.org/10.1016/j.rser.2022.112666.
11. Atallah, R.F.; Assi, C.M.; Fawaz, W.; Tushar, M.H.K.; Khabbaz, M.J. Optimal Supercharge Scheduling of Electric Vehicles: Centralized Versus Decentralized Methods. *IEEE Trans. Veh. Technol.* **2018**, *67*, 7896–7909. https://doi.org/10.1109/TVT.2018.2842128.
12. Richardson, P.; Flynn, D.; Keane, A. Local versus centralized charging strategies for electric vehicles in low voltage distribution systems. *IEEE Trans. Smart Grid* **2012**, *3*, 1020–1028. https://doi.org/10.1109/TSG.2012.2185523.
13. Statnett.
Distributed balancing of the power grid. Technical report, 2021. Available online https://www.statnett.no/contentassets/5f177747331347f1b5da7c87f9cf0733/2021.02.24-results-from-the-efleks-pilot-in-the-mfrr-market--.pdf (accessed on 10 August 2024).
14. Han, X.; Heussen, K.; Gehrke, O.; Bindner, H.W.; Kroposki, B. Taxonomy for Evaluation of Distributed Control Strategies for Distributed Energy Resources. *IEEE Trans. Smart Grid* **2018**, *9*, 5185–5195. https://doi.org/10.1109/TSG.2017.2682924.
15. Anwar M. B.; Muratori, M.; Jadun, P.; Hale, E.; Bush, B.; Denholm, P.; Ma O.; Podkaminer, K. Assessing the value of electric vehicle managed charging: A review of methodologies and results. *Energy Environ. Sci.* **2022**, *15*, 466–498 . https://doi.org/10.1039/d1ee02206g.
16. Knez, M.; Zevnik, G. K.; Obrecht, M. A review of available chargers for electric vehicles: United States of America, European Union, and Asia. *Renew. Sustain. Energy Rev.* **2019**, *109*, 284–293. https://doi.org/10.1016/j.rser.2019.04.013.
17. Thompson, A. W.; Perez, Y. Vehicle-to-Everything (V2X) energy services, value streams, and regulatory policy implications. *Energy Policy* **2020**, *137*, 111136. https://doi.org/10.1016/j.enpol.2019.111136.
18. Thingvad, A.; Ziras, C.; Marinelli, M. Economic value of electric vehicle reserve provision in the Nordic countries under driving requirements and charger losses. *J. Energy Storage* **2019**, *21*, 826–834. https://doi.org/10.1016/j.est.2018.12.018.
19. Yao, E.; Wong, V.W.S.; Schober, R. Robust Frequency Regulation Capacity Scheduling Algorithm for Electric Vehicles. *IEEE Trans. Smart Grid* **2017**, *8*, 984–997. https://doi.org/10.1109/TSG.2016.2530660.
20. Falahati, S.; Taher, S.A.; Shahidehpour, M. A new smart charging method for EVs for frequency control of smart grid. *Int. J. Electr. Power Energy Syst.* **2016**, *83*, 458–469. https://doi.org/https://doi.org/10.1016/j.ijepes.2016.04.039.
21. Orihara, D.; Kimura, S.; Saitoh, H. *Frequency Regulation by Decentralized V2G Control with Consensus-Based SOC Synchronization*; Elsevier B.V.: Amsterdam, The Netherlands, 2018; Volume 51, pp. 604–609. https://doi.org/10.1016/j.ifacol.2018.11.770.
22. Meesenburg, W.; Thingvad, A.; Elmegaard, B.; Marinelli, M. Combined provision of primary frequency regulation from Vehicle-to-Grid (V2G) capable electric vehicles and community-scale heat pump. *Sustain. Energy Grids Netw.* **2020**, *23*, 100382. https://doi.org/10.1016/j.segan.2020.100382.
23. Yang, Q.; Li, J.; Yang, R.; Zhu, J.; Wang, X.; He, H. New hybrid scheme with local battery energy storages and electric vehicles for the power frequency service. *eTransportation* **2021**, *11*, 100151. https://doi.org/10.1016/j.etran.2021.100151.
24. Meng, J.; Mu, Y.; Jia, H.; Wu, J.; Yu, X.; Qu, B. Dynamic frequency response from electric vehicles considering travelling behavior in the Great Britain power system. *Appl. Energy* **2016**, *162*, 966–979. https://doi.org/10.1016/j.apenergy.2015.10.159.

25. Marinelli, M.; Martinenas, S.; Knezović, K.; Andersen, P.B. Validating a centralized approach to primary frequency control with series-produced electric vehicles. *J. Energy Storage* **2016**, *7*, 63–73. https://doi.org/10.1016/j.est.2016.05.008.
26. Arias, N.B.; Hashemi, S.; Andersen, P.B.; Traeholt, C.; Romero, R. V2G Enabled EVs Providing Frequency Containment Reserves: Field Results. In Proceedings of the 2018 IEEE international conference on industrial technology (ICIT), Lyon, France, 20–22 February 2018.
27. Striani, S.; Sevdari, K.; Marinelli, M.; Lampropoulos, V.; Kobayashi, Y.; Suzuki, K. *Wind Based Charging via Autonomously Controlled EV Chargers under Grid Constraints*; Institute of Electrical and Electronics Engineers Inc.: Piscataway, NJ, USA, 2022. https://doi.org/10.1109/UPEC55022.2022.9917883.
28. European Committee for Electrotechnical Standardization. *DS/EN 61851-1:2019 Electric Vehicle Conductive Charging System—Part 1: General Requirements.* Rue de la Science 23, B-1040 Brussels. 2019.
29. Sevdari, K.; Calearo, L.; Bakken, B.H.; Andersen, P.B.; Marinelli, M. Experimental validation of onboard electric vehicle chargers to improve the efficiency of smart charging operation. *Sustain. Energy Technol. Assess.* **2023**, *60*, 103512. https://doi.org/10.1016/j.seta.2023.103512.

**Department of Wind and Energy Systems**
Division for Power and Energy Systems
Technical University of Denmark
Frederiksborgvej 399
DTU Risø Campus, 4000 Roskilde
Denmark

https://windenergy.dtu.dk/english
Tel: (+45) 46 77 50 85
E-mail: communication@windenergy.dtu.dk